Quantum Information Capacities for Networks and Higher Dimensional Channels

PhD program

Nanoscience

Academic year

2021/2022

Scuola Normale Superiore

Candidate
Stefano Chessa

Supervisors
Prof. Vittorio Giovannetti

Except where acknowledged in the customary manner, the material presented in this thesis is, to the best of my knowledge, original and has not been submitted in whole or part for a degree in any university.

Stefano Chessa

Acknowledgements

List of publications

- **S. Chessa**, V. Giovannetti
Time-polynomial Lieb-Robinson bounds for finite-range spin-network models,
Phys. Rev. A **100**, 052309 (2019).

- **S. Chessa**, M. Fanizza, and V. Giovannetti
Quantum-capacity bounds in spin-network communication channels,
Phys. Rev. A **100**, 032311 (2019).

- **S. Chessa**, V. Giovannetti
Partially Coherent Direct Sum Channels,
Quantum **5**, 504 (2021).

- **S. Chessa**, V. Giovannetti
Quantum capacity analysis of multi-level amplitude damping channels,
Commun. Phys. **4**, 22 (2021).

- **S. Chessa**, V. Giovannetti
Resonant multi-level amplitude damping channels, a quantum capacity analysis,
In preparation, (2022).

- S. Tirone, **S. Chessa**, R. Salvia, and V. Giovannetti
Quantum advantage in noisy work extraction,
In preparation, (2022).

Contents

1 Introduction

> "The discussion is suggestive throughout, rather than mathematical, and it is not always clear that the author's mathematical intentions are honorable."
>
> *Joseph L. Doob*, speaking about one of the most influential intellectual productions in human history.

When in 1948 Claude Shannon published "A Mathematical Theory of Communication" [Sha48] he little could know and probably little could expect about how the notion of information would have been central and pervasive in our days. Apparently, also some of his reviewers could know pretty little, they were more focused on the honorability of the mathematical intentions[1] [Doo49, Pie73]. However, maybe luckily for us, the impact of Shannon's findings in the theory of communication wasn't shadowed by his contemporaries' mathematical taste and the consequences of his work now permeate almost every facet of our daily life. All the information needed to produce this thesis throughout these four years has been accessible thanks to the technology stemmed from Shannon's production. The scientific papers encoded as data stored in servers, the communication protocols to transfer them reliably from node to node over the internet network, the software needed to compress, decompress and convert the digital data to user-enjoyable form (including this PDF file) are all a consequence of his seminal work. As the reader may have guessed, also the conceptual content of this thesis is a consequence of Shannon findings (clearly with a different pretense of impact but with an at least comparable lack of honorability), we'll see later on how.

[1] When asked for an opinion about this review he declared [SSW93]: "I didn't like his review. He hadn't read the paper carefully". Sounds familiar?

Roughly during the same years in which Shannon set the foundations of Communication Theory, physics was living an extremely active and flourishing time. Relativity and Quantum Mechanics were formalized and elementary aspects of nature were brought to the light with the foundation of Quantum Field Theory. These new theories offered new grounds for technological revolutions such as, relevantly, the ability to exploit nuclear energy and information technologies. It's not the goal of this thesis to deliver an exhaustive depiction of how nuclear and electronic technologies are pivotal in contemporary society. This appears self-evident from the geopolitical picture to the most basic facets of our daily life. What may come as a surprise is that, despite being now more than a century old and the deep technological exploitation that it triggered, Quantum Mechanics still has proven to be able to provide new windows to observe our reality under a different point of view. In 1982 Richard Feynman, that curiously also took part in the other revolution (the nuclear one), gave a now famous conference seminar about the relation between computers and the quantumness of reality [Fey82]. Trying to be concise here, in that talk he stated that, given the structure and capabilities of modern computers, the faithful simulation of natural systems must have been quantum. In consequence, only "quantum behaving" systems could achieve that with constrained resources. While this claim in this form today may be debated, Feynman's observation is considered the first milestone on the journey of Quantum Information. The peculiar features of quantum mechanics started then to attract interest not only for their "non-classicality" per se, but also because they shed a different light over the concepts of information and its processing. Three years later David Deutsch conceived the Quantum Turing Machine and the first instance of a quantum algorithm as we know them [Deu85], providing an advantageous application of quantum computers. Around those same years, thanks to the work of Wiesner, Bennett, Brassard and Ekert it was shown that Quantum mechanics could ensure intrinsic safety resources for quantum cryptography [Wie83, BB14, Eke91]. The early 90's witnessed the birth of new quantum algorithms [DJ92, Kit95, Gro96, BV97, Sim97], with culminating point the 1994 Peter Shor's algorithm, where he proved that a quantum computer could break RSA encryption system efficiently [Sho94]. This last event marked a turning point in the field. Quantum Information switched rapidly from a relatively small speculative topic to a strategic research field in the realm of information science and technologies. So, in the background of this picture, the advent of quantum mechanics in the landscape of Information Theory stimulated a revisitation of Shannon's theory of communication by equipping it with the new resources that quantum theory could provide. Also in this regard the additional quantum features were crucial to exhibit increased communication performances and to enlarge the variety of protocols that could be imagined in the framework of communication. This thesis will focus on a small corner of this new formulations of Communication Theory (Quantum Communication) and Shannon Theory (Quantum Shannon Theory). Specifically we'll deal with noise models in specific systems, spin networks and qudits, and characterize some of their information capacities.

Motivations and outlook

As we hinted above, in recent years the field of Quantum Information has witnessed a fast growth in both its theoretical and experimental manifestations. This is due to its claims that promise to revolutionize the realms of information and communication. In this perspective, this thesis aims to contribute to the efforts dedicated to the exploration of the features of Quantum Communication and its applications, specifically the quantification of limits in information transfer expressed in terms of information capacities. This issue has attracted the efforts of our community since, as the reader may know, Quantum Mechanics allows the existence of communication protocols that are inaccessible classically. The characterization of these protocols though is typically provably harder, analytically and computationally, to be tackled. A corpus of literature has therefore been built up in order to approach this challenging endeavor: the pieces of work that we'll present in the following can be considered as incremental steps in this direction. We'll discuss how (some of the known) capacities can be bounded in quantum networks and then we'll deal with new classes of noise models in higher dimensional systems for which we'll exhibit an extensive analysis with focus on quantum and private classical capacities.
We sketch below the structure of the thesis.

The thesis is structured in two main groups of chapters.

In the first group, that comprises Chapter 2 and 3, we'll give a very self contained introduction to the most basic concepts in Quantum Communication. Our goal is far from trying to give a comprehensive review, we'll present only the strictly necessary notions useful to give a reasonable but synthetic contextualization to the pieces of work that will be discussed in the results in Chapters 4, 5, 6 and 7. The interested readers will be able to deepen each topic by referring to the references that will be provided along the road. This brief introduction is structured as follows.

- **Chapter 2**

  Quantum communications: models for implementations

  In Sec. 2.1 we'll introduce DiVincenzo's criteria while discussing what properties a quantum computing device will be required to display in order to reliably perform the desired tasks. Some of these criteria will affect also quantum communication features. In Sec. 2.2 we'll start the analysis of possible ways, in terms of physical implementations, of effectively transferring quantum states from one point in the spacetime to another one. We'll see that one can conceive two kind of models:

  - Flying qubit model, Sec. 2.2.1: the means of communication (carrier) physically moves from the sender to the receiver.
  - Static model, Sec. 2.2.2: the means of communication is a static infrastructure connecting sender and receiver.

- Chapter **3**

  Quantum Shannon Theory

  In Sec. 3.1 we'll sketch some of the most relevant results in noisy classical communication and Shannon theory, specifically we'll introduce the concept of capacity of a communication channel.

  In Sec. 3.2 we'll enumerate the basic definitions of quantum states, channels and von Neumann entropy that we'll need in the following.

  In Sec. 3.3 we'll examine how the communication settings and the definitions of information rates are built in presence of quantum mechanical systems and effects. Functionally to the discussions that will take place in the results in Chapters 4, 5, 6 and 7, we'll introduce the following communication protocols:

  - In Sec. 3.3.1: classical communication via quantum channels with the associated classical capacity C.
  - In Sec. 3.3.2: private classical communication via quantum channels with the associated private classical capacity C_{p}.
  - In Sec. 3.3.3: quantum communication via quantum channels with the associated quantum capacity Q.
  - In Sec. 3.3.4: entanglement assisted classical and quantum communication via quantum channels with the associated entanglement-assisted classical capacity C_{ea} and Q_{ea}.

In the second group of chapters of the thesis, that comprises Chapters 4, 5, 6 and 7, we'll discuss some of the results that we obtained in the last (almost) four years of my PhD. As discussed in the introduction and in Chapters 2 and 3, they refer to topics in the Quantum Communications landscape, in particular estimates of information capacities in quantum networks employed as means of communication and models of quantum noise for higher dimensional (qudit) systems. Considering the non complete homogeneity of the topics and reasons of practicality I decided to present them in separate chapters, each one corresponding to one of the publications that stemmed from our work. I substantially preserved the original structure of each paper in order for each chapter to be self contained and to be more easily accessible, independently one from the other, for those who'll be required to read this piece of work. In light of this, the results chapters are structured as follows:

- **Chapter 4**

  Bounding capacities in quantum networks

  This chapter is based on [CFG19] : S. Chessa, M. Fanizza, and V. Giovannetti, Quantum-capacity bounds in spin-network communication channels, *Phys. Rev. A* **100**, 032311 (2019).

  We present the issue of communication protocols in quantum spin networks equipped with short range interaction. We show that by exploiting a well known result in

mathematical physics, the Lieb-Robinson bound, one can characterize several information capacities associated to the information transmission between two regions of the network.

- **Chapter 5**

  Multi-level amplitude damping channels, a capacity analysis

  This chapter is based on [CG21b] : S. Chessa, V. Giovannetti, Quantum capacity analysis of multi-level amplitude damping channels, *Comm. Phys.* **4**, 22 (2021).

  We introduce a new class of quantum channels, Multi-level amplitude damping channels, as a construction arising from the generalization of the well known qubit amplitude damping channel. We give a characterization of this class in terms of Kraus operators. We proceed then at the analysis of quantum capacity, private classical capacity with a study of degradability and antidegradability conditions, and of entanglement assisted quantum and classical capacities.

- **Chapter 6**

  Resonant multi-level amplitude damping channels channels, a quantum capacity analysis

  This chapter is based on: S. Chessa, V. Giovannetti, Resonant multi-level amplitude damping channels, a quantum capacity analysis, *in preparation*, 2022.

  We show how in the context of higher dimensional systems, by directly looking at the interaction with the environment through the Stinespring representation one can evade the class of multilevel amplitude damping channels, seeing that an unusual action on the off diagonal coherences is present. This despite having an identical behaviour on the state populations. We recognize then a new class of channels and study degradability and antidegradability in order to approach their quantum capacity and private classical capacity, we compute entanglement assisted quantum and classical capacities.

- **Chapter 7**

  Partially Coherent Direct Sum channels

  This chapter is based on [CG21a] : S. Chessa, V. Giovannetti, Partially Coherent Direct Sum channels, *Quantum* **5**, 504 (2021).

  We introduce the class of Partially Coherent Direct Sum channels, generalizing a construction from Fukuda and Wolf. In brief, this is done by a coherent composition of channels in direct sum. We characterize their structure and show necessary an sufficient conditions for degradability. We exhibit some applications by computing the quantum capacity of composition of physical low dimensional channels shaping higher dimensional channels.

In Chapter 8 we'll draw our conclusions.

2

Quantum communications: models for implementations

2.1 Quantum in practice: DiVincenzo's criteria

As we discussed in the introduction, the unexplored capabilities that Quantum Information promises to express in the realm of information technologies have triggered an ever growing effort from the scientific community aimed to harness them. Unfortunately theoretical results often are not easily translated into immediately achievable and scalable practical solutions. This meant that at the early stages of Quantum Computation it wasn't clear what kind of device would have been able to deliver the expectations. In 2000 David DiVincenzo tried then to summarize some of the necessary features that such devices needed to exhibit and drew up what are now known as DiVincenzo's criteria [DiV00]:

- A scalable physical system with well characterized qubits.
- The ability to initialize the state of the qubits to a simple fiducial state.
- Long relevant decoherence times, much longer than the gate operation time.
- A "universal" set of quantum gates.
- A qubit-specific measurement capability.

These five features were discussed by DiVincenzo as minimal requirements to be held by actual devices in order to achieve reliable quantum computation. Each one of them implies deep consequences in technological terms and the last two decades have seen an extended variety of efforts to close the gaps between the reality of today accessible systems and the standards set by the criteria. Obviously we will not be able to talk through these aspects here. What we are interested in though is that he also recognized

how the ability to connect separate devices and transfer quantum states would prove crucial in the perspective of a distributed network of "quantum nodes". In consequence of this he added to the list 2 more criteria:

- The ability to interconvert stationary and flying qubits.
- The ability to faithfully transmit flying qubits between specified locations.

These two additional requirements identify almost completely those that will be the scientific context and (hopefully) contribution to the existing literature of this thesis. As we'll see later, our results are concerned with quantifying the amount of information that quantum communication channels can transmit from a point in space to the another one and understanding how noise processes interfere with this transmission.

In the next section we'll go a little bit deeper in the details, introducing a first basic distinction between the possible structures that quantum communication facilities can display to perform actual quantum state transfer.

2.2 Moving quantum states

As it was superficially hinted in the introduction, the production, storage and transfer of quantum states are, at the current state of the art of the technologies involved, highly nontrivial tasks. The issues that may get in the way of such tasks are inherently device dependent and of a multitude of originating natures. From a more abstract perspective though, the failures associated with quantum state manipulation can be fit in two large classes that encompass these phenomena. The first one is given by the presence of environmental noise: microscopic systems, as much as isolated, can interact with degrees of freedom that are not accessible or controllable by the experimenter. This interaction will induce an evolution on the system and produce a shift on the original quantum state. In general that shift may not be reversed and the uncertainty on the state will translate to a noisy effect. The second one is given by the intrinsic non deterministic nature of quantum operations: even in optimal experimental settings there may be fundamental uncertainties concerning state preparation, processing and measurements. In many cases also these uncertainties can be modeled as the effect of noise processes.

It's clear then that the overall enterprise of quantum communication will incur in technical limitations. These limitations, as stated before, will depend on the physical implementation of the communication protocol. Therefore, depending on the selected platform, there always will be a trade-off involving performance, complexity and costs. Because of these trade offs, depending on the context, one implementation may be more advantageous than other ones. The literature then evolved by proposing a variety of different (conceptually and practically) possible approaches that promise at least the potential to achieve a faithful quantum communication. In the following we discuss the two macro areas to which quantum communication systems can ascribe: the "flying qubit" model and the static model.

2.2.1 Flying qubit model

The flying qubit model refers to the possibility, from the sending party A, of encoding their quantum state on a physical systems that will travel from one point of the spacetime to a different point of the spacetime where the receiver B will collect it[1]. This picture is fairly simple and does not require specific assumptions about the local structures at disposal of the two communicating parties A and B. Without loss of generality we can imagine them to possess a quantum register each that possibly will be an ensemble of quantum systems in a definite quantum state. The goal will be then to transfer the register state, or maybe of one of its subsystems state, to the moving carrier. To do this we'll assume A to be able to perform coherent operations between the register and the carrier. Once the carrier will be in proximity of B the same will happen with the associated quantum register. See Fig. 2.1 for a depiction of the process.

This setting is quite intuitive and finds its realization for instance in those applications involving electro-magnetic waves employed as carriers [WPGP+12], that comprise already diffused optical fibers quantum communication, where the information (quantum state)

[1]The term flying *qubit* is a little bit misleading here since the state carrier needs not to be generally a 2 levels system, but for the sake of simplicity we'll keep this denomination in the following

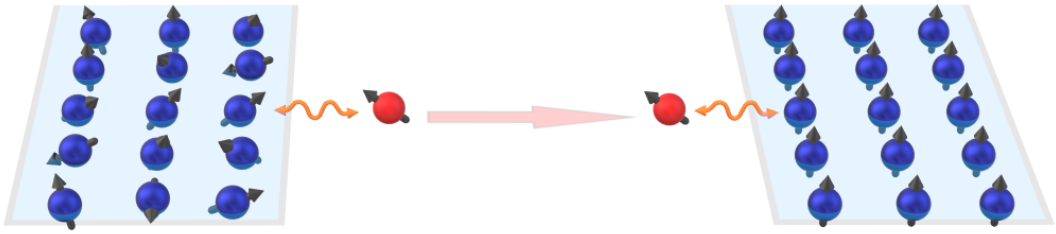

FIGURE 2.1: Flying qubit model. A quantum system is encoded on a carrier through the interaction with a register A. The carrier moves to the register B and interacting with it transfers the quantum state.

is encoded in photons or wave packets and which has been proven to be effective up to 600 km for quantum key distribution purposes [PML+21]. Photons are also used in satellite quantum communication, hence in a free space setting [VBD+15, Pir21, SJG+], atmospheric setting [HPK+14] and even in the sea water settings [JGY+17]. Proof of principle implementations of flying qubit quantum communication have also been realized with electrons in solid state devices [HTY+11, MKF+11], ions in traps [PDF+21] and phonons [DJP+21].

2.2.2 Static model

If we try to picture how a future quantum computer will look like, we may find ourselves projecting the current computers typical architectural structure onto the new coming breed of devices. We'll likely imagine a number of processors that must be able to communicate more or less rapidly with layers of memory, depending on the necessities of the computation in place. Now, leaving aside the technical issues related to the effective realization of such components, what is reasonable to expect is that all these components will be as much as possible miniaturized in order to reduce latency times and noise exposure. This is true in conventional computers and likely will be in quantum computers, think for instance to superconducting-circuit based quantum devices: the volume inside a cryostat that can be functionally cooled to the requisite working temperatures is limited, hence the whole machine needs to be compressed in few cubic centimeters. The miniaturization predicament, in the quantum as in the classical setting, finds a solution in the integration of the communication lines between processing units and memory cells directly into the computational apparatus. So, as an integrated bus connects a CPU to another CPU or to a memory, a quantum bus formed by an array of static (i.e. not flying) interacting qubits may be able to connect two quantum processing units or quantum memories.

Compared to the flying qubit scenario, the static setting will then witness similar protocols for the communicating parties (granted the possible difference in underlying technology) but a stark difference in the transmission. Specifically, we can still imagine without loss of generality a quantum register A in possess of the sender party with a definite quantum state encoded in it. Something similar holds for the receiver that has

access to a quantum register B. Both sender and receiver will be able to operate on their own registers and to perform operations also on a limited portion of the bus. The bus will be a static structure composed by a number of quantum systems, we can presume a chain or a network, and will be spatially located and distributed in order for its ends to be sufficiently close to A and B. In this case there is no spatial displacement of a carrier, the quantum state will need to "jump" from a site of the bus to the neighbours. See Fig. 2.2 for a depiction of the setting.

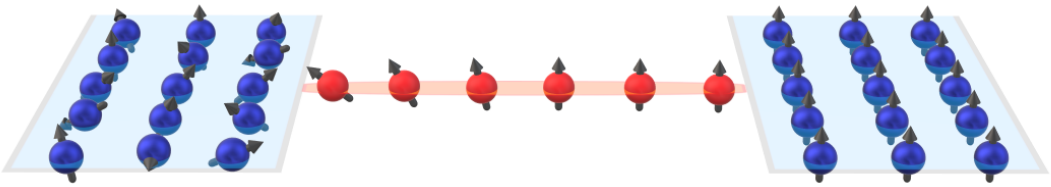

Figure 2.2: Static model. The registers of the two communicating parties registers A and B are put in contact with an intermediary infrastructure. The state is encoded on one end of the "quantum bus" by A and the internal interaction transfers the state to B that retrieves the state with suitable operations.

It's clear that this configuration will require an interaction between the sites. This interaction may be artificially induced in the case of a quantum bus made of a very limited number of quantum systems, otherwise we'd expect a fixed interaction that needs not external management. The latter case, the autonomous quantum bus, results particularly appealing with respect to the flying qubit model and the controlled bus because reduces the amount of resources that are directed towards the state propagation and that consequently can be employed elsewhere. As we said above though advantages come often with trade-offs, in this case the decrease of needed resources translates trivially into a decrease of control in the transfer: depending on the morphology of the system and the interaction considered the faithful state transfer may get more difficult. What can be said in general terms is that the quantum bath and the associated interaction will be modeled via the expression of an Hamiltonian $\hat{H}$, that in typical practical settings will be written as a sum of local terms:

$$\hat{H} = \sum_X \hat{H}_X, \tag{2.1}$$

where the subscripts X refer to possible local subsets of the quantum bus composing systems, with locality defined with a suitable notion of distance on the bus network. A large range of well known models that can be described in this fashion. Among the 1-D models we count for instance the exchange interaction Hamiltonian $\hat{H}^{\text{ex}}$:

$$\hat{H}^{\text{ex}} = \sum_{i,j} J_{ij}\, \hat{\mathbf{S}}_i \cdot \hat{\mathbf{S}}_j, \tag{2.2}$$

being J_{ij} the coupling between the spins $\hat{\mathbf{S}}_i = (S_i^X, S_i^Y, S_i^Z)$ and $\hat{\mathbf{S}}_j = (S_j^X, S_j^Y, S_j^Z)$ on the sites i and j. These models can of course be generalized to higher dimensions

(say 2D or 3D structures) and arbitrary geometries where the linear quantum bus of Fig. 2.2 gets replaced by a networks of interconnected elements (see Chapter 4). Also in this context however the overall picture remains the same: two communicating parties with local accessible registers, produce signals that travel on the network, propagated by the network Hamiltonian. We stress that at this level we don't need though to focus too much on the underlying physics of these kind of models, which represents *per se* a vast area of research in condensed matter. This is because the only feature that will be relevant to the results that we'll present later is for our quantum bus to be equipped with a local or equivalently finite range interaction, so that sufficiently distant sites will not influence directly each others.

As discussed above, the static model for quantum communication is more suited for quantum state transfer in miniaturized and compact architectures. Considering current candidates for quantum computation, the static model finds its natural application in solid state devices. Among the proposals and demonstrations in this sense we saw quantum communication with Josephson junctions arrays [RFB05], with nuclei controlled by NMR pulses [FXBJ07], chains of nitrogen-vacancy centers in diamonds [PLBG13], chains of cold atoms [MVV+16], see [Bos07] and references therein for other examples.

Recap

Trying to summarize briefly this introductory section, we'll say here that our interest will concentrate on information theoretic aspects of quantum communication. As displayed above, being able to transfer quantum states is of paramount importance if we realistically aim to achieve an advantageous use-case for quantum technologies. This transfer can in principle be realized via several implementations or strategies, but can be reduced to two main typologies: flying qubit and static. Our work will address both, we'll try to give a characterization of the amount of information that can be transmitted in these settings, possibly in presence of noise.

3 Quantum Shannon Theory

In this chapter we'll introduce the basic definitions in Shannon Theory and Quantum Shannon Theory that will come useful in the derivation and discussion of the results of our work in the second part of this thesis. For reasons of space and time the exposition needs to be as self-contained as possible. Therefore we refer the reader to the standard textbooks of Classical Shannon Theory, e.g. [CT05], and Quantum Shannon Theory, e.g. [Wil17, Hay17, Wat18, Hol19], by which substantially this introduction will be inspired.

3.1 Shannon theory and noisy classical communication

When we talk about communication we refer to an operative process in which messages, composed by symbols $\{s_i\}_i$ extracted from a set Σ (that here we'll consider finite), need to be transferred from a party A to a party B that is spatio-temporally separated from A. The probability distribution $\mathbf{p} \equiv \{p_i\}_i \equiv \{p(s_i)\}$ of occurrences of the symbols, together with the symbols $\{s_i\}_i$, identify what is called an information source. Here and in the following we'll assume that each sampling of the source will be independent from the others: the information source behaves as a memoryless, independent and identically distributed (i.i.d.) random variable. It's possible to associated to any information source a "measure" of its information content, so to speak, and this measure is given by the Shannon entropy $H(\mathbf{p})$:

$$H(\mathbf{p}) = -\sum_i p_i \log_2 p_i, \tag{3.1}$$

where the intuition is given by the fact that one can define the "surprise" relative to the outcome i as $-\log p_i$ and in consequence the Shannon entropy is the average surprise of the source. The Shannon entropy has also an additional operational meaning. In his source coding theorem Shannon showed that messages extracted from n instances of a source X with entropy $H(X)$, in the asymptotic limit can be compressed without information loss in at least $nH(X)$ bits [Sha48].

In the physical world the communication procedure will necessarily be carried out by physical systems undergoing physical processes. In the typical reasonable scenarios these processes will not be fully controlled by the communicating parties and some of the messages will be corrupted, introducing uncertainty to the end of the receiver. They can't assess with certainty whether the message received is the original one or a corrupted one: the communication is noisy. If the noise model is known though, the two parties may agree on an engineered a protocol that optimizes the chances that the message passes untouched. This is translated in the realization of an encoding procedure $\mathcal{E}$ and a decoding procedure $\mathcal{D}$ tailored in order to store messages into agreed "codewords" that are resilient to the noise Φ and that the receiver will be able to faithfully map back to the original message X, see Fig. 3.1 for a schematic representation of the process.

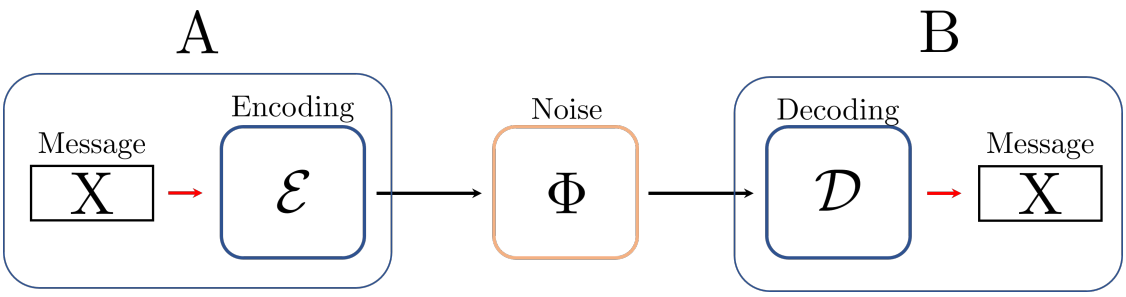

FIGURE 3.1: Representation of an error correcting communication scheme: a message X is encoded by A in a suitable state that undergoes through the noise, the output is then reconverted to the original message by the decoding procedure.

These codewords will correspond to physical states that will remain somewhat distinguishable after the application of the noise. The question that naturally arises is: given n noisy channel uses how much information will we be able to transmit without errors? Shannon answered also this question. We can define the rate R of our code for a message space M and n uses of the channel as

$$R = \frac{\log_2 |M|}{n} , \tag{3.2}$$

being $|M|$ the dimension of our message space. The Shannon's noisy channel theorem states that for each noise model Φ will exist a capacity C such that if we choose $R < C$ then messages will be decoded with arbitrary small probability of error, while for $R > C$ the transfer will happen with non vanishing errors. The capacity of a channel is the supremum of all the achievable rates and it can be expressed as

$$C(\Phi) = \sup_{p_A} I(A : B) , \tag{3.3}$$

being p_A a probability distribution of the generating source of the code for A and $I(A : B) = H(A) + H(B) - H(AB)$ the mutual information between A and B after the application of the channel.

The results that here we synthetically portrayed constitute the milestones of information theory. They hold for communication of classical information through classical channels. Our contribution will deal with communication carried out by quantum channels but, with distinctions that will be made clear in the following, the underlying framework over which Quantum Shannon Theory is built overlaps with the one we laid above.

3.2 Quantum states, channels and measurement

Quantum states

We'll set here some of the basics of the notation that we'll need to define quantum information capacities and in general in the rest of the thesis.

We'll denote as $\mathcal{H}_{\mathrm{S}}$ the Hilbert space associated with the quantum system S, which is a complex vector space equipped with an inner product $\langle \cdot , \cdot \rangle : \mathcal{H}_{\mathrm{S}} \times \mathcal{H}_{\mathrm{S}} \to \mathbb{C}$. In this thesis we'll only deal with finite dimensional Hilbert spaces.

We can denote as $\mathcal{L}(\mathcal{H}_{\mathrm{S}})$ the algebra of linear operators acting over $\mathcal{H}_{\mathrm{S}}$. In general we'll express such operators with a hat symbol in order to facilitate the distinction between scalars, operators, channels. We'll add a subscript to specify the underlying Hilbert space when needed or we'll drop it if the context will be unambiguous. For instance we'll write $\hat{O}_{\mathrm{S}}$ to identify the operator $\hat{O}$ belonging to $\mathcal{L}(\mathcal{H}_{\mathrm{S}})$. We'll denote with $\hat{O}^\dagger$ the conjugate-transpose of the operator $\hat{O}$, call Hermitian those operators for which $\hat{O}^\dagger = \hat{O}$ holds, call positive definite those operators for which $\langle v, \hat{O}_{\mathrm{S}} v\rangle > 0 \; \forall v \in \mathcal{H}_{\mathrm{S}}$ and positive semidefinite those operators for which $\langle v, \hat{O}_{\mathrm{S}} v\rangle \geq 0 \; \forall v \in \mathcal{H}_{\mathrm{S}}$.

When dealing with a set of systems S_i, each one equipped with its own Hilbert space $\mathcal{H}_{\mathrm{S}_i}$, the overall composed system S_{t} Hilbert space will be given by the tensor product of the individual subsystems Hilbert spaces like $\mathcal{H}_{\mathrm{S}_{\mathrm{t}}} = \bigotimes_i \mathcal{H}_{\mathrm{S}_i}$. The construction of linear operators over composite systems goes the same way: if we have a collection of local operators $\hat{O}_{\mathrm{S}_i} \in \mathcal{L}(\mathcal{H}_{\mathrm{S}_i})$ acting on $\mathcal{H}_{\mathrm{S}_i}$ the overall action will be described by the operator $\hat{O}_{\mathrm{S}_{\mathrm{t}}} = \bigotimes_i \hat{O}_{\mathrm{S}_i}$.

Among all the linear operators we'll be particularly interested in positive semidefinite operators such that their trace is 1 and, in consequence of positive semidefiniteness, that are Hermitian. In quantum theory they identify quantum states and are called density matrices, in the text will be typically expressed as $\hat{\rho}$. Once specified an Hilbert space $\mathcal{H}_{\mathrm{S}}$, density matrices over said Hilbert space form a convex set that we'll denote as $\mathfrak{S}(\mathcal{H}_{\mathrm{S}})$. Density matrices of rank 1 are called pure states and, exploiting Dirac's bra-ket notation, can be expressed as $|\psi\rangle\langle\psi|$. Here $|\psi\rangle$ represents a vector in the Hilbert space such that $\langle\psi,\psi\rangle \equiv \langle\psi|\psi\rangle = 1$. If states are not rank 1 then they are called mixed states and, fixed a suitable orthonormal basis $\{|i\rangle\}_{i=0}^{d-1}$, they can be expressed as

$$\hat{\rho} = \sum_{i=0}^{d-1} p_i \, |i\rangle\langle i| \ , \tag{3.4}$$

where the real and positive coefficients p_i can be interpreted as probabilities and they sum up to 1. This is an immediate consequence of the Hermiticity of density matrices and the fact that their trace is 1.

It is possible to give a notion of distance in the set of density operators $\mathfrak{S}(\mathcal{H}_{\mathrm{S}})$. This can be done for instance introducing the trace distance $T(\hat{\rho}, \hat{\sigma})$:

$$T(\hat{\rho}, \hat{\sigma}) = \frac{1}{2} \|\hat{\rho} - \hat{\sigma}\|_1 \ , \tag{3.5}$$

that exploits the definition of trace norm of an operator $\hat{O}$ that goes as

$$\|\hat{O}\|_1 = \mathrm{tr}\left[\sqrt{\hat{O}^\dagger \hat{O}}\right] . \tag{3.6}$$

As linear operators, density matrices representing states of multipartite systems behave following the tensorization as explained above. In quantum information is also relevant though the typology of structure that quantum states display in these multipartite. Specifically quantum states can be distinguished in separable states and entangled states. Separable states are those states that can be expressed as a convex combination of product states, i.e.

$$\hat{\rho}_{\mathrm{S}_1,\mathrm{S}_2,\cdots,\mathrm{S}_N} = \sum_i p_i \, \hat{\sigma}^i_{\mathrm{S}_1} \otimes \hat{\sigma}^i_{\mathrm{S}_2} \otimes \cdots \otimes \hat{\sigma}^i_{\mathrm{S}_N} \quad \text{with} \quad \hat{\sigma}^i_{\mathrm{S}_j} \in \mathfrak{S}(\mathcal{H}_{\mathrm{S}_j}) . \tag{3.7}$$

Entangled states are those states that are not separable and hence that cannot be expressed as in Eq. (3.7).

The issue of discriminating between entangled states and separable states has proved to be a really tough challenge to address. Criteria to establish separability or entanglement have been proposed but an universal characterization is not available yet for the generic multipartite scenario. The problem was showed to be NP-complete [Gur03, Gur04]. Luckily in the following we won't need to worry about the intricacies of the separability problem and we refer the interested reader for instance to [BŻ17] to get a broader perspective on the issue. What we'll need to keep in mind is that these two categories of states express a deep separation between the classical and quantum descriptions of nature. Entangled states are an exclusive feature of quantum theory and entanglement is, as we'll see later, one of the resources that mark the departure between classical and quantum communication.

von Neumann entropy

The statistical nature of quantum states, and in particular of density matrices in the form of Eq. (eq: density matrix), allows us to associate to them a "measure of uncertainty" as Shannon did with sources. The generalization of Shannon entropy to quantum states is attributed to John von Neumann [vN27, vN18] and referred to as von Neumann entropy. The von Neumann entropy of a density matrix $\hat{\rho}$ is expressed as

$$S(\hat{\rho}) = -\,\mathrm{tr}[\hat{\rho}\log_2\hat{\rho}] , \tag{3.8}$$

being here $\log_2$ the operator logarithm. It can be shown that von Neumann entropy is invariant under unitary transformations, so, taking $\dim(\mathcal{H}_\mathrm{S}) = d$ and $\hat{U} \in SU(d)$ follows that $S(\hat{\rho}) = S(\hat{U}\hat{\rho}\hat{U}^\dagger)$. This is equivalent to saying that $S(\hat{\rho})$ is invariant under a change of basis. The same can be generalized to linear isometries $\hat{V} : \mathcal{H}_\mathrm{A} \to \mathcal{H}_\mathrm{B}$ such that $\hat{V}^\dagger\hat{V} = \hat{\mathbb{1}}_\mathrm{A}$, with in general $\dim(\mathrm{A}) \neq \dim(\mathrm{B})$. From this fact follows that von Neumann entropy can be reduced to Shannon entropy when the state is expressed in the basis that diagonalizes it. $S(\hat{\rho}) = 0$ if and only if $\hat{\rho}$ is a pure state and has its maximum value $\log_2 d$ on the completely mixed state $\hat{\rho} = \hat{\mathbb{1}}_d/d$. As we'll see in the following, von Neumann entropy plays a central role in the definition of other information quantities, we report here some of the simplest and most useful properties it displays:

- Positivity: $0 \leq S(\hat{\rho}) \leq \log_2 d$, with $\hat{\rho} \in \mathfrak{S}(\mathcal{H}_\mathrm{S})$ and $\dim(\mathcal{H}_\mathrm{S}) = d$.
- Concavity in the input state: $S(\sum_i p_i \hat{\rho}_i) \geq \sum_i p_i S(\hat{\rho}_i)$, with $p_i \geq 0$ and $\sum_i p_i = 1$.
- Additivity under tensorization: $S(\hat{\rho}_\mathrm{A} \otimes \hat{\rho}_\mathrm{B}) = S(\hat{\rho}_\mathrm{A}) + S(\hat{\rho}_\mathrm{B})$.
- Subadditivity: $S(\hat{\rho}_\mathrm{AB}) \leq S(\hat{\rho}_\mathrm{A}) + S(\hat{\rho}_\mathrm{A})$, with $\hat{\rho}_\mathrm{A} = \mathrm{Tr}_\mathrm{B}\, \hat{\rho}_\mathrm{AB}$ and $\hat{\rho}_\mathrm{B} = \mathrm{Tr}_\mathrm{A}\, \hat{\rho}_\mathrm{AB}$.
- Strong subadditivity: $S(\hat{\rho}_\mathrm{ABC}) + S(\hat{\rho}_\mathrm{C}) \leq S(\hat{\rho}_\mathrm{AC}) + S(\hat{\rho}_\mathrm{BC})$.

Quantum Channels

Physical processes involving quantum systems can be expressed as transformations over quantum states and, consequently, as transformations over the associated density matrices. We'll denote them as $\Phi : \mathcal{L}(\mathcal{H}_\mathrm{A}) \to \mathcal{L}(\mathcal{H}_\mathrm{B})$. Not all mathematically admissible transformations though have a corresponding physical equivalent. In particular all physical transformations need to map physical states into physical states. In non relativistic quantum mechanics this translates to: first requiring the final state to be trace 1 as the initial state, in general then we'll require that

$$\mathrm{tr}[\Phi(\hat{\rho})] = \mathrm{tr}[\hat{\rho}] \,, \tag{3.9}$$

the channel is said then to be trace preserving; second also to requiring the final state to be positive, for any input state. This second condition needs to be made stronger: what is necessary to ask is:

$$(\mathbb{1}_n \otimes \Phi)(\hat{\rho}) > 0 \quad \forall \hat{\rho},\ \forall n \,, \tag{3.10}$$

where $\mathbb{1}_n$ is the identity map over a generic n-dimensional auxiliary Hilbert space. The requirement expressed by Eq. (3.10) is called complete positivity. The physical interpretation of complete positivity can be put in these terms: a local physical operation must preserve its "physicality" also on the rest of the universe which is unaffected by the action of the operation. This set of requirements defines a class of operations, that since they are defined over linear operators are called superoperators, and this class is the set of Completely Positive and Trace Preserving (CPTP) linear superoperators (or alternatively CPTP maps). In general allowed quantum operations and channels must satisfy Eq. (3.9) and Eq. (3.10) and therefore are CPTP maps, these terms will be interchangeable in the text. CPTP maps are closed under convex combinations. Unitary evolutions induced by a Hamiltonian are a subclass of CPTP maps.

There are more than one way to represent the action of a CPTP map over a density matrix, e.g. Stinespring representation and Kraus representation. We'll discuss Kraus representation in the Results section where it will be employed extensively . Similarly only later we'll talk about how we may find a map to be CPTP, in particular that Eq. (3.10) is satisfied: we'll see how the Choi representation of a channel allows us to establish the complete positivity. Here we will briefly present the Stinespring representation which will be needed in the next section while introducing information capacities. As we have seen any physical process can be represented by a quantum channel, also dissipative and non unitary ones. It can be shown that the action of any CPTP map $\Phi_{A\to B}$ can be realized

by a unitary interaction $\hat{U}_{AE\to BE'}$ between the input system A and an environment E in a fixed pure state $|\psi\rangle$ [Sti55], so that

$$\Phi_{A\to B}(\hat{\rho}_A) = \mathrm{tr}_{E'}\left[\hat{U}_{AE\to BE'}(\hat{\rho}_A \otimes |\psi\rangle\langle\psi|_E)\hat{U}^\dagger_{AE\to BE'}\right] . \tag{3.11}$$

This representation highlights the fact that in general evolutions on local systems may be induced by interaction with an external environment. It follows that the unitary interaction $\hat{U}_{AE\to BE'}$ will affect also environmental degrees of freedom, producing an effective channel $\tilde{\Phi}_{A\to E'}$, called complementary channel of Φ, expressed as

$$\tilde{\Phi}_{A\to E'}(\hat{\rho}_A) = \mathrm{tr}_{B}\left[\hat{U}_{AE\to BE'}(\hat{\rho}_A \otimes |\psi\rangle\langle\psi|_E)\hat{U}^\dagger_{AE\to BE'}\right] . \tag{3.12}$$

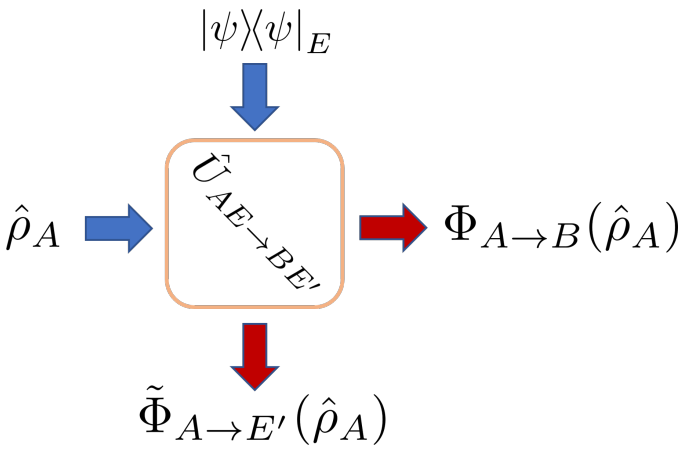

Figure 3.2: Representation of the Stinespring representation for quantum channels Φ and associated complementary channels $\tilde{\Phi}$.

Measurements

Measurements are those procedures that allow us to extract information from a quantum state about the system that it represents. Intuitively it can be modeled as a quantum process that drives the system into a state that we associate with a specific outcome. In the so called "noiseless measurement" setting the outcomes $\{j\}_j$ are linked to projectors $\{\hat{\Pi}_j\}_j$ such that:

$$\hat{\Pi}_j > 0\,, \quad \hat{\Pi}_j^\dagger = \hat{\Pi}_j\,, \quad \hat{\Pi}_i\hat{\Pi}_j = \delta_{ij}\hat{\Pi}_j\,, \quad \sum_j \hat{\Pi}_j = \hat{\mathbb{1}}\,. \tag{3.13}$$

The action on a generic quantum state of these projective measurements defines the evolution:

$$\hat{\rho} \to \frac{\hat{\Pi}_j\hat{\rho}\hat{\Pi}_j^\dagger}{p_j} \quad \text{with} \quad p_j = \mathrm{tr}\left[\hat{\Pi}_j\hat{\rho}\right] = \mathrm{tr}\left[\hat{\Pi}_j\hat{\rho}\hat{\Pi}_j^\dagger\right]\,, \tag{3.14}$$

where the parameters p_j, accordingly with the Born rule, correspond to the probabilities of getting the outcome j. From the equation above we can see that the measurement process can be seen as a quantum channel that allows us to store information about the exact projective subspace in which the system lives after the measurement.

This condition can be relaxed in order to obtain a more general definition of measurements where we just know the probability of the specific outcomes and not necessarily also a specific projective subspace. In this case we associate to the outcomes $\{j\}_j$ a set of positive valued operators $\{\hat{\Lambda}_j\}_j$ such that:

$$\hat{\Lambda}_j \geq 0 \,, \quad \sum_j \hat{\Lambda}_j = \hat{\mathbb{1}} \,. \tag{3.15}$$

The measurement procedures exhibiting these features are called positive operator-valued measures (POVM). By writing $\hat{\Lambda}_j = \hat{M}_j^\dagger \hat{M}_j$, as for projective measurements we can express the post measurement quantum state and the associated probability:

$$\hat{\rho} \to \frac{\hat{M}_j \hat{\rho} \hat{M}_j^\dagger}{p_j} \quad \text{with} \quad p_j = \mathrm{tr}\Big[\hat{\Lambda}_j \hat{\rho}\Big] = \mathrm{tr}\Big[\hat{M}_j \hat{\rho} \hat{M}_j^\dagger\Big] \,. \tag{3.16}$$

3.3 Communicating with quantum channels

In the following we'll introduce the information capacities that we'll approach in the results section. The list that follows is far from being comprehensive of the state of the art in the field and it is just instrumental in our purposes. The interested reader will be able to find more comprehensive treatises in specialized reviews and books, such as for instance [HG12, Hay17, Wil17, GIN18, Hol19, KW20].

The presentation will be again as synthetic and as schematic as possible: we'll introduce the communication setting and the relevant resources, define the significant entropic quantities and express the associated capacity.

3.3.1 Classical communication with quantum channels

Recalling what we said about the capacity of a noisy classical channel, one could think that it would suffice encode a codeword x into a quantum state $\hat{\rho}_x$ to transmit classical information through a noisy quantum channel. This can be done but as was shown by Holevo it does not represent the best achievable strategy. As it turns out, in the quantum picture also entanglement plays a role and entangled input blocks or entangled measurements can provide better performances.

More in detail, the "classical-quantum" strategy could for instance consist, mimicking the classical case, in the production from A of a classical random code of size n where symbols from $\{s_i\}_i \in \Sigma$ are extracted with probability p_X^i and associated with quantum states $\hat{\rho}_A^{s_i}$ to produce separable codewords of the form $\hat{\rho}_{A^n}^{s^n} = \hat{\rho}_A^{s_1} \otimes \hat{\rho}_A^{s_2} \otimes \cdots \otimes \hat{\rho}_A^{s_n}$. The codewords are transmitted through n uses of the channel Φ and measured with a separable POVM Λ_{SEP} at the output. The output conditional probability allows us to extract the mutual information $I(X:B)$ and then apply the noisy channel theorem, with maximum achievable rate $R_{\max}$ given by:

$$R_{\max}(\Phi) = \max_{\{p_X, \hat{\rho}_{A^n}^{s^n}, \Lambda_{\text{SEP}}\}} I(X:B) \, . \tag{3.17}$$

It's clear though that in principle the same exact scheme could be employed but without restricting ourselves to separable codewords and separable POVMs, see Fig. 3.3 for a pictorial depiction of a generic classical-communication-with-quantum-channels scheme. The issue arising here is that allowing entangled POVMs prevents the naive application of Shannon theorem as above. In general we'll need to repeat the computation for any block-size n, take the maximum and regularize dividing by n for a functional that can't be easily expressed: we need a different figure of merit. This was provided by Holevo [Hol73] who firstly showed that χ, called Holevo information, is an upper bound for $R_{\max}(\Phi)$ and is defined on an ensemble $\{\{p^i\}, \{\hat{\rho}^i\}\}$ such that the probabilities $\{p^i\} = p_X$ of Eq. (3.17) and writes [Hol73]

$$\chi(\{\{p^i\}, \{\hat{\rho}^i\}\}) = S\left(\sum_i p_i \hat{\rho}^i\right) - \sum_i p^i S(\hat{\rho}^i) \, . \tag{3.18}$$

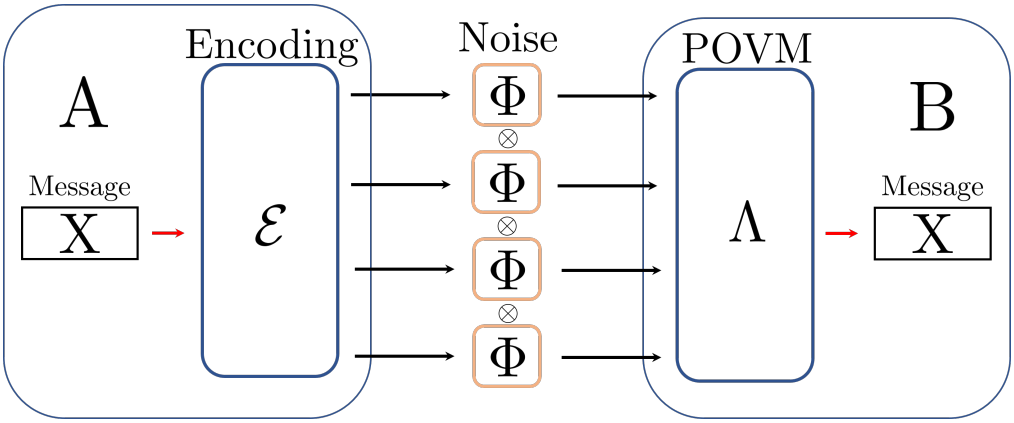

FIGURE 3.3: Representation of the communication setting for classical communication with quantum channels.

Later Holevo [Hol79, Hol98], Schumacher and Westmoreland [SW97] showed that $\chi(\Phi)$, defined as :

$$\chi(\Phi) = \sup_{\{\{p^i\},\{\hat{\rho}^i\}\}} \chi(\{\{p^i\},\{\Phi(\hat{\rho}^i)\}\}) \tag{3.19}$$

is also an achievable rate and therefore the regularized formula

$$C(\Phi) = \lim_{n\to\infty} \frac{\chi(\Phi^{\otimes n})}{n} \tag{3.20}$$

correctly expresses the value of the classical capacity for the quantum channel Φ.

Despite $\chi(\Phi)$ having a simple expression as the one in Eq. (3.19), the expression for $C(\Phi)$ in Eq. (3.20) is of little practical utility because of the unbounded sequence of optimizations that it is implied with $n \to \infty$. One could hope though the $\chi(\Phi)$ functional to be well behaved and exhibit additivity, that is to say:

$$\chi(\Phi^{\otimes n}) = n\chi(\Phi) \ , \tag{3.21}$$

that would trivialize the regularized formula into $C(\Phi) = \chi(\Phi)$. Unfortunately it has been explicitly shown that there exist channels for which $\chi(\Phi \otimes \bar{\Phi}) > \chi(\Phi) + \chi(\bar{\Phi})$: the Holevo information can be superadditive [HW08, Has09]. There are examples in the literature though of channels that display the additivity as in Eq. (3.21). Among finite dimensional quantum channels it was proved for entanglement breaking channels [Sho02a], for unital qubit channels [Kin02], for depolarizing channels [Kin03] and Hadamard channels [KMNR05, Kin]. Techniques to find "approximately additive" channels, i.e. close to additive channels in the suitable norm, were discussed in [LKDW18].

3.3.2 Classical private communication with quantum channels

In the introduction we briefly mentioned how applications in cryptography were among the first ones to be recognized as potential candidates to the exploitation of quantum effects to improve existing communication protocols, such as secret key distribution. These

tasks require a reliable estimation of the amount of information that can be transferred without an eavesdropper being able to intercept it. Intuitively this boils down to ask how many secret bits can be sent using once the channel.

The communication setting is then equivalent to the setting analyzed in the previous section, with the addition here that the state that the eavesdropper has access to, i.e. the environmental state $\tilde{\Phi}^{\otimes n}_{A\to E'}(\hat{\rho}_{A^n})$ after n applications of the quantum channel $\Phi_{A\to B}$ to the input message encoding $\hat{\rho}_{A^n}$, must be arbitrarily close to a fixed state $\hat{\pi}_{E'^n}$, see Fig. 3.4. The explicit requirement will be:

$$\|\tilde{\Phi}^{\otimes n}_{A\to E'}(\hat{\rho}_{A^n}) - \hat{\pi}_{E'^n}\|_1 < \epsilon \,, \tag{3.22}$$

with ϵ positive constant and arbitrarily small.

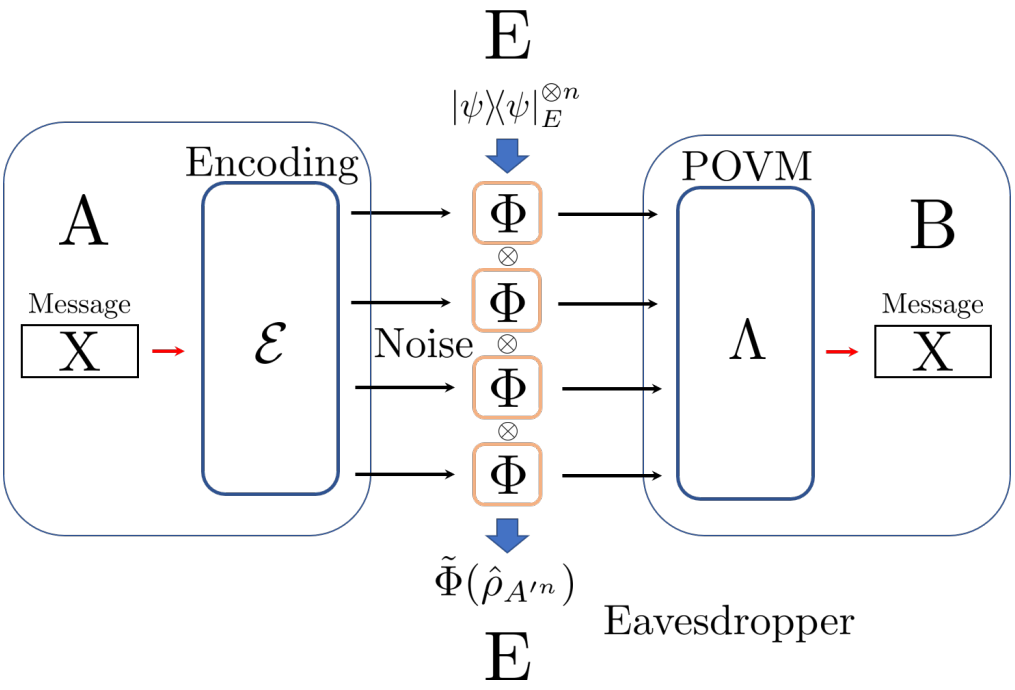

Figure 3.4: Representation of a private classical communication setting involving a quantum channel Φ.

Without deepening the details of the proof, it was shown [Dev05] that it is always possible to express an achievable rate, attainable enforcing the privacy requirement in Eq. (3.22). This is done by what is called the private information $I_{\mathrm{p}}(\Phi)$ of a channel Φ:

$$I_{\mathrm{p}}(\Phi) = \max_{\{\{p_i\},\{\hat{\rho}_i\}\}} \chi\left(\{\{p_i\},\{\Phi(\hat{\rho}_i)\}\}\right) - \chi(\{\{p_i\},\{\tilde{\Phi}(\hat{\rho}_i)\}\}) \,, \tag{3.23}$$

being χ the Holevo information defined in Eq. (3.18). The statement generalizes to n uses of the channels: $I_{\mathrm{p}}(\Phi^{\otimes n})$ is an achievable rate too. As one could have guessed taking the parallel with the case of the classical capacity, the private information is also instrumental in expressing an upper bound on the achievable rates and consequently the

private classical capacity $C_{\mathrm{p}}(\Phi)$ of a quantum channel Φ. Specifically, independently Devetak [Dev05] and Cai, Winter, Yeung [CWY04] proved that

$$C_{\mathrm{p}}(\Phi) = \lim_{n\to\infty} \frac{I_{\mathrm{p}}(\Phi^{\otimes n})}{n} \,. \tag{3.24}$$

This expression suffers again of the regularization predicament: in order to have an exact characterization of the private classical capacity we would need to perform an optimization over an infinite number of block-sizes n. Again, we could hope $I_{\mathrm{p}}(\Phi^{\otimes n})$ to scale trivially with n and being additive. Unfortunately, also in this case explicit examples of superadditivity of the private classical capacity in various settings have been provided, see e.g. [LWZG09, SRS08, ES15]. In general then the task of computing $C_{\mathrm{p}}(\Phi)$ is a highly nontrivial endeavour. There are classes of channels though for which useful properties can be leveraged and the problem simplified. It is the case for instance of degradable and antidegradable channels that display additive private capacity. We'll discuss more in detail degradable channels in the Results section.

3.3.3 Quantum communication with quantum channels

Until now we have dealt only with protocols involving the transmission of classical messages through quantum channels, mediated by an encoding over quantum states. In a quantum communication and computation oriented scenario it is plausible though to think that the goal of the sender A may be delivering quantum states to a receiver B. The desiderata in this setting will be then the received state to be very close to the state that was sent and the possible correlations (entanglement) with a separate reference system R to be preserved. The overall setting can then be laid out as the other protocols we saw, see Fig. 3.5 for a depiction. A will own a quantum state $\hat{\rho}_A$ which is a share of a multipartite state $\hat{\rho}_{AR} \in \mathfrak{S}(\mathcal{H}_A \otimes \mathcal{H}_R)$ so that $\mathrm{tr}_R[\hat{\rho}_{AR}] = \hat{\rho}_A$. In order to protect the state from the noise $\Phi_{A'\to B'}$ they'll encode it into a block A'^n of n systems A' via an encoding operation $\mathcal{E}_{A\to A'^n}$ and send the block through n uses of the channels. At the output of the channel B will try to retrieve the quantum state by applying a decoding operation $\mathcal{D}_{B'^n\to B}$. In order for our protocol to succeed, in the sense we talked about above, we'll ask:

$$\|\mathcal{D}_{B'^n\to B} \circ \Phi^{\otimes n}_{A'\to B'} \circ \mathcal{E}_{A\to A'^n}(\hat{\rho}_{AR}) - \hat{\rho}_{AR}\|_1 < \epsilon \,, \tag{3.25}$$

with ϵ positive and arbitrarily small.

Similarly to the classical case, we'll define a rate R_{q} that depends on the size of the messages space that can be transferred reliably from A to B. In this case, being quantum states our messages, we'll have

$$R_{\mathrm{q}} = \frac{\log_2 \dim(\mathcal{H}_A)}{n} \,. \tag{3.26}$$

Again, as for the classical and private classical scenarios, we are interested in understanding whether it's possible to express a superior limit for the rates in Eq. (3.26) to define a quantum capacity Q. The answer is affirmative and requires the introduction

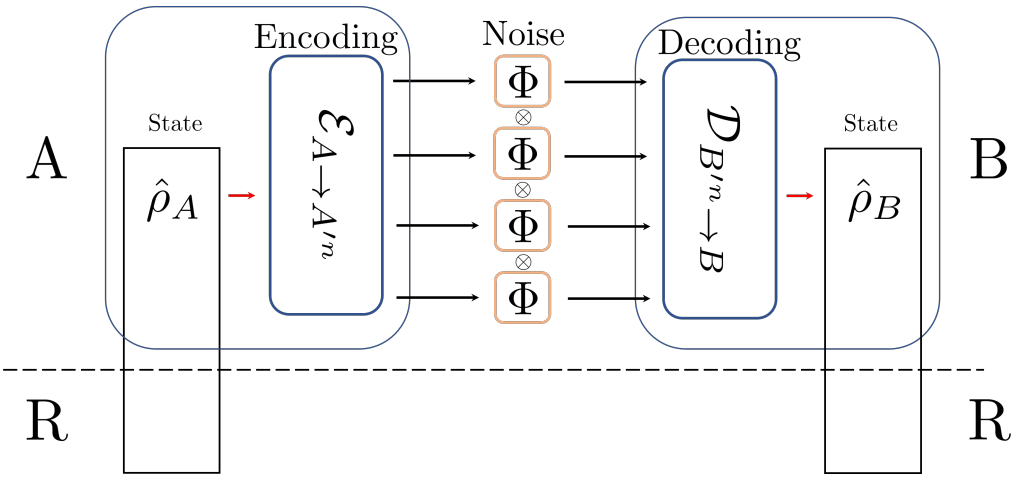

FIGURE 3.5: Depiction of a quantum communication setting involving a quantum channel Φ.

of an additional entropic quantity called coherent information. The coherent information I_{coh} was firstly defined by Nielsen and Schumacher in [SN96] and exploiting the Stinespring representation can be written as

$$I_{\text{coh}}(\hat{\rho}_A, \Phi) = S(\Phi(\hat{\rho}_A)) - S(\tilde{\Phi}(\hat{\rho}_A)) \,, \tag{3.27}$$

from which immediately follows the channel-related definition:

$$I_{\text{coh}}(\Phi) = \max_{\hat{\rho}_A \in \mathfrak{S}(\mathcal{H}_A)} I_{\text{coh}}(\hat{\rho}_A, \Phi) \,. \tag{3.28}$$

The coherent information was proved to be an upper bound for the quantum capacity [Sch96, SN96, BNS98, BKN00] and later $I_{\text{coh}}(\Phi)$ and the n uses version $I_{\text{coh}}(\Phi^{\otimes n})/n$ were proved to be also achievable rates. This allowed to define the quantum capacity $Q(\Phi)$ for a channel Φ [Llo97, Sho02b, Dev05]:

$$Q(\Phi) = \lim_{n\to\infty} \frac{I_{\text{coh}}(\Phi^{\otimes n})}{n} \,. \tag{3.29}$$

This formula, as the other ones found for communication capacities with quantum channels, involves an infinite regularization that makes it impractical to be actually used for estimating exactly the quantum capacity. The coherent information, in general, is not additive. It has indeed been showed to be superadditive, for finite dimensional channels see e.g. [SS96, DSS98, SS07, FW08, CEM+15, LLS18a, BL21, SG21a, Sid21, LLS+22b] and it has also been experimentally observed [YMP+20]. The quantum capacity can also exhibit superactivation [SY08], i.e. quantum channels with null quantum capacity, if used together, allow a nonzero quantum capacity. As for the private classical capacity though, there are classes of quantum channels for which the capacity can be computed exactly. Among these we find degradable channels, antidegradable channels, that we'll discuss later, and some other instances such as [GJL18a, GJL18b, CG21b, CG21a, LLS+22c] among which we find also MAD channels and PCDS channels that we'll introduce in the Results section.

3.3.4 Entanglement assisted communication

We mentioned in the introduction how the presence of entanglement shared between sender and receiver allows the realizations of communication protocols, such as quantum teleportation [BBC+93] and superdense coding [BW92], that prove advantageous with respect to a purely classical setting. The existence of such protocols opens the question related to the possible enhancement of communication capabilities in terms of rates. Does the presence of shared entanglement, despite the impossibility of information transfer through it, improve classical and quantum communication? The answer, as you can guess, is yes.

The description of the communication setting is similar to those already encountered, with the addition of an arbitrarily large amount of shared entanglement between A and B, see Fig. 3.6 for a representation of the entanglement assisted classical communication setting.

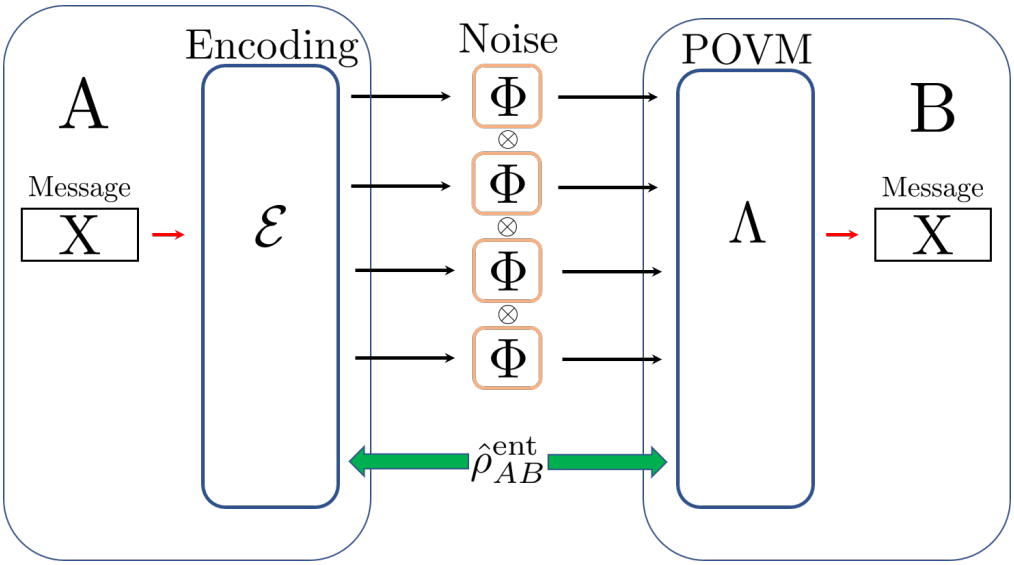

FIGURE 3.6: Depiction of an entanglement assisted communication setting involving a quantum channel Φ.

Maybe surprisingly though, in this case the formulas defining the entanglement assisted classical capacity $C_{\text{ea}}(\Phi)$ and the entanglement assisted quantum capacity $Q_{\text{ea}}(\Phi)$ of a quantum channel Φ do not require a regularized formula. This is because the entropic quantity involved in their definitions is the quantum mutual information $I(\hat{\rho}, \Phi)$ associated with an input state and a channel $\Phi_{A\to B}$ that writes:

$$I(\hat{\rho}, \Phi) = S(\hat{\rho}) + S(\Phi(\hat{\rho})) - S(\tilde{\Phi}(\hat{\rho})) \, . \tag{3.30}$$

The expressions for $C_{\text{ea}}(\Phi)$ and $Q_{\text{ea}}(\Phi)$ are then:

Entanglement assisted classical capacity

$$C_{\text{ea}}(\Phi) = \max_{\hat{\rho}_A \in \mathfrak{S}(\mathcal{H}_A)} I(\hat{\rho}_A, \Phi) \, . \tag{3.31}$$

The coding theorem bringing to Eq. (3.31) was provided by Bennett, Shor, Smolin and Thapliyal [BSST99, BSST02]. The single-letter formula is achieved thanks to the property of subadditivity that quantum mutual information displays [AC97], so we have $C_{\text{ea}}(\Phi^{\otimes n}) = nC_{\text{ea}}(\Phi)$. It's also evident by construction that $C_{\text{ea}}(\Phi) \geq C(\Phi)$.

Entanglement assisted quantum capacity

$$Q_{\text{ea}}(\Phi) = \max_{\hat{\rho}_A \in \mathfrak{S}(\mathcal{H}_A)} \frac{1}{2} I(\hat{\rho}_A, \Phi) \, . \tag{3.32}$$

As it can be immediately observed by inspection, the entanglement assisted quantum capacity $Q_{\text{ea}}(\Phi)$ of a quantum channel is just half of the classical counterpart. This can be intuitively explained as follows [BSST99]. Since the quantum capacity is a rate that relates to the maximum input space dimension that can be transmitted noiselessly, taking for instance the case of qubits, we already know from quantum teleportation that we can transfer perfectly any quantum state by sending 2 classical bits. But we also know from superdense coding that 2 bits can be transferred with only a single use of the channel, hence the factor 2. Being defined through the quantum mutual information, $Q_{\text{ea}}(\Phi)$ shares the additivity property of $C_{\text{ea}}(\Phi)$, so $Q_{\text{ea}}(\Phi^{\otimes n}) = nQ_{\text{ea}}(\Phi)$.

4

Bounding capacities in quantum networks

Preface

What follows is based on the published paper [CFG19]:

- S. Chessa, M. Fanizza, and V. Giovannetti, Quantum-capacity bounds in spin-network communication channels, *Phys. Rev. A* **100**, 032311 (2019).

This chapter is focused on communication properties of quantum spin networks. In the framework that we consider, spin networks are imagined as static quantum communication infrastructures, in the sense discussed in Chapter 2, Sec. 2.2 where we compared the static model to the flying qubit model. The communication will be modeled in a simplified fashion, assuming the communicating parties to be able to communicate by local operations on separated portions of the network. The signals will be propagated by the interaction with which the network is equipped. To estimate our bounds we'll exploit the so called Lieb-Robinson bound, a well established result in mathematical physics that allows us to give an upper bound to the correlations between two portions of a quantum spin network. Lieb-Robinson bounds are an important result with a number of relevant consequences and we gave a contribution also on that topic in [CG19], that we report as an appendix. We decided though to not include it in the main text of the thesis since it is not directly related to the issue of information capacities. The interested reader may check [CG19] (Appendix A) and the references therein for a deeper dive in the topic of Lieb-Robinson bounds.

4.1 Introduction

As we have seen in Chapter 2, Sec. 2.2, in the flying qubit model of quantum communication messages are conveyed from the sender (Alice) to the intended receiver (Bob) after being encoded into some degree of freedom which actually "moves" from the location of the first party to the location of the second party [Hol19, Wil17, Wat18]. This scenario is the most widely studied in the literature as it finds application in many realistic scenarios which, for instance, employ electro-magnetic pulses as quantum carriers. An intriguing alternative is provided by the spin-network communication (SNC) model, that belongs to the static models of quantum communication discussed in in Chapter 2, Sec. 2.2.2, where instead Alice and Bob are assumed to have access to different portions of an extended many-body quantum infrastructure. This infrastructure is formed by interacting particles which occupy fixed locations but which are mutually coupled via an assigned, fixed Hamiltonian that, as in a solid, allows the spread of local perturbations along the medium, see e.g. Ref. [Bos07] and references therein. While being intrinsically limited to short distance applications, SNC schemes have been suggested as an effective way to avoid interfacing issues in the engineering of connections between clusters of otherwise independent quantum processors [Bos03, CDEL04, CVDC03, BGB07, EPBH04, PHE04, HRP06, GB06]. The study of these models is also motivated by the need of better understanding how the many-body system reacts to the spreading of local perturbations. The main result in this context is the well known bound by Lieb and Robinson (LR) [LR72, NSY19] on the maximum group velocity for two-points correlation functions of the network, see also [NS06, Has04b, HK06, NOS06]. For sufficiently regular models, it basically identifies the presence of an effective light cone with exponentially decaying tails implying that information that leaks out to space-like separated regions is negligible, so that for large enough distances non-signaling is preserved. Several applications of the LR inequality in a quantum information theoretical treatment of SNC models have been presented in the literature. For instance in Ref. [EO06] the LR bound was used to set a limit on the entanglement that can develop across the boundary of a distinguished region for short times. In Ref. [Osb06] instead the bound was used to show that dynamics of 1D quantum spin systems can be approximated efficiently. In Ref. [BHV06] finally, making use of the Fannes inequality [Fan73], Bravyi *et al.* succeeded in linking the LR inequality to the Holevo information capacity χ [Hol98, SW97] attainable for a special example of SNC model where Alice tries to communicate classical messages to Bob by "overwriting" them into the initial state of the spin-network she controls. A generalization of this result was presented in Ref. [EW17] where the LR bound was employed to set the limits within which high-fidelity quantum state transfer and entanglement generation can be performed in general spin-network systems. The aim of the present Chapter is to go beyond these findings, by generalizing the inequality derived in Ref. [BHV06] to the whole plethora of quantum channel capacities [HG12] that one can associate to the underlying SNC model and to the arbitrary encoding strategies Alice may adopt to upload her messages into the network. For this purpose we shall make explicit use of the continuity argument of Refs. [LS09, Shi17] which allows one to connect the capacities values of two channels via their relative distance measured in terms of the diamond norm metric [Kit97, KSVV02]. While our derivation in many respects mimics the one presented

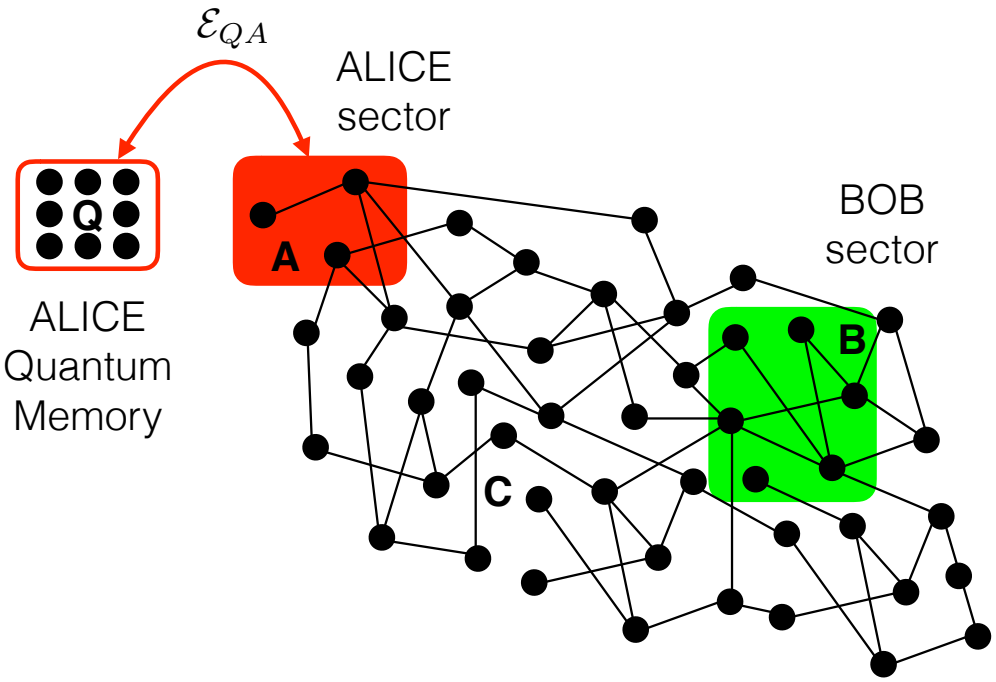

Figure 4.1: (Color online) Schematic representation of a spin-network model for quantum communication. The network $\mathcal{N}$ is divided into three components: the sector A (controlled by the sender of the message Alice), the sector B (controlled by the receiver Bob), and the sector C on which neither Alice nor Bob can operate. The element Q represents an external ancillary memory element Alice uses to store the information she wants to transmit. At time $t = 0$ Alice couples A with Q via an arbitrary encoding mapping $\mathcal{E}_{QA}$ which fully characterizes the adopted communication strategy; Bob, on his side, will try to pick up the message at some later time t from B.

by Bravyi *et al.*, we stress that in order to account for all possible encoding strategies, we have explicitly to deal with the dimension of the ancillary memory element Q Alice can use in the process. The presence of such element, which does not enter in the definition of the spin-network (and hence in the associated LR inequality), introduces a divergent contribution which, if not properly tamed, tends to spoil the connection between the LR bound and the diamond norm distance, compromising the possibility of using the results of Refs. [LS09, Shi17] to constrain the capacities values of the underlying SNC model (a problem which, due to the intrinsic sub-additivity of the Holevo information χ, needed not to be addressed in Ref. [BHV06]).

The Chapter is organized as follows: we start in Sec. 4.2 by introducing the SNC scheme and reviewing some basic facts about the LR bound. The main results of the Chapter are presented in Sec. 4.3. Here, in Sec. 4.3.1, first we exploited the LR inequality to put an upper limit on the induced trace-norm distance [Wat18] between the map associated with the SNC scheme and a (zero-capacity) replacement channel [Kin03, NC10].

From this, in Sec. 4.3.2 we hence derive an analogous bound for the diamond distance [Kit97, KSVV02] from which ultimately the bounds on the SNC communication capacities follow. The Chapter ends with the conclusions in Sec. 4.4. Technical material is presented in the Appendix.

4.2 The model

In the scenario we are interested in, two distant parties (Alice the sender and Bob the receiver) try to exchange (classical or quantum) messages by locally manipulating portions of a many-body quantum system $\mathcal{N}$ that, as schematically shown in Fig. 4.1, acts as the mediator of the information exchange [Bos03, Bos07, CDEL04, CVDC03, BGB07, EPBH04, PHE04, HRP06, BHV06]. An exhaustive characterization of $\mathcal{N}$ is provided by the spin network formalism [NS06] where the (fixed) locations of the quantum subsystems are specified by a graph $\mathbb{G} := (V, E)$ defined by a set of vertices V and by a set E of edges. The model is equipped with a metric $d(x, y)$ defined as the shortest path (least number of edges) connecting $x, y \in V$ ($d(x, y)$ being set equal to infinity in the absence of a connecting path), which induces a measure for the diameter $D(X)$ of a given subset $X \subset V$, and a distance $d(X, Y)$ between the subsets $X, Y \subset V$,

$$\begin{aligned} D(X) &:= \max_{x,y}\{d(x, y)|x, y \in X\} , \\ d(X, Y) &:= \min\{d(x, y)|x \in X, y \in Y\} . \end{aligned} \tag{4.1}$$

Indicating with $\mathcal{H}_x$ the Hilbert space associated with the spin that occupies the vertex x of the graph, the Hamiltonian of $\mathcal{N}$, which ultimately is responsible for the information propagation in the medium, can be expressed as

$$\hat{H} := \sum_{X \subset V} \hat{H}_X , \tag{4.2}$$

where the summation runs over the subsets X of V with $\hat{H}_X$ being a self-adjoint operator that is local on the Hilbert space $\mathcal{H}_X := \otimes_{x \in X} \mathcal{H}_x$, i.e. it acts non-trivially on the spins of X while being the identity everywhere else.

Assume then that Alice and Bob control respectively two non-overlapping sections A and B of the network $\mathcal{N}$, their distance being $d(A, B) > 0$. The model includes also a domain C of $\mathcal{N}$ that represents the spins which are neither under Bob's nor Alice's control. The two parties agree about a protocol according to which Alice signals to Bob by locally perturbing the input state of the chain $\hat{\tau}_{ABC}$ via a set of local operations acting on the spins belonging to her domain A. Such actions will hence propagate according to the natural Hamiltonian (4.2) of the network for some transferring time t after which Bob will try to recover them via some proper local operations on the domain B. The question we want to address is how much Bob will be able to discern about Alice's encoding action by performing arbitrary (local) operations on the output state (4.12). In the next section we shall approach this problem by generalizing the work of Ref. [BHV06] where, using the Lieb-Robinson (LR) inequality [LR72, NSY19] an upper limit was set for the Holevo capacity χ [HG12] attainable using a specific spin-network communication strategy (explicitly the model defined in Eq. (4.16) below). We remind that the LR is a

universal bound on the correlations that can be established between distant portions of the network due to the dynamics induced by the system Hamiltonian $\hat{H}$ under minimal assumptions about the structure of involved couplings. In particular, given any two operators $\hat{A}$ and $\hat{B}$ that are local on Alice's and Bob's subsets A and B respectively, the LR inequality imposes the constraint

$$\frac{\|[\hat{A}(t),\hat{B}]\|}{\|\hat{A}\|\|\hat{B}\|} \leq \epsilon_{AB}(t) , \tag{4.3}$$

where

$$\|\hat{\Theta}\| := \max_{|\psi\rangle} \|\hat{\Theta}|\psi\rangle\| , \tag{4.4}$$

represents the standard operator norm, and where given

$$\hat{U}(t) := \exp\left[-i\hat{H}t\right] , \tag{4.5}$$

the unitary operator associated with the network Hamiltonian (4.2) ($\hbar = 1$),

$$\hat{A}(t) := \hat{U}^{\dagger}(t)\hat{A}\hat{U}(t) , \tag{4.6}$$

is the evolved counterpart of $\hat{A}$ in the Heisenberg representation. According to the LR analysis, the quantity $\epsilon_{AB}(t)$ appearing on the r.h.s. of (4.3) exhibits an explicit dependence upon the coupling strengths but is independent of the actual state of the network $\hat{\tau}_{ABC}$. Most importantly it depends upon t via its absolute value $|t|$, and tends to zero when this parameter is small and/or $d(A,B)$ is large enough, pointing out that modifications on A sites require a certain time to affect the sector B when the two are disjoint. In particular, as shown in Ref. [CG19], for finite range Hamiltonians admitting $\bar{D}$ such that $\hat{H}_X = 0$ whenever $D(X) > \bar{D}$, we can express the LR quantity $\epsilon_{AB}(t)$ in the following compact form

$$\epsilon_{AB}(t) = 2|A||B| \left(\frac{2\, e\, \zeta\, \bar{D}\, |t|}{d(A,B)} \right)^{\frac{d(A,B)}{\bar{D}}} , \tag{4.7}$$

where $|X|$ is the total number of sites in the domain $X \subset V$, and where ζ is a finite, positive constant characterizing the graph topology and the intensity of the couplings (but not on the size of the graph). If instead the Hamiltonian is explicitly of long-range couplings but sufficiently well behaved so that there exist μ, s positive constants such that $\sup_{x\in V} \sum_{X\ni x} |X|\, \|\hat{H}_X\| e^{\mu_2 D(X)} \leq s$ (exponential decay), or $\sup_{x\in V} \sum_{X\ni x} |X|\, \|\hat{H}_X\| [1 + D(X)]^{\mu} \leq s$ (power-law decay), then Eq. (4.7) gets replaced by

$$\epsilon_{AB}(t) = C|A||B|(e^{v|t|} - 1)e^{-\mu d(A,B)} , \tag{4.8}$$

in the first case, and by

$$\epsilon_{AB}(t) = C|A||B| \frac{e^{v|t|} - 1}{(1 + d(A,B))^{\mu}} , \tag{4.9}$$

in the second case, v and C being positive constants that again depend upon the metric of the network and on the Hamiltonian, but do not scale with the size of the model [HK06, NS06].

4.2.1 SNC channels

Without loss of generality we can describe the perturbation induced by Alice on the network in an effort to communicate with Bob as a Linear, Completely Positive, Trace preserving (LCPT) [Cho75, Hol19, Wil17, NC10] encoding map $\mathcal{E}_{QA}$ which at time $t = 0$ locally couples the portion A of $\mathcal{N}$ with an external memory element Q that stores the information she wants Bob to receive, see Fig. 4.1. Specifically, indicating with $\hat{\tau}_{ABC}$ the initial state of the network we have

$$\hat{\rho}_Q \to \mathcal{E}_{QA}[\hat{\rho}_Q \otimes \hat{\tau}_{ABC}] := (\mathcal{E}_{QA} \otimes \mathcal{I}_{BC})[\hat{\rho}_Q \otimes \hat{\tau}_{ABC}] \,, \tag{4.10}$$

where $\mathcal{I}_{BC}$ represents the identity superoperator on the BC domains. Once introduced into the system, the perturbation (4.10) propagates freely for a transferring time t along the spin-network, i.e.

$$\mathcal{E}_{QA}[\hat{\rho}_Q \otimes \hat{\tau}_{ABC}] \longrightarrow \hat{U}(t)\mathcal{E}_{QA}[\hat{\rho}_Q \otimes \hat{\tau}_{ABC}]\hat{U}^\dagger(t) \,, \tag{4.11}$$

with $\hat{U}(t)$ being the unitary transformation (4.5) defining the dynamics of $\mathcal{N}$. Bob on his sites will have hence the possibility of perceiving it as a modification of the reduced density matrix of the portion of spin-network he controls, i.e.

$$\begin{aligned} \hat{\rho}_B(t) = \Phi[\hat{\rho}_Q] &:= \mathrm{Tr}_{QAC}\Big(\hat{U}(t)\mathcal{E}_{QA}[\hat{\rho}_Q \otimes \hat{\tau}_{ABC}]\hat{U}^\dagger(t)\Big) \\ &= \mathrm{Tr}_{AC}\Big(\hat{U}(t)\mathcal{E}_A[\hat{\tau}_{ABC}]\hat{U}^\dagger(t)\Big) \,, \end{aligned} \tag{4.12}$$

where in the second line we used the fact that $\hat{U}(t)$ does not operate on Q, to introduce the LCPT mapping locally acting on A

$$\hat{\tau}_{ABC} \to \mathcal{E}_A[\hat{\tau}_{ABC}] := \mathrm{Tr}_Q\Big(\mathcal{E}_{QA}[\hat{\rho}_Q \otimes \hat{\tau}_{ABC}]\Big) \,, \tag{4.13}$$

that depends on the selected message $\hat{\rho}_Q$ and encoding operation $\mathcal{E}_{QA}$.

Equation (4.12) defines the SNC channel Φ connecting Alice's quantum memory Q to Bob's location. By construction it is explicitly LCPT and besides the properties of the network (namely its Hamiltonian $\hat{H}$ and its input state $\hat{\tau}_{ABC}$) and the propagation time t, it explicitly depends upon Alice's choice of the encoding transformation $\mathcal{E}_{QA}$. A trivial option is represented for instance by the case where $\mathcal{E}_{QA}$ is the identity mapping $\mathcal{I}_{QA}$: under this assumption no information is transferred from Q either to the A or to the B portion of the network, leading (4.12) to coincide with the replacement map $\Phi^{(0)}_{RP}$ defined by the identity

$$\Phi^{(0)}_{RP}[\hat{\rho}_Q] := \hat{\rho}^{(0)}_B(t)\ \mathrm{Tr}[\hat{\rho}_Q] \,, \tag{4.14}$$

where

$$\hat{\rho}^{(0)}_B(t) := \mathrm{Tr}_{AC}[\hat{U}(t)\hat{\tau}_{ABC}\hat{U}^\dagger(t)] \,, \tag{4.15}$$

is the state Bob would have received if Alice decided not to perturb her spins at time $t = 0$. Identifying instead $\mathcal{E}_{QA}$ with a control gate activated by different choices of $\hat{\rho}_Q$,

we can force $\mathcal{E}_A$ to belong to a generic list $\{\mathcal{E}_A^{(\alpha)}\}_\alpha$ of possible operations, each associated with a classical symbol labeled by the index α. With this choice the scheme (4.12) induces the mapping

$$\alpha \longrightarrow \hat{\rho}_B^{(\alpha)}(t) := \mathrm{Tr}_{AC}\Big(\hat{U}(t)\mathcal{E}_A^{(\alpha)}[\hat{\tau}_{ABC}]\hat{U}^\dagger(t)\Big) , \tag{4.16}$$

that corresponds to the signaling strategy analysed in Ref. [BHV06] to allow the transferring of classical messages from A to B. On the contrary, by identifying Q with a memory element Q_A that is isomorphic with A and taking $\mathcal{E}_{QA}$ to be a unitary swap gate, Eq. (4.13) reduces to

$$\hat{\tau}_{ABC} \to \hat{\rho}_A \otimes \hat{\tau}_{BC} , \tag{4.17}$$

with $\hat{\rho}_A$ being the isomorphic copy of $\hat{\rho}_{Q_A}$ on A and $\hat{\tau}_{BC} := \mathrm{Tr}_A[\hat{\tau}_{ABC}]$ being the reduced state of the BC domains obtained by tracing away A from the input $\hat{\tau}_{ABC}$. Accordingly, under this construction the SNC channel (4.12) becomes

$$\Phi_{SW}[\hat{\rho}_{Q_A}] \;\; = \;\; \mathrm{Tr}_{AC}\Big(\hat{U}(t)[\hat{\rho}_A \otimes \hat{\tau}_{BC}]\hat{U}^\dagger(t)\Big) , \tag{4.18}$$

which represents the swap-in/swap-out spin-network communication strategy extensively studied in the literature (see e.g. Refs. [Bos03, Bos07, CDEL04, CVDC03, BGB07, EPBH04, PHE04, HRP06, GB06]) that, at least in principle, is capable to convey both classical and quantum messages.

Of course, Eqs. (4.14), (4.16), and (4.18) are just three examples out of a large (possibly infinite) set of possible maps (4.12) that we can realize for fixed $\hat{\tau}$, $\hat{H}$ and t, by using different choices of the mapping $\mathcal{E}_{QA}$. Determining what is the optimal option in terms of communication efficiency is a rather complex problem which arguably depends upon the property of the network, the value of transferring time t, the relative distance of the locations A and B, as well as upon the kind of messages (classical, private classical, quantum, etc.) one wishes to transfer. Our aim is to show that however, irrespectively of the freedom to select the encoding $\mathcal{E}_{QA}$, the LR inequality (4.3) poses a fundamental limitation on the resulting communication efficiency.

4.3 Distance of the received message from the non-signaling state

To determine the amount of information that can be effectively retrieved by Bob at the end of the transmission (4.12) associated with an arbitrary coding strategy $\mathcal{E}_{QA}$, we have to compute the distance between the SNC channel Φ and the replacement channel $\Phi_{RP}^{(0)}$ of Eq. (4.14) associated with the non-signaling protocol. Specifically in Sec. 4.3.1 we first analyze the induced trace-norm distance [Wat18] between Φ and $\Phi_{RP}^{(0)}$ showing that irrespectively of the choice of $\mathcal{E}_{QA}$ we get the inequality

$$\|\Phi - \Phi_{RP}^{(0)}\|_1 \leq M_A^2 \, \epsilon_{AB}(t) , \tag{4.19}$$

where M_A is the dimension of the Hilbert space associated with the spins of the domain A under Alice's control and where $\epsilon_{AB}(t)$ is the LR quantity appearing on the r.h.s. of

Eq. (4.3). Equation (4.19) is a clear indication that for small enough values of t and/or large enough values of $d(A,B)$, the spin-network channel performances are close to the non-signaling regime, irrespectively of the initial state $\hat{\tau}_{ABC}$ of the network and from the encoding procedure $\mathcal{E}_{QA}$ selected by Alice. In particular from Eq. (75) of Ref. [Shi17] it is possible to use Eq. (4.19) to bound the value of the Holevo information χ [Hol98, SW97], defined in Eq. 3.19 in Sec. 3.3.1, associated with Φ as

$$\chi(\Phi) \leq \frac{M_A^2\, \epsilon_{AB}(t)}{2} \log_2 M_B + g(\tfrac{M_A^2\, \epsilon_{AB}(t)}{2}) , \tag{4.20}$$

where we exploited the fact that $\chi(\Phi_{RP}^{(0)})$ is trivially null (no information being transferred via the replacement map) and where $g(x)$ is a function that tends to zero as $x \to 0$, defined by the identities

$$g(x) := (1+x) H_2(x/(1+x)) , \tag{4.21}$$

$$H_2(y) := -y \log_2 y - (1-y) \log_2 (1-y) . \tag{4.22}$$

Equation (4.20) generalizes an analogous result obtained in Ref. [BHV06] in the special case of the classical-to-quantum encoding strategy (4.16). Extending this to all possible encodings and to the full set of communication capacities [HG12, Hol19, Wil17] (i.e. the classical capacity $C(\Phi)$ [Hol98, SW97], the private capacity $C_{\rm p}(\Phi)$ [Dev05], the quantum capacity $Q(\Phi)$ [Dev05, Llo97, Sho02b], and the entanglement assisted capacity $C_{\rm ea}(\Phi)$ [BSST02, BSST99] of the map Φ), all defined in Sec. 3.3 requires however a little more effort. For this purpose in Sec. 4.3.2 we focus on the diamond distance [Kit97, KSVV02] between Φ and a slightly different version of the replacement channel $\Phi_{RP}^{(0)}$, namely the channel

$$\Phi_{DP}^{(1)}[\hat{\rho}_Q] := \hat{\rho}_B^{(1)}(t)\, \mathrm{Tr}[\hat{\rho}_Q] , \tag{4.23}$$

obtained by replacing in Eq. (4.14) the state $\hat{\rho}_B^{(0)}(t)$ of (4.15) with the density matrix

$$\hat{\rho}_B^{(1)}(t) := \mathrm{Tr}_{AC}[\hat{U}(t)(\hat{\tau}_A \otimes \hat{\tau}_{BC})\hat{U}^\dagger(t)] , \tag{4.24}$$

with $\hat{\tau}_A := \mathrm{Tr}_{BC}[\hat{\tau}_{ABC}]$ and $\hat{\tau}_{BC} := \mathrm{Tr}_A[\hat{\tau}_{ABC}]$ the reduced density matrices of the sectors (A and BC respectively) of the input state of the network $\hat{\tau}_{ABC}$. According to our analysis we shall see that the following inequality holds

$$\|\Phi - \Phi_{DP}^{(1)}\|_\diamond \leq M\, \epsilon_{AB}(t) , \tag{4.25}$$

where again $\epsilon_{AB}(t)$ is the LR quantity and where M is upper bounded by $2M_A^4$, specifically

$$M := 2 \min\{M_A^4, M_A^3 M_B M_C\} . \tag{4.26}$$

Notice that as for Eq. (4.19), the r.h.s. of this inequality involves only quantities that ultimately just depend upon properties of the spin-network: specifically the distance of the sectors A and B, the number of spins they contain, the transferring time t, the

dimension of the Hilbert space of A. From the results of Leung and Smith [LS09] and the subsequent improvement by Shirokov [Shi17] we can now turn Eq. (4.25) into a bound for the communication capacities [HG12, Hol19, Wil17] of the map Φ in terms of the corresponding ones associated with the replacement map $\Phi_{DP}^{(1)}$. Explicitly, observing that by definition we have

$$\begin{aligned} \chi(\Phi_{DP}^{(1)}) &= C(\Phi_{DP}^{(1)}) = 0 \,, \\ C_{\rm p}(\Phi_{DP}^{(1)}) &= Q(\Phi_{DP}^{(1)}) = 0 \,, \\ C_{\rm ea}(\Phi_{DP}^{(1)}) &= 0 \,, \end{aligned} \tag{4.27}$$

equations (81) and (82) of Ref. [Shi17] lead us to

$$Q(\Phi), C(\Phi) \leq M\, \epsilon_{AB}(t) \log_2 M_B + g(\tfrac{M\, \epsilon_{AB}(t)}{2}) \,, \tag{4.28}$$

while Eq. (76) of Ref. [Shi17] to

$$C_{\rm ea}(\Phi) \leq M\, \epsilon_{AB}(t) \log_2 M' + g(\tfrac{M\, \epsilon_{AB}(t)}{2}) \,, \tag{4.29}$$

where M' is the minimum between the dimensions of A and B, i.e.

$$M' := \min\{M_A, M_B\} \,. \tag{4.30}$$

As a matter of fact the last of the inequalities presented above happens to be the strongest of all: indeed due to the natural ordering among the capacities [BDSS06]

$$C_{\rm p}(\Phi) \leq C(\Phi) \leq C_{\rm ea}(\Phi) \,, \qquad Q(\Phi) \leq C_{\rm ea}(\Phi)/2 \,, \tag{4.31}$$

our final bounds read

$$C_{\rm p}(\Phi), C(\Phi), C_{\rm ea}(\Phi) \leq M\, \epsilon_{AB}(t) \log_2 M' + g(\tfrac{M\, \epsilon_{AB}(t)}{2}) \,, \tag{4.32}$$

$$Q(\Phi) \leq \frac{M\, \epsilon_{AB}(t)}{2} \log_2 M' + \frac{1}{2} g(\tfrac{M\, \epsilon_{AB}(t)}{2}) \,. \tag{4.33}$$

4.3.1 Induced trace-norm distance

The induced trace distance between Φ of Eq. (4.12) and the replacement channel $\Phi_{RP}^{(0)}$ of Eq. (4.14) related to the non-signaling protocol is defined as

$$\|\Phi - \Phi_{RP}^{(0)}\|_1 := 2 \max_{\hat{\rho}_Q} D(\Phi(\hat{\rho}_Q), \Phi_{RP}^{(0)}(\hat{\rho}_Q)) \,, \tag{4.34}$$

where the maximum is taken over the whole set of possible input states $\hat{\rho}_Q$ of the memory Q, and $D(\Phi(\hat{\rho}_Q), \Phi_{RP}^{(0)}(\hat{\rho}_Q))$ is the trace-distance [NC10] between the corresponding output configurations $\hat{\rho}_B(t)$ and $\hat{\rho}_B^{(0)}(t)$ of Φ and $\Phi_{RP}^{(0)}$. According to the Helstrom theorem [Hol19, Wil17], $D(\Phi(\hat{\rho}_Q), \Phi_{RP}^{(0)}(\hat{\rho}_Q))$ gauges the minimum error probability that one can get trying to discriminate $\Phi(\hat{\rho}_Q)$ from $\Phi_{RP}^{(0)}(\hat{\rho}_Q))$, in particular it writes

$$\begin{aligned} D(\Phi(\hat{\rho}_Q), \Phi_{RP}^{(0)}(\hat{\rho}_Q)) &= D(\hat{\rho}_B(t), \hat{\rho}_B^{(0)}(t)) \\ &:= \frac{1}{2} \|\hat{\rho}_B(t) - \hat{\rho}_B^{(0)}(t)\|_1 \,, \end{aligned} \tag{4.35}$$

with $\|\hat{X}\|_1 := \mathrm{Tr}[\sqrt{\hat{X}^\dagger \hat{X}}]$ being the trace-norm of the operator $\hat{X}$, not to be confused with the operator norm introduced in Eq. (4.4). A useful way to express (4.35) is

$$D(\hat{\rho}_B(t), \hat{\rho}_B^{(0)}(t)) = \max_{\hat{\Theta}_B} \left| \mathrm{Tr}_B \left[\hat{\Theta}_B (\hat{\rho}_B(t) - \hat{\rho}_B^{(0)}(t)) \right] \right| , \tag{4.36}$$

where the maximum can be taken either over the set of positive operators $\hat{\mathbb{1}}_B \geq \hat{\Theta}_B \geq 0$, or, equivalently, on the set of operators $\hat{\Theta}_B = \hat{V}_B/2$ with $\hat{V}_B$ being a unitary operator acting locally on the spins of the domain B (in what follows we'll find more convenient the latter option). Introducing the operator $\hat{\Theta}_B(t) := \hat{U}^\dagger(t)\hat{\Theta}_B\hat{U}(t)$ and using Eqs. (4.11), (4.12), and (4.15) we can then write

$$\begin{aligned} D(\hat{\rho}_B(t), \hat{\rho}_B^{(0)}(t)) &= \max_{\hat{\Theta}_B} \left| \mathrm{Tr} \left[\hat{\Theta}_B(t) \, (\mathcal{E}_A[\hat{\tau}_{ABC}] - \hat{\tau}_{ABC}) \right] \right| \\ &= \max_{\hat{\Theta}_B} \left| \sum_{k=1}^{K} \mathrm{Tr} \left[\hat{M}_k^\dagger \hat{\Theta}_B(t) \hat{M}_k \hat{\tau}_{ABC} - \hat{\Theta}_B(t) \hat{M}_k^\dagger \hat{M}_k \hat{\tau}_{ABC} \right] \right| \\ &= \max_{\hat{\Theta}_B} \left| \sum_{k=1}^{K} \mathrm{Tr} \left[[\hat{M}_k^\dagger, \hat{\Theta}_B(t)] \; \hat{M}_k \; \hat{\tau}_{ABC} \right] \right| , \end{aligned}$$

where $\{\hat{M}_k; k = 1, \cdots, K\}$ are a Kraus set of local operators on A which represents the action of the LCPT map $\mathcal{E}_A$, i.e.

$$\mathcal{E}_A[\cdots] = \sum_{k=1}^{K} \hat{M}_k [\cdots] \hat{M}_k^\dagger, \qquad \sum_{k=1}^{K} \hat{M}_k^\dagger \hat{M}_k = \hat{\mathbb{1}} . \tag{4.37}$$

Now bounding the expectation value of $[\hat{M}_k^\dagger, \hat{\Theta}_B(t)]\hat{M}_k$ over $\hat{\tau}_{ABC}$ with the associated operator norm (4.4), exploiting the triangular inequality we obtain

$$D(\hat{\rho}_B(t), \hat{\rho}_B^{(0)}(t)) \leq \max_{\hat{\Theta}_B} \sum_{k}^{K} \|[\hat{M}_k^\dagger, \hat{\Theta}_B(t)]\| \|\hat{M}_k\| , \tag{4.38}$$

Observe that by unitary equivalence of the norm we have $\|[\hat{M}_k^\dagger, \hat{\Theta}_B(t)]\| = \|[\hat{M}_k^\dagger(-t), \hat{\Theta}_B]\|$ where now $\hat{M}_k^\dagger(t) = \hat{U}^\dagger(t)\hat{M}_k^\dagger\hat{U}(t)$ is the time evolved version of the local operator $\hat{M}_k^\dagger$ of A under the action of the network Hamiltonian. Accordingly we can use (4.3) and (4.7) to write

$$\|[\hat{M}_k^\dagger, \hat{\Theta}_B(t)]\| \leq \|\hat{M}_k^\dagger\| \|\hat{\Theta}_B\| \epsilon_{AB}(t) \leq \epsilon_{AB}(t)/2 , \tag{4.39}$$

where we used the fact that

$$\|\hat{M}_k^\dagger\| = \|\hat{M}_k\| = \sqrt{\|\hat{M}_k^\dagger \hat{M}_k\|} \leq 1 , \tag{4.40}$$

due to the normalization condition of the Kraus elements, and $\|\hat{\Theta}_B\| = \|\hat{V}_B/2\| \leq 1/2$. Replacing this into the bound on $D(\hat{\rho}_B(t), \hat{\rho}_B^{(0)}(t))$ we hence can write

$$D(\hat{\rho}_B(t), \hat{\rho}_B^{(0)}(t)) \leq (K/2) \;\; \epsilon_{AB}(t) , \tag{4.41}$$

with the r.h.s. that depends upon the specific choice of the encoding channel $\mathcal{E}_A$ only via the total number K of Kraus elements that enter the decomposition (4.37). In case we restrict Alice to adopt only unitary encodings, this yields $K = 1$. Alternatively, if we allow for arbitrary LCPT operations $\mathcal{E}_A$ on A, i.e. arbitrary LCPT operations $\mathcal{E}_{QA}$ on Q and A, an universal bound can be established by reminding that, irrespectively of the choice of $\mathcal{E}_A$ it is always possible to have a Kraus set with at most $K = M_A^2$ [Cho75]. This leads to

$$D(\hat{\rho}_B(t), \hat{\rho}_B^{(0)}(t)) \leq (M_A^2/2)\, \epsilon_{AB}(t) \,, \tag{4.42}$$

and hence to Eq. (4.19) via Eq. (4.34) exploiting the fact that the r.h.s. of Eq. (4.42) holds true for all possible choices of the input $\hat{\rho}_Q$.

4.3.2 Diamond norm distance

The diamond-distance [Kit97, KSVV02] between two channels Φ and Φ' connecting Q to B is defined as

$$\|\Phi - \Phi'\|_\diamond = \max_{|\psi\rangle_{QQ'}} \|(\Phi \otimes \mathcal{I} - \Phi' \otimes \mathcal{I})(|\psi\rangle_{QQ'}\langle\psi|)\|_1 \,, \tag{4.43}$$

where the maximization now is performed for extensions $\Phi \otimes \mathcal{I}$ and $\Phi' \otimes \mathcal{I}$ of the original channels involving purifications $|\psi\rangle_{QQ'}$ of the possible inputs of Q constructed on an ancillary system Q' that is isomorphic to Q. A naive way to bound this quantity would be given by using the natural ordering with the induced trace-norm distance (see Appendix 4.5), according to which one has

$$\|\Phi - \Phi'\|_1 \leq \|\Phi - \Phi'\|_\diamond \leq 2M_Q \|\Phi - \Phi'\|_1 \,, \tag{4.44}$$

with M_Q being the dimension of Alice's memory Q. Applying this to the maps Φ, associated with a generic encoding $\mathcal{E}_{QA}$, and to the replacement channel $\Phi_{RP}^{(0)}$ of Eq. (4.14) yields

$$\|\Phi - \Phi_{RP}^{(0)}\|_\diamond \leq 2M_Q \|\Phi - \Phi_{RP}^{(0)}\|_1 \leq 2M_Q M_A^2 \epsilon_{AB}(t) \,, \tag{4.45}$$

where in writing the last term we invoked the bound (4.19). In many cases of physical interest where M_Q is directly linked to the dimensionality of A, Eq. (4.45) is sufficiently strong for our purposes. For instance this happens for the swap-in/swap-out coding map Φ_{SW} of Eq. (4.18), where by construction the memory element is isomorphic to A, i.e. $M_{Q_A} = M_A$. Accordingly, in this case Eq. (4.45) leads to

$$\|\Phi_{SW} - \Phi_{RP}^{(0)}\|_\diamond \leq 2M_A^3 \epsilon_{AB}(t) \,, \tag{4.46}$$

which can be used to replace (4.25) in our study of the channel capacities reported at the beginning of Sec. 4.3. For a generic choice of $\mathcal{E}_{QA}$ however, the presence of M_Q on the r.h.s. of Eq. (4.45) poses a severe limitation to this inequality as the dimension of Q is not a property of the spin-network model and can in principle assume unbounded values. To deal with this problem we now consider the diamond norm

$$\|\Phi - \Phi_{RP}^{(1)}\|_\diamond = \max_{|\psi\rangle_{QQ'}} \|(\Phi \otimes \mathcal{I} - \Phi_{RP}^{(1)} \otimes \mathcal{I})(|\psi\rangle_{QQ'}\langle\psi|)\|_1 \,, \tag{4.47}$$

between the map Φ associated with the encoding operation $\mathcal{E}_{QA}$ and the replacement map $\Phi^{(1)}_{DP}$ defined in Eq. (4.23). Notice that the actions of Φ and $\Phi^{(1)}_{DP}$ can be expressed as a concatenation of two processes, i.e.

$$\Phi[\cdots] = \Psi \circ \mathcal{E}[\cdots] , \tag{4.48}$$

$$\Phi^{(1)}_{DP}[\cdots] = \Psi^{(1)}_{DP} \circ \mathcal{E}[\cdots] , \tag{4.49}$$

where

$$\mathcal{E}[\cdots] := \mathrm{Tr}_Q[\mathcal{E}_{QA}[\cdots \otimes \hat{\tau}_{ABC}]] , \tag{4.50}$$

is a LCPT channel from Q to ABC and where

$$\Psi[\cdots] := \mathrm{Tr}_{AC}\left[\hat{U}(t)[\cdots]\hat{U}^\dagger(t)\right] , \tag{4.51}$$

$$\Psi^{(1)}_{DP}[\cdots] := \mathrm{Tr}_{AC}\left[\hat{U}(t)\left(\hat{\tau}_A \otimes \mathrm{Tr}_A[\cdots]\right)\hat{U}^\dagger(t)\right] , \tag{4.52}$$

are instead LCPT transformations operating from ABC to B which do not depend upon the special choice of $\mathcal{E}_{QA}$.

Consider first the case where the input state $\hat{\tau}_{ABC}$ of the network $\mathcal{N}$ is a pure vector $|\tau\rangle_{ABC}$. For a generic choice of the pure states $|\psi\rangle_{QQ'}$ of QQ' entering the maximization (4.47), we have that globally the $QQ'ABC$ system is described by the product vector $|\psi,\tau\rangle_{QQ'ABC} := |\psi\rangle_{QQ'}|\tau\rangle_{ABC}$, which, after a Schmidt decomposition of $|\psi\rangle_{QQ'}$ and $|\tau\rangle_{ABC}$ along the partitions Q, Q' and A, BC respectively, can be written as

$$\begin{aligned} |\psi,\tau\rangle_{QQ'ABC} &= \sum_{i=1}^{r}\sum_{j=1}^{s}\sqrt{\alpha_i\beta_j}\,|\psi_i,\psi_i,\tau_j,\tau_j\rangle_{Q'QABC} , \\ |\psi_i,\psi_i,\tau_j,\tau_j\rangle_{Q'QABC} &:= |\psi_i\rangle_{Q'}|\psi_i\rangle_{Q}|\tau_j\rangle_{A}|\tau_j\rangle_{BC} , \end{aligned} \tag{4.53}$$

with $r \leq M_Q$ and $s \leq \min\{M_A, M_B M_C\}$ with $|\psi_i\rangle_{Q/Q'}$ and $|\tau_j\rangle_{A/BC}$ forming an orthogonal set of pure states of their respective systems. Completing hence $|\psi_i\rangle_Q$ to a basis of Q, we then define the vectors

$$\left|\tilde{\lambda}_{\ell,q}\right\rangle_{Q'ABC} := \sum_{i=1}^{r}\sum_{j=1}^{s}\sqrt{\alpha_i\beta_j}\,|\psi_i\rangle_{Q'}|\chi_{\ell,q,i,j}\rangle_A|\tau_j\rangle_{BC} , \tag{4.54}$$

where

$$|\chi_{\ell,q,i,j}\rangle_A := {}_Q\langle\psi_q|\hat{N}_\ell|\psi_i,\tau_j\rangle_{QA} , \tag{4.55}$$

and where $\hat{N}_\ell$ are the Kraus operators associated with the channel $\mathcal{E}_{QA}$

$$\mathcal{E}_{QA}[\cdots] = \sum_{\ell=1}^{L}\hat{N}_\ell[\cdots]\hat{N}_\ell^\dagger, \qquad \sum_{\ell=1}^{L}\hat{N}_\ell^\dagger\hat{N}_\ell = \hat{\mathbb{1}} , \tag{4.56}$$

with L which can be always chosen to be smaller than $M_Q^2 M_A^2$. Upon normalization Eq. (4.54) gives the pure states

$$|\lambda_{\ell,q}\rangle_{Q'ABC} := |\tilde{\lambda}_{\ell,q}\rangle_{Q'ABC}/g_{\ell,q} \,, \tag{4.57}$$

the norms $g_{\ell,q} := \||\tilde{\lambda}_{\ell,q}\rangle_{Q'ABC}\|$ satisfying the constraint

$$\sum_{\ell=1}^{L}\sum_{q=1}^{M_Q} g_{\ell,q}^2 = 1. \tag{4.58}$$

Notice that since terms (4.55) are elements of the Hilbert space of $\mathcal{H}_A$, it follows that for each given q and ℓ, when varying indexes i, j, vectors $|\chi_{\ell,q,i,j}\rangle_A |\tau_j\rangle_{BC}$ span a space of dimension not larger than

$$\begin{aligned} M_* &:= M_A \times \min\{M_A, M_B M_C\} \\ &= \min\{M_A^2, M_A M_B M_C\} \,. \end{aligned} \tag{4.59}$$

Accordingly this number also bounds the maximum number of non-zero terms entering the Schmidt decomposition of $|\lambda_{\ell,q}\rangle_{Q'ABC}$ along the partition Q', ABC, i.e.

$$|\lambda_{\ell,q}\rangle = \sum_{m=1}^{M_*} \sqrt{\gamma_m} |m\rangle_{Q'} |m\rangle_{ABC} \,, \tag{4.60}$$

for a proper choice of orthogonal sets of vectors $|m\rangle_{Q'}$ and $|m\rangle_{ABC}$. Exploiting the above identities the state of $Q'BC$ after the encoding stage through the mapping Eq. (4.50) can be casted in the following form

$$\mathcal{E} \otimes \mathcal{I}\Big[\, |\psi,\tau\rangle \langle\psi,\tau| \,\Big] = \sum_{\ell=1}^{L}\sum_{q=1}^{M_Q} g_{\ell,q}^2 \, |\lambda_{\ell,q}\rangle \langle\lambda_{\ell,q}| \,, \tag{4.61}$$

where for ease of notation we set $|\psi,\tau\rangle := |\psi,\tau\rangle_{QQ'ABC}$ and $|\lambda_{\ell,q}\rangle := |\lambda_{\ell,q}\rangle_{Q'ABC}$. From (4.48) and (4.49) we hence get

$$\begin{aligned} &\|(\Phi \otimes \mathcal{I} - \Phi_{DP}^{(1)} \otimes \mathcal{I})[|\psi\rangle_{QQ'} \langle\psi|]\|_1 \\ &\quad = \|\sum_{\ell=1}^{L}\sum_{q=1}^{M_Q} g_{\ell,q}^2 (\Psi \otimes \mathcal{I} - \Psi_{DP}^{(1)} \otimes \mathcal{I})[|\lambda_{\ell,q}\rangle \langle\lambda_{\ell,q}|]\|_1 \\ &\quad \leq \sum_{\ell=1}^{L}\sum_{q=1}^{M_Q} g_{\ell,q}^2 \|(\Psi \otimes \mathcal{I} - \Psi_{DP}^{(1)} \otimes \mathcal{I})[|\lambda_{\ell,q}\rangle \langle\lambda_{\ell,q}|]\|_1, \end{aligned} \tag{4.62}$$

the last inequality deriving from Eq. (4.58) by convexity of the trace-norm. Remember now that each one of the vectors $|\lambda_{\ell,q}\rangle$ has Schmidt rank smaller than M_* as indicated in Eq. (4.60). Therefore, being the following steps identical to those in Appendix 4.5 we

get

$$\|(\Psi\otimes\mathcal{I}-\Psi^{(1)}_{DP}\otimes\mathcal{I})[|\lambda_{\ell,q}\rangle\langle\lambda_{\ell,q}|]\|_1 \tag{4.63}$$
$$\leq \sum_{m,m'=1}^{M_*}\sqrt{\gamma_m\gamma_{m'}}\Big\|(\Psi-\Psi^{(1)}_{DP})[|m\rangle\langle m'|]\otimes|m\rangle\langle m'|\Big\|_1$$
$$= \sum_{m,m'=1}^{M_*}\sqrt{\gamma_m\gamma_{m'}}\|(\Psi-\Psi^{(1)}_{DP})[|m\rangle\langle m'|]\|_1$$
$$\leq 2M_*\|\Psi-\Psi^{(1)}_{DP}\|_1\ , \tag{4.64}$$

with $\|\Psi-\Psi^{(1)}_{DP}\|_1$ being the induced trace-distance between Ψ and $\Psi^{(1)}_{DP}$, i.e. the quantity

$$\|\Psi-\Psi^{(1)}_{DP}\|_1 := \max_{\hat{\tau}'_{ABC}}\|(\Psi-\Psi^{(1)}_{DP})[\hat{\tau}'_{ABC}]\|_1\ . \tag{4.65}$$

A crucial observation now is that, indicating with Q_A Alice's memory which is isometric to A, for all $\hat{\tau}'_{ABC}$ we can write

$$\begin{aligned}\Psi[\hat{\tau}'_{ABC}] &= \mathrm{Tr}_{AC}[\hat{U}(t)\hat{\tau}'_{ABC}\hat{U}^\dagger(t)] = \Phi'_{DP}[\hat{\tau}_{Q_A}]\ ,\\ \Psi^{(1)}_{DP}[\hat{\tau}'_{ABC}] &= \Phi'_{SW}[\hat{\tau}_{Q_A}]\ ,\end{aligned} \tag{4.66}$$

where $\hat{\tau}_{Q_A}$ represents the copy of $\hat{\tau}_A$ on Q_A, while Φ'_{DP} and Φ'_{SW} are respectively the non-signaling and the swap-in/swap-out channels associated with the input state $\hat{\tau}'_{ABC}$ of the network. Hence invoking (4.19) we can write

$$\begin{aligned}\|(\Psi-\Psi^{(1)}_{DP})[\hat{\tau}'_{ABC}]\|_1 &= \|(\Phi'_{DP}-\Phi')[\hat{\tau}_{Q_A}]\|_1\\ &\leq \|\Phi'_{DP}-\Phi'\|_1 \leq M_A^2\ \epsilon_{AB}(t)\ ,\end{aligned} \tag{4.67}$$

which, by reminding that $\epsilon_{AB}(t)$ does not depend upon the initial state of the spin-network, gives

$$\|\Psi-\Psi^{(1)}_{DP}\|_1 \leq M_A^2\ \epsilon_{AB}(t)\ . \tag{4.68}$$

Accordingly from Eq. (4.65) and (4.62) we have

$$\|(\Phi\otimes\mathcal{I}-\Phi^{(1)}_{DP}\otimes\mathcal{I})[|\psi\rangle_{QQ'}\langle\psi|]\|_1 \leq 2M_*M_A^2\ \epsilon_{AB}(t)\ , \tag{4.69}$$

for all $|\psi\rangle_{QQ'}$, which replaced into Eq. (4.47) leads to

$$\|\Phi-\Phi^{(1)}_{DP}\|_\diamond \leq 2M_*M_A^2\ \epsilon_{AB}(t)\ , \tag{4.70}$$

hence proving Eq. (4.25).

The above argument can be also used to deal with the case where the initial state of the network $\hat{\tau}_{ABC}$ is not pure. Indeed, by writing it as a convex sum over a set of pure states

$$\hat{\tau}_{ABC} = \sum_i p_i\,|\tau_i\rangle_{ABC}\langle\tau_i|\ , \tag{4.71}$$

equation (4.61) gets replaced by

$$\mathcal{E}\otimes\mathcal{I}\Big[\left|\psi\right\rangle\left\langle\psi\right|\otimes\hat{\tau}_{ABC}\Big]=\sum_{i}\sum_{\ell=1}^{L}\sum_{q=1}^{M_Q}p_i\left(g_{\ell,q}^{(i)}\right)^2\left|\lambda_{\ell,q}^{(i)}\right\rangle\left\langle\lambda_{\ell,q}^{(i)}\right|\ , \tag{4.72}$$

with $g_{\ell,q}^{(i)}$ and $\left|\lambda_{\ell,q}^{(i)}\right\rangle$ being associated with the i-th pure vector $\left|\tau_i\right\rangle_{ABC}$ entering Eq. (4.71) via the construction detailed in Eqs. (4.53-4.57). Consequently we can still invoke convexity to arrive at

$$\begin{aligned}&\|(\Phi\otimes\mathcal{I}-\Phi_{DP}^{(1)}\otimes\mathcal{I})[\left|\psi\right\rangle_{QQ'}\left\langle\psi\right|]\|_1 \\ &\leq\sum_{i}\sum_{\ell=1}^{L}\sum_{q=1}^{M_Q}p_i\left(g_{\ell,q}^{(i)}\right)^2\|(\Psi\otimes\mathcal{I}-\Psi_{DP}^{(1)}\otimes\mathcal{I})[\left|\lambda_{\ell,q}^{(i)}\right\rangle\left\langle\lambda_{\ell,q}^{(i)}\right|]\|_1,\end{aligned} \tag{4.73}$$

that formally replaces (4.62). From here we can exploit the same steps reported in Eqs. (4.63-4.70).

4.4 Conclusions

We propose a study of a broad set of information capacities associated with spin-networks employed as means of communication. In our analysis we considered as a quantum channel Φ a generic spin-network in a generic initial state equipped with an encoding represented by a local LCTP map, which results to be more general with respect to specific solutions adopted previously in the literature. Here we made use of the tools offered by the diamond norm and we exploited established results such as the Lieb-Robinson bound [LR72], which describes how correlations spread in spin systems, and Fannes inequality [Fan73], which states continuity properties of the Von Neumann entropy. We were able in such a way to upper bound the whole set of quantum capacities of the map Φ. Possible extensions of our work should include the presence of memory effects [CGLM14] in the information transferring which may arise when allowing Alice to perform sequences of encoding operations during the time it takes for one of them to reach Bob's location.

4.5 Appendix: Bounds on the diamond norm

The lower bound in Eq. (4.44) is a direct consequence of the definition of the diamond norm [Kit97, KSVV02, Wat18]. To prove the upper bound of (4.44) let us observe that introducing the Schmidt decomposition of the state $\left|\psi\right\rangle$ of Q and Q', $\left|\psi\right\rangle:=\sum_{j=1}^{M_Q}\lambda_j\left|j\right\rangle\otimes$

$|j\rangle$, we can write

$$\begin{aligned}
&2D((\Phi\otimes\mathcal{I})(|\psi\rangle\langle\psi|),(\Phi_{RP}^{(0)}\otimes\mathcal{I})(|\psi\rangle\langle\psi|))\\
&=\|\sum_{j,j'=1}^{M_A}\lambda_j\lambda_{j'}(\Phi-\Phi_{RP}^{(0)})[|j\rangle\langle j'|]\otimes|j\rangle\langle j'|\|_1\\
&\leq\sum_{j,j'=1}^{M_A}\lambda_j\lambda_{j'}\|(\Phi-\Phi_{RP}^{(0)})[|j\rangle\langle j'|]\otimes|j\rangle\langle j'|\|_1\\
&\leq\sum_{j,j'=1}^{M_A}\lambda_j\lambda_{j'}\|(\Phi-\Phi_{RP}^{(0)})[|j\rangle\langle j'|]\|_1\\
&\leq 2\|\Phi-\Phi_{RP}^{(0)}\|_1\Big(\sum_{j=1}^{M_A}\lambda_j\Big)^2\leq 2M_A\|\Phi-\Phi_{RP}^{(0)}\|_1\ ,
\end{aligned}\tag{4.74}$$

where first we used the convexity of the trace-distance, then the fact that for all $|j\rangle$, $|j'\rangle$ we have

$$\|(\Phi-\Phi_{RP}^{(0)})[|j\rangle\langle j'|]\|_1\leq 2\|\Phi-\Phi_{RP}^{(0)}\|_1\ ,\tag{4.75}$$

and finally the Chauchy-Schwarz inequality and the normalization condition for the Schmidt coefficients. Replacing hence (4.74) into (4.43), Eq. (4.44) finally follows.

5

Multi-level amplitude damping channels, a capacity analysis

Preface

What follows is based on the published paper [CG21b]:

- S. Chessa, V. Giovannetti, Quantum capacity analysis of multi-level amplitude damping channels, *Comm. Phys.* **4**, 22 (2021).

In this chapter we'll introduce Multi-level amplitude damping (MAD) channels. Concerning qubits, the analysis of noise models was carried out relatively quickly at the early stages of Quantum Information. This is no surprise, firstly since qubits are simpler and more accessible with respect to systems with more degrees of freedom, secondly because from a practical point of view they represented the only realistic experimental testbed for actual physical implementations. Nowadays though the thought of controlling qutrits or ququarts (and other dimensionalities) it's not anymore unrealistic. With our work we filled then a gap in the characterization of noise models in non-qubit systems with an immediate and intuitive generalization of the qubit amplitude damping channel. This kind of noise model may be more suited for the flying qubit (qudit in this case) scenario described in Chapter 2, Sec. 2.2 but as was shown in [GF05] the amplitude damping channel can emerge also in spin-chains, so it can model phenomena also in the static model of quantum communication infrastructures.

5.1 Introduction

In this Chapter we will focus on the specific and well known model for quantum noise given by the amplitude damping channel (ADC). While the ADC has been thoroughly studied and characterized, in terms of capacities in various settings, for the qubit framework [GF05, DBFM13, JAT15, DBFM15], a general treatise for qudit (d-dimensional) systems is still missing and likely not possible to attain. Because of these reasons ADC for $d > 2$ has to be approached case by case, and the literature regarding capacities of fixed finite dimensions ADC is still remarkably short [DBFM15, Ouy14, MS19]. Our interest in the topic is due to the fact that higher dimensional systems have attracted the attention of a growing number of researchers in recent years, since they have been shown to provide potential advantages both in terms of computation (see e.g. [MS00, LBA+09, RRG07, ITV12, GSÇ+15, KNX+20]) and communication or error correction (see e.g. [CDLBO19, LYGG08, GBDG+14, MZL+17]) together with the fact that more experimental implementations have been progressively made available (see e.g. [LNG+11, NJDH+13, MMP+15, BEW+17, KRR+17, MPGB+18, GPE+19, SBG+20]). Among non-qubit systems, three-dimensional systems (qutrit) have received particular consideration because of their relative accessibility both theoretically and experimentally (see e.g. [BM02, KGRS03, KOC+03, BČF+06, LWL+08, BRS17, SZS+18, LZE+19, BKL+19, LYF13]). In addition to that, new results on the quantum capacity of finite dimensional channels can also be applied to higher dimensional maps via the *Partially Coherent Direct Sum* (PCDS) channels approach [CG21a], placing in a wider context the efforts dedicated to the analysis of non-qubit channels. Considering this, we will start a first systematic analysis of the ADC on the qutrit space: while we will not approach the issue of the classical capacity of the channel, we will focus on the quantum capacity, private classical capacity and entanglement assisted capacities, trying to understand in which conditions these quantities can be known.

The Chapter is structured as follows. In Sec. 5.2 we introduce the model and notations we used for the qutrit MAD. In Sec. 5.3 we proceed to the study of the quantum capacity and private classical capacity of the qutrit MAD in various configurations. In Sec. 5.4 we repeat the same analysis for the entanglement assisted quantum and classical capacities.

5.2 Settings

The transformations we focus on in the present work are special instances of the multi-level versions of the qubit ADC [GF05], hereafter indicated as MAD channels in brief, which effectively describe the decaying of energy levels of a d-dimensional quantum system A. In its most general form, given $\{|i\rangle\}_{i=0,\cdots,d-1}$ an orthonormal basis of the Hilbert space $\mathcal{H}_{\mathrm{A}}$ associated with A (hereafter dubbed the computational basis of the problem), a MAD channel $\mathcal{D}$ is a Completely Positive Trace Preserving (CPTP) mapping [Hol19, Wil17, Wat18, HG12, NC10, GIN18] acting on the set $\mathcal{L}(\mathcal{H}_{\mathrm{A}})$ of linear operators of the system,

defined by the following set of $d(d-1)/2+1$ Kraus operators

$$\begin{aligned} \hat{K}_{ij} &\equiv \sqrt{\gamma_{ji}}\,|i\rangle\langle j|\,, \qquad \forall\ i,j \text{ s.t. } 0 \le i < j \le d-1, \\ \hat{K}_0 &\equiv |0\rangle\langle 0| + \sum_{1\le j\le d-1} \sqrt{1-\xi_j}\,|j\rangle\langle j|\ , \end{aligned} \tag{5.1}$$

with γ_{ji} real quantities describing the decay rate from the j-th to the i-th level that fulfill the conditions

$$\begin{cases} 0 \le \gamma_{ji} \le 1\,, \qquad \forall\ i,j \text{ s.t. } 0 \le i < j \le d-1, \\ \xi_j \equiv \sum\limits_{0\le i<j} \gamma_{ji} \le 1\,, \qquad \forall j = 1,\cdots,d-1\,. \end{cases} \tag{5.2}$$

Accordingly, given $\hat{\rho} \in \mathfrak{S}(\mathcal{H}_A)$ a generic density matrix of the system A, the MAD

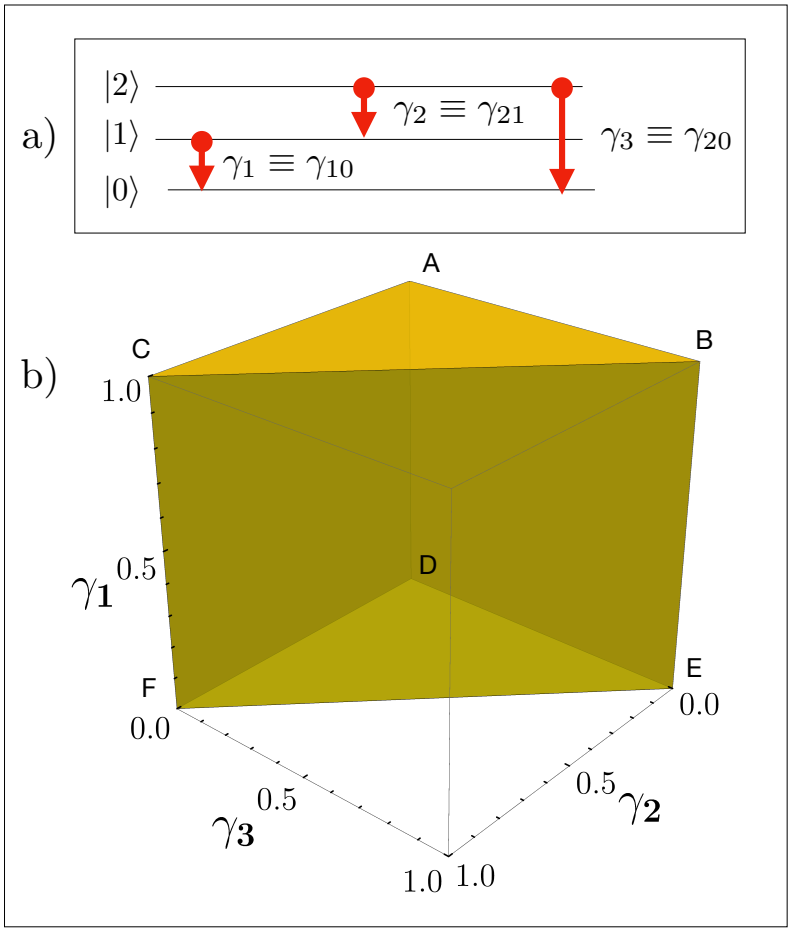

FIGURE 5.1: Top panel: schematic representation of the action of the MAD channel $\mathcal{D}_{\vec{\gamma}}$ on a 3-level system. Bottom panel: the admitted region of the damping parameters space: the transformation is CPTP if and only if the rate vector $\vec{\gamma}$ belongs to the yellow region defined in Eq. (5.6).

channel $\mathcal{D}$ will transform it into the output state defined as

$$\begin{aligned}\mathcal{D}(\hat{\rho}) &= \hat{K}_0\hat{\rho}\hat{K}_0^\dagger + \sum_{0\le i<j\le d-1}\hat{K}_{ij}\hat{\rho}\hat{K}_{ij}^\dagger\,,\\ &= \hat{K}_0\hat{\rho}\hat{K}_0^\dagger + \sum_{0\le i<j\le d-1}\gamma_{ji}|i\rangle\langle i|\,\langle j|\hat{\rho}|j\rangle\,.\end{aligned} \tag{5.3}$$

By construction $\mathcal{D}$ always admits the ground state $|0\rangle$ as a fixed point, i.e. $\mathcal{D}(|0\rangle\langle 0|) = |0\rangle\langle 0|$, even though, depending on the specific values of the coefficients γ_{ji}, other input states may fulfill the same property as well. Limit cases are $\gamma_{ji} = 0\ \forall\, i,\, j$, where all levels are untouched and $\mathcal{D}$ reduces to the noiseless identity channel Id which preserves all the input states of A. On the opposite extreme are those examples in which for some j we have $\xi_j = 1$, corresponding to the scenario where the j-th level becomes totally depopulated at the end of the transformation. The maps (5.3) provide also a natural playground to describe Partially Coherent Direct Sum (PCDS) channels [CG21a]. Last but not the least, an important and easy to verify property of the maps (5.3) is that they are covariant under the group formed by the unitary transformations $\hat{U}$ which are diagonal in the computational basis $\{|i\rangle\}_{i=0,\cdots,d-1}$, i.e.

$$\mathcal{D}(\hat{U}\hat{\rho}\hat{U}^\dagger) = \hat{U}\mathcal{D}(\hat{\rho})\hat{U}^\dagger\,, \tag{5.4}$$

for all inputs $\hat{\rho}$.

For what concerns the present work, we shall restrict our analysis to the special set of MAD channels (5.3) associated with a qutrit system ($d = 3$) whose decay processes, pictured in the top panel of Fig. 5.1, are fully characterized by only three rate parameters γ_{ji} that for the ease of notation we rename with the cartesian components of a 3D vector $\vec{\gamma} \equiv (\gamma_1, \gamma_2, \gamma_3)$. Accordingly, expressed in terms of the matrix representation induced by the computational basis $\{|0\rangle, |1\rangle, |2\rangle\}$, the Kraus operators (5.1) write explicitly as

$$\begin{aligned}\hat{K}_0 &= \begin{pmatrix}1 & 0 & 0\\ 0 & \sqrt{1-\gamma_1} & 0\\ 0 & 0 & \sqrt{1-\gamma_2-\gamma_3}\end{pmatrix}, \quad \hat{K}_{01} = \begin{pmatrix}0 & \sqrt{\gamma_1} & 0\\ 0 & 0 & 0\\ 0 & 0 & 0\end{pmatrix},\\ \hat{K}_{12} &= \begin{pmatrix}0 & 0 & 0\\ 0 & 0 & \sqrt{\gamma_2}\\ 0 & 0 & 0\end{pmatrix}, \quad \hat{K}_{03} = \begin{pmatrix}0 & 0 & \sqrt{\gamma_3}\\ 0 & 0 & 0\\ 0 & 0 & 0\end{pmatrix},\end{aligned} \tag{5.5}$$

with CPTP conditions (5.2) given by

$$\begin{cases} 0 \le \gamma_j \le 1\,, & \forall j = 1,2,3\,,\\ \\ \gamma_2 + \gamma_3 \le 1\,, \end{cases} \tag{5.6}$$

which produce the volume visualized in the bottom panel of Fig. 5.1.

The resulting mapping (5.3) for the channel $\mathcal{D}_{(\gamma_1,\gamma_2,\gamma_3)}$ reduces hence to the following expression

$$\mathcal{D}_{\vec{\gamma}}(\hat{\rho}) = \begin{pmatrix}\rho_{00}+\gamma_1\rho_{11}+\gamma_3\rho_{22} & \sqrt{1-\gamma_1}\rho_{01} & \sqrt{1-\gamma_2-\gamma_3}\rho_{02}\\ \sqrt{1-\gamma_1}\rho_{01}^* & (1-\gamma_1)\rho_{11}+\gamma_2\rho_{22} & \sqrt{1-\gamma_1}\sqrt{1-\gamma_2-\gamma_3}\rho_{12}\\ \sqrt{1-\gamma_2-\gamma_3}\rho_{02}^* & \sqrt{1-\gamma_1}\sqrt{1-\gamma_2-\gamma_3}\rho_{12}^* & (1-\gamma_2-\gamma_3)\rho_{22}\end{pmatrix}, \tag{5.7}$$

while the associated complementary CPTP transformation [Hol19, Wil17, Wat18, HG12] computed as in Eq. (B.5) of Appendix B.1, for generic choices of the system parameters, transforms A into a 4-dimensional state via the mapping

$$\tilde{\mathcal{D}}_{\vec{\gamma}}(\hat{\rho}) = \begin{pmatrix} \rho_{00} + (1-\gamma_1)\rho_{11} + (1-\gamma_2-\gamma_3)\rho_{22} & \sqrt{\gamma_1}\rho_{01} & \sqrt{1-\gamma_1}\sqrt{\gamma_2}\rho_{12} & \sqrt{\gamma_3}\rho_{02} \\ \sqrt{\gamma_1}\rho_{01}^* & \gamma_1\rho_{11} & 0 & \sqrt{\gamma_1}\sqrt{\gamma_3}\rho_{12} \\ \sqrt{1-\gamma_1}\sqrt{\gamma_2}\rho_{12}^* & 0 & \gamma_2\rho_{22} & 0 \\ \sqrt{\gamma_3}\rho_{02}^* & \sqrt{\gamma_1}\sqrt{\gamma_3}\rho_{12}^* & 0 & \gamma_3\rho_{22} \end{pmatrix} , \tag{5.8}$$

where for $i, j \in 0, 1, 2$, $\rho_{ij} \equiv \langle i|\hat{\rho}|j\rangle$ are the matrix entries of the input density operator $\hat{\rho} \in \mathfrak{S}(\mathcal{H}_{\rm A})$.

5.2.1 Composition rules

It is relatively easy to verify that the set of qutrit MAD channels (5.7) is close under concatenation. Specifically we notice that given $\mathcal{D}_{\vec{\gamma}'}$ and $\mathcal{D}_{\vec{\gamma}''}$ with $\vec{\gamma}'' = (\gamma_1'', \gamma_2'', \gamma_3'')$ and $\vec{\gamma}' = (\gamma_1', \gamma_2', \gamma_3')$ two rate vectors fulfilling the conditions (5.6), we have

$$\mathcal{D}_{\vec{\gamma}'} \circ \mathcal{D}_{\vec{\gamma}''} = \mathcal{D}_{\vec{\gamma}} , \tag{5.9}$$

with $\vec{\gamma} = (\gamma_1, \gamma_2, \gamma_3)$ a new rate vector of components

$$\begin{cases} \gamma_1 = \gamma_1'' + \gamma_1' - \gamma_1'\gamma_1'' , \\ \gamma_2 = \gamma_2''(1-\gamma_1'-\gamma_2') + \gamma_2'(1-\gamma_3'') , \\ \gamma_3 = \gamma_3'' + \gamma_2''(\gamma_1'-\gamma_3') + \gamma_3'(1-\gamma_3'') . \end{cases} \tag{5.10}$$

which also satisfies (5.6) (hereafter we shall use the symbol "$\circ$" to represent super-operator composition). The importance of Eq. (5.9) for the problem we are facing stems from channel data-processing inequalities (or bottleneck) inequalities [Key02, KSW20, NC10], according to which, any information capacity functional Γ [HG12] such as the quantum capacity Q, the classical capacity C, the private classical capacity $C_{\rm p}$, the entanglement assisted classical capacity $C_{\rm ea}$ etc., computed for a CPTP map $\Phi = \Phi' \circ \Phi''$ obtained by concatenating channel Φ' with channel Φ'', must fulfill the following relation

$$\Gamma(\Phi) \leq \min\{\Gamma(\Phi'), \Gamma(\Phi'')\} . \tag{5.11}$$

Applied to Eq. (5.9), the above inequality can be used to predict monotonic behaviors for the capacity $\Gamma(\mathcal{D}_{\vec{\gamma}})$ as a function of the rate vector $\vec{\gamma}$, that allows us to provide useful lower and upper bounds which in some case permit to extend the capacity formula to domain where other techniques (e.g. degradability analysis) fail. In particular we notice that for single-decay MAD channels where only one component of the rate vector is different from zero (say γ_1) we get

$$\mathcal{D}_{(\gamma_1',0,0)} \circ \mathcal{D}_{(\gamma_1'',0,0)} = \mathcal{D}_{(\gamma_1'',0,0)} \circ \mathcal{D}_{(\gamma_1',0,0)} = \mathcal{D}_{(\gamma_1,0,0)} , \tag{5.12}$$

with γ_1 as in the first identity of Eq. (5.10). Accordingly we can conclude that all the capacities $\Gamma(\mathcal{D}_{(\gamma_1,0,0)})$ should be non increasing functionals of the parameter γ_1, i.e.

$$\Gamma(\mathcal{D}_{(\gamma_1,0,0)}) \geq \Gamma(\mathcal{D}_{(\gamma_1',0,0)}), \qquad \forall \gamma_1 \leq \gamma_1' , \tag{5.13}$$

(the same expressions and conclusions apply also for $\mathcal{D}_{(0,\gamma_2,0)}$ and $\mathcal{D}_{(0,0,\gamma_3)}$). Composing single-decay MAD channels characterized by rate vectors pointing along different cartesian axis, in general creates maps with higher rank of the resulting vector rate. Specifically from Eq. (5.9) it follows that, for an arbitrary choice of the rate vector $\vec{\gamma} = (\gamma_1, \gamma_2, \gamma_3)$ in the allowed CPTP domain the MAD channel $\mathcal{D}_{(\gamma_1,\gamma_2,\gamma_3)}$ can be expressed as

$$\mathcal{D}_{(\gamma_1,\gamma_2,\gamma_3)} = \mathcal{D}_{(0,0,\bar{\gamma}_3)} \circ \mathcal{D}_{(0,\gamma_2,0)} \circ \mathcal{D}_{(\gamma_1,0,0)} \tag{5.14}$$

$$= \mathcal{D}_{(0,\bar{\gamma}_2,0)} \circ \mathcal{D}_{(0,0,\gamma_3)} \circ \mathcal{D}_{(\gamma_1,0,0)} \ , \tag{5.15}$$

with

$$\bar{\gamma}_3 \equiv \frac{\gamma_3}{1-\gamma_2} \ , \qquad \bar{\gamma}_2 \equiv \frac{\gamma_2}{1-\gamma_3} \ , \tag{5.16}$$

which because of the constraint (5.6) are properly defined rates. As a direct consequence of Eqs. (5.11) and (5.12) it then follows that the capacities $\Gamma(\mathcal{D}_{(\gamma_1,\gamma_2,\gamma_3)})$ must be non-increasing functionals of all the cartesian components of rate vector $\vec{\gamma}$, i.e.

$$\Gamma(\mathcal{D}_{(\gamma_1,\gamma_2,\gamma_3)}) \geq \Gamma(\mathcal{D}_{(\gamma_1',\gamma_2',\gamma_3')}), \quad \forall \gamma_i' \geq \gamma_i \ . \tag{5.17}$$

and must be restricted by the upper bound

$$\Gamma(\mathcal{D}_{(\gamma_1,\gamma_2,\gamma_3)}) \leq \min\{\Gamma(\mathcal{D}_{(\gamma_1,0,0)}), \mathcal{D}_{(0,\bar{\gamma}_2,0)}), \mathcal{D}_{(0,0,\bar{\gamma}_3)})\} \ . \tag{5.18}$$

As a further refinement notice that, setting $\gamma_2 = 0$ in Eqs. (5.14) and (5.15) we get

$$\mathcal{D}_{(\gamma_1,0,\gamma_3)} = \mathcal{D}_{(\gamma_1,0,0)} \circ \mathcal{D}_{(0,0,\gamma_3)} = \mathcal{D}_{(0,0,\gamma_3)} \circ \mathcal{D}_{(\gamma_1,0,0)} \ , \tag{5.19}$$

which replaced back into Eq. (5.15) gives us

$$\mathcal{D}_{(\gamma_1,\gamma_2,\gamma_3)} = \mathcal{D}_{(0,\bar{\gamma}_2,0)} \circ \mathcal{D}_{(\gamma_1,0,\gamma_3)} \ , \tag{5.20}$$

which allows us to replace (5.18) with the stronger requirement

$$\Gamma(\mathcal{D}_{(\gamma_1,\gamma_2,\gamma_3)}) \leq \min\{\Gamma(\mathcal{D}_{(0,\bar{\gamma}_2,0)}), \Gamma(\mathcal{D}_{(\gamma_1,0,\gamma_3)})\} \ . \tag{5.21}$$

Similarly by setting $\gamma_1 = 0$ we get

$$\mathcal{D}_{(0,\gamma_2,\gamma_3)} = \mathcal{D}_{(0,0,\bar{\gamma}_3)} \circ \mathcal{D}_{(0,\gamma_2,0)} = \mathcal{D}_{(0,\bar{\gamma}_2,0)} \circ \mathcal{D}_{(0,0,\gamma_3)} \ , \tag{5.22}$$

that yields

$$\mathcal{D}_{(\gamma_1,\gamma_2,\gamma_3)} = \mathcal{D}_{(0,\gamma_2,\gamma_3)} \circ \mathcal{D}_{(\gamma_1,0,0)} \ , \tag{5.23}$$

and

$$\Gamma(\mathcal{D}_{(\gamma_1,\gamma_2,\gamma_3)}) \leq \min\{\Gamma(\mathcal{D}_{(0,\gamma_2,\gamma_3)}), \Gamma(\mathcal{D}_{(\gamma_1,0,0)})\} \ . \tag{5.24}$$

Finally setting $\gamma_3 = 0$ in Eqs. (5.14) we get

$$\mathcal{D}_{(\gamma_1,\gamma_2,0)} = \mathcal{D}_{(0,\gamma_2,0)} \circ \mathcal{D}_{(\gamma_1,0,0)} \ , \tag{5.25}$$

that leads to

$$\mathcal{D}_{(\gamma_1,\gamma_2,\gamma_3)} = \mathcal{D}_{(0,0,\bar{\gamma}_3)} \circ \mathcal{D}_{(\gamma_1,\gamma_2,0)} \ , \tag{5.26}$$

and

$$\Gamma(\mathcal{D}_{(\gamma_1,\gamma_2,\gamma_3)}) \leq \min\{\Gamma(\mathcal{D}_{(\gamma_1,\gamma_2,0)}), \mathcal{D}_{(0,0,\bar{\gamma}_3)}\} \ . \tag{5.27}$$

5.3 Quantum and private classical capacities for qutrit MAD

The quantum capacity Q of a quantum channel is a measure of how faithfully quantum states can be transmitted from the input to the output of the associated CPTP map by exploiting proper encoding and decoding procedures that act on multiple transmission stages [Hol19, Wil17, Wat18, HG12, NC10, GIN18]. The private classical capacity $C_{\rm p}$ instead quantifies the amount of classical information transmittable per channel use under the extra requirement that the entire signaling process allows the communicating parties to be protected by eavesdropping by an adversary agent that is controlling the communication line. The explicit evaluation of these important functionals is one of the most elusive task of quantum information theory, as testified by the limited number of examples which allow for an explicit solution. For a comprehensive, self-consistent introduction to the technical problems involved in this calculation we refer the reader to the Appendix B.1, where we present the notions of complementary channel, coherent information, and degradability and where we introduce the explicit functionals [Llo97, Sho02b, Dev05] we need to optimize. Building up from these premises here we present a thoughtful characterization of the quantum capacity $Q(\mathcal{D}_{\vec{\gamma}})$ and the private classical capacity $C_{\rm p}(\mathcal{D}_{\vec{\gamma}})$ of the qutrit MAD channel $\mathcal{D}_{\vec{\gamma}}$ defined in Eq. (5.7). We stress that while failing to provide the explicit solution for all rate vectors $\vec{\gamma}$ in the allowed domain defined by Eq. (5.6), in what follows we manage to deliver the exact values of $Q(\mathcal{D}_{\vec{\gamma}})$ and $C_{\rm p}(\mathcal{D}_{\vec{\gamma}})$ for a quite a large class of qutrit MAD channels by making use of degradability properties [DS05], data-processing (or bottleneck) inequalities [Key02, KSW20], and channel isomorphism. In particular we anticipate here that, for those $\mathcal{D}_{\vec{\gamma}}$ which are provably degradable [DS05], we shall exploit the covariance property (5.4) to further simplify the single-letter formula (B.17) as

$$Q(\mathcal{D}_{\vec{\gamma}}) = C_{\rm p}(\mathcal{D}_{\vec{\gamma}}) = \max_{\hat{\rho}_{\rm diag}} \left\{ S(\mathcal{D}_{\vec{\gamma}}(\hat{\rho}_{\rm diag})) - S(\tilde{\mathcal{D}}_{\vec{\gamma}}(\hat{\rho}_{\rm diag})) \right\} , \tag{5.28}$$

where $S(\cdots)$ is the von Neumann entropy, and where the maximization is performed on input states of A which are diagonal in the computational basis of the problem, i.e. the density matrices of the form $\hat{\rho}_{\rm diag} = \sum_{i=0}^{2} p_i |i\rangle\langle i|$ with $p_0, p_1, p_2 \in [0,1]$ fulfilling the normalization constraint $p_0 + p_1 + p_2 = 1$ – see discussion at the end of Appendix B.1.2 for details. Notably, when applicable, Eq. (5.28) relies on an optimization of a functional of only two real variables (namely the populations p_0 and p_1) which can be easily carried on (at least numerically).

To begin with, observe that, as anticipated in Eq. (5.8), the complementary map $\tilde{\mathcal{D}}_{\vec{\gamma}}$ of a generic qutrit MAD channel $\mathcal{D}_{\vec{\gamma}}$ sends the input states of A into a 4-dimensional "environment state". In the end this is a consequence of the fact that the (minimal) number of Kraus operators we need to express (5.7) is 4. Unfortunately this number also ensures us that the channel is not degradable: it has been indeed shown [CRS08] that a necessary condition for any CPTP map with output dimension 3 to be degradable is that its associated Choi rank, and consequently the minimal number of Kraus operators we need to express such transformation, is at most 3. This brings us to consider some simplification in the problem, e.g. by fixing some of the values of the damping parameters. One approach is represented by the selective suppression of one (or two) of the decaying channels, i.e. imposing one (or two) of the parameters γ_i equal to 0, which we will

do in Secs. 5.3.1, 5.3.3, and 5.3.4. For each of these subclasses of channels we'll give a characterization, when possible, in terms of degradability, antidegradability and quantum capacity. A second approach that we adopt in Secs. 5.3.2 and 5.3.5, consists instead to fix one of the damping parameters to its maximum allowed value, a choice that as we shall see, will effectively allow us to reduce the number of degrees of freedom of the problem.

5.3.1 Single-decay qutrit MAD channels

We consider here instances of the qutrit MAD channel in which only one of the three damping parameters γ_i is explicitly different from zero, i.e. the maps $\mathcal{D}_{(\gamma_1,0,0)}$, $\mathcal{D}_{(0,\gamma_2,0)}$, and $\mathcal{D}_{(0,0,\gamma_3)}$ associated respectively with the edges DA, DF and DE of Fig. 5.1. It is easy to verify that these three sets of transformations can be mapped into each other via unitary conjugations that simply permute the energy levels of the system: for instance $\mathcal{D}_{(0,0,\gamma_3=\gamma)}$ can be transformed into $\mathcal{D}_{(\gamma_1=\gamma,0,0)}$ by simply swapping levels $|1\rangle$ and $|2\rangle$. Accordingly, as a consequence of (5.11), the capacities of these three sets must coincide, i.e.

$$Q(\mathcal{D}_{(\gamma,0,0)}) = Q(\mathcal{D}_{(0,\gamma,0)}) = Q(\mathcal{D}_{(0,0\gamma)}) \ , \quad \forall \gamma \in [0,1] \ , \tag{5.29}$$

(similarly for $C_{\rm p}$). By virtue of this fact, without loss of generality, in the following we report the analysis only for $\mathcal{D}_{(\gamma_1,0,0)}$, being the results trivially extendable to the remaining two.

It turns out that the channel $\mathcal{D}_{(\gamma_1,0,0)}$ is a special instance of the PCDS maps analyzed in Ref. [CG21a] where an explicit formula for Q has been already derived. Still, for the sake of completeness, we find it useful to present here an alternative derivation of those results which does not make explicit reference to the PCDS structure. For this purpose we observe that from Eq. (5.5) it follows that $\mathcal{D}_{(\gamma_1,0,0)}$ possesses only two non zero Kraus operators, i.e.

$$\hat{K}_0 = \begin{pmatrix} 1 & 0 & 0 \\ 0 & \sqrt{1-\gamma_1} & 0 \\ 0 & 0 & 1 \end{pmatrix} \quad \hat{K}_{01} = \begin{pmatrix} 0 & \sqrt{\gamma_1} & 0 \\ 0 & 0 & 0 \\ 0 & 0 & 0 \end{pmatrix} . \tag{5.30}$$

Transformation (5.7) is then given by

$$\mathcal{D}_{(\gamma_1,0,0)}(\hat{\rho}) = \begin{pmatrix} \rho_{00}+\gamma_1\rho_{11} & \sqrt{1-\gamma_1}\rho_{01} & \rho_{02} \\ \sqrt{1-\gamma_1}\rho_{01}^* & (1-\gamma_1)\rho_{11} & \sqrt{1-\gamma_1}\rho_{12} \\ \rho_{02}^* & \sqrt{1-\gamma_1}\rho_{12}^* & \rho_{22} \end{pmatrix} , \tag{5.31}$$

and the complementary channel $\tilde{\mathcal{D}}_{(\gamma_1,0,0)}$ that can be expressed as a mapping that connects the system A to a 2-dimensional environmental system E, i.e.

$$\tilde{\mathcal{D}}_{(\gamma_1,0,0)}(\hat{\rho}) = \begin{pmatrix} 1-\gamma_1\rho_{11} & \sqrt{\gamma_1}\rho_{01} \\ \sqrt{\gamma_1}\rho_{01}^* & \gamma_1\rho_{11} \end{pmatrix} . \tag{5.32}$$

From Eq. (5.31) it follows that, irrespectively of the value of γ, the model always owns a 2-dim noiseless subspace spanned by the vectors $|0\rangle$ and $|2\rangle$ ensuring a non zero lower bound for both the quantum and the private classical capacity

$$Q(\mathcal{D}_{(\gamma_1,0,0)}), C_{\rm p}(\mathcal{D}_{(\gamma_1,0,0)}) \geq \log_2(2) = 1, \tag{5.33}$$

which incidentally implies that the channel $\mathcal{D}_{(\gamma_1,0,0)}$ is never anti-degradable. By methods discussed in Appendix B.1.1 we can also show that $\mathcal{D}_{(\gamma_1,0,0)}$ is always mathematically invertible for all $\gamma_1 < 1$, with $\tilde{\mathcal{D}}_{(\gamma_1,0,0)} \circ \mathcal{D}^{-1}_{(\gamma_1,0,0)}$ CPTP for all $\gamma_1 \leq \frac{1}{2}$. Accordingly, invoking (B.10) we can ensure the channel to be degradable if and only if $\gamma_1 \leq \frac{1}{2}$ and use Eq. (5.28) to compute its capacity value (notice that in principle the above argument leaves open the possibility that the channel would be degradable also for $\gamma_1 = 1$, this however can be excluded by direct calculation or invoking the analysis of [CG21a]). Consequently for $\gamma_1 \leq \frac{1}{2}$ we can write

$$
\begin{aligned}
&Q(\mathcal{D}_{(\gamma_1,0,0)}) = C_{\mathrm{p}}(\mathcal{D}_{(\gamma_1,0,0)}) \\
&= \max_{p_0,p_1} \Big\{ -(1-p_0-p_1)\log_2(1-p_0-p_1) \\
&- (p_0+\gamma_1 p_1)\log_2(p_0+\gamma_1 p_1) - (1-\gamma_1)p_1 \log_2((1-\gamma_1)p_1) \\
&+ (1-\gamma_1 p_1)\log_2(1-\gamma_1 p_1) + \gamma_1 p_1 \log_2(\gamma_1 p_1)\Big\},
\end{aligned}
$$

which can be solved numerically (the maximization being performed over all possible values $p_0, p_1 \in [0,1]$ under the constraint that $p_0 + p_1 \leq 1$).

Despite the fact that the channel is degradable only for $0 \leq \gamma_1 \leq \frac{1}{2}$ and that we know that it's not anti-degradable, we can still compute the value of the capacity of $\mathcal{D}_{(\gamma_1,0,0)}$ showing that

$$
Q(\mathcal{D}_{(\gamma_1,0,0)}) = C_{\mathrm{p}}(\mathcal{D}_{(\gamma_1,0,0)}) = 1\,, \qquad \forall \gamma_1 \geq 1/2. \tag{5.34}
$$

This indeed is a direct consequence of the lower bound (5.33), the fact that $Q(\mathcal{D}_{(\gamma_1,0,0)})$ and $C_{\mathrm{p}}(\mathcal{D}_{(\gamma_1,0,0)})$ are non-increasing functions of γ_1 as explicitly shown in Eq. (5.13), and of the fact that from Eq. (5.34) we get $Q(\mathcal{D}_{(\gamma_1=1/2,0,0)}) = C_{\mathrm{p}}(\mathcal{D}_{(\gamma_1=1/2,0,0)}) = 1$ by direct evaluation. Putting all this together we obtain

$$
1 = Q(\mathcal{D}_{(\gamma_1=1/2,0,0)}) \geq Q(\mathcal{D}_{(\gamma_1,0,0)}) \geq 1\,, \qquad \forall \gamma_1 \geq 1/2, \tag{5.35}
$$

that implies (5.34), the same conclusion of course holding true for $C_{\mathrm{p}}(\mathcal{D}_{(\gamma_1,0,0)})$. The results discussed above are summarized in the plot in Fig. 5.2.

5.3.2 Complete damping of the first excited state ($\gamma_1 = 1$)

Assume next that our qutrit MAD channel of Eq. (5.7) is characterized by the maximum value of γ_1 allowed by CPTP constraint of Eq. (5.6), i.e. $\gamma_1 = 1$, region represented by the ABC triangle of Fig. 5.1. This map corresponds to the case where the initial population of the first excited level $|1\rangle$, gets completely lost in favor of the ground state $|0\rangle$ of the model so that Eqs. (5.7), (5.8) rewrite as

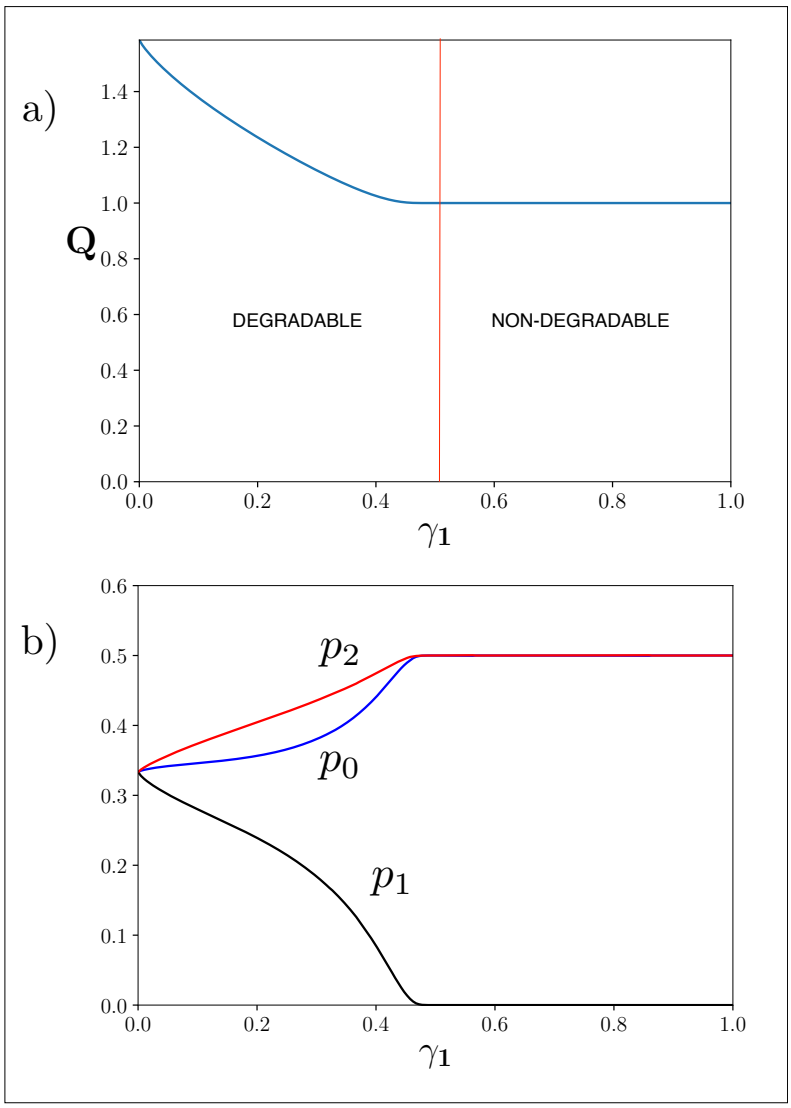

FIGURE 5.2: Upper panel: profile of the quantum and the private classical capacity for the channel $\mathcal{D}_{(\gamma_1,0,0)}$ w.r.t. the damping parameter γ_1. For $\gamma_1 \leq 1/2$ the channel is degradable and the reported value follows from the numerical solution of Eq. (5.34). For $\gamma > 1/2$ instead the channel is neither degradable nor antidegradable: here the associated capacity value is equal to 1 (see main text). Notice that the reported values respect the monotonicity property (5.13). Lower panel: populations p_0, p_1 and p_2 of those states that maximize the quantum capacity formula (5.34) for the channel $\mathcal{D}_{(\gamma_1,0,0)}$ w.r.t. the damping parameter γ_1.

$$\mathcal{D}_{(1,\gamma_2,\gamma_3)}(\hat{\rho}) = \begin{pmatrix} 1-(1-\gamma_3)\rho_{22} & 0 & \sqrt{1-\gamma_2-\gamma_3}\rho_{02} \\ 0 & \gamma_2\rho_{22} & 0 \\ \sqrt{1-\gamma_2-\gamma_3}\rho_{02}^* & 0 & (1-\gamma_2-\gamma_3)\rho_{22} \end{pmatrix}, \tag{5.36}$$

$$\tilde{\mathcal{D}}_{(1,\gamma_2,\gamma_3)}(\hat{\rho}) = \begin{pmatrix} \rho_{00}+(1-\gamma_2-\gamma_3)\rho_{22} & \rho_{01} & 0 & \sqrt{\gamma_3}\rho_{02} \\ \rho_{01}^* & \rho_{11} & 0 & \sqrt{\gamma_3}\rho_{12} \\ 0 & 0 & \gamma_2\rho_{22} & 0 \\ \sqrt{\gamma_3}\rho_{02}^* & \sqrt{\gamma_3}\rho_{12}^* & 0 & \gamma_3\rho_{22} \end{pmatrix}, \tag{5.37}$$

for $\gamma_2, \gamma_3 \in [0,1]$ such that $\gamma_2 + \gamma_3 \leq 1$. The above expressions make it explicit that, at variance with the case discussed in the previous section and in agreement with the conclusions of Ref. [CRS08], the map $\mathcal{D}_{(1,\gamma_2,\gamma_3)}$ is not degradable. Indeed we notice that while $\tilde{\mathcal{D}}_{(1,\gamma_2,\gamma_3)}(\hat{\rho})$ preserves information about the components ρ_{11}, ρ_{01}, ρ_{10}, ρ_{12}, ρ_{21} of the input state $\hat{\rho}$, no trace of those terms is left in $\mathcal{D}_{(1,\gamma_2,\gamma_3)}(\hat{\rho})$: accordingly it is technically impossible to identify a linear (not mentioning CPTP) map $\mathcal{N}$ which applied to $\mathcal{D}_{(1,\gamma_2,\gamma_3)}(\hat{\rho})$ would reproduce $\tilde{\mathcal{D}}_{(1,\gamma_2,\gamma_3)}(\hat{\rho})$ for all $\hat{\rho}$. Despite this fact it turns out that also for $\mathcal{D}_{(1,\gamma_2,\gamma_3)}$, the capacity can still be expressed as the single letter expression (5.28). Specifically, as we shall see in the following, in this case we can write

$$\begin{aligned} Q(\mathcal{D}_{(1,\gamma_2,\gamma_3)}) &= C_{\rm p}(\mathcal{D}_{(1,\gamma_2,\gamma_3)}) \\ &= Q^{(1)}(\mathcal{D}_{(1,\gamma_2,\gamma_3)}) = \mathcal{Q}(\gamma_2,\gamma_3) \, , \end{aligned} \tag{5.38}$$

with the function $\mathcal{Q}(\gamma_2,\gamma_3)$ being formally defined as

$$\begin{aligned} \mathcal{Q}(\gamma_2,\gamma_3) &\equiv \max_{\hat{\tau}_{\rm diag}} \left\{ S(\mathcal{D}_{(1,\gamma_2,\gamma_3)}(\hat{\tau}_{\rm diag})) - S(\tilde{\mathcal{D}}_{(1,\gamma_2,\gamma_3)}(\hat{\tau}_{\rm diag})) \right\} \\ &= \max_{p\in[0,1]} \Big\{ -(1-(1-\gamma_3)p)\log_2(1-(1-\gamma_3)p) - (1-\gamma_2-\gamma_3)p\log_2(1-\gamma_2-\gamma_3)p) \\ &\quad +(1-(\gamma_2+\gamma_3)p)\log_2(1-(\gamma_2+\gamma_3)p) + \gamma_3 p\log_2\gamma_3 p) \Big\} \, , \end{aligned} \tag{5.39}$$

where the maximization is restricted to the diagonal density matrices $\hat{\tau}_{\rm diag} = (1-p)|0\rangle\langle 0| + p|2\rangle\langle 2|$ of A', associated with the linear subspace $\mathcal{H}_{\mathrm{A}'} \equiv \mathrm{Span}\{|0\rangle, |2\rangle\}$. The explicit value of $\mathcal{Q}(\gamma_2,\gamma_3)$ has been numerically plotted in Fig. 5.3: we remark here that for $\gamma_3 \geq \frac{1-\gamma_2}{2}$ this function assumes zero value, i.e. $\mathcal{Q}(\gamma_2,\gamma_3) = 0$, in agreement with the fact that in such regime the channel $\mathcal{D}_{(1,\gamma_2,\gamma_3)}$ has zero capacity, i.e.

$$\begin{aligned} Q(\mathcal{D}_{(1,\gamma_2,\gamma_3)}) &= C_{\rm p}(\mathcal{D}_{(1,\gamma_2,\gamma_3)}) = 0 \, , \\ &\quad \forall\, 1-\gamma_2 \geq \gamma_3 \geq \tfrac{1-\gamma_2}{2} \, . \end{aligned} \tag{5.40}$$

To prove Eq. (5.38) let us start by observing that $\mathcal{Q}(\gamma_2,\gamma_3)$ provides a natural lower bound for $Q(\mathcal{D}_{(1,\gamma_2,\gamma_3)})$ and hence for $C_{\rm p}(\mathcal{D}_{(1,\gamma_2,\gamma_3)})$: this is a simple consequence of (B.16), which allows us to write

$$\begin{aligned} Q(\mathcal{D}_{(1,\gamma_2,\gamma_3)}) &\geq \max_{\hat{\rho}} I_{\rm coh}(\mathcal{D}_{(1,\gamma_2,\gamma_3)},\hat{\rho}) \\ &\geq \max_{\hat{\tau}_{\rm diag}} I_{\rm coh}(\mathcal{D}_{(1,\gamma_2,\gamma_3)},\hat{\tau}_{\rm diag}) = \mathcal{Q}(\gamma_2,\gamma_3) \, , \end{aligned}$$

with $I_{\rm coh}$ being the coherent information functional (B.15). Next step is now to show that the function $\mathcal{Q}(\gamma_2,\gamma_3)$ provides also an upper bound for $Q(\mathcal{D}_{(1,\gamma_2,\gamma_3)})$: we do this by constructing a new channel $\mathcal{D}'_{(\gamma_2,\gamma_3)}$ whose capacity is provably larger than the capacity of $\mathcal{D}_{(1,\gamma_2,\gamma_3)}$, i.e.

$$Q(\mathcal{D}_{(1,\gamma_2,\gamma_3)}) \leq Q(\mathcal{D}'_{(\gamma_2,\gamma_3)}) \, , \tag{5.41}$$

$$C_{\rm p}(\mathcal{D}_{(1,\gamma_2,\gamma_3)}) \leq C_{\rm p}(\mathcal{D}'_{(\gamma_2,\gamma_3)}) \, , \tag{5.42}$$

and for which we can explicitly show that

$$Q(\mathcal{D}'_{(\gamma_2,\gamma_3)}) = C_{\rm p}(\mathcal{D}'_{(\gamma_2,\gamma_3)}) = \mathcal{Q}(\gamma_2,\gamma_3)\ . \tag{5.43}$$

For this purpose notice that since the population of level $|1\rangle$ is washed away, the output produced by $\mathcal{D}_{(1,\gamma_2,\gamma_3)}$ can be simulated by the CPTP map $\mathcal{D}'_{(\gamma_2,\gamma_3)} : \mathcal{L}(\mathcal{H}_{\rm A'}) \to \mathcal{L}(\mathcal{H}_{\rm A})$ operating on the two levels quantum system associated with the Hilbert space $\mathcal{H}_{\rm A'} \equiv {\rm Span}\{|0\rangle, |2\rangle\}$, and producing qutrit states of A as outputs. In particular defining $\hat{\tau}$ a generic density matrix on $\mathcal{H}_{\rm A'}$ we have

$$\mathcal{D}'_{(\gamma_2,\gamma_3)}(\hat{\tau}) = \begin{pmatrix} 1-(1-\gamma_3)\tau_{22} & 0 & \sqrt{1-\gamma_2-\gamma_3}\tau_{02} \\ 0 & \gamma_2\tau_{22} & 0 \\ \sqrt{1-\gamma_2-\gamma_3}\tau^*_{02} & 0 & (1-\gamma_2-\gamma_3)\tau_{22} \end{pmatrix} \tag{5.44}$$

with the corresponding complementary channel (B.5) given by

$$\tilde{\mathcal{D}}'_{(\gamma_2,\gamma_3)}(\hat{\tau}) = \begin{pmatrix} 1-(\gamma_2+\gamma_3)\tau_{22} & 0 & \sqrt{\gamma_3}\tau_{02} \\ 0 & \gamma_2\tau_{22} & 0 \\ \sqrt{\gamma_3}\tau^*_{02} & 0 & \gamma_3\tau_{22} \end{pmatrix}, \tag{5.45}$$

where for $i,j = 0,2$ we set $\tau_{ij} \equiv \langle i|\hat{\tau}|j\rangle$.

The reason why $\mathcal{D}'_{(\gamma_2,\gamma_3)}$ fulfills the inequality (5.41) is a direct consequence of the fact that $\mathcal{D}_{(1,\gamma_2,\gamma_3)}$, while yielding the same outcomes of $\mathcal{D}'_{(\gamma_2,\gamma_3)}$, is also "wasting" resources in the useless level $|1\rangle$. To formalize this, notice that we can write

$$\mathcal{D}_{(1,\gamma_2,\gamma_3)} = \mathcal{D}'_{(\gamma_2,\gamma_3)} \circ \mathcal{A}\ , \tag{5.46}$$

where $\mathcal{A} : \mathcal{L}(\mathcal{H}_{\rm A}) \to \mathcal{L}(\mathcal{H}_{\rm A'})$ is the CPTP transformation which maps the input state of the qutrit A to the qubit system A$'$ by completely erasing the level $|1\rangle$ and moving its population to $|0\rangle$, i.e.

$$\mathcal{A}(\hat{\rho}) \quad = \quad \begin{pmatrix} \rho_{00}+\rho_{11} & \rho_{02} \\ \rho_{20} & \rho_{22} \end{pmatrix}, \tag{5.47}$$

where $\rho_{ij} = \langle i|\hat{\rho}|j\rangle$ with $\hat{\rho} \in \mathfrak{S}(\mathcal{H}_{\rm A})$. Equation (5.41) can hence be derived as a direct consequence of the bottleneck inequality (5.11) applied to the case in which Γ is indeed the quantum capacity Q. The second part of the argument, i.e. Eq. (5.43), can instead be derived by noticing that at variance with the original mapping $\mathcal{D}_{(1,\gamma_2,\gamma_3)}$ which is never degradable, it turns out that $\mathcal{D}'_{(\gamma_2,\gamma_3)}$ is degradable for

$$0 \leq \gamma_3 \leq (1-\gamma_2)/2\ , \tag{5.48}$$

and antidegradable otherwise, i.e. for $(1-\gamma_2)/2 \leq \gamma_3 \leq 1-\gamma_2$. This can be shown for instance by observing that in the region identified by the inequality (5.48) the quantity

$$\bar{\gamma}_3 \equiv \frac{1-\gamma_2-2\gamma_3}{1-\gamma_2-\gamma_3}\ , \tag{5.49}$$

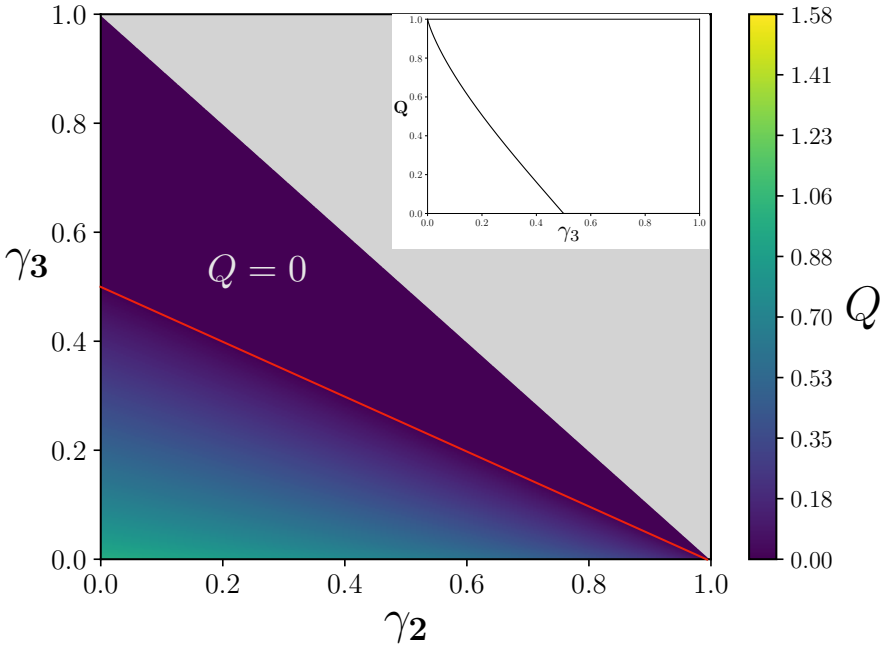

Figure 5.3: Quantum and private classical capacity of the MAD channel $\mathcal{D}_{(1,\gamma_2,\gamma_3)}$ w.r.t. γ_2 and γ_3, computed according to Eq. (5.38) – the associated parameter region corresponds to the ABC triangle of Fig. 5.1. The grey region represent points where $\mathcal{D}_{(1,\gamma_2,\gamma_3)}$ is not CPTP; the points above the red line ($\gamma_3 = (1-\gamma_2)/2$) have zero capacity, $Q(\mathcal{D}_{(1,\gamma_2,\gamma_3)}) = 0$. The equivalent channel $\mathcal{D}'_{(\gamma_2,\gamma_3)}$ of Eq. (5.44) is anti-degradable for points above the red line and degradable below. For $\gamma_2 = 0$ the value of $Q(\mathcal{D}_{(1,\gamma_2,\gamma_3)})$ and $C_{\rm p}(\mathcal{D}_{(1,\gamma_2,\gamma_3)})$ coincides with the quantum capacity [GF05] of a qubit ADC channel of transmissivity γ_3 (see inset): this should be compared with the value of $Q(\mathcal{D}_{(1,\gamma_2,\gamma_3)})$ and $C_{\rm p}(\mathcal{D}_{(1,\gamma_2,\gamma_3)})$ on the other border (i.e. $\gamma_3 = 0$), which we report in Fig. 5.4. Notice finally that the reported values respect the monotonicity requirement of Eq. (5.17).

belongs to the interval $[0, 1]$ and can be used to build up a proper CPTP single-decay qutrit MAD channel $\mathcal{D}_{(0,0,\bar{\gamma}_3)}$ – see Sec. 5.3.1. Furthermore by direct calculation we also get

$$\mathcal{D}_{(0,0,\bar{\gamma}_3)} \circ \mathcal{D}'_{(\gamma_2,\gamma_3)} = \tilde{\mathcal{D}}'_{(\gamma_2,\gamma_3)} \ , \tag{5.50}$$

which shows that $\mathcal{D}_{(0,0,\bar{\gamma}_3)}$ acts as the connecting channel $\mathcal{N}$ entering the degradability condition (B.8) of $\mathcal{D}'_{(\gamma_2,\gamma_3)}$. From Eqs. (5.44) and (5.45) it is also immediately visible that $\mathcal{D}'_{(\gamma_2,\gamma_3)}$ can be obtained from $\tilde{\mathcal{D}}'_{(\gamma_2,\gamma_3)}$ by the substitution $\gamma_3 \to 1-\gamma_2-\gamma_3$. Consequently using the same construction (5.50) we can conclude that $\mathcal{D}'_{(\gamma_2,\gamma_3)}$ is antidegradable for $(1-\gamma_2)/2 \leq \gamma_3 \leq 1-\gamma_2$.

To derive Eq. (5.43) we finally observe that as the original mapping $\mathcal{D}_{(1,\gamma_2,\gamma_3)}$, also $\mathcal{D}'_{(\gamma_2,\gamma_3)}$ is covariant under the group of unitary transformations which are diagonal in the computational basis of the model: accordingly, following the same argument that led

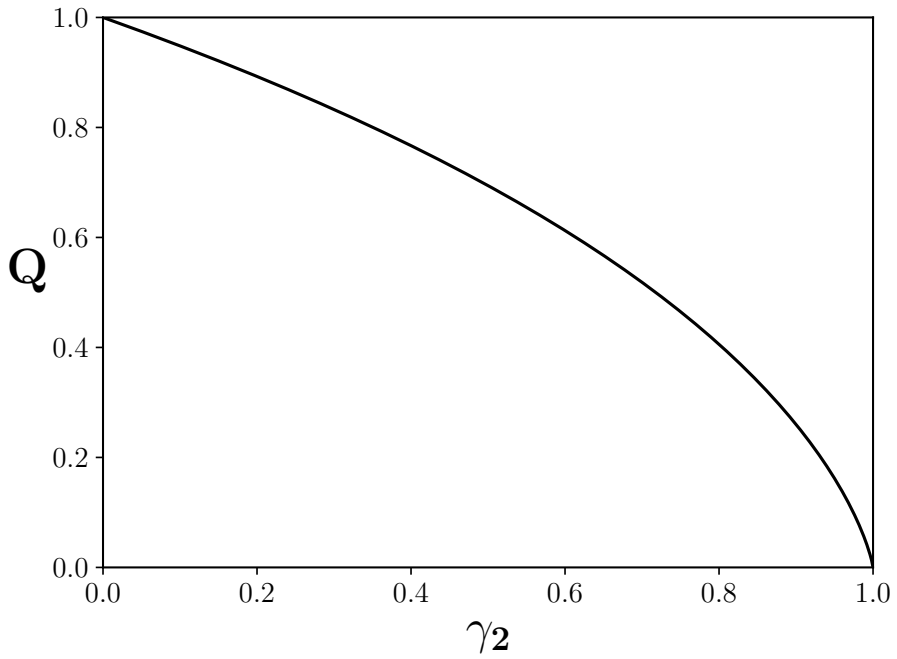

FIGURE 5.4: Quantum (and private classical) capacity of the channel $\mathcal{D}_{(1,\gamma_2,0)}$ w.r.t. γ_2. Region corresponding to the edge AC of Fig. 5.1.

us to (5.28), we can express its capacity as

$$\begin{aligned} Q(\mathcal{D}'_{(\gamma_2,\gamma_3)}) &= C_{\rm p}(\mathcal{D}'_{(\gamma_2,\gamma_3)}) = \max_{\hat\tau_{\rm diag}} \Big\{ S(\mathcal{D}'_{(\gamma_2,\gamma_3)}(\hat\tau_{\rm diag})) \\ &- S(\tilde{\mathcal{D}}'_{(\gamma_2,\gamma_3)}(\hat\tau_{\rm diag})) \Big\} = \mathcal{Q}(\gamma_2,\gamma_3), \end{aligned} \tag{5.51}$$

the last identity following from the fact that $\mathcal{D}'_{(\gamma_2,\gamma_3)}(\hat\tau_{\rm diag}))$ coincides with $\mathcal{D}_{(1,\gamma_2,\gamma_3)}(\hat\tau_{\rm diag})$ and by the fact that the positive component of the spectrum of $\tilde{\mathcal{D}}'_{(\gamma_2,\gamma_3)}(\hat\tau_{\rm diag})$ coincides with the one of $\tilde{\mathcal{D}}_{(1,\gamma_2,\gamma_3)}(\hat\tau_{\rm diag})$ (strictly speaking the above derivation holds true only in the degradable region (5.48) of $\mathcal{D}'_{(\gamma_2,\gamma_3)}(\hat\tau_{\rm diag}))$: still since $\mathcal{Q}(\gamma_2,\gamma_3)$ nullifies for $1-\gamma_2 \geq \gamma_3 \geq (1-\gamma_2)/2$, we can apply (5.51) also in the antidegradability region of the channel where $Q(\mathcal{D}'_{(\gamma_2,\gamma_3)}) = 0$).

As a concluding remark we comment on a special limit of the above construction obtained by setting $\gamma_2 = 0$: in this case we notice that the effective map (5.44) can be replaced with the quantum channel

$$\mathcal{D}'_{\gamma_3}(\hat\tau) = \begin{pmatrix} 1-(1-\gamma_3)\tau_{22} & \sqrt{1-\gamma_3}\tau_{02} \\ \sqrt{1-\gamma_3}\tau^*_{02} & (1-\gamma_3)\tau_{22} \end{pmatrix}, \tag{5.52}$$

which now maps the two-level system A′ into itself via a standard qubit ADC map with rate γ_3. Accordingly, following the same analysis we did before we can conclude that $Q(\mathcal{D}_{(1,0,\gamma_3)})$ coincides with the capacity value of the latter, computed in Ref. [GF05].

5.3.3 Double-decay qutrit MAD channel with $\gamma_2 = 0$

Here we consider the value of the capacity for $\vec{\gamma}$ belonging to the square surface ABED of Fig. 5.1, identified by the condition $\gamma_2 = 0$. From Eq. (5.5) we have that the Kraus operators for the MAD channel $\mathcal{D}_{(\gamma_1,0,\gamma_3)}$ are three:

$$\hat{K}_0 = \begin{pmatrix} 1 & 0 & 0 \\ 0 & \sqrt{1-\gamma_1} & 0 \\ 0 & 0 & \sqrt{1-\gamma_3} \end{pmatrix}, \quad \hat{K}_{01} = \begin{pmatrix} 0 & \sqrt{\gamma_1} & 0 \\ 0 & 0 & 0 \\ 0 & 0 & 0 \end{pmatrix},$$
$$\hat{K}_{03} = \begin{pmatrix} 0 & 0 & \sqrt{\gamma_3} \\ 0 & 0 & 0 \\ 0 & 0 & 0 \end{pmatrix} \tag{5.53}$$

while Eqs. (5.7) and (5.8) become

$$\mathcal{D}_{(\gamma_1,0,\gamma_3)}(\hat{\rho}) = \begin{pmatrix} \rho_{00} + \gamma_1\rho_{11} + \gamma_3\rho_{22} & \sqrt{1-\gamma_1}\rho_{01} & \sqrt{1-\gamma_3}\rho_{02} \\ \sqrt{1-\gamma_1}\rho_{01}^* & (1-\gamma_1)\rho_{11} & \sqrt{1-\gamma_1}\sqrt{1-\gamma_3}\rho_{12} \\ \sqrt{1-\gamma_3}\rho_{02}^* & \sqrt{1-\gamma_1}\sqrt{1-\gamma_3}\rho_{12}^* & (1-\gamma_3)\rho_{22} \end{pmatrix} \tag{5.54}$$

$$\tilde{\mathcal{D}}_{(\gamma_1,0,\gamma_3)}(\hat{\rho}) = \begin{pmatrix} 1 - \gamma_1\rho_{11} - \gamma_3\rho_{22} & \sqrt{\gamma_1}\rho_{01} & \sqrt{\gamma_3}\rho_{02} \\ \sqrt{\gamma_1}\rho_{01}^* & \gamma_1\rho_{11} & \sqrt{\gamma_1}\sqrt{\gamma_3}\rho_{12} \\ \sqrt{\gamma_3}\rho_{02}^* & \sqrt{\gamma_1}\sqrt{\gamma_3}\rho_{12}^* & \gamma_3\rho_{22} \end{pmatrix}. \tag{5.55}$$

As evident from Fig. 5.2 and from the formal structure of Eq. (5.54), for $\gamma_2 = 0$ the model exhibits a symmetry under the exchange of γ_1 and γ_3. Indeed, indicating with $\hat{V}$ the unitary gate that swaps levels $|2\rangle$ and $|3\rangle$ we have that

$$\mathcal{D}_{(\gamma_3,0,\gamma_1)}(\hat{\rho}) = \hat{V}\mathcal{D}_{(\gamma_1,0,\gamma_3)}(\hat{V}\hat{\rho}\hat{V}^\dagger)\hat{V}^\dagger\,, \tag{5.56}$$

which by data-processing inequality implies

$$Q(\mathcal{D}_{(\gamma_1,0,\gamma_3)}) = Q(\mathcal{D}_{(\gamma_3,0,\gamma_1)})\,, \tag{5.57}$$

with an analogous identity applying in the case of the private classical capacity. Following the procedure in Appendix B.1.1 we now observe that $\mathcal{D}_{(\gamma_1,0,\gamma_3)}$ is invertible for $\gamma_1, \gamma_3 < 1$, while $\tilde{\mathcal{D}}_{(\gamma_1,0,\gamma_3)} \circ \mathcal{D}^{-1}_{(\gamma_1,0,\gamma_3)}$ is CPTP for $\gamma_1, \gamma_3 \leq \frac{1}{2}$, implying that in this range of parameters the channel is degradable (region DEG of Fig. 5.5). Comparing Eqs. (5.54) with (5.55) we also realize that

$$\tilde{\mathcal{D}}_{(\gamma_1,0,\gamma_3)} = \mathcal{D}_{(1-\gamma_1,0,1-\gamma_3)}\,. \tag{5.58}$$

Therefore, by the same argument above, we can conclude that the channel is antidegradable for $\gamma_1, \gamma_3 \geq \frac{1}{2}$ (region ANTI-DEG of Fig. 5.5) so that $Q(\mathcal{D}_{(\gamma_1,0,\gamma_3)})$ is null for that range of values. Notice that resulting from Eq. (5.21) this translates to the following stronger statement:

$$Q(\mathcal{D}_{(\gamma_1,\gamma_2,\gamma_3)}) = C_{\rm p}(\mathcal{D}_{(\gamma_1,\gamma_2,\gamma_3)}) = 0\,, \quad \forall \gamma_1, \gamma_3 \geq \frac{1}{2}\,, \tag{5.59}$$

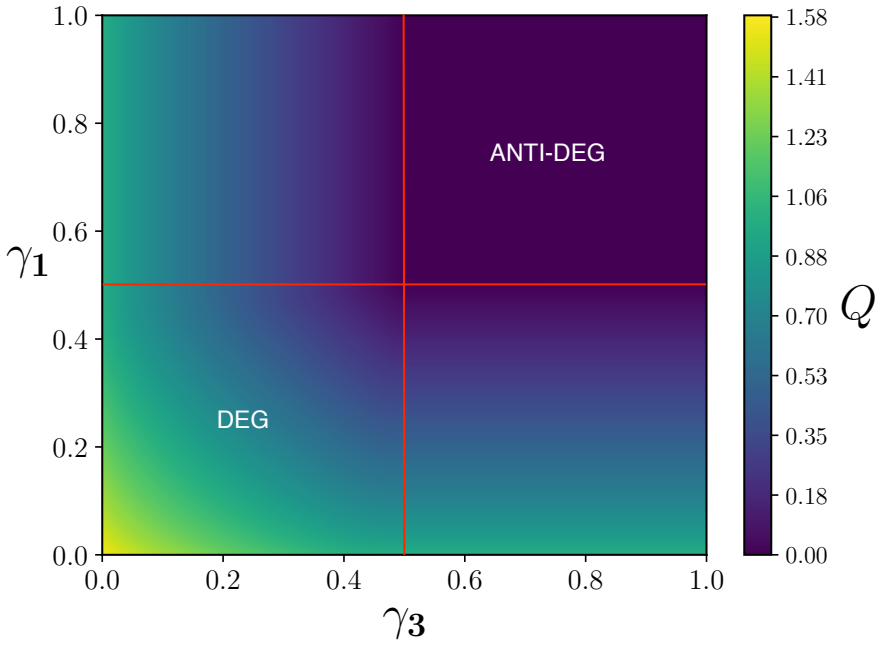

FIGURE 5.5: Quantum (and private classical) capacity for the channel $\mathcal{D}_{(\gamma_1,0,\gamma_3)}$ w.r.t. the damping parameters γ_1 and γ_3 – square surface ABED of Fig. 5.1. For $\gamma_1, \gamma_3 \leq 1/2$ (region DEG), the channel is degradable and its capacity Q is computed by solving numerically the maximization (5.60); for $\gamma_1, \gamma_3 \geq 1/2$ (region ANTI-DEG) instead it is explicitly antidegradable and its capacity is zero. Values in the SE and NW quadrants of the picture follow from the monotonicity behaviors Eq. (5.17) and by the symmetry (5.57): in particular in the SE sector the capacity is constant w.r.t. γ_1 (see Eq. (5.61)), while the NW is constant w.r.t. to γ_3.

(see green region of Fig. 5.6).

To evaluate $Q(\mathcal{D}_{(\gamma_1,0,\gamma_3)})$ and $C_{\mathrm{p}}(\mathcal{D}_{(\gamma_1,0,\gamma_3)})$ in the region DEG of Fig. 5.5, where the map $\mathcal{D}_{(\gamma_1,0,\gamma_3)}$ is provably degradable, we exploit Eq. (5.28) obtaining

$$\begin{aligned} Q(\mathcal{D}_{(\gamma_1,0,\gamma_3)}) &= C_{\mathrm{p}}(\mathcal{D}_{(\gamma_1,0,\gamma_3)}) \\ &= \max_{p_1,p_2} \Big\{ -[1-(1-\gamma_1)p_1+(1-\gamma_3)p_2]\log_2[1-(1-\gamma_1)p_1+(1-\gamma_3)p_2] \\ &\quad -(1-\gamma_1)p_1\log_2((1-\gamma_1)p_1) - (1-\gamma_3)p_2\log_2((1-\gamma_3)p_2) \\ &\quad +(1-\gamma_1p_1-\gamma_3p_2)\log_2(1-\gamma_1p_1-\gamma_3p_2) + \gamma_1p_1\log_2(\gamma_1p_1) + \gamma_3p_2\log_2(\gamma_3p_2)\Big\}, \end{aligned} \tag{5.60}$$

the maximization running over all possible values $p_1, p_2 \in [0,1]$ under the constraint that $p_1 + p_2 \leq 1$.

Notice that the capacities are known also on the borders of the parameters space, since when one of the rates is 0 we reduce to the single-decay MAD we solved in Sec. 5.3.1.

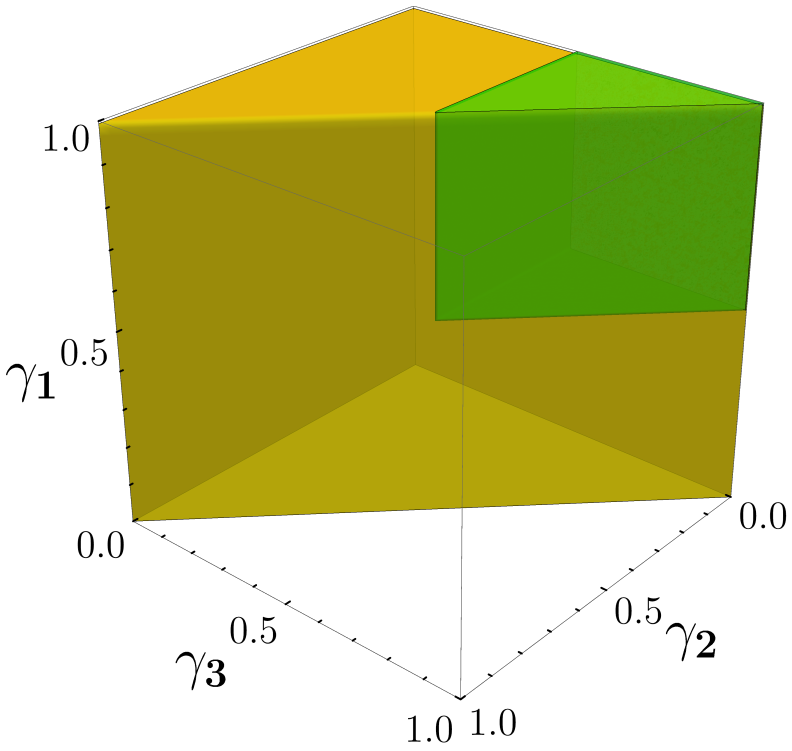

Figure 5.6: According to Eq. (5.59) all points included in the green region of the plot have zero quantum (and private classical) capacity.

When one of the rates is instead 1 we reduce to the MAD channel discussed in Sec. 5.3.2, for which Q is already available. More precisely in Sec. 5.3.2 we computed $Q(\mathcal{D}_{(1,0,\gamma_3)})$, verifying that it coincides with the capacity of the qubit ADC: the value of $Q(\mathcal{D}_{(\gamma_1,0,1)})$ follows from the latter via the symmetry (5.57). Since the value of Q is available also on the borders of the DEG region, we can now compare $Q(\mathcal{D}_{(\gamma_1,0,\gamma_3)})$ at $\gamma_3 = \frac{1}{2}$ and $\gamma_3 = 1$, for all $\gamma_1 \leq 1/2$. We find that the two are the same, i.e. $Q(\mathcal{D}_{(\gamma_1,0,1)}) = Q(\mathcal{D}_{(\gamma_1,0,1/2)})$, Accordingly, invoking the monotonicity constraint (5.17), we can finally conclude that

$$Q(\mathcal{D}_{(\gamma_1,0,1)}) = Q(\mathcal{D}_{(\gamma_1,0,\gamma_3)} \qquad \forall \gamma_3 \geq \frac{1}{2}\,, \tag{5.61}$$

which invoking the symmetry (5.57) allows us to evaluate the quantum capacity on the entire parameters region, see Fig. 5.5.

5.3.4 Double-decay qutrit MAD channel with $\gamma_1 = 0$

Here we consider the triangular surface DEF of Fig. 5.1. From Eq. (5.1) we have that the Kraus operators for the MAD channel $\mathcal{D}_{(0,\gamma_2,\gamma_3)}$ are three:

$$\hat{K}_0 = \begin{pmatrix} 1 & 0 & 0 \\ 0 & 1 & 0 \\ 0 & 0 & \sqrt{1-\gamma_2-\gamma_3} \end{pmatrix} \quad \hat{K}_{12} = \begin{pmatrix} 0 & 0 & 0 \\ 0 & 0 & \sqrt{\gamma_2} \\ 0 & 0 & 0 \end{pmatrix}$$
$$\hat{K}_{03} = \begin{pmatrix} 0 & 0 & \sqrt{\gamma_3} \\ 0 & 0 & 0 \\ 0 & 0 & 0 \end{pmatrix}. \tag{5.62}$$

The actions of $\mathcal{D}_{(0,\gamma_2,\gamma_3)}$ and its complementary counterpart $\tilde{\mathcal{D}}_{(0,\gamma_2,\gamma_3)}$ on a generic density matrix $\hat{\rho}$ can hence be described as

$$\mathcal{D}_{(0,\gamma_2,\gamma_3)}(\hat{\rho}) = \begin{pmatrix} \rho_{00}+\gamma_3\rho_{22} & \rho_{01} & \sqrt{1-\gamma_2-\gamma_3}\rho_{02} \\ \rho_{01}^* & \rho_{11}+\gamma_2\rho_{22} & \sqrt{1-\gamma_2-\gamma_3}\rho_{12} \\ \sqrt{1-\gamma_2-\gamma_3}\rho_{02}^* & \sqrt{1-\gamma_2-\gamma_3}\rho_{12}^* & (1-\gamma_2-\gamma_3)\rho_{22} \end{pmatrix}, \tag{5.63}$$

$$\tilde{\mathcal{D}}_{(0,\gamma_2,\gamma_3)}(\hat{\rho}) = \begin{pmatrix} 1-(\gamma_2+\gamma_3)\rho_{22} & \sqrt{\gamma_2}\rho_{12} & \sqrt{\gamma_3}\rho_{02} \\ \sqrt{\gamma_2}\rho_{12}^* & \gamma_2\rho_{22} & 0 \\ \sqrt{\gamma_3}\rho_{02}^* & 0 & \gamma_3\rho_{22} \end{pmatrix}, \tag{5.64}$$

(notice that in this case, differently of what happens with $\mathcal{D}_{(\gamma_1,0,\gamma_3)}$, the complementary channel is not an element of the MAD set). By close inspection of Eq. (5.63), and as intuitively suggested by Fig. 5.1, also these channels exhibit a symmetry analogous to the one reported in Eq. (5.56), but this time with $\hat{V}$ being the swap operation exchanging levels $|0\rangle$ and $|1\rangle$, which gives us

$$Q(\mathcal{D}_{(0,\gamma_2,\gamma_3)}) = Q(\mathcal{D}_{(0,\gamma_3,\gamma_2)}) \,, \tag{5.65}$$

and an analogous identity for the private classical capacity. Furthermore, as in the case of the single-decay qutrit MAD channel $\mathcal{D}_{(0,\gamma_2,0)}$, we notice that $\mathcal{D}_{(0,\gamma_2,\gamma_3)}$ has a noiseless subspace, given here by $\{|0\rangle, |1\rangle\}$, and we can establish the following lower bound:

$$C_{\mathrm{p}}(\mathcal{D}_{(0,\gamma_2,\gamma_3)}) \geq Q(\mathcal{D}_{(0,\gamma_2,\gamma_3)}) \geq \log_2(2) = 1 \,. \tag{5.66}$$

In particular this tells us that $\mathcal{D}_{(0,\gamma_2,\gamma_3)}$ cannot be antidegradable (the same conclusion can be obtained by noticing that [CRS08] the map $\tilde{\mathcal{D}}_{(\gamma_2,0,\gamma_3)}$ has a kernel that cannot be included into the kernel set of $\mathcal{D}_{(\gamma_2,0,\gamma_3)}$ – e.g. the former contains $|0\rangle\langle 1|$ while the latter does not).

Following the usual approach we find that $\mathcal{D}_{(0,\gamma_2,\gamma_3)}$ is invertible for $\gamma_2+\gamma_3 < 1$, and that $\tilde{\mathcal{D}}_{(0,\gamma_2,\gamma_3)} \circ \mathcal{D}^{-1}_{(0,\gamma_2,\gamma_3)}$ is CPTP for $\gamma_2+\gamma_3 \leq \frac{1}{2}$, which defines hence the degradability region for the map. So, invoking (5.28) we compute the quantum capacity in the

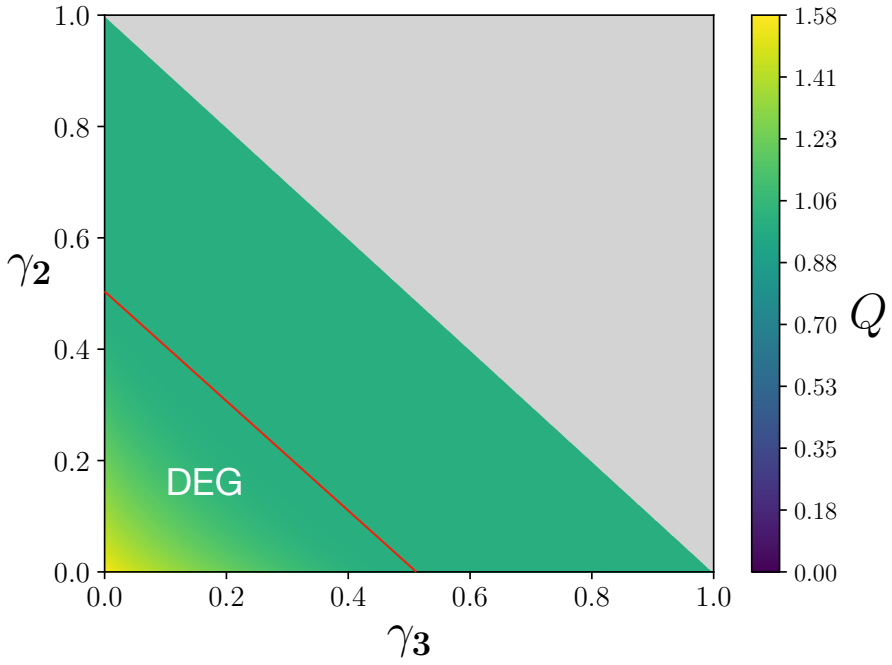

Figure 5.7: Quantum (and private classical) capacity of the channel $\mathcal{D}_{(0,\gamma_2,\gamma_3)}$ w.r.t. γ_2 and γ_3 – triangular surface DEF of Fig. 5.1. The DEG zone below the red curve, $\gamma_2+\gamma_3=\frac{1}{2}$, is the degradability region for the channel: here we compute $Q(\mathcal{D}_{(0,\gamma_2,\gamma_3)})$ solving numerically the maximization of Eq. (5.67). Above the red curve the channel capacity assumes constant value (5.66). Notice that the reported function exhibits the symmetry (5.65) and the monotonicity conditions (5.17). The grey zone indicates the non-accessible region (5.6).

degradability region as

$$\begin{aligned} Q(\mathcal{D}_{(0,\gamma_2,\gamma_3)}) &= C_{\rm p}(\mathcal{D}_{(0,\gamma_2,\gamma_3)}) \\ &= \max_{p_0,p_1}\Big\{ -(p_1+\gamma_2 p_2)\log_2(p_1+\gamma_2 p_2) \\ &\quad -[1-p_1-(1-\gamma_3)p_2]\log_2[1-p_1-(1-\gamma_3)p_2] \\ &\quad -(1-\gamma_2-\gamma_3)p_2\log_2((1-\gamma_2-\gamma_3)p_2) \\ &\quad +(1-(\gamma_2+\gamma_3)p_2)\log_2(1-(\gamma_2+\gamma_3)p_2) \\ &\quad +\gamma_2 p_2\log_2(\gamma_2 p_2)+\gamma_3 p_2\log_2(\gamma_3 p_2)\Big\}. \end{aligned} \tag{5.67}$$

Via numerical inspection we are also able to evaluate the magnitude of Q on the border of the degradability region, designated by $\gamma_2+\gamma_3=\frac{1}{2}$, showing that here it equals the lower bound (5.66). This, in addition to the monotonicity (5.17), allows us to conclude that $\mathcal{D}_{(0,\gamma_2,\gamma_3)}$ assumes the value 1 over all the region above the degradability borderline (red curve of Fig. 5.7), i.e.

$$\begin{aligned} Q(\mathcal{D}_{(0,\gamma_2,\gamma_3)}) \;&=\; C_{\rm p}(\mathcal{D}_{(0,\gamma_2,\gamma_3)})=1\,, \\ &\qquad \forall \gamma_2+\gamma_3\geq 1/2\,. \end{aligned} \tag{5.68}$$

5.3.5 The qutrit MAD channel on the $\gamma_2 + \gamma_3 = 1$ plane

Let us now consider the regime with $\gamma_2 + \gamma_3 = 1$ where rate vectors $\vec{\gamma}$ belong to the rectangular area BEFC of Fig. 5.1.

Under this condition the map (5.7) still admits four Kraus operators and becomes

$$\mathcal{D}_{(\gamma_1,\gamma_2,1-\gamma_2)}(\hat{\rho}) = \begin{pmatrix} \rho_{00}+\gamma_1\rho_{11}+(1-\gamma_2)\rho_{22} & \sqrt{1-\gamma_1}\rho_{01} & 0 \\ \sqrt{1-\gamma_1}\rho_{01}^* & (1-\gamma_1)\rho_{11}+\gamma_2\rho_{22} & 0 \\ 0 & 0 & 0 \end{pmatrix}. \tag{5.69}$$

We notice that the level $|2\rangle$ gets completely depopulated and that the channel can be expressed as

$$\mathcal{D}_{(\gamma_1,\gamma_2,1-\gamma_2)} = \mathcal{C} \circ \mathcal{D}_{\gamma_1} \ , \tag{5.70}$$

where $\mathcal{D}_{\gamma_1}$ is a standard qubit ADC channel connecting level $|1\rangle$ to level $|0\rangle$ with damping rate γ_1, while now $\mathcal{C}$ is a CPTP transformation sending the qutrit A to the qubit system spanned by vectors $|0\rangle, |1\rangle$ and completely erasing the level $|2\rangle$, moving its population in part to $|1\rangle$ and in part to $|0\rangle$, i.e.

$$\mathcal{C}(\hat{\rho}) \quad = \quad \begin{pmatrix} \rho_{00}+(1-\gamma_2)\rho_{22} & \rho_{01} \\ \rho_{10} & \rho_{11}+\gamma_2\rho_{22} \end{pmatrix}. \tag{5.71}$$

Accordingly the quantum capacity of $\mathcal{D}_{\gamma_1}$ computed in Ref. [GF05] is an explicit upper bound for $Q(\mathcal{D}_{(\gamma_1,\gamma_2,1-\gamma_2)})$ and $C_{\rm p}(\mathcal{D}_{(\gamma_1,\gamma_2,1-\gamma_2)})$ (remember that for the qubit ADC Q and $C_{\rm p}$ coincide). On the other hand, $Q(\mathcal{D}_{\gamma_1})$ is also a lower bound for $Q(\mathcal{D}_{(\gamma_1,\gamma_2,1-\gamma_2)})$ and $C_{\rm p}(\mathcal{D}_{(\gamma_1,\gamma_2,1-\gamma_2)})$ as its rate can be achieved by simply using input states of A that live on the subspace $\{|0\rangle, |1\rangle\}$. Consequently we can conclude that the following identity holds true

$$Q(\mathcal{D}_{(\gamma_1,\gamma_2,1-\gamma_2)}) = C_{\rm p}(\mathcal{D}_{(\gamma_1,\gamma_2,1-\gamma_2)}) = Q(\mathcal{D}_{\gamma_1}) \ , \tag{5.72}$$

as shown in Fig. 5.8.

5.3.6 Double-decay qutrit MAD channel with $\gamma_3 = 0$

Here we consider the square region CADF of Fig. 5.1 identified by $\gamma_3 = 0$. From Eq. (5.1) we have that the Kraus operators for $\mathcal{D}_{(\gamma_1,\gamma_2,0)}$ are three:

$$\hat{K}_0 = \begin{pmatrix} 1 & 0 & 0 \\ 0 & \sqrt{1-\gamma_1} & 0 \\ 0 & 0 & \sqrt{1-\gamma_2} \end{pmatrix} \quad \hat{K}_{01} = \begin{pmatrix} 0 & \sqrt{\gamma_1} & 0 \\ 0 & 0 & 0 \\ 0 & 0 & 0 \end{pmatrix}$$
$$\hat{K}_{02} = \begin{pmatrix} 0 & 0 & 0 \\ 0 & 0 & \sqrt{\gamma_2} \\ 0 & 0 & 0 \end{pmatrix}, \tag{5.73}$$

while the actions of $\mathcal{D}_{(\gamma_1,\gamma_2,0)}$ and $\tilde{\mathcal{D}}_{(\gamma_1,\gamma_2,0)}$ on a generic density matrix $\hat{\rho}$ are:

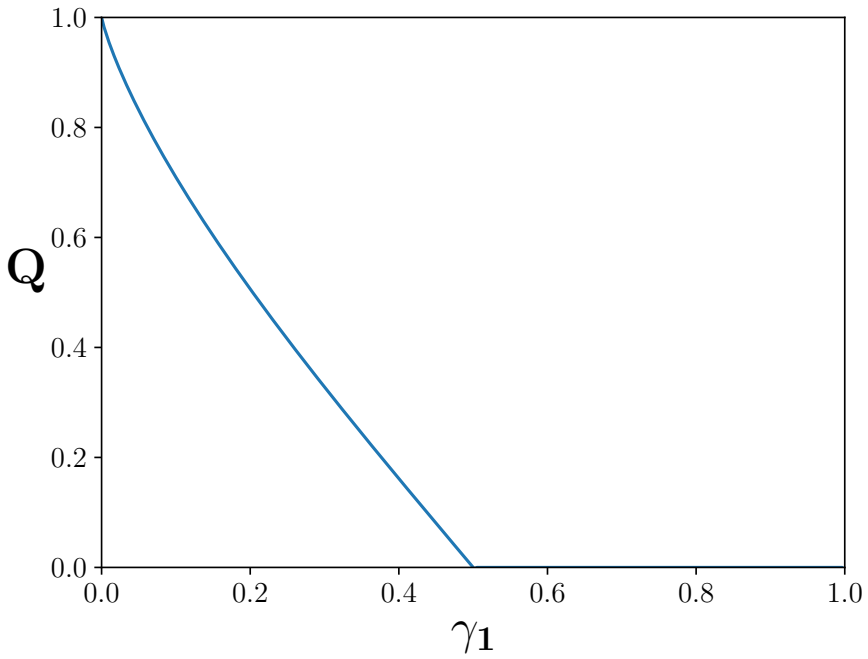

FIGURE 5.8: Evaluation of $Q(\mathcal{D}_{(\gamma_1,\gamma_2,1-\gamma_2)})$ w.r.t. γ_1, equivalent to the qubit ADC quantum capacity (i.e. the rectangular region BEFC of Fig. 5.1): as shown in Eq. (5.72) the capacity exhibits no dependence upon γ_2 in this case.

$$\mathcal{D}_{(\gamma_1,\gamma_2,0)}(\hat{\rho}) = \begin{pmatrix} \rho_{00}+\gamma_1\rho_{11} & \sqrt{1-\gamma_1}\rho_{01} & \sqrt{1-\gamma_2}\rho_{02} \\ \sqrt{1-\gamma_1}\rho_{01}^* & (1-\gamma_1)\rho_{11}+\gamma_2\rho_{22} & \sqrt{1-\gamma_1}\sqrt{1-\gamma_2}\rho_{12} \\ \sqrt{1-\gamma_2}\rho_{02}^* & \sqrt{1-\gamma_1}\sqrt{1-\gamma_2}\rho_{12}^* & (1-\gamma_2)\rho_{22} \end{pmatrix}, \quad (5.74)$$

$$\tilde{\mathcal{D}}_{(\gamma_1,\gamma_2,0)}(\hat{\rho}) = \begin{pmatrix} 1-\gamma_1\rho_{11}-\gamma_2\rho_{22} & \sqrt{\gamma_1}\rho_{01} & \sqrt{1-\gamma_1}\sqrt{\gamma_2}\rho_{02} \\ \sqrt{\gamma_1}\rho_{01}^* & \gamma_1\rho_{11} & 0 \\ \sqrt{1-\gamma_1}\sqrt{\gamma_2}\rho_{02}^* & 0 & \gamma_2\rho_{22} \end{pmatrix}. \quad (5.75)$$

At variance with the previous sections, we have that while $\mathcal{D}_{(\gamma_1,\gamma_2,0)}$ is invertible for $\gamma_1,\gamma_2 < 1$, for no range of these values the application $\tilde{\mathcal{D}}_{(\gamma_1,\gamma_2,0)} \circ \mathcal{D}^{-1}_{(\gamma_1,\gamma_2,0)}$ produces a CPTP map. We can hence conclude that the map is never degradable. About antidegradability, here also we have that $\ker\{\tilde{\mathcal{D}}_{(\gamma_1,\gamma_2,0)}\} \not\subseteq \ker\{\mathcal{D}_{(\gamma_1,\gamma_2,0)}\}$, so $\mathcal{D}_{(\gamma_1,\gamma_2,0)}$ is also not antidegradable [CRS08]. As a matter of fact the only cases for which we can produce explicit values of $Q(\mathcal{D}_{(\gamma_1,\gamma_2,0)})$ are the limiting cases where either γ_1 or γ_2 equals 0 (in these cases the map is a single-rate MAD channel discussed in Sec. 5.3.1), or 1 where instead the results of Sec. 5.3.2 or Sec. 5.3.5 can be applied. For the remaining cases we resort in presenting a lower bound for $Q(\mathcal{D}_{(\gamma_1,\gamma_2,0)})$ and $C_{\mathrm{p}}(\mathcal{D}_{(\gamma_1,\gamma_2,0)})$.

A straightforward approach is to exploit the right-hand-side of Eq. (5.28) and run them also outside the degradability region, in synthesis evaluating the maximum of the coherent information of $\mathcal{D}_{(\gamma_1,\gamma_2,0)}$ on the diagonal sources. Notice that since the map is not degradable, the coherent information is not necessarily concave and the restriction

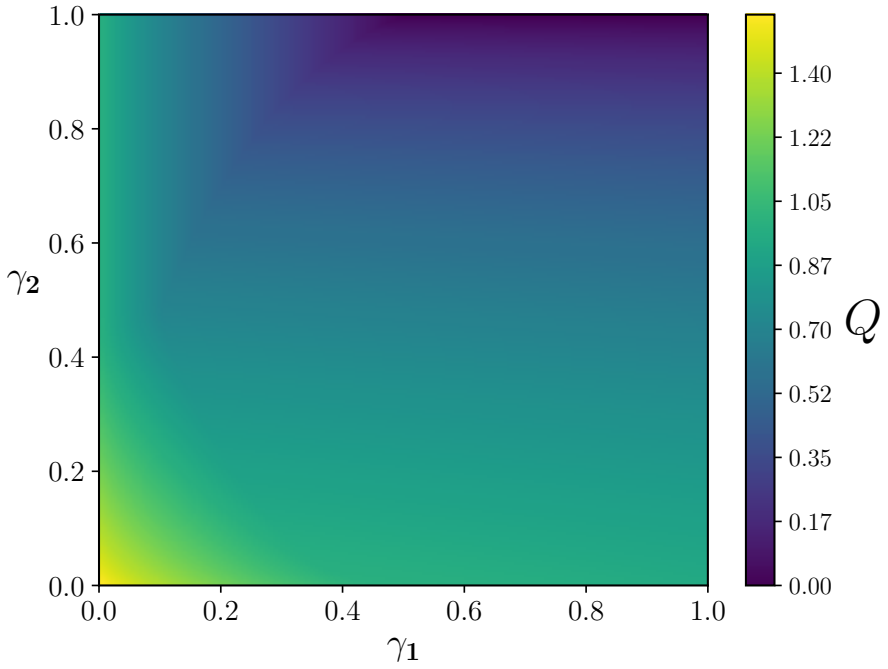

FIGURE 5.9: Numerical evaluation of a lower bound for $Q(\mathcal{D}_{(\gamma_1,\gamma_2,0)})$ (and $C_{\mathrm{p}}(\mathcal{D}_{(\gamma_1,\gamma_2,0)})$) obtained by maximizing the single use coherent information of the channel over all possible diagonal inputs – the parameters region corresponds to the CADF square of Fig. 5.1. Notice that reported plot does not fulfill the monotonicity constraint (5.17), hence explicitly proving that the function we present is certainly not the real capacity of the system.

to diagonal sources does not even guarantee that the computed expression corresponds to the true $Q^{(1)}(\mathcal{D}_{(\gamma_1,\gamma_2,0)})$ functional. Clearly the task can be refined as much as needed, e.g. by choosing less specific families of states or by computing $Q^{(i)}(\mathcal{D}_{(\gamma_1,\gamma_2,0)})$ for $i > 1$, but these aspects are beyond the focus of this work and will be considered in future research. The results we obtain are reported in Fig. (5.9).

5.4 Entanglement Assisted Quantum Capacity of qutrit MAD channels

For the sake of completeness the present section is devoted to studying the entanglement assisted quantum capacity $Q_{\mathrm{ea}}(\mathcal{D})$ of MAD CPTP maps which quantifies the amount of quantum information transmittable per channel use assuming the communicating parties to share an arbitrary amount of entanglement. A general introduction to the subject is presented in Appendix B.1.4 where we review some basic properties and derive a simplified expression which in the case of MAD channels of arbitrary dimension translates into

$$Q_E(\mathcal{D}) = \frac{1}{2} \max_{\hat{\rho}_{\mathrm{diag}}} \left\{ S(\hat{\rho}_{\mathrm{diag}}) + S(\mathcal{D}(\hat{\rho}_{\mathrm{diag}})) - S(\tilde{\mathcal{D}}(\hat{\rho}_{\mathrm{diag}})) \right\} , \tag{5.76}$$

where $\hat{\rho}_{\text{diag}}$ are input density matrices which are diagonal in the computational basis of the system. In the case of the single-rate qutrit MAD transformations this translates to solving the following maximization:

$$\begin{aligned} Q_{\text{ea}}(\mathcal{D}_{(\gamma_1,0,0)}) = \frac{1}{2}\max_{p_0,p_1}\Big\{ & -p_0\log_2 p_0 - p_1\log_2 p_1 \\ & -2(p_0+\gamma_1 p_1)\log_2(p_0+\gamma_1 p_1) \\ & -(1-\gamma_1)p_1\log_2((1-\gamma_1)p_1) \\ & +(1-\gamma_1 p_1)\log_2(1-\gamma_1 p_1)+\gamma_1 p_1\log_2(\gamma_1 p_1)\Big\}, \end{aligned} \tag{5.77}$$

the result being reported in Fig. 5.10 a). In a similar fashion we also numerically compute Q_{ea} for all the two-rate qutrit MAD channels scenarios we analyzed in the previous sections, reporting the associated results in Fig. 5.10 b), c), d). Notice that also the three-rate qutrit MAD channels Q_{ea} can be computed but not easily visualized, hence it's not reported.

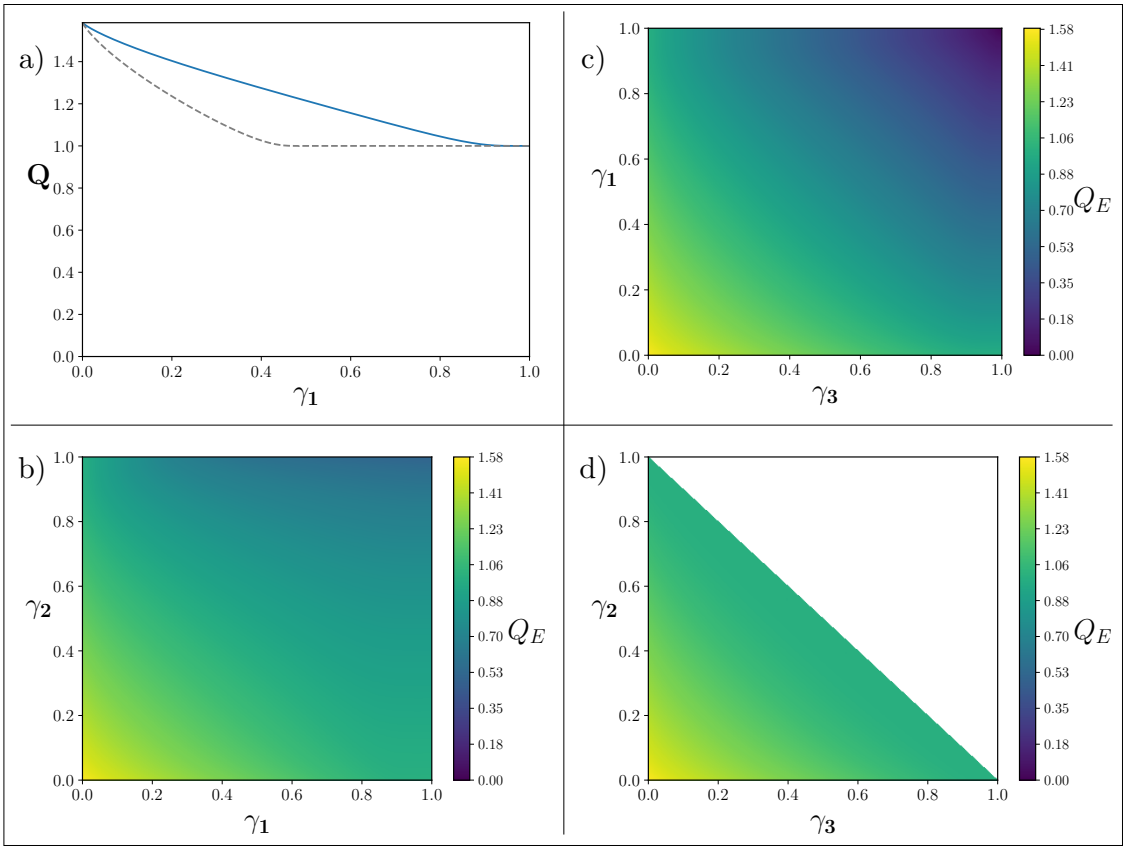

FIGURE 5.10: **a)** Profile of the entanglement assisted quantum capacity $Q_{\text{ea}}(\mathcal{D}_{(\gamma_1,0,0)})$ w.r.t. the damping parameter γ_1 (results should be compared with those of Fig. 5.2 where we present $Q(\mathcal{D}_{(\gamma_1,0,0)})$ and $C_{\text{p}}(\mathcal{D}_{(\gamma_1,0,0)})$). Notice that also in this case the expression fulfills the monotonicity constraint (5.13). In **b)**, **c)**, **d)** Entanglement assisted quantum capacity for the CADF square region of Fig. 5.1, for the ABED region, and for the DEF region, respectively.

5.5 Conclusions

We introduce a finite dimensional generalization of the qubit ADC model which represents one of the most studied examples of quantum noise in quantum information theory. In this context the quantum (and private classical) capacity of a large class of quantum channels (namely the qutrit MAD channels) has been explicitly computed, vastly extending the set of models whose capacity is known: : this effort in particular includes some non-trivial examples of quantum maps which are explicitly non-degradable (neither antidegradable) – see e.g. the results of Sec. 5.3.3. Besides allowing generalizations to higher dimensional systems (see e.g. Ref. [CG21a]), the analysis here presented naturally spawns further research, e.g. extending it to include other capacity measures, such as the classical capacity or the two-way quantum capacity [KSW20, PLOB17]. We finally conclude by noticing that the MAD channel scheme discussed in the present Chapter can be also easily adapted to include generalizations of the (qubit) generalized amplitude

damping channel scheme [KSW20], by allowing reverse *damping* processes which promote excitations from lower to higher levels that could mimic, e.g., thermalization events.

6

Resonant multi-level amplitude damping channels, a capacity analysis

Preface

What follows is based on the yet unpublished paper:

- S. Chessa, V. Giovannetti, Resonant multi-level amplitude damping channels, *in preparation*, 2022.

The work that constitute this chapter saw the light as an evolution and a follow-up of the topic encountered in Chapter 5. The underlying motivations are the same: higher dimensional quantum channels have been overlooked in the early stages of Quantum Information, but now they are becoming increasingly relevant. With respect to the previous chapter though we approach in a different way the construction of the channel, postulating (reasonably) the action of the Stinespring unitary representation on our system and the associated environment. What we show is that in higher dimensional systems, due to the increased margin for action allowed by the larger number of degrees of freedom, the physically plausible processes that can affect quantum systems are more than expected. We show that amplitude damping in qudits don't reduce to those channels identified by the Kraus structure laid out in Chapter 5. We characterize this additional damping channels that we call Resonant multi-level amplitude (ReMAD) damping channels.

6.1 Intro

As discussed in Chapter 3 and in the previous Chapter, the literature has evolved to find capacities bounds and to find channel properties to be leveraged in order to overcome the difficulties of the direct computation or at least provide meaningful upper bounds. Among others, concerning the unassisted quantum and private classical capacities, we find: degradability [DS05], antidegradability [CG06], weak degradability [CG06], existence of additive extensions [SS08], conjugate degradability [BDHM10], being less noisy or more capable [Wat12], partial degradability [Gyo14], approximate degradability [SSWR17], allowing teleportation-stretching [PLOB17], being unital [Ans17], existence of low noise approximations [LLS18b]. In this sense a corpus of literature is being built with the aim to produce efficiently computable bounds and approximations of these capacities, see e.g. [TWW17, WTB17, CMH17, WFD19, HRF20, FF21, HL22, FST22]. Coherently with this perspective, the main results of this work are related to the study of degradability and the estimation of the quantum capacity Q and the private classical capacity C_p of a new class of qudit channels that we introduce in the following.

Qudit systems have captured increasing interest in the community of Quantum Information science. This is because they have been proven to provide advantages in terms of communication and cryptography (see e.g. [CDLBO19] and references therein) and of computation (see e.g. [WHSK20] and references therein), with qutrits that recently made their first appearance on commercial quantum devices [Hil21]. Despite this fact, except for a small number of very fundamental channels, the landscape of higher dimensional channels describing physical noise and the computation of their information capacities is still relatively unexplored. Concerning the unassisted quantum and private classical capacities, significant results have been obtained in: bounds for the qudit depolarizing channel [FKG20] bounds for qudit Pauli channels [KFG22], degradability conditions for qudit dephasing channels [DS05] and qudit dephasing with memory effects [DBF07], degradability and antidegradability conditions for multi-level amplitude damping (MAD) channels [CG21b], degradability and antidegradability conditions for combinations of MAD and dephasing channels and in general direct-sum compositions of quantum channels [CG21a], channels hybridizations in higher dimensions that allow the exact computation of capacities [LLS+22a], more general results regarding the degradability of channels with specific input/output dimensions [CRS08], results on the positivity of the quantum capacity (or complementary quantum capacity) of MAD channels, qudit Pauli channels, qudit depolarizing channels [SD22]. It's clear then that the number of noise models exactly characterized in terms of quantum (and private classical) capacity is still limited, often restricted to specific input dimensions. What we are here to argue is that, other than this lack of knowledge, in the context of higher dimensional systems also realistic noise models are still ignored when not directly derived from the qubit setting. We provide here an instance of this kind of models by describing what we called Resonant multi-level amplitude damping (ReMAD) channels. This class of channels behaves as an usual amplitude damping channel on the populations but exhibits a nontrivial effect on the coherences that is not present in other known damping channels. It describes an exchange of excitations mediated by an interaction of the type $\sigma_{\mathrm{S}}^{-} \otimes \sigma_{\mathrm{E}}^{+}$ between a system

S and an environment E, both d dimensional. As we'll see, the "mixing" action on the coherences is such that there is no qubit counterpart for such channels.
We show that these channels can be degradable or antidegradable in large portions of the allowed parameter space and, taking the case of $d = 3$ as an example, there we compute exactly Q and C_p.

The Chapter is structured as follows: in Sec. 6.2 we define ReMAD channels, their complementary channels and their composition rules; in Sec. 6.3 we address the issue of degradability, antidegradability and the computation of Q and C_p; conclusions are drawn in Sec. 6.4.

6.2 Definitions

6.2.1 Channel

Let $\mathcal{H}_{\mathrm{S}}$ be the Hilbert space associated with a system S and $\mathfrak{S}(\mathcal{H}_{\mathrm{S}})$ the related convex hull of density operators. We can specify the action of a completely positive and trace preserving (CPTP) linear map [Cho75] (quantum channel) $\Phi : \mathcal{L}(\mathcal{H}_{\mathrm{S}}) \to \mathcal{L}(\mathcal{H}_{\mathrm{S}'})$ over a density matrix $\hat{\rho} \in \mathfrak{S}(\mathcal{H}_{\mathrm{S}})$ by: explicitly giving $\Phi(\hat{\rho})$, expressing the Kraus operators set [Kra71] or expressing its Stinespring representation [Sti55].
If we wanted to generalize the action of the qubit amplitude damping channel to qudits the most immediate procedure would be, as done in [CG21b], to enlarge the set of Kraus operators in order to include each desired damping process between levels. This procedure generates MAD channels. Assuming to deal with a minimal Kraus set, fixing the number of Kraus operators also fixes the Stinespring representation and the environment size. So for a generic d dimensional MAD channel we'd have $d(d-1)/2$ damping processes, $d(d-1)/2+1$ Kraus operators and $d(d-1)/2+1$ dimensional environment. In this scenario each damping transition in the system S induces an excitation on the environment E from the ground state to one of the excited levels. Each transition in S excites a different level in E.
We could think instead of going the other way around and derive the channel by directly imposing its damping effects on the levels of S and E. This is equivalent to fixing first the Stinespring dilation of the channel. To do so we need to assume the environment to be in a pure state. Without loss of generality we choose the pure state to be $|0\rangle_{\mathrm{E}}$. For a generic qudit system, the transitions we consider are

$$|0\rangle_{\mathrm{S}}|0\rangle_{\mathrm{E}} \to |0\rangle_{\mathrm{S}}|0\rangle_{\mathrm{E}} \ , \qquad |j\rangle_{\mathrm{S}}|0\rangle_{\mathrm{E}} \to \sqrt{1-\sum_{k<j}\gamma_{jk}}\,|j\rangle_{\mathrm{S}}|0\rangle_{\mathrm{E}} + \sum_{k=1}^{j}\sqrt{\gamma_{j,j-k}}\,|j-k\rangle_{\mathrm{S}}|k\rangle_{\mathrm{E}} \ . \tag{6.1}$$

where the coefficients γ_{ji} represent the transition probabilities from level j to i, with $j > i$. They are real coefficients and are constrained as:

$$0 \le \gamma_{ji} \le 1 \ , \qquad \sum_{k<j}\gamma_{jk} \le 1 \ . \tag{6.2}$$

In the case of a qutrit Eqs. (6.1) reduce to

$$\begin{aligned}
&|0\rangle_S|0\rangle_E \to |0\rangle_S|0\rangle_E \\
&|1\rangle_S|0\rangle_E \to \sqrt{1-\gamma_{10}}\,|1\rangle_S|0\rangle_E + \sqrt{\gamma_{10}}\,|0\rangle_S|1\rangle_E \\
&|2\rangle_S|0\rangle_E \to \sqrt{1-\gamma_{21}-\gamma_{20}}\,|2\rangle_S|0\rangle_E + \sqrt{\gamma_{20}}\,|0\rangle_S|2\rangle_E + \sqrt{\gamma_{21}}\,|1\rangle_S|1\rangle_E\ .
\end{aligned} \tag{6.3}$$

These transitions capture the interaction between two d-dimensional systems for which energy spacing between levels is uniform, transferring excitations from the system S to the environment E. Notice how here we have a d-dimensional environment, while in the case of MAD channels we had a $d(d-1)/2+1$ dimensional environment, see Fig. 6.1. The two processes are not physically equivalent.

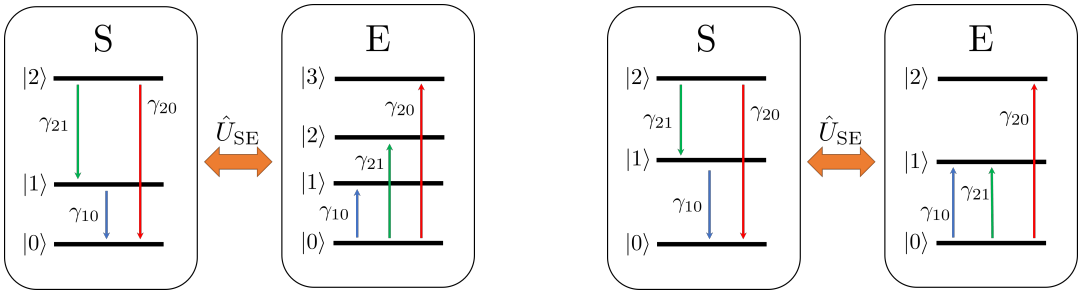

FIGURE 6.1: **Left:** depiction of the MAD excitations exchange between the system S and the environment E. **Right:** depiction of the ReMAD excitations exchange between the system S and the environment E, notice the environment size.

What makes this noise model interesting is its simplicity and the fact that it can emerge in a variety of scenarios. To enumerate some of the ones relevant in quantum information processing and quantum communications we can mention: atomic systems in quantum memories and quantum repeaters [HSP10, SSdRG11, RR15], optical qudits transmitted through lines such as optical fibers with polarization dependent losses [Dam05], optical qudits interacting with beam splitters and qudits encoded in harmonic oscillators [GKP01, BdGS02], see [TCV20, CMW+21] and references therein for applications and implementations of bosonic codes.

As already discussed, once we specify the Stinespring representation of our channel we can retrieve also the Kraus set. So, from Eq. (6.1) we can infer the Stinespring dilation for the channel and, from that, the Kraus operators. In general, at dimension d we have a diagonal Kraus operator $\hat{K}_0^d$ and $d-1$ non diagonal operators $\hat{K}_i^d$ (see Appendix C.1 for details), expressed as

$$\hat{K}_0^d = \sum_{l=0}^{d-1} \sqrt{1-\sum_{m<l}\gamma_{lm}}\,|l\rangle\langle l|\ , \qquad \hat{K}_i^d = \sum_{l=0}^{d-i-1} \sqrt{\gamma_{i+l,l}}\,|l\rangle\langle i+l|\ . \tag{6.4}$$

For the qutrit setting we will have then

$$\hat{K}_0 = \begin{pmatrix} 1 & 0 & 0 \\ 0 & \sqrt{1-\gamma_{10}} & 0 \\ 0 & 0 & \sqrt{1-\gamma_{21}-\gamma_{20}} \end{pmatrix}, \quad \hat{K}_1 = \begin{pmatrix} 0 & \sqrt{\gamma_{10}} & 0 \\ 0 & 0 & \sqrt{\gamma_{21}} \\ 0 & 0 & 0 \end{pmatrix}, \quad \hat{K}_2 = \begin{pmatrix} 0 & 0 & \sqrt{\gamma_{20}} \\ 0 & 0 & 0 \\ 0 & 0 & 0 \end{pmatrix}. \tag{6.5}$$

We can see how, unlike MAD channels, some of the non diagonal Kraus operators can allow more than one decay rate γ_{ij}.
Now, by applying Kraus operators to a generic density matrix $\hat{\rho}$ we retrieve the overall action of the channel:

$$\Phi_{\vec{\gamma}}(\hat{\rho}) = \sum_{i=0}^{d-1} \hat{K}_i \hat{\rho} \hat{K}_i^\dagger \,, \tag{6.6}$$

we denoted by $\vec{\gamma}$ the set of all decay rates γ_{ij}. By exploiting the expressions for the Kraus operators in Eq. (6.4), in arbitrary dimensions d we can compactly state the components of the channel output $\Phi_{\vec{\gamma}}(\hat{\rho})$ as:

$$\begin{aligned}
[\Phi_{\vec{\gamma}}(\hat{\rho})]_{00} &= \rho_{00} + \sum_{l=0}^{d-1} \gamma_{l0}\rho_{ll} \,, \\
[\Phi_{\vec{\gamma}}(\hat{\rho})]_{jj} &= (1 - \sum_{l<j} \gamma_{jl})\rho_{jj} + \sum_{l=1}^{d-j-1} \gamma_{l+j,j}\rho_{l+j,l+j} \,, \\
[\Phi_{\vec{\gamma}}(\hat{\rho})]_{0j} &= \sqrt{1 - \sum_{l<j} \gamma_{jl}}\rho_{0j} + \sum_{l=1}^{d-j-1} \sqrt{\gamma_{l0}}\sqrt{\gamma_{l+j,j}}\rho_{l,l+j} \,, \\
[\Phi_{\vec{\gamma}}(\hat{\rho})]_{ij} &= \sqrt{1 - \sum_{l<i} \gamma_{il}}\sqrt{1 - \sum_{l<j} \gamma_{jl}}\rho_{ij} + \sum_{l=1}^{d-j-1} \sqrt{\gamma_{l+i,i}}\sqrt{\gamma_{l+j,j}}\rho_{l+i,l+j} \,,
\end{aligned} \tag{6.7}$$

where in the last line we assumed $i < j$.
To give an intuition of the action of this kind of channels we explicitly show how the qutrit version behaves on a generic density matrix:

$$\Phi_{\vec{\gamma}}(\hat{\rho}) = \begin{pmatrix} \rho_{00} + \gamma_{10}\rho_{11} + \gamma_{20}\rho_{22} & \sqrt{1-\gamma_{10}}\rho_{01} + \sqrt{\gamma_{10}\gamma_{21}}\rho_{12} & \sqrt{1-\gamma_{21}-\gamma_{20}}\rho_{02} \\ \sqrt{1-\gamma_{10}}\rho_{01}^* + \sqrt{\gamma_{10}\gamma_{21}}\rho_{12}^* & (1-\gamma_{10})\rho_{11} + \gamma_{21}\rho_{22} & \sqrt{(1-\gamma_{10})(1-\gamma_{21}-\gamma_{20})}\rho_{12} \\ \sqrt{1-\gamma_{21}-\gamma_{20}}\rho_{02}^* & \sqrt{(1-\gamma_{10})(1-\gamma_{21}-\gamma_{20})}\rho_{12}^* & (1-\gamma_{21}-\gamma_{20})\rho_{22} \end{pmatrix}. \tag{6.8}$$

As you can observe, on the diagonal elements we have the usual decay of populations from higher to lower levels typical of amplitude damping channels. On off-diagonal elements though we can see that there is a coherence mixing which is not contemplated in qubit (you have only one coherence term) or MAD channels. This phenomenon represents another signature of the fact that we are dealing with a different underlying physical process.

To this class of channels belongs a simple group of amplitude damping channels that was already discussed in the literature but that was not recognized as a member

of a more general class. In [Ouy14] were introduced the so called *beam splitter type* amplitude damping channels. This kind of amplitude damping channels describes the evolution of a qudit encoded in the first d states in the Fock basis of an harmonic oscillator passing through a beam splitter of transmittance γ. It's straightforward to verify that the j-th level (Fock state with j photons) will decay into the i-th level with probability $p_{ji} = \binom{j}{i}\gamma^{n-i}(1-\gamma)^i$ and consequently $\gamma_{ji} = \sqrt{p_{ji}}$. At variance with the parameter γ these channels constitute a subclass of the ReMAD channels. We show in Fig. 6.2 their configuration in the parameters space for the qutrit case. These channels were shown to be degradable for $\gamma \geq 1/2$ and antidegradable for $\gamma \leq 1/2$ (see Sec. 6.3 and Appendix C.2 for definitions and discussion of these properties), we'll show how these properties can be extended to channels with unconstrained values of γ_{ji}.

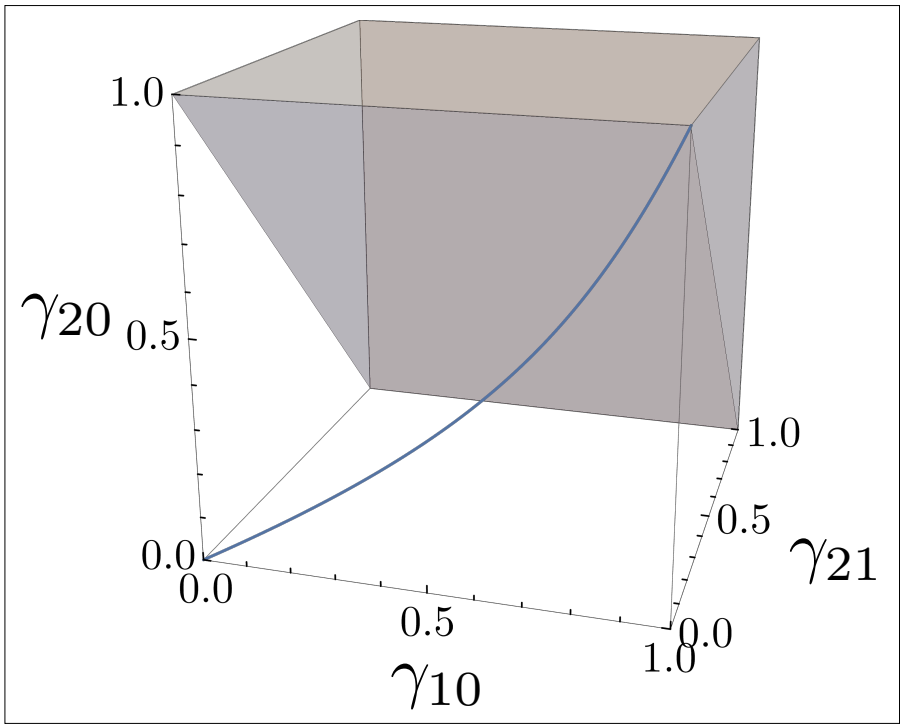

Figure 6.2: Set of beam splitter type amplitude damping channels in the parameters space for a qutrit (blue line).

6.2.2 Complementary channel

From the Kraus operators we can also retrieve the complementary channel $\tilde{\Phi}_{\vec{\gamma}}$ (see Appendix C.1), resulting in

$$
\begin{aligned}
[\tilde{\Phi}_{\vec{\gamma}}(\hat{\rho})]_{00} &= \rho_{00} + \sum_{l=0}^{d-1}(1 - \sum_{m<l}\gamma_{lm})\rho_{ll} \ , \\
[\tilde{\Phi}_{\vec{\gamma}}(\hat{\rho})]_{jj} &= \gamma_{j0}\rho_{jj} + \sum_{l=1}^{d-j-1}\gamma_{l+j,l}\rho_{l+j,l+j} \ , \\
[\tilde{\Phi}_{\vec{\gamma}}(\hat{\rho})]_{0j} &= \sqrt{\gamma_{j0}}\rho_{0j} + \sum_{l=1}^{d-j-1}\sqrt{1 - \sum_{m<l}\gamma_{lm}}\sqrt{\gamma_{l+j,l}}\rho_{l,l+j} \ , \\
[\tilde{\Phi}_{\vec{\gamma}}(\hat{\rho})]_{ij} &= \sqrt{\gamma_{i0}}\sqrt{\gamma_{j0}}\rho_{ij} + \sum_{l=1}^{d-j-1}\sqrt{\gamma_{l+i,l}}\sqrt{\gamma_{l+j,l}}\rho_{l+i,l+j} \ ,
\end{aligned}
\tag{6.9}
$$

with $i < j$ in the last line. By inspection we can see that the complementary channel of a ReMAD channel is itself a ReMAD channel. In particular $\tilde{\Phi}_{\vec{\gamma}}$ can be put in correspondence with $\Phi_{\vec{\gamma}}$ by transforming the decay rates a s follows:

$$
\gamma_{l0} \to 1 - \sum_{m<l}\gamma_{lm} \ , \qquad \gamma_{l+j,j} \to \gamma_{l+j,l} \ . \tag{6.10}
$$

Again, we can check an instance of this behaviour in the qutrit setting by comparing Eq. (6.8) and Eq. (6.11):

$$
\tilde{\Phi}_{\vec{\gamma}}(\hat{\rho}) = \begin{pmatrix}
\rho_{00} + (1-\gamma_{10})\rho_{11} + (1-\gamma_{21}-\gamma_{20})\rho_{22} & \sqrt{\gamma_{10}}\rho_{01} + \sqrt{(1-\gamma_{10})\gamma_{21}}\rho_{12} & \sqrt{\gamma_{20}}\rho_{02} \\
\sqrt{\gamma_{10}}\rho_{01}^* + \sqrt{(1-\gamma_{10})\gamma_{21}}\rho_{12}^* & \gamma_{10}\rho_{11} + \gamma_{21}\rho_{22} & \sqrt{\gamma_{10}\gamma_{20}}\rho_{12} \\
\sqrt{\gamma_{20}}\rho_{02}^* & \sqrt{\gamma_{10}\gamma_{20}}\rho_{12}^* & \gamma_{20}\rho_{22}
\end{pmatrix} . \tag{6.11}
$$

6.2.3 Composition rules

Since MAD channels are closed under composition we could ask ourselves whether ReMAD channels behave similarly. Given two ReMAD channels $\Phi_{\vec{\eta}}$ and $\Phi_{\vec{\gamma}}$, is the composed channel $\Phi_{\vec{\eta}} \circ \Phi_{\vec{\gamma}}$ still a ReMAD channel? Maybe surprisingly, it turns out that it's not always the case.

The shape of a generic $\Phi_{\vec{\eta}} \circ \Phi_{\vec{\gamma}}$ can be obtained by applying Eqs. (6.7) that yield:

$$
\begin{aligned}
[\Phi_{\vec{\eta}} \circ \Phi_{\vec{\gamma}}(\hat{\rho})]_{00} &= \rho_{00} + \sum_{l=0}^{d-1} \eta_{l0}(1 - \sum_{m<l} \gamma_{lm})\rho_{ll} + \sum_{l=1}^{d-1}\sum_{m=1}^{d-l-1} \eta_{l0}\gamma_{l+m,l}\rho_{l+m,l+m} \ , \\
[\Phi_{\vec{\eta}} \circ \Phi_{\vec{\gamma}}(\hat{\rho})]_{jj} &= (1 - \sum_{l<j} \eta_{jl}) \left[(1 - \sum_{l<j} \gamma_{jl})\rho_{jj} + \sum_{l=1}^{d-j-1} \gamma_{l+j,j}\rho_{l+j,l+j} \right] + \\
&\quad + \sum_{l=1}^{d-j-1} \eta_{l+j,j} \left[(1 - \sum_{m<l+j} \gamma_{l+j,m})\rho_{l+j,l+j} + \sum_{m=1}^{d-(l+j)-1} \gamma_{m+l+j,l+j}\rho_{m+l+j,m+l+j} \right] \ , \\
[\Phi_{\vec{\eta}} \circ \Phi_{\vec{\gamma}}(\hat{\rho})]_{0j} &= \sqrt{1 - \sum_{l<j} \eta_{jl}} \left[\sqrt{1 - \sum_{l<j} \gamma_{jl}}\rho_{0j} + \sum_{l=1}^{d-j-1} \sqrt{\gamma_{l0}}\sqrt{\gamma_{l+j,j}}\rho_{l,l+j} \right] + \\
&\quad + \sum_{l=1}^{d-j-1} \sqrt{\eta_{l0}}\sqrt{\eta_{l+j,j}} \Big[\sqrt{1 - \sum_{m<l} \gamma_{lm}} \sqrt{1 - \sum_{m<l+j} \gamma_{l+j,m}}\rho_{l,l+j} + \\
&\quad + \sum_{m=1}^{d-(l+j)-1} \sqrt{\gamma_{m+l,l}}\sqrt{\gamma_{m+l+j,l+j}}\rho_{m+l,m+l+j} \Big] \ , \\
[\Phi_{\vec{\eta}} \circ \Phi_{\vec{\gamma}}(\hat{\rho})]_{ij} &= \sqrt{1 - \sum_{l<i} \eta_{il}} \sqrt{1 - \sum_{l<j} \eta_{jl}} \left[\sqrt{1 - \sum_{l<i} \gamma_{il}} \sqrt{1 - \sum_{l<j} \gamma_{jl}}\rho_{ij} + \sum_{l=1}^{d-j-1} \sqrt{\gamma_{l+i,i}}\sqrt{\gamma_{l+j,j}}\rho_{l+i,l+j} \right] + \\
&\quad + \sum_{l=1}^{d-j-1} \sqrt{\eta_{l+i,i}}\sqrt{\eta_{l+j,j}} \left[\sqrt{1 - \sum_{m<l+i} \gamma_{l+i,m}} \sqrt{1 - \sum_{m<l+j} \gamma_{l+j,m}}\rho_{l+i,l+j} + \right. \\
&\quad \left. + \sum_{m=1}^{d-(l+j)-1} \sqrt{\gamma_{m+l+i,l+i}}\sqrt{\gamma_{m+l+j,l+j}}\rho_{m+l+i,m+l+j} \right] \ .
\end{aligned}
\tag{6.12}
$$

We can see that these expressions are a little bit too much convoluted to be addressed generally in a meaningful way. To prove our point though we just need to show that for a specific instance of Eqs. (6.12) composition rules are nontrivial. To do so we analyze the simplest non qubit case of $d = 3$. Applying Eqs. (6.12) on the composition of two qutrit channels as the on in Eq. (6.8) we get

$$
\begin{aligned}
[\Phi_{\vec{\eta}} \circ \Phi_{\vec{\gamma}}(\hat{\rho})]_{00} &= \rho_{00} + (\eta_{10}\gamma_{10} + 1 - \gamma_{10})\rho_{11} + (\eta_{10}\gamma_{21} + \eta_{20}\gamma_{20} + 1 - \gamma_{21} - \gamma_{20})\rho_{22} \ , \\
[\Phi_{\vec{\eta}} \circ \Phi_{\vec{\gamma}}(\hat{\rho})]_{01} &= \sqrt{1 - \eta_{10}}\sqrt{1 - \gamma_{10}}\rho_{01} + (\sqrt{\eta_{10}\eta_{21}(1 - \gamma_{10})(1 - \gamma_{21} - \gamma_{20})} + \sqrt{\gamma_{10}\gamma_{21}(1 - \eta_{10})})\rho_{12} \ , \\
[\Phi_{\vec{\eta}} \circ \Phi_{\vec{\gamma}}(\hat{\rho})]_{02} &= \sqrt{1 - \eta_{21} - \eta_{20}}\sqrt{1 - \gamma_{21} - \gamma_{20}}\rho_{02} \ , \\
[\Phi_{\vec{\eta}} \circ \Phi_{\vec{\gamma}}(\hat{\rho})]_{11} &= (1 - \eta_{10})(1 - \gamma_{10})\rho_{11} + [\eta_{21}(1 - \gamma_{21} - \gamma_{20}) + (1 - \eta_{10})\gamma_{21}]\rho_{22} \ , \\
[\Phi_{\vec{\eta}} \circ \Phi_{\vec{\gamma}}(\hat{\rho})]_{12} &= \sqrt{(1 - \eta_{10})(1 - \eta_{21} - \eta_{20})}\sqrt{(1 - \gamma_{10})(1 - \gamma_{21} - \gamma_{20})}\rho_{12} \ , \\
[\Phi_{\vec{\eta}} \circ \Phi_{\vec{\gamma}}(\hat{\rho})]_{22} &= (1 - \eta_{21} - \eta_{20})(1 - \gamma_{21} - \gamma_{20})\rho_{22} \ ,
\end{aligned}
\tag{6.13}
$$

plus the Hermitian conjugate of off-diagonal elements.
We are interested in understanding whether a set of parameters $\vec{\delta}$ exists or not such that we are able to construct a ReMAD channel $\Phi_{\vec{\delta}} = \Phi_{\vec{\eta}} \circ \Phi_{\vec{\gamma}}$. Among equations above, those

referring to elements 00, 02, 11, 12, 22 are all consistent with:

$$\begin{aligned}\delta_{10} &= \gamma_{10} + \eta_{10}(1-\gamma_{10}) \,, \\ \delta_{20} &= \gamma_{20} + \eta_{10}\gamma_{21} + \eta_{20}(1-\gamma_{21}-\gamma_{20}) \,, \\ \delta_{21} &= (1-\eta_{10})\gamma_{21} + \eta_{21}(1-\gamma_{21}-\gamma_{20}) \,. \end{aligned} \tag{6.14}$$

Element 01 instead forces an additional constraint, i.e.

$$\sqrt{\delta_{21}\delta_{10}} = \sqrt{\eta_{10}\eta_{21}(1-\gamma_{10})(1-\gamma_{21}-\gamma_{20})} + \sqrt{\gamma_{10}\gamma_{21}(1-\eta_{10})} \,. \tag{6.15}$$

By substituting in this constraint the values for δ_{21} and δ_{10} obtained in Eq. (6.14) we get that in order to satisfy it we need

$$\gamma_{10}\eta_{21}(1-\gamma_{21}-\gamma_{20}) = \gamma_{21}\eta_{10}(1-\gamma_{10})(1-\eta_{10}) \,. \tag{6.16}$$

This, together with the usual constraints for the decay parameters $0 \leq \delta_{ij} \leq 1$, defines a specific region for the parameters $\vec{\gamma}$ and $\vec{\eta}$ outside of which the resulting $\Phi_{\vec{\delta}}$ is not a ReMAD channel.

6.3 Degradability, Quantum Capacity and Private Classical Capacity

The evaluation of those functionals describing maximum achievable communication rates, whether analytically or numerically, has been proven to be one of the most challenging tasks in Quantum Information Theory. Indeed the number of examples that allow for explicit solutions is quite limited. In the following, after introducing basic definitions, we show how ReMAD channels are in identifiable regions fully characterized in terms of quantum and private classical capacities.

6.3.1 Quantum Capacity and Private Classical Capacity

The quantum capacity $Q(\Phi)$ of a quantum channel Φ defines the maximum rate of transmitted quantum information achievable per channel use, assuming Φ to act in the regime of i.i.d. noise [Hol19, Wil17, Wat18, Hay17, HG12, NC10, IG12, GIN18]. Intuitively it tells you how faithfully a quantum state, possibly correlated with an external system, can be sent and received by two communication parties if the communication line is noisy. Recently Q has also been showed to provide a lower bound to the space overhead necessary for fault tolerant quantum computation in presence of noise [FMHS22].

The formal definition of the quantum capacity Q relies on the coherent information I_{coh} [SN96]. Assuming n uses of the channel Φ and a generic state $\hat{\rho}^{(n)} \in \mathfrak{S}(\mathcal{H}_{\text{S}}^{\otimes n})$ we have

$$I_{\text{coh}}\left(\Phi^{\otimes n}, \hat{\rho}^{(n)}\right) \equiv S\left(\Phi^{\otimes n}(\hat{\rho}^{(n)})\right) - S\left(\tilde{\Phi}^{\otimes n}(\hat{\rho}^{(n)})\right) . \tag{6.17}$$

with $S(\hat{\rho}) \equiv -\text{Tr}[\hat{\rho}\log_2\hat{\rho}]$ the von Neumann entropy of the state $\hat{\rho}$, and $\tilde{\Phi}$ the complementary channel of Φ. Maximizing over $\mathfrak{S}(\mathcal{H}_{\text{S}}^{\otimes n})$ we get the maximized coherent information

$Q^{(n)}$ for n instances of the channel

$$Q^{(n)}(\Phi) \equiv \max_{\hat{\rho}^{(n)} \in \mathfrak{S}(\mathcal{H}_{\mathrm{S}}^{\otimes n})} I_{\mathrm{coh}}\left(\Phi^{\otimes n}, \hat{\rho}^{(n)}\right) , \tag{6.18}$$

and by regularization of this expression we get the maximized coherent information per channel use, that is the quantum capacity $Q(\Phi)$ [Llo97, Sho02b, Dev05]

$$Q(\Phi) = \lim_{n\to\infty} \frac{Q^{(n)}(\Phi)}{n} . \tag{6.19}$$

The private classical capacity $C_{\mathrm{p}}(\Phi)$ instead quantifies the maximum rate of classical information achievable per channel use assuming also the privacy of communication. Privacy is intended as limiting to arbitrarily small the amount of information that an eavesdropper can extract from the environment during the communication.
To define the private classical capacity we have to introduce the Holevo information functional χ [Hol73]. Being $\mathcal{E}_n \equiv \{p_i, \hat{\rho}_i^{(n)}\}$ an ensemble of quantum states $\hat{\rho}_i^{(n)} \in \mathfrak{S}(\mathcal{H}_{\mathrm{S}}^{\otimes n})$, we have

$$\chi(\Phi^{\otimes n}, \mathcal{E}_n) \equiv S\left(\Phi^{\otimes n}\left(\sum_i p_i \hat{\rho}_i^{(n)}\right)\right) - \sum_i p_i S\left(\Phi^{\otimes n}\left(\hat{\rho}_i^{(n)}\right)\right) . \tag{6.20}$$

Through the Holevo information we define the private information for n uses $C_{\mathrm{p}}^{(n)}(\Phi)$, that involves a maximization over all ensembles $\mathcal{E}_n$

$$C_{\mathrm{p}}^{(n)}(\Phi) \equiv \max_{\mathcal{E}_n} \left(\chi\left(\Phi^{\otimes n}, \mathcal{E}_n\right) - \chi\left(\tilde{\Phi}^{\otimes n}, \mathcal{E}_n\right)\right) . \tag{6.21}$$

As for the quantum capacity, we regularize this formula to get the maximum achievable private classical rate per channel use, i.e. the private classical capacity $C_{\mathrm{p}}(\Phi)$: [Dev05, CWY04]:

$$C_{\mathrm{p}}(\Phi) = \lim_{n\to\infty} \frac{C_{\mathrm{p}}^{(n)}(\Phi)}{n} . \tag{6.22}$$

The difficulties related to the evaluation of the above formulas are well known and ultimately the reason underlying our efforts here. An exception to this predicament is given by degradable [DS05] and antidegradable [CG06] channels, see Sec. 6.3.2 for definitions. For degradable channels Q and C_{p} result to be additive, so the regularization over n in Eq. (6.19) isn't needed, leading to the following single-letter formula [Smi08]

$$C_{\mathrm{p}}(\Phi) = Q(\Phi) = Q^{(1)}(\Phi). \tag{6.23}$$

For antidegradable channels instead, due to a no-cloning argument [BDS97], $Q = 0$. Similarly, $C_{\mathrm{p}} = 0$: the environment can reconstruct the channel output simply by applying the antidegrading channel, so no private information can be transmitted. Therefore for channels exhibiting antidegradability no maximizations are needed.

6.3.2 Degradability and antidegradability

As discussed in deeper details in Appendix C.2, degradable channels are those for which exists a CPTP map $\mathcal{N}$ s.t. $\tilde{\Phi} = \mathcal{N} \circ \Phi$, while antidegradable channels are those for which exists a CPTP map $\mathcal{M}$ s.t. $\Phi = \mathcal{M} \circ \tilde{\Phi}$.

To assess these two properties for ReMAD channels we can always make use of the matrix inversion technique described in Appendix C.2, since system and environment have always the same size.

Alternatively, mimicking the approach used for other amplitude damping channels, we can try to exploit the "almost" closure under composition of ReMAD channels and check whether the degrading (or antidegrading) channel is itself a ReMAD channel. With a procedure similar to the one employed in Sec. 6.2.3 for the composition rules, we need to find a set of decay parameters $\vec{\eta}$ that define a $\Phi_{\vec{\eta}}$ s.t. $\tilde{\Phi}_{\vec{\gamma}} = \Phi_{\vec{\eta}} \circ \Phi_{\vec{\gamma}}$. This constraint will yield equations delimiting the parameters region in which this composition is allowed, as it happens in Eq. (6.15) for the qutrit ReMAD channel composition. Again, in this case a self contained treatise for arbitrary dimension d cannot be obtained, therefore we take the qutrit case as a pedagogic instance. So, with $d = 3$, asking $\tilde{\Phi}_{\vec{\gamma}} = \Phi_{\vec{\eta}} \circ \Phi_{\vec{\gamma}}$ leads to

$$\begin{aligned}
&\gamma_{10} + \eta_{10}(1 - \gamma_{10}) = 1 - \gamma_{10} \,, \\
&(1 - \eta_{10})\gamma_{21} + \eta_{21}(1 - \gamma_{21} - \gamma_{20}) = \gamma_{20} \,, \\
&\gamma_{20} + \eta_{10}\gamma_{21} + \eta_{20}(1 - \gamma_{21} - \gamma_{20}) = 1 - \gamma_{21} - \gamma_{20} \,.
\end{aligned} \tag{6.24}$$

This implies

$$\begin{aligned}
\eta_{10} &= \frac{1 - 2\gamma_{10}}{1 - \gamma_{10}} \,, \\
\eta_{21} &= \frac{1 - 2\gamma_{10}}{1 - \gamma_{10}} \frac{\gamma_{21}}{1 - \gamma_{21} - \gamma_{20}} \,, \\
\eta_{20} &= \frac{1 - \gamma_{21} - 2\gamma_{20}}{1 - \gamma_{21} - \gamma_{20}} - \frac{\gamma_{21}}{1 - \gamma_{21} - \gamma_{20}} \frac{1 - 2\gamma_{10}}{1 - \gamma_{10}} \,.
\end{aligned} \tag{6.25}$$

Imposing now that $0 \leq \eta_{ij} \leq 1$ and $\eta_{21} + \eta_{20} \leq 1$ we get the degradability region. We report the depiction of the degradable region in the parameters space in Fig. 6.3 (yellow).

To check antidegradability we follow the same path, by looking for a set of parameter $\vec{\eta}$ s.t. there exists $\Phi_{\vec{\gamma}} = \Phi_{\vec{\eta}} \circ \tilde{\Phi}_{\vec{\gamma}}$, that implies:

$$\begin{aligned}
&1 - \gamma_{10}(1 - \eta_{10}) = \gamma_{10} \,, \\
&1 - \gamma_{21}(1 - \eta_{10}) - \gamma_{20}(1 - \eta_{20}) = \gamma_{20} \,, \\
&(1 - \eta_{10})\gamma_{21} + \eta_{21}\gamma_{20} = \gamma_{21} \,,
\end{aligned} \tag{6.26}$$

from which we get

$$\begin{aligned}\eta_{10} &= \frac{2\gamma_{10}-1}{\gamma_{10}}\,,\\ \eta_{21} &= \frac{\gamma_{21}}{\gamma_{20}}\frac{2\gamma_{10}-1}{\gamma_{10}}\,,\\ \eta_{21} &= 2+\frac{\gamma_{21}(1-\gamma_{10})-\gamma_{10}}{\gamma_{10}\gamma_{20}}\,.\end{aligned} \tag{6.27}$$

Again, imposing $0 \leq \eta_{ij} \leq 1$ and $\eta_{21}+\eta_{20} \leq 1$ gives us antidegradability region. We report the depiction of the antidegradable region in the parameters space in Fig. 6.3 (blue).

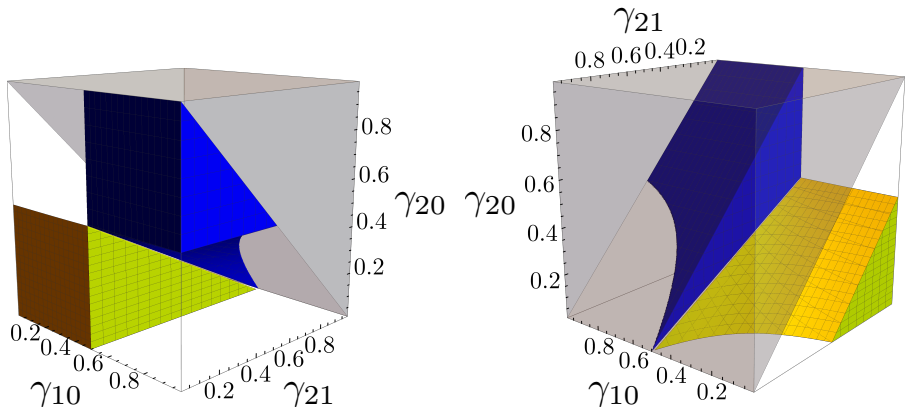

Figure 6.3: Degradability region (yellow) and antidegradability region (blue) from different perspectives.

Interestingly, the degradability and antidegradability regions found with the composition method turn out to be the same that we obtain via the matrix inversion method. This resembles the behaviour of the other classes of amplitude damping channels known: heuristically we can say that an amplitude damping channel is (anti)degradable if exists another amplitude damping channel that acts as (anti)degrading channel.
In the degradable region we are then able to compute exactly the quantum capacity Q and the private classical capacity C_{p} by maximizing over a single use Hilbert space. The maximization is further simplified by the fact hat ReMAD channels exhibit a covariance property, see Appendix C.3 for definitions and details, which allows us to maximize only over diagonal states. We report in Fig. 6.4 the evaluation of Q and C_{p} (in the degradable region they are equivalent) for a qutrit ReMAD channel at variance with the values of the parameters γ_{10}, γ_{21} and γ_{20}. In the cases of $\gamma_{21}=0$ and $\gamma_{10}=0$ Q and C_{p} were already known in the whole parameter space, since there ReMAD channels reduce to double-decay MAD channels, already studied in [CG21b].

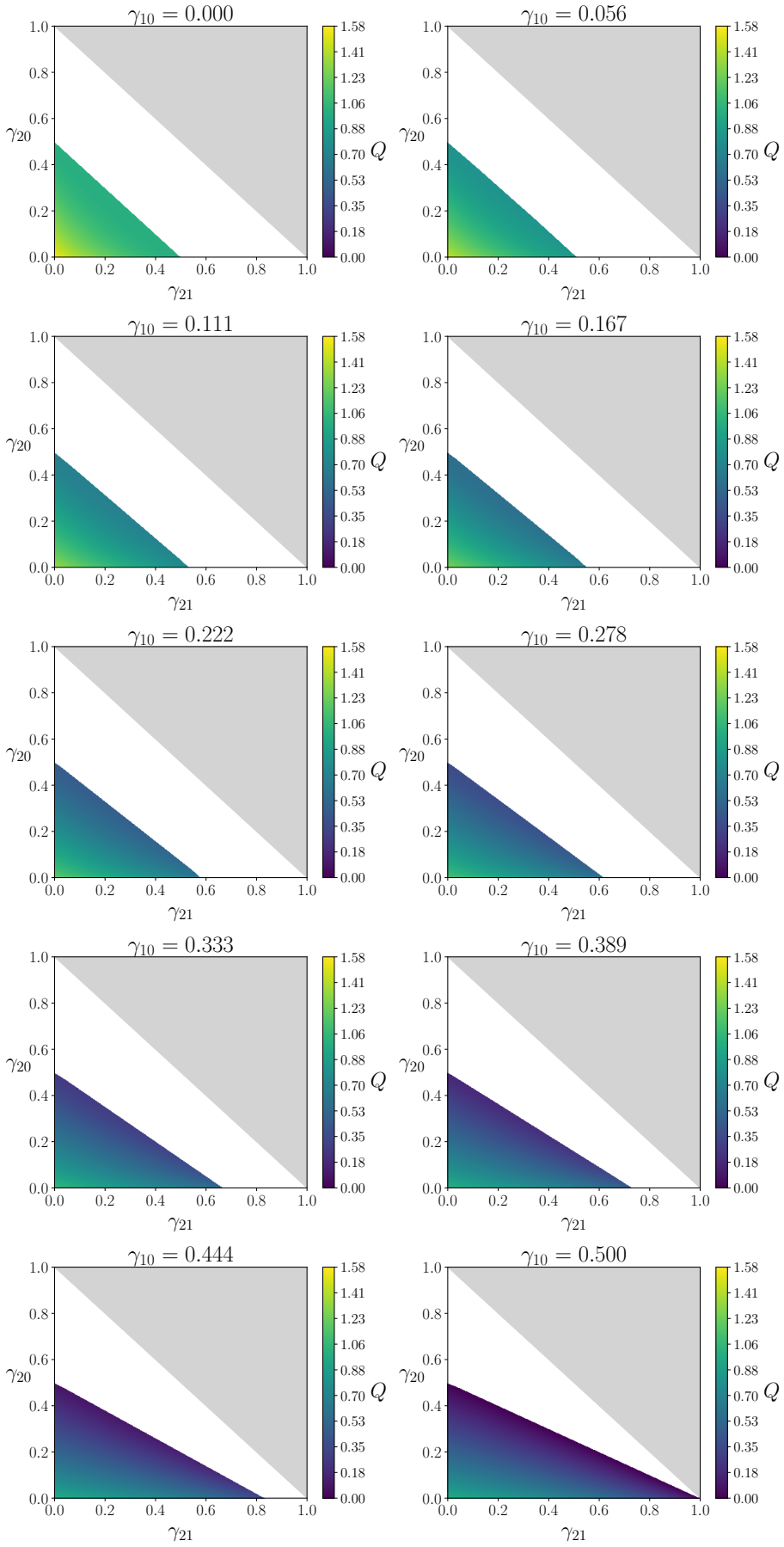

Figure 6.4: Quantum (and private classical) capacity for different γ_{10}, γ_{21} and γ_{20} in the degradable region.

6.3.3 Capacities in non-degradable and non-antidegradable regions

In those regions of parameters for which degradability or antidegradability are not achieved an expression for Q and C_{p} is lacking. It is still possible to exploit some information theoretic properties and known results in the literature to obtain computationally efficient upper bounds. An immediately available upper bound is given by noticing that the quantum capacity Q is always smaller than the entanglement-assisted quantum capacity Q_{ea}. This latter quantity doesn't need a regularized expression and, as showed in App. C.4, can be efficiently computed. The tightness of the bound given by Q_{ea} is not guaranteed though: in the following we sketch some of the more immediate strategies, given the properties of our channel, that may provide an improvement.

- **Data processing and composition rules.** Consider a degradable ReMAD channel $\Phi_{\vec{\gamma}}$ on the border of the degradable region and another ReMAD channel Φ_{η_3} s.t. $\eta_{10} = \eta_{21} = 0$ and $\eta_{20} = \eta_3$. From composition rules and constraints in Eq. (6.14) and Eq. (6.16), we have that $\Phi_{\eta_3} \circ \Phi_{\vec{\gamma}}$ is an ReMAD channel $\Phi_{\vec{\delta}}$ s.t. $\delta_{20} = \gamma_{20} + \eta_3(1 - \gamma_{21} - \gamma_{20}) > \gamma_{20}$. Hence by the composition with Φ_{η_3} we get a ReMAD channel outside of the degradability region. We can then apply the data processing inequality for the coherent information and get $Q(\Phi_{\vec{\delta}}) \leq \min\{Q(\Phi_{\vec{\gamma}}), Q(\Phi_{\eta_3})\}$. The same holds for C_{p}.

- **Data processing and inversion.** If our non degradable channel $\Phi_{\vec{\delta}}$ has parameters δ_{10}, δ_{21} not compatible with a degradable ReMAD channel we may still ask ourselves whether channels Γ and Γ' exist s.t. $\Phi_{\vec{\delta}} = \Gamma \circ \Phi_{\vec{\gamma}}$ or $\Phi_{\vec{\delta}} = \Phi_{\vec{\gamma}} \circ \Gamma'$, being $\Phi_{\vec{\gamma}}$ a degradable ReMAD channel. In the matrix representation of the channels discussed in App. C.2 this is equivalent to computing matrices $\hat{\mathrm{M}}_{\Gamma} = \hat{\mathrm{M}}_{\Phi_\delta} \hat{\mathrm{M}}_{\Phi_\gamma}^{-1}$ and $\hat{\mathrm{M}}_{\Gamma'} = \hat{\mathrm{M}}_{\Phi_\gamma}^{-1} \hat{\mathrm{M}}_{\Phi_\delta}$ and check whether the associated Choi matrices are positive definite. If this is verified (it can easily be done numerically for fixed $\vec{\delta}$ and $\vec{\gamma}$) then due to data processing we have $Q(\Phi_{\vec{\delta}}) \leq \min\{Q(\Phi_{\vec{\gamma}}), Q(\Gamma), Q(\Gamma')\} \leq Q(\Phi_{\vec{\gamma}})$. The same holds for C_{p}.

- **ϵ-(anti)degradability and ϵ-close-(anti)degradability.** If our channel $\Phi_{\vec{\delta}}$ is not (anti)degradable we can ask how distant it is from a (anti)degradable channel $\Phi_{\vec{\gamma}}$ and exploit then results on the continuity of the quantum capacity to bound $Q(\Phi_{\vec{\delta}})$ (ϵ-close-degradability). In our case we already have some 'reference' channels given by those contained in the (anti)degradable region. Alternatively we could try to find the best approximate-degrading channel $\mathcal{D}_\epsilon$ that brings $\Phi_{\vec{\delta}}$ close to $\tilde{\Phi}_{\vec{\delta}}$ and again exploit continuity results to bound $Q(\Phi_{\vec{\delta}})$ (ϵ-degradability). These approaches were firstly introduced in [SSWR17] and rely respectively on the computation of $||\Phi_{\vec{\delta}} - \Phi_{\vec{\gamma}}||_\diamond$ and $||\tilde{\Phi}_{\vec{\delta}} - \mathcal{D}_\epsilon \circ \Phi_{\vec{\delta}}||_\diamond$, that can be done efficiently via semi-definite programming. The upper bound needs though also the computation of $Q^{(1)}(\Phi_{\vec{\delta}})$, which is a non-convex maximization problem and presents nontrivial aspects in terms of convergence.

6.4 Conclusions

We introduced the class of ReMAD channels. We showed that this class differs from the other known classes of amplitude damping channels studied in the literature. In particular, the existence of this new type of channel highlights the fact, often disregarded, that in higher dimensions the richness of degrees of freedom can allow the emergence of effects that are absent in the qubit setting. In the context of Quantum Computation and Quantum Communication this issue is of paramount importance: the fragility of quantum information in practical scenarios demands a detailed knowledge of the possible error models affecting quantum devices. In this sense what we provided is a description of a noise channel that can reproduce e.g. the energy exchange between qudits encoded in harmonic oscillators and a bosonic environment. As a first step we gave a characterization of the unassisted quantum capacity Q and private classical capacity C_{p} exploiting degradability and antidegradability and computed the entanglement-assisted quantum capacity Q_{ea} and entanglement-assisted classical capacity C_{ea}. The full characterization in terms of information capacities, such as for instance classical capacity and two-way capacities, is then still missing for ReMAD channels and will require further investigations. As well, we hope that this work will motivate a comprehensive analysis of higher dimensional quantum channels deriving from possible realistic environment and interaction models.

7
PCDS channels

Preface

What follows is based on the published paper [CG21a]:

- S. Chessa, V. Giovannetti, Partially Coherent Direct Sum channels, *Quantum* **5**, 504 (2021).

In the following chapter we present what is probably the most abstract among the results discussed until now. It fits though the general picture delineated by Chapter 5 and Chapter 6. As a "bibliographic note" it was conceived while producing [CG21b], over which Chapter 6 is based, while trying to simplify the procedure of computation of MAD channels quantum capacities. What we observed is that the action of some channels can be decomposed in blocks by looking at the underlying Hilbert space as a direct sum. Fukuda and Wolfe provided a similar approach even though without coherences among subspaces. Our construction generalizes theirs and allows us to state new theorems about the degradability of composed channels starting from knowledge of subchannels and viceversa. In turn, this provide tools to compute exactly the quantum capacity and private classical capacity of high dimensional channels that otherwise would be hardly approachable.

7.1 Introduction

As mentioned in Chapter 3, even for few uses of the channel considered, in absence of useful properties or further symmetries, maximizations over Hilbert spaces to find capacities can reveal themselves computationally hard. Especially in higher dimensions. This makes the study, in terms of information capacities, of a wide realm of channels unattractive and unexplored, despite quantum information in higher dimensions being a well established field of research. For this family of systems and channels potential advantages are showed either from the quantum computation (see e.g. [MS00, RRG07, LBA+09, GSÇ+15]) and quantum communication (see e.g. [CDLBO19, LYGG08, GBDG+14, MZL+17]) perspectives, and are now also increasingly experimentally accessible [LNG+11, NJDH+13, MMP+15, BEW+17, KRR+17, MPGB+18, GPE+19, SBG+20, LZE+19]. All this considered, methods to overcome these kind of obstacles are still researched and this Chapter aims to contribute to this corpus of literature. Specifically, we present compact expressions for the quantum capacity and entanglement assisted quantum capacity of a new class of channels that we called *Partially Coherent Direct Sum* (PCDS) channels, a generalization of the direct sum (DS) channels described in [FW07]. This formalism appears in a variety of contexts [GJL18a, GJL18b, BHP09, BDHM10, BHTW10, Brá11, BJOJ11], among which recently the "gluing" procedure in [SG21b] derived as a generalization of the construction in [LLS18a]. DS channels were initially introduced in [FW07] in the context of the additivity conjecture for the classical capacity, later proven wrong [Has09]. There, the direct-sum structure was proposed in order to simplify the expressions of those functionals, e.g. output entropy and Holevo information, whose additivity was conjectured. Among these results also an expression for the coherent information for DS channels was found. In the subsequent literature the direct-sum structure has been mainly exploited to show superadditivity features of quantum channels.

We draw attention to PCDS because, other than encompassing the already known DS channels, they provide a framework for the efficient description of wide classes of physical noise models and their capacities. An instance is given by damping processes in multi-level systems, denominated multi-level amplitude damping (MAD) channels [CG21b]. In addition to that, PCDS appear to be interesting because their capacity is in principle exactly computable with reduced complexity also for high dimensional systems. In this sense, the knowledge already acquired about low dimensional quantum channels can be exploited to compose new PCDS channels. At the same time the introduction of the PCDS can push the study of all accessible zoology of low dimensional channels. In addition to that, through the techniques here developed, in some cases we are able to evaluate exactly the quantum capacity even if the channel can be proven not to be degradable [DS05]. Finally we also see that PCDS channels, despite the similar construction, have higher capacities w.r.t. DS channels. This enhancement is associated with the direct sum structure of the Hilbert space and the introduction of coherences.

The Chapter is organized as follows: in Sec. 7.2 we introduce the model for the channels we consider; in Sec 7.3 we analyze complementary channels and degradability properties; in Sec. 7.4 we study the quantum capacity and entanglement assisted quantum capacity; in Sec 7.5 we apply results to instances of quantum channels that include

dephasing channels, amplitude damping channels and combinations of the two. Conclusions and perspectives are presented in Sec. 7.6 while technical material is presented in the Appendix.

7.2 The model

Let us start fixing some notation: given $\mathcal{H}_{\rm X}$ and $\mathcal{H}_{\rm Y}$ two Hilbert spaces associated with two (possibly unrelated) quantum systems X and Y, we shall use the symbol

$$\mathcal{L}_{\rm X\to Y} := \{\hat{\Theta}_{\rm YX} : \mathcal{H}_{\rm X} \longrightarrow \mathcal{H}_{\rm Y}\} \,, \tag{7.1}$$

to represent the set of linear operators $\hat{\Theta}_{\rm YX}$ mapping the input vectors of X into the output vectors of Y. The symbol $\mathfrak{S}_{\rm X} = \mathfrak{S}(\mathcal{H}_{\rm X})$ will describe the special subset of $\mathcal{L}_{\rm X\to X}$ formed by the density operators $\hat{\rho}_{\rm XX}$ of the system X. We also define

$$\mathcal{M}_{\rm X\to Y} := \{\Phi_{\rm YX} : \mathcal{L}_{\rm X\to X} \longrightarrow \mathcal{L}_{\rm Y\to Y}\} \,, \tag{7.2}$$

to be the set of super-operators $\Phi_{\rm YX}$ which transform operators $\hat{\Theta}_{\rm XX} \in \mathcal{L}_{\rm X\to X}$ into elements of $\mathcal{L}_{\rm Y\to Y}$. We'll indicate with $\mathcal{M}^{\rm (cpt)}_{\rm X\to Y}$ the special subset formed by the quantum channels of $\mathcal{M}_{\rm X\to Y}$, i.e. by the super-operators $\Phi_{\rm YX}$ which are Completely Positive and Trace preserving (CPT) [Cho75]. Finally, for X$\neq$Y we shall use the special symbol

$$\mathcal{M}^{\rm (off)}_{\rm X\to Y} := \{\Phi^{\rm (off)}_{\rm YX} : \mathcal{L}_{\rm X\to Y} \longrightarrow \mathcal{L}_{\rm X\to Y}\} \,, \tag{7.3}$$

to describe linear mappings $\Phi^{\rm (off)}_{\rm YX}$ which connect operators $\mathcal{L}_{\rm X\to Y}$ into themselves.

Consider next C, a quantum system described by a Hilbert space $\mathcal{H}_{\rm C}$ admitting the following direct sum decomposition

$$\mathcal{H}_{\rm C} = \mathcal{H}_{\rm A} \oplus \mathcal{H}_{\rm B} \,, \tag{7.4}$$

with $\mathcal{H}_{\rm A}$ and $\mathcal{H}_{\rm B}$ two nontrivial subspaces of dimensions $d_{\rm A}$, $d_{\rm B} = d_{\rm C} - d_{\rm A}$. We'll associate with them the projectors $\hat{P}_{\rm AA}$ and $\hat{P}_{\rm BB}$ that fulfill the orthonormalization conditions

$$\hat{P}_{\rm AA}\hat{P}_{\rm BB} = \hat{P}_{\rm BB}\hat{P}_{\rm AA} = 0 \,, \quad \hat{P}_{\rm AA} + \hat{P}_{\rm BB} = \hat{I}_{\rm CC} \,, \tag{7.5}$$

$\hat{I}_{\rm CC}$ being the identity operator on $\mathcal{H}_{\rm C}$. Accordingly, any operator $\hat{\Theta}_{\rm CC} \in \mathcal{L}_{\rm C\to C}$ mapping the space of C into itself can then be written as a sum of diagonal and off-diagonal block terms, i.e.

$$\hat{\Theta}_{\rm CC} = \bigoplus_{\rm X,Y=A,B} \hat{\Theta}_{\rm YX} \equiv \left[\begin{array}{c|c} \hat{\Theta}_{\rm AA} & \hat{\Theta}_{\rm AB} \\ \hline \hat{\Theta}_{\rm BA} & \hat{\Theta}_{\rm BB} \end{array}\right] , \tag{7.6}$$

with X,Y = A,B and $\hat{\Theta}_{\rm XY}$ is an element of $\mathcal{L}_{\rm Y\to X}$ defined by the identity

$$\hat{\Theta}_{\rm XY} \equiv \hat{P}_{\rm XX}\hat{\Theta}_{\rm CC}\hat{P}_{\rm YY} \,. \tag{7.7}$$

Let now $\Phi_{\rm CC} \in \mathcal{M}^{\rm (cpt)}_{\rm C\to C}$ be a CPT channel mapping C into itself. We say that it is a *Partially Coherent Direct Sum* (PCDS) map if it preserves the block structure in

Eq. (7.6). Or equivalently if we can identify super-operators $\Phi_{\rm AA} \in \mathcal{M}_{\rm A\to A}$, $\Phi_{\rm BB} \in \mathcal{M}_{\rm B\to B}$, $\Phi^{(\rm off)}_{\rm AB} \in \mathcal{M}^{(\rm off)}_{\rm B\to A}$, and $\Phi^{(\rm off)}_{\rm BA} \in \mathcal{M}^{(\rm off)}_{\rm A\to B}$ such that

$$\Phi_{\rm CC}\left[\begin{array}{c|c} \hat{\Theta}_{\rm AA} & \hat{\Theta}_{\rm AB} \\ \hline \hat{\Theta}_{\rm BA} & \hat{\Theta}_{\rm BB} \end{array}\right] = \left[\begin{array}{c|c} \Phi_{\rm AA}[\hat{\Theta}_{\rm AA}] & \Phi^{(\rm off)}_{\rm AB}[\hat{\Theta}_{\rm AB}] \\ \hline \Phi^{(\rm off)}_{\rm BA}[\hat{\Theta}_{\rm BA}] & \Phi_{\rm BB}[\hat{\Theta}_{\rm BB}] \end{array}\right], \tag{7.8}$$

for all input $\hat{\Theta}_{\rm CC} \in \mathcal{L}_{\rm C\to C}$. In brief, simplifying the notation

$$\Phi_{\rm CC} = \Phi_{\rm AA} + \Phi_{\rm BB} + \Phi^{(\rm off)}_{\rm AB} + \Phi^{(\rm off)}_{\rm BA}\,, \tag{7.9}$$

where each channel $\Phi_{\rm XX}$ implicitly assumes the projection on the suitable subspace as in Eq. (7.7). Quantum channels that can be cast in form of Eq. (7.9) arise whenever the quantum system C is affected by a (possibly noisy) evolution that preserves the relative populations associated with the subsystems $\mathcal{H}_{\rm A}$ and $\mathcal{H}_{\rm B}$, but (possibly) deteriorates the quantum coherence among them. In Appendix D.1 it is shown a necessary and sufficient condition for this to happen. This condition is that, given $\{\hat{M}^{(j)}_{\rm CC}\}_j$ a Kraus set [Kra71] for $\Phi_{\rm CC}$, its elements must only involve diagonal terms when cast into the block form as in Eq. (7.6), i.e.

Theorem 1. *A quantum channel Φ_{CC} described by a Kraus set $\{\hat{M}^{(j)}_{CC}\}_j$ admits the PCDS structure (7.9) if and only if*

$$\hat{M}^{(j)}_{CC} = \hat{M}^{(j)}_{AA} + \hat{M}^{(j)}_{BB}\,, \tag{7.10}$$

or equivalently that $\hat{M}^{(j)}_{AB} = \hat{M}^{(j)}_{BA} = 0$, for all j.

The explicit proof of this result is given in Appendix D.1. There we also show that the maps on the right-hand-side of Eq. (7.9) can be expressed in terms of the operators $\hat{M}^{(j)}_{\rm AA}$ and $\hat{M}^{(j)}_{\rm BB}$ of Eq. (7.10) as

$$\Phi_{\rm XX}[\cdots] \;=\; \sum_j \hat{M}^{(j)}_{\rm XX}\cdots\hat{M}^{(j)\dagger}_{\rm XX}\,, \tag{7.11}$$

for all X=A,B and

$$\Phi^{(\rm off)}_{\rm XY}[\cdots] \;=\; \sum_j \hat{M}^{(j)}_{\rm XX}\cdots\hat{M}^{(j)\dagger}_{\rm YY}\,, \tag{7.12}$$

for all X≠Y=A,B. Notice that in particular Eq. (7.11) implies that the diagonal terms define proper CPT channels on A and B respectively, i.e. $\Phi_{\rm AA} \in \mathcal{M}^{(\rm cpt)}_{\rm A\to A}$ and $\Phi_{\rm BB} \in \mathcal{M}^{(\rm cpt)}_{\rm B\to B}$, with Kraus sets provided by $\{\hat{M}^{(j)}_{\rm AA}\}_j$ and $\{\hat{M}^{(j)}_{\rm BB}\}_j$.

One can easily check that given $\Phi'_{\rm CC}, \Phi''_{\rm CC} \in \mathcal{M}^{(\rm cpt)}_{\rm C\to C}$ fulfilling the constraint of Eq. (7.9), then the same holds true for both the channel $p\Phi'_{\rm CC} + (1-p)\Phi''_{\rm CC}$ with $p \in [0,1]$ and for the channel $\Phi'_{\rm CC} \circ \Phi''_{\rm CC}$, with " $\circ$ " representing super-operator composition. The first property implies that the set of PCDS quantum evolutions is closed under convex

combination. The second property instead, together with the observation that the identity channel $\mathrm{Id}_{\mathrm{CC}}$ is also trivially PCDS, tells us that the set forms a semi-group under channel concatenation. Observe also that a special instance of PCDS transformations is provided by the purely dephasing channels $\Delta^{(\kappa)}_{\mathrm{CC}}$, which induce the mapping

$$\Delta^{(\kappa)}_{\mathrm{CC}}\left[\begin{array}{c|c} \hat{\Theta}_{\mathrm{AA}} & \hat{\Theta}_{\mathrm{AB}} \\ \hline \hat{\Theta}_{\mathrm{BA}} & \hat{\Theta}_{\mathrm{BB}} \end{array}\right] = \left[\begin{array}{c|c} \hat{\Theta}_{\mathrm{AA}} & \kappa\hat{\Theta}_{\mathrm{AB}} \\ \hline \kappa^{*}\hat{\Theta}_{\mathrm{BA}} & \hat{\Theta}_{\mathrm{BB}} \end{array}\right] , \tag{7.13}$$

with κ being a complex parameter of norm $|\kappa| \leq 1$. The semi-group property mentioned above also allows us to state the following. Starting from any PCDS channel Φ_{CC}, described as in Eq. (7.9) for some proper choice of the maps Φ_{AA}, Φ_{BB}, $\Phi^{(\mathrm{off})}_{\mathrm{AB}}$, and $\Phi^{(\mathrm{off})}_{\mathrm{BA}}$, we can construct an entire family of new PCDS elements

$$\Phi^{(\kappa)}_{\mathrm{CC}} \equiv \Delta^{(\kappa)}_{\mathrm{CC}} \circ \Phi_{\mathrm{CC}} = \Phi_{\mathrm{CC}} \circ \Delta^{(\kappa)}_{\mathrm{CC}} , \tag{7.14}$$

whose off-diagonal components are rescaled versions of $\Phi^{(\mathrm{off})}_{\mathrm{AB}}$, and $\Phi^{(\mathrm{off})}_{\mathrm{BA}}$, i.e.

$$\Phi^{(\kappa)}_{\mathrm{CC}} = \Phi_{\mathrm{AA}} + \Phi_{\mathrm{BB}} + \kappa\Phi^{(\mathrm{off})}_{\mathrm{AB}} + \kappa^{*}\Phi^{(\mathrm{off})}_{\mathrm{BA}} . \tag{7.15}$$

(Here the commutativity property exhibited in Eq. (7.14) follows from the linearity of the super-operators $\Phi^{(\mathrm{off})}_{\mathrm{AB}}$ and $\Phi^{(\mathrm{off})}_{\mathrm{BA}}$). In particular by setting $\kappa = 0$, Eq. (7.15) describes the *Direct Sum* (DS) channels discussed in Ref. [FW07] which completely suppress coherence among $\mathcal{H}_{\mathrm{A}}$ and $\mathcal{H}_{\mathrm{B}}$. This special condition is met whenever the Kraus elements in Eq. (7.10) of a PCDS map are given by operators that have support exclusively either on $\mathcal{H}_{\mathrm{A}}$ or on $\mathcal{H}_{\mathrm{B}}$. We can summarize this constraint in terms of the following simple relation

$$\hat{M}^{(j)}_{\mathrm{AA}} \neq 0 \Longrightarrow M^{(j)}_{\mathrm{BB}} = 0 , \qquad \forall j . \tag{7.16}$$

It is worth stressing that the properties discussed above, as well as the results we are going to present in the following sections, admit a simple generalization in case of multi-block decompositions of the map PCDS – see Appendix D.3.

7.3 Complementary channels and degradability for PCDS maps

We remind that, via the Stinespring dilation theorem [Sti55], given $\Phi_{\mathrm{XX}} \in \mathcal{M}^{(\mathrm{cpt})}_{\mathrm{X}\to\mathrm{X}}$ a generic CPT transformation on an arbitrary system X, its complementary channel can be identified with a CPT map $\tilde{\Phi}_{\mathrm{EX}} \in \mathcal{M}^{(\mathrm{cpt})}_{\mathrm{X}\to\mathrm{E}}$ coupling X with the (sufficiently large) auxiliary quantum system E that plays the role of the system environment. Let $\{M^{(j)}_{\mathrm{XX}}\}_j$ be a Kraus set for Φ_{XX} and $\{|j_{\mathrm{E}}\rangle\}_j$ be a fixed set of orthonormal vectors on the Hilbert space $\mathcal{H}_{\mathrm{E}}$ of E. Then the action of $\tilde{\Phi}_{\mathrm{EX}}$ on a generic operator $\hat{\Theta}_{\mathrm{XX}} \in \mathcal{L}_{\mathrm{X}\to\mathrm{X}}$ can be expressed as

$$\tilde{\Phi}_{\mathrm{EX}}[\hat{\Theta}_{\mathrm{XX}}] = \sum_{j,j'} |j_{\mathrm{E}}\rangle\langle j'_{\mathrm{E}}| \, \mathrm{Tr}[M^{(j')\dagger}_{XX} M^{(j)}_{XX} \hat{\Theta}_{\mathrm{XX}}] , \tag{7.17}$$

(notice that due to the arbitrariness of the choice of $\{|j_{\rm E}\rangle\}_j$, $\tilde{\Phi}_{\rm EX}$ can always be redefined up to a unitary rotation on E). We also remind that the map $\Phi_{\rm XX}$ is said to be degradable [DS05] if we can identify a degrading CPT quantum channel $\Lambda_{\rm EX} \in \mathcal{M}^{(\rm cpt)}_{\rm X\to E}$ which allows us to reconstruct the action of $\tilde{\Phi}_{\rm EX}$ by acting on the corresponding output of $\Phi_{\rm XX}$, i.e.

$$\tilde{\Phi}_{\rm EX} = \Lambda_{\rm EX} \circ \Phi_{\rm XX} \; . \tag{7.18}$$

Similarly we say that $\Phi_{\rm XX}$ is antidegradable [CG06] if exists $\Lambda_{\rm XE} \in \mathcal{M}^{(\rm cpt)}_{\rm E\to X}$ such that

$$\Phi_{\rm XX} = \Lambda_{\rm XE} \circ \tilde{\Phi}_{\rm EX} \; . \tag{7.19}$$

In the case of DS channel $\Phi_{\rm CC}$, using Eq. (7.16) and the orthogonality between $\hat{M}^{(j)}_{\rm AA}$ and $\hat{M}^{(j)}_{\rm BB}$, from Eq. (7.17) one can then easily verify that for all input operators $\hat{\Theta}_{\rm CC}$ the following identity holds

$$\tilde{\Phi}_{\rm EC}[\hat{\Theta}_{\rm CC}] \;\; = \;\; \tilde{\Phi}_{\rm EA}[\hat{\Theta}_{\rm AA}] + \tilde{\Phi}_{\rm EB}[\hat{\Theta}_{\rm BB}] \; . \tag{7.20}$$

Here $\tilde{\Phi}_{\rm EA}$ and $\tilde{\Phi}_{\rm EB}$ are, respectively, the complementary channels associated with the diagonal components $\Phi_{\rm AA}$ and $\Phi_{\rm BB}$ entering in the decomposition of Eq. (7.9), while $\hat{\Theta}_{\rm AA}$ and $\hat{\Theta}_{\rm BB}$ are the diagonal terms of Eq. (7.6). We refer the reader to Appendix D.2 for a physical insight on this identity. As we'll see next, Eq. (7.20) holds also for PCDS. Notice though that, while for generic PCDS channels $\Phi_{\rm CC}$ the operators $\tilde{\Phi}_{\rm EA}[\hat{\Theta}_{\rm AA}]$ and $\tilde{\Phi}_{\rm EB}[\hat{\Theta}_{\rm BB}]$ may have nontrivial commutation relations, in the special case of the DS channels $\Phi^{(0)}_{\rm CC}$ [FW07] they have always zero overlap, i.e.

$$\tilde{\Phi}^{(0)}_{\rm EA}[\hat{\Theta}_{\rm AA}]\tilde{\Phi}^{(0)}_{\rm EB}[\hat{\Theta}_{\rm BB}] = \tilde{\Phi}^{(0)}_{\rm EB}[\hat{\Theta}_{\rm BB}]\tilde{\Phi}^{(0)}_{\rm EA}[\hat{\Theta}_{\rm AA}] = 0 \; . \tag{7.21}$$

In this scenario this implies that the sum appearing in Eq. (7.20) is indeed a direct sum.

We can now prove a necessary and sufficient condition for the degradability of a generic PCDS channel $\Phi_{\rm CC}$. This condition establishes that such property only depends upon the diagonal blocks entering in the decomposition of Eq. (7.9):

Theorem 2. *A PCDS quantum channel Φ_{CC} is degradable if and only if all of its diagonal block terms Φ_{AA}, Φ_{BB} are degradable too.*

Proof: First of all let us show that the degradability of $\Phi_{\rm AA}$ and $\Phi_{\rm BB}$ implies the degradability of $\Phi_{\rm CC}$. Indeed for X = A,B, let $\Lambda_{\rm XE}$ be the CPT degrading map from X to E, which allows us to express $\tilde{\Phi}_{\rm XX}$ in terms of $\Phi_{\rm XX}$ as in Eq. (7.18). Consider then the super-operator $\Lambda_{\rm EC}$ from C to E defined as

$$\Lambda_{\rm EC}[\hat{\Theta}_{\rm CC}] \equiv \Lambda_{\rm EA}[\hat{\Theta}_{\rm AA}] + \Lambda_{\rm EB}[\hat{\Theta}_{\rm BB}] \; , \tag{7.22}$$

which is CPT thanks to the fact that both $\Lambda_{\rm EA}$ and $\Lambda_{\rm EB}$ fulfill the same constraint by hypothesis – see Appendix D.2.1 for details. Furthermore for all $\hat{\Theta}_{\rm CC}$ we have

$$\begin{aligned}
\Lambda_{\rm EC} \circ \Phi_{\rm CC}[\hat{\Theta}_{\rm CC}] &= \Lambda_{\rm EC}\left[\begin{array}{c|c} \Phi_{\rm AA}[\hat{\Theta}_{\rm AA}] & \Phi^{(\rm off)}_{\rm AB}[\hat{\Theta}_{\rm AB}] \\ \hline \Phi^{(\rm off)}_{\rm BA}[\hat{\Theta}_{\rm BA}] & \Phi_{\rm BB}[\hat{\Theta}_{\rm BB}] \end{array}\right] \\
&= \Lambda_{\rm EA} \circ \Phi_{\rm AA}[\hat{\Theta}_{\rm AA}] + \Lambda_{\rm EB} \circ \Phi_{\rm BB}[\hat{\Theta}_{\rm BB}] \\
&= \tilde{\Phi}_{\rm EA}[\hat{\Theta}_{\rm AA}] + \tilde{\Phi}_{\rm EB}[\hat{\Theta}_{\rm BB}] = \tilde{\Phi}_{\rm EC}[\hat{\Theta}_{\rm BB}] \; ,
\end{aligned}$$

that proves that Φ_{CC} is degradable with degrading channel as in Eq. (7.22).

Let's now show next that if Φ_{CC} is degradable then also Φ_{AA} and Φ_{BB} must be degradable. For this purpose, given Λ_{EC} the CPT transformation from C to E which allows us to reconstruct $\tilde{\Phi}_{EC}$ from Φ_{CC}, from Eqs. (7.9) and (7.20) we get

$$\tilde{\Phi}_{EA}[\hat{\Theta}_{AA}] + \tilde{\Phi}_{EB}[\hat{\Theta}_{BB}] = \sum_{X,Y=A,B} (\Lambda_{EC} \circ \Phi_{YX})[\hat{\Theta}_{YX}] \,, \tag{7.23}$$

which must hold true for all $\hat{\Theta}_{YX} \in \mathcal{L}_{X\to Y}$. In the particular case $\hat{\Theta}_{BB} = \hat{\Theta}_{AB} = \hat{\Theta}_{BA} = 0$, this implies that for all $\hat{\Theta}_{AA} \in \mathcal{L}_{A\to A}$ we have

$$\tilde{\Phi}_{EA}[\hat{\Theta}_{AA}] = (\Lambda_{EC} \circ \Phi_{AA})[\hat{\Theta}_{AA}] = (\Lambda_{EA} \circ \Phi_{AA})[\hat{\Theta}_{AA}] \,, \tag{7.24}$$

where in the last identity we introduced

$$\Lambda_{EA}[\cdots] \equiv \Lambda_{EC}[\hat{P}_{AA} \cdots \hat{P}_{AA}] \,, \tag{7.25}$$

by exploiting the fact that Φ_{AA} maps operators of A into A, i.e. that $\hat{P}_{BB}\Phi_{AA}[\hat{\Theta}_{AA}] = \Phi_{AA}[\hat{\Theta}_{AA}]\hat{P}_{BB} = 0$. Since the map in Eq. (7.25) is CPT – see Appendix D.2.1, we can finally conclude that Φ_{AA} is degradable. The degradability of Φ_{BB} can be proved in the same way. □

7.4 Computing the quantum capacity of PCDS channels

As firstly shown in [Llo97, Sho02b, Dev05], the quantum capacity $Q(\Phi_{XX})$ of a channel Φ_{XX} is expressed as:

$$Q(\Phi_{XX}) = \lim_{n\to\infty} \frac{1}{n} \max_{\hat{\rho}_{XX}^{(n)} \in \mathfrak{S}(\mathcal{H}_X^{\otimes n})} I_{coh}(\Phi_{XX}^{\otimes n}; \hat{\rho}_{XX}^{(n)}), \tag{7.26}$$

where $I_{coh}(\Phi_{XX}; \hat{\rho}_{XX})$ is the *coherent information* and is defined as

$$I_{coh}(\Phi_{XX}; \hat{\rho}_{XX}) \equiv S(\Phi_{XX}(\hat{\rho}_{XX})) - S(\tilde{\Phi}_{EX}(\hat{\rho}_{XX})) \,, \tag{7.27}$$

being $S(\hat{\rho}_{XX}) \equiv -\mathrm{Tr}_X [\hat{\rho}_{XX} \log_2 \hat{\rho}_{XX}]$ the von Neumann entropy and $\tilde{\Phi}_{EX}$ the complementary channel of Φ_{XX} as defined in Eq. (7.17). As already mentioned in the introduction, the challenging aspect of the computation of the quantum capacity is given by the regularization over the number n of channel uses. This since the behavior for many uses doesn't scale linearly w.r.t. the single shot formula, due to the well known property of non additivity of quantum channels. The issue can be bypassed when the channel is degradable (see Sec. 7.4.1) for which the single letter formula is sufficient [DS05], or antidegradable (the complementary channel is degradable) for which, due to no-cloning argument, we have $Q(\Phi_{XX}) = 0$. Since we'll make use of this feature, it is finally worth noticing that from the invariance of the von Neumann entropy under unitary transformations it follows that the capacity formula reported above does not depend on the specific form of the complementary channel. Indeed as already mentioned, the complementary channel can be chosen freely up to a unitary rotation acting on the environment E – see

more about this in App. D.2.

Moving now towards DS and PCDS channels, in Ref. [FW07] it was shown that the quantum capacity of DS channels is given by the maximum of the quantum capacity of their diagonal contributions. Expressed in our notation

$$Q(\Phi_{\mathrm{CC}}^{(0)}) = \max\{Q(\Phi_{\mathrm{AA}}), Q(\Phi_{\mathrm{BB}})\} \, , \tag{7.28}$$

with Φ_{AA} and Φ_{BB} being the diagonal block terms. The presence of non-zero off-diagonal contributions in Eq. (7.9) is clearly bound to challenge the above result. To begin with, invoking the channel *data-processing inequality* (DPI) [Hol19, Wat18, Wil17, Key02, KSW20, NC10] from Eq. (7.14), it follows that the right-hand-side of Eq. (7.28) is an explicit lower bound for the quantum capacity of an arbitrary PCDS channel Φ_{CC} having the same diagonal block terms of $\Phi_{\mathrm{CC}}^{(0)}$, i.e.

$$Q(\Phi_{\mathrm{CC}}) \geq Q(\Phi_{\mathrm{CC}}^{(0)}) = \max\{Q(\Phi_{\mathrm{AA}}), Q(\Phi_{\mathrm{BB}})\} \, . \tag{7.29}$$

This fact alone paves the way to higher communication performances. The easiest way to see this is by comparing the case of the identity map $\mathrm{Id}_{\mathrm{CC}}$, which has capacity

$$Q(\mathrm{Id}_{\mathrm{CC}}) = \log_2 d_{\mathrm{C}} = \log_2(d_{\mathrm{A}} + d_{\mathrm{B}}) \, , \tag{7.30}$$

with the case of the completely dephasing channel $\Delta_{\mathrm{CC}}^{(\kappa=0)}$ of Eq. (7.13). $\Delta_{\mathrm{CC}}^{(\kappa=0)}$ shares the same diagonal terms of $\mathrm{Id}_{\mathrm{CC}}$ (i.e. $\Phi_{\mathrm{AA}} = \mathrm{Id}_{\mathrm{AA}}$ and $\Phi_{\mathrm{BB}} = \mathrm{Id}_{\mathrm{BB}}$) but, according to Eq. (7.28), has instead quantum capacity equal to

$$Q(\Delta_{\mathrm{CC}}^{(\kappa=0)}) = \max\{\log_2 d_{\mathrm{A}}, \log_2 d_{\mathrm{B}}\} \, . \tag{7.31}$$

Exploiting the results of the previous section we are going to set this observation on a broader context, computing the explicit value of the quantum capacity of large class of PCDS channels. Interestingly enough this will allow us to determine the quantum capacity of channels which are not degradable.

7.4.1 The quantum capacity of degradable PCDS channels

Consider the case of a PCDS channel Φ_{CC} which is degradable. According to [DS05] we can hence express it in terms of the following single-letter expression

$$Q(\Phi_{\mathrm{CC}}) = \max_{\hat{\rho}_{\mathrm{CC}} \in \mathfrak{S}_{\mathrm{C}}} I_{\mathrm{coh}}(\Phi_{\mathrm{CC}}; \hat{\rho}_{\mathrm{CC}}) \, , \tag{7.32}$$

with $I_{\mathrm{coh}}(\Phi_{\mathrm{CC}}; \hat{\rho}_{\mathrm{CC}})$ the single-use coherent information functional introduced in Eq. (7.27). Observe next that from Eq. (7.8) and the monotonicity of S under block diagonalization,

it follows that

$$\begin{aligned} S(\Phi_{\rm CC}(\hat{\rho}_{\rm CC})) &= S\left(\left[\begin{array}{c|c} p\Phi_{\rm AA}[\hat{\tau}_{\rm AA}] & \Phi^{(\rm off)}_{\rm AB}[\hat{\rho}_{\rm AB}] \\ \hline \Phi^{(\rm off)}_{\rm BA}[\hat{\rho}_{\rm BA}] & (1-p)\Phi_{\rm BB}[\hat{\tau}_{\rm BB}] \end{array}\right]\right) \\ &\leq S\left(\left[\begin{array}{c|c} p\Phi_{\rm AA}[\hat{\tau}_{\rm AA}] & 0 \\ \hline 0 & (1-p)\Phi_{\rm BB}[\hat{\tau}_{\rm BB}] \end{array}\right]\right) \\ &= S\left(p\Phi_{\rm AA}[\hat{\tau}_{\rm AA}]\right) + S\left((1-p)\Phi_{\rm BB}[\hat{\tau}_{\rm BB}]\right) \\ &= pS\left(\Phi_{\rm AA}[\hat{\tau}_{\rm AA}]\right) + (1-p)S\left(\Phi_{\rm BB}[\hat{\tau}_{\rm BB}]\right) + H_2(p)\ . \end{aligned} \tag{7.33}$$

Here we fixed $p \equiv {\rm Tr}[\hat{\rho}_{\rm AA}]$, we introduced the density matrices of A and B defined as $\hat{\tau}_{\rm AA} = \hat{\rho}_{\rm AA}/p$ and $\hat{\tau}_{\rm BB} = \hat{\rho}_{\rm BB}/(1-p)$, and called $H_2(p) \equiv -p\log_2 p - (1-p)\log_2(1-p)$ the binary entropy function. Considering then that Eq. (7.33) can be saturated by focusing on density matrices $\hat{\rho}_{\rm CC}$ with zero off-diagonal blocks (i.e. $\hat{\rho}_{\rm AB} = \hat{\rho}_{\rm BA} = 0$), and using the fact that according to Eq. (7.20) $\tilde{\Phi}_{\rm EC}(\hat{\rho}_{\rm CC})$ does not depend upon such terms, Eq. (7.32) reduces to

$$\begin{aligned} Q(\Phi_{\rm CC}) = \max_{p\in[0,1]} \Big\{ & H_2(p) \\ & + \max_{\hat{\tau}_{\rm AA}\in\mathfrak{S}_{\rm A}} \max_{\hat{\tau}_{\rm BB}\in\mathfrak{S}_{\rm B}} J_p(\Phi_{\rm AA};\hat{\tau}_{\rm AA},\Phi_{\rm BB};\hat{\tau}_{\rm BB}) \Big\}\ . \end{aligned} \tag{7.34}$$

We can see that this expression involves an optimization only on the diagonal components of $\hat{\rho}_{\rm CC}$. The functional J_p appearing in the above expression can be expressed as a rescaled convex combination of the coherent information terms of the channels $\Phi_{\rm AA}$ and $\Phi_{\rm BB}$. Explicitly

$$\begin{aligned} J_p \ \equiv\ & pI_{\rm coh}(\Phi_{\rm AA};\hat{\tau}_{\rm AA}) + (1-p)I_{\rm coh}(\Phi_{\rm BB};\hat{\tau}_{\rm BB}) \\ & -\Delta S_p(\tilde{\Phi}_{\rm EA}[\hat{\tau}_{\rm AA}],\tilde{\Phi}_{\rm EB}[\hat{\tau}_{\rm BB}])\ , \end{aligned} \tag{7.35}$$

where for generic density matrices $\hat{\rho}'_{\rm EE}$ and $\hat{\rho}''_{\rm EE}$ of E, we introduced

$$\begin{aligned} \Delta S_p(\hat{\rho}'_{\rm EE},\hat{\rho}''_{\rm EE}) \ \equiv\ & S\Big(p\hat{\rho}'_{\rm EE} + (1-p)\hat{\rho}''_{\rm EE}\Big) \\ & -pS\left(\hat{\rho}'_{\rm EE}\right) - (1-p)S\left(\hat{\rho}''_{\rm EE}\right)\ , \end{aligned} \tag{7.36}$$

which is non-negative due to the concavity of the von Neumann entropy. Notice that by simply specifying the above expression for the extreme cases $p = 1$ and $p = 0$ one can easily verify that Eq. (7.34) correctly complies with the bound in Eq. (7.29). On the contrary, an upper bound for $Q(\Phi_{\rm CC})$ can be obtained by dropping $\Delta S_p(\hat{\rho}'_{\rm EE},\hat{\rho}''_{\rm EE})$ in the right-hand-side of Eq. (7.35), leading to the following inequality

$$\begin{aligned} Q(\Phi_{\rm CC}) \ &\leq\ \max_{p\in[0,1]} \Big\{H_2(p) + pQ(\Phi_{\rm AA}) + (1-p)Q(\Phi_{\rm BB})\Big\} \\ &=\ \log_2(2^{Q(\Phi_{\rm AA})} + 2^{Q(\Phi_{\rm BB})})\ , \end{aligned} \tag{7.37}$$

where we introduced $Q(\Phi_{AA})$ and $Q(\Phi_{BB})$ using the optimization over $\hat{\tau}_{AA}$ and $\hat{\tau}_{BB}$, and where in the second line we carried out the maximization over p. This bound makes physical sense as it implies that the dimension of the optimal noiseless subspace of Φ_{CC} cannot be larger than the direct sum of the noise-free subspace associated with the channels Φ_{AA} and Φ_{BB} when used independently. Notice also that the inequality (7.37) is saturated by taking Φ_{CC} to be the identity channel.

7.4.2 Entanglement-assisted quantum capacity formula for PCDS channels

For the sake of completeness we report here the value of the entanglement assisted quantum capacity $Q_{ea}(\Phi_{XX})$ [BSST02, BSST02, BDSS06] for the case of arbitrary (non-necessarily degradable) PCDS channels. We remind that if we allow shared entanglement between sender and receiver the reliable transferring of quantum messages through the map Φ_{XX} can be improved via teleportation. The associated improvement is captured by the following expression

$$Q_{ea}(\Phi_{XX}) = \frac{1}{2} \max_{\rho_{XX} \in \mathfrak{S}_X} I(\Phi_{XX}; \hat{\rho}_{XX}) , \tag{7.38}$$

where now

$$I(\Phi_{XX}; \hat{\rho}_{XX}) \equiv S(\hat{\rho}_{XX}) + I_{coh}(\Phi_{XX}; \hat{\rho}_{XX}) , \tag{7.39}$$

is the *quantum mutual information*, which being sub-additive needs no regularization even if the map Φ_{XX} is not degradable.

In this case, besides Eq. (7.33) we also invoke the inequality

$$S(\hat{\rho}_{CC}) \leq pS(\hat{\tau}_{AA}) + (1-p)S(\hat{\tau}_{BB}) + H_2(p) , \tag{7.40}$$

that can be derived along the same line of reasoning. Replacing all this into Eq. (7.38) we get

$$\begin{aligned} Q_{ea}(\Phi_{CC}) = \max_{p \in [0,1]} \Big\{ & H_2(p) \\ & + \frac{1}{2} \max_{\hat{\tau}_{AA} \in \mathfrak{S}_A} \max_{\hat{\tau}_{BB} \in \mathfrak{S}_B} I_p(\Phi_{AA}; \hat{\tau}_{AA}, \Phi_{BB}; \hat{\tau}_{BB}) \Big\} , \end{aligned} \tag{7.41}$$

where now

$$\begin{aligned} I_p \equiv & \; pI(\Phi_{AA}; \hat{\tau}_{AA}) + (1-p) I(\Phi_{BB}; \hat{\tau}_{BB}) \\ & - \Delta S_p(\tilde{\Phi}_{EA}[\hat{\tau}_{AA}], \tilde{\Phi}_{EB}[\hat{\tau}_{BB}]) , \end{aligned} \tag{7.42}$$

with $I(\Phi_{AA}; \hat{\tau}_{AA})$ and $I(\Phi_{BB}; \hat{\tau}_{BB})$ the quantum mutual information functional of Eq. (7.39) of Φ_{AA} and Φ_{BB} respectively. As in the case of the formula in Eq. (7.34) we can get a lower bound for it by taking $p = 0, 1$ and an upper bound by dropping the term $\Delta S_p(\tilde{\Phi}_{EA}[\hat{\tau}_{AA}], \tilde{\Phi}_{EB}[\hat{\tau}_{BB}])$ in Eq. (7.42). This leads to the inequality

$$Q_{ea}(\Phi^{(0)}_{CC}) \leq Q_{ea}(\Phi_{CC}) \leq \log_2(2^{Q_{ea}(\Phi_{AA})} + 2^{Q_{ea}(\Phi_{BB})}) , \tag{7.43}$$

with $Q_{ea}(\Phi^{(0)}_{CC}) = \min\{Q_{ea}(\Phi^{(0)}_{AA}), Q_{ea}(\Phi^{(0)}_{BB})\}$ as in Ref. [FW07].

7.4.3 The special case of $\Phi_{BB} = \mathrm{Id}_{BB}$

We now focus on the special case where the diagonal block Φ_{BB} of the PCDS channel Φ_{CC} defined in Eq. (7.9) corresponds to the identity map Id_{BB}. Under this condition $\mathcal{H}_B$ is a decoherence-free subspace for the communication model. This implies that the value of $Q(\Phi_{CC})$ can always be lower bounded by $\log_2 d_B$, a condition that is automatically granted by the inequality (7.29), noticing that in this case $Q(\Phi_{BB}) = \log_2 d_B$. Deeper insight on the model arises by observing that from Eq. (7.17) we get

$$\tilde{\Phi}_{EB}[\hat{\Theta}_{BB}] = |0_E\rangle\langle 0_E| \, \mathrm{Tr}_B[\hat{\Theta}_{BB}] \, , \tag{7.44}$$

with $|0_E\rangle$ being an element of the orthonormal set $\{|j_E\rangle\}_j$ of $\mathcal{H}_E$. Accordingly from Eq. (7.35) we have

$$\begin{aligned} J_p &= pS\left(\Phi_{AA}[\hat{\tau}_{AA}]\right) + (1-p)S\left(\hat{\tau}_{BB}\right) \\ &\quad -S\Big(p\tilde{\Phi}_{EA}(\hat{\tau}_{AA}) + (1-p)|0_E\rangle\langle 0_E|\Big) \\ &\leq pS\left(\Phi_{AA}[\hat{\tau}_{AA}]\right) + (1-p)\log_2 d_B \\ &\quad -S\Big(p\tilde{\Phi}_{EA}(\hat{\tau}_{AA}) + (1-p)|0_E\rangle\langle 0_E|\Big) \, , \end{aligned} \tag{7.45}$$

the upper bound being achieved by taking as input $\hat{\tau}_{BB}$ for B the completely mixed state $\hat{P}_{BB}/d_B$. Hence the capacity formulas in Eqs. (7.34) and (7.41) now write respectively

$$\begin{aligned} Q(\Phi_{CC}) &= \max_{p\in[0,1]} \Big\{ H_2(p) + (1-p)\log_2 d_B \\ &\quad + \max_{\hat{\tau}_{AA}\in\mathfrak{S}_A} \Big\{ pS\left(\Phi_{AA}[\hat{\tau}_{AA}]\right) \\ &\quad -S(p\tilde{\Phi}_{EA}[\hat{\tau}_{AA}] + (1-p)|0_E\rangle\langle 0_E|) \Big\} \Big\} \, , \end{aligned} \tag{7.46}$$

which holds true for all choices of CPT maps Φ_{AA} that are degradable, and

$$\begin{aligned} Q_{ea}(\Phi_{CC}) &= \max_{p\in[0,1]} \Big\{ H_2(p) + (1-p)\log_2 d_B \\ &\quad + \frac{1}{2} \max_{\hat{\tau}_{AA}\in\mathfrak{S}_A} \Big\{ pS\left(\hat{\tau}_{AA}\right) + pS\left(\Phi_{AA}[\hat{\tau}_{AA}]\right) \\ &\quad -S(p\tilde{\Phi}_{EA}[\hat{\tau}_{AA}] + (1-p)|0_E\rangle\langle 0_E|) \Big\} \Big\} \, , \end{aligned} \tag{7.47}$$

that instead applies also for non degradable CPT maps Φ_{AA} – both expressions now involving only an optimization with respect to $\hat{\tau}_{AA}$ and p.

Notice that the relatively simple expression reported in Eq. (7.46) paves the way to refine a little the lower bound discussed in Sec. 7.4 for general PCDS channels. In particular, assume that there exists a density matrix $\hat{\rho}^*_{AA}$ of A such that the complementary channel $\tilde{\Phi}_{EA}$ of $\tilde{\Phi}_{AA}$ fulfills the following identity

$$\tilde{\Phi}_{EA}[\hat{\rho}^*_{AA}] = |0_E\rangle\langle 0_E| \, , \tag{7.48}$$

with $|0_E\rangle$ being the pure vector that via Eq. (7.44) defines the action of $\tilde{\Phi}_{\rm EB}$. Interestingly enough, in Appendix D.2.2 we show that this special requirement can always be met if the channel $\Phi_{\rm AA}$ admits a fixed point state that is pure (examples of those maps are provided by the cases studied in Sec. 7.5.2 and Sec. 7.5.3). Under the hypothesis in Eq. (7.48), setting $\hat{\tau}_{\rm AA} = \hat{\rho}^*_{\rm AA}$ in the right-end-side of Eqs. (7.46) and dropping a positive term we can then arrive to the inequality

$$\begin{aligned} Q(\Phi_{\rm CC}) &\geq \max_{p\in[0,1]} \Big\{ H_2(p) + (1-p)\log_2 d_{\rm B} \Big\} \\ &= \log_2(d_{\rm B}+1) \, . \end{aligned} \tag{7.49}$$

For $\log_2(d_{\rm B}+1) > Q(\Phi_{\rm AA})$ represents an improvement with respect to the general lower bound given in Eq. (7.29). At the physical level Eq. (7.49) implies that under the condition in Eq. (7.48) the model admits the presence of a decoherence-free subspace. The dimension of this subspace is $d_{\rm B}+1$ and is slightly larger than the value $d_{\rm B}$ that is granted for free by having the block B preserved during the evolution. An interesting consequence of Eq. (7.49) can finally be drawn by comparing it with Eq. (7.37). Indeed in the present case, due to the fact that $Q(\Phi_{\rm BB} = {\rm Id}_{\rm BB}) = \log_2 d_{\rm B}$, such an upper bound reduces to

$$Q(\Phi_{\rm CC}) \leq \log_2(2^{Q(\Phi_{\rm AA})} + d_{\rm B}) \, , \tag{7.50}$$

whose right-hand-side term exactly matches that of the lower bound of Eq. (7.49) whenever $Q(\Phi_{\rm AA}) = 0$. Putting all this together we can then arrive to the following observation

Lemma 3. *Let Φ_{CC} be a PCDS quantum channel (7.9) with $\Phi_{BB} = Id_{BB}$. If Φ_{AA} is a zero-capacity (i.e. $Q(\Phi_{AA}) = 0$), degradable map admitting a pure fixed point state then we have*

$$Q(\Phi_{CC}) = \log_2(d_B+1) \, . \tag{7.51}$$

Explicit examples of $\Phi_{\rm CC}$ obeying the structural constraints imposed by the Lemma will be presented in Secs. 7.5.2 and 7.5.3, together with a rather important consequence of the identity in Eq. (7.51).

7.5 Applications

Here we report few applications of the identity in Eq. (7.46) that allows us to fully characterize the quantum capacity of a large class of nontrivial PCDS quantum channels, including some specific examples of CPT maps which are not degradable.

7.5.1 Purely Dephasing channels

As a first example of PCDS channels $\Phi_{\rm CC}$ described in Sec. 7.4.3 we focus on the purely dephasing maps [DBF07, TWW17] $\Delta^{(\kappa)}_{\rm CC}$ of Eq. (7.13). Accordingly in this case both $\Phi_{\rm BB}$

and $\Phi_{\rm AA}$ are the identity transformation and we can assign the Kraus set of the model by taking the following operators

$$\hat{M}^{(0)}_{\rm CC} = \kappa \hat{P}_{\rm AA} + \hat{P}_{\rm BB} \ , \quad \hat{M}^{(1)}_{\rm CC} = \sqrt{1-|\kappa|^2}\hat{P}_{\rm AA} \ . \tag{7.52}$$

Via Eq. (7.17) this leads us to Eq. (7.44) for the complementary channel $\tilde{\Phi}_{\rm EB}$ and to

$$\tilde{\Phi}_{\rm EA}[\hat{\Theta}_{\rm AA}] = |v^{(\kappa)}_{\rm E}\rangle\langle v^{(\kappa)}_{\rm E}| \, {\rm Tr}_{\rm A}[\hat{\Theta}_{\rm AA}] \ , \tag{7.53}$$

where now $|v_{\rm E}\rangle$ is the pure state vector

$$|v^{(\kappa)}_{\rm E}\rangle \equiv \kappa |0_{\rm E}\rangle + \sqrt{1-|\kappa|^2}|1_{\rm E}\rangle \ . \tag{7.54}$$

Since in the present case $\Phi_{\rm AA}$ is the identity channel, hence degradable, we can compute the quantum capacity of $\Delta^{(\kappa)}_{\rm CC}$ via the single letter formula in Eq. (7.46) which, by trivially upper-bounding $S\left(\Phi_{\rm AA}[\hat{\tau}_{\rm AA}]\right)$ with $\log_2 d_{\rm A}$, rewrites as

$$\begin{aligned} Q(\Delta^{(\kappa)}_{\rm CC}) \ &= \ \max_{p\in[0,1]} \Big\{ H_2(p) + p\log_2 d_{\rm A} + (1-p)\log_2 d_{\rm B} \\ &\quad -S(p|v^{(\kappa)}_{\rm E}\rangle\langle v^{(\kappa)}_{\rm E}| + (1-p)|0_{\rm E}\rangle\langle 0_{\rm E}|) \Big\} \\ &= \ \log_2 d_{\rm B} + \max_{p\in[0,1]} \Big\{ H_2(p) + p\log_2(d_{\rm A}/d_{\rm B}) \\ &\quad -H_2\left(\tfrac{1+\sqrt{1-4p(1-p)(1-|\kappa|^2)}}{2}\right) \Big\} \ . \end{aligned} \tag{7.55}$$

In the limiting cases $|\kappa| = 1$ (no noise) and $\kappa = 0$ (full dephasing) the maximization can be explicitly performed leading to the expected results of Eqs. (7.30) and (7.31), respectively. For all the other choices of κ we resort to numerical evaluation and report the obtained results in Fig. 7.1 a). Partial analytical information can however be recovered by noticing that the function we have to optimize with respect to p depends, apart from the noise coefficient $|\kappa|$, only upon the ratio $d_{\rm A}/d_{\rm B}$. From this fact, by simple analytical considerations it follows that functions $Q(\Delta^{(\kappa)}_{\rm CC})$ associated with models with same value of ratio $d_{\rm A}/d_{\rm B}$ will only differ by an additive constant. Furthermore, in the special case where $d_{\rm A}/d_{\rm B} = 1$ the maximization can be again carried out analytically, e.g. by noticing that the associated functional is symmetric for exchange of p and $1-p$: accordingly we can conclude that in this case the optimal value for p is $1/2$, implying

$$Q(\Delta^{(\kappa)}_{\rm CC}) \ = \ 1 - H_2((1-|\kappa|^2)/2) + \log_2(d_{\rm A}) \ , \tag{7.56}$$

For $d_{\rm A} = 1$ this expression correctly reproduces the capacity formula of Ref. [DS05] for the qubit ($d_{\rm C} = 2$) dephasing channel. It's worth noticing from Fig. 7.1 a) that depending on the combination of $(d_{\rm A}, d_{\rm B})$ a structure among the channels emerges. The noiseless subspace associated with $d_{\rm B}$ defines a "multiplet" of curves that converge to $\log_2(d_{\rm B})$ at $\kappa \sim 0$ and spread with increasing κ toward the values $\log_2(d_{\rm A} + d_{\rm B})$, never intersecting each other. Intersections can take place between elements of different multiplets, as

happens e.g. for the curves (3,3) and (1,4). In this case we can see that when $\kappa \gtrsim 0.75$, having 3 decohering levels and 3 noiseless performs better than having only 1 decohering level and 4 noiseless.

Similar conclusions can be drawn for the entanglement assisted capacity of $\Delta_{\rm CC}^{(\kappa)}$, which from Eq. (7.47) we express as

$$\begin{aligned} Q_{\rm ea}(\Delta_{\rm CC}^{(\kappa)}) &= \max_{p\in[0,1]} \Big\{ H_2(p) + p\log_2 d_{\rm A} + (1-p)\log_2 d_{\rm B} \\ &\quad -\frac{1}{2} S(p|v_{\rm E}^{(\kappa)}\rangle\langle v_{\rm E}^{(\kappa)}| + (1-p)|0_{\rm E}\rangle\langle 0_{\rm E}|) \Big\} \\ &= \log_2 d_{\rm B} + \max_{p\in[0,1]} \Big\{ H_2(p) + p\log_2(d_{\rm A}/d_{\rm B}) \\ &\quad -\frac{1}{2} H_2\left(\tfrac{1+\sqrt{1-4p(1-p)(1-|\kappa|^2)}}{2} \right) \Big\} , \end{aligned} \tag{7.57}$$

whose values are plotted in Fig. 7.1 b) (notice again that for $d_{\rm A} = d_{\rm B}$ the optimization can be performed analytically resulting in $Q_{\rm ea}(\Delta_{\rm CC}^{(\kappa)}) = 1 - \frac{1}{2}H_2((1-|\kappa|^2)/2) + \log_2(d_{\rm A})$).

7.5.2 Multi-level Amplitude Damping channels

As a second example we now focus on a multi-level version of the qubit Amplitude Damping channel [GF05], hereafter indicated as MAD channels in brief, which describes the probability for levels of a $d_{\rm C}$-dimensional system to decay into each other [CG21b]. In their most general form, given $\{|i_{\rm C}\rangle\}_{i=0,\cdots,d_{\rm C}-1}$ an orthornormal basis for $\mathcal{H}_{\rm C}$, these maps can be assigned by introducing the set of Kraus operators $\{\hat{M}_{\rm CC}^{(0)}\} \bigcup \{\hat{M}_{\rm CC}^{(ij)}\}_{i<j}$ formed by the $d_{\rm C}(d_{\rm C}-1)/2$ matrices

$$\hat{M}_{\rm CC}^{(ij)} \equiv \sqrt{\gamma_{ji}}\, |i_{\rm C}\rangle\langle j_{\rm C}| , \qquad \forall i < j , \tag{7.58}$$

with γ_{ji} real quantities on the interval $[0,1]$ describing the decay rate from the j-th to the i-th level (see Fig. 7.2). The damping parameters fulfill the conditions

$$\xi_j \equiv \sum_{0\le i<j} \gamma_{ji} \le 1 , \qquad \forall j = 1, \cdots, d_{\rm C}-1 . \tag{7.59}$$

The Kraus set is completed by

$$\hat{M}_{\rm CC}^{(0)} \equiv |0_{\rm C}\rangle\langle 0_{\rm C}| + \sum_{1\le j\le d_{\rm C}-1} \sqrt{1-\xi_j}\, |j_{\rm C}\rangle\langle j_{\rm C}| . \tag{7.60}$$

Besides providing effective description of the noisy evolution of energy dissipation of atomic models, MAD channels have a rather rich structure. Limit cases are those where all the γ_{ji} are zero, corresponding to the identity channel $\mathrm{Id}_{\rm CC}$, and the cases where equality holds in Eq. (7.59) leaving the level j totally depopulated. Most importantly for us, by properly tailoring the values of the parameters γ_{ji}, MAD channels can be used to construct nontrivial examples of PCDS channels. This happens, for instance, whenever

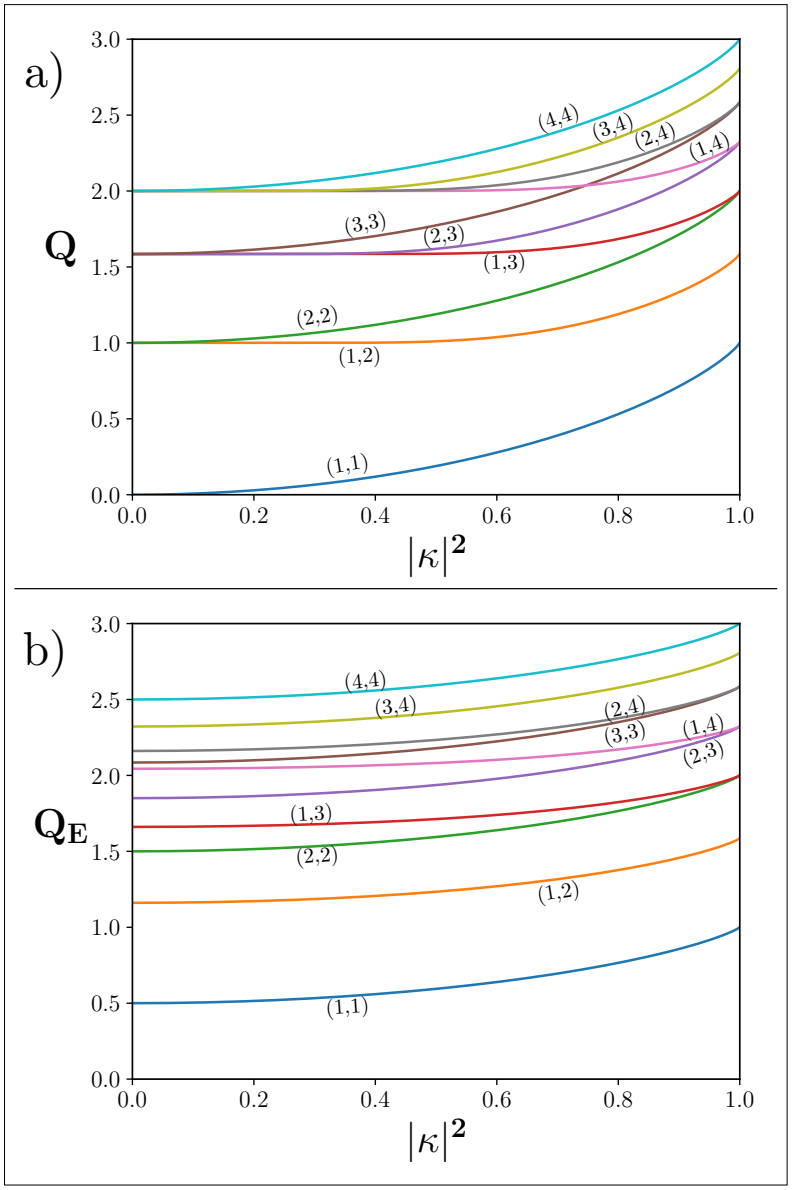

Figure 7.1: **a)** Quantum capacity Q of the purely dephasing channel $\Delta_{CC}^{(\kappa)}$ of Eq. (7.13) for some values of the couple (d_A, d_B) w.r.t. the dephasing parameter $|\kappa|^2$. For $d_A = d_B = 1$ we recover the quantum capacity of the qubit dephasing channel of [DS05]. **b)** Entanglement assisted quantum capacity Q_{ea} of $\Delta_{CC}^{(\kappa)}$ for some values of the couple (d_A, d_B) w.r.t. the dephasing parameter $|\kappa|^2$. It is worth observing that the curves associated with the same value of the ratio d_A/d_B differs only by an additive constant as predicted in the main text, and that the presence of the entanglement resource removes the degeneracy of the $Q(\Delta_{CC}^{(\kappa)})$ capacity for $\kappa = 0$. The monotonic behavior of the plotted curves follows from the channel DPI and from the trivial composition rules obeyed by the maps $\Delta_{CC}^{(\kappa)}$.

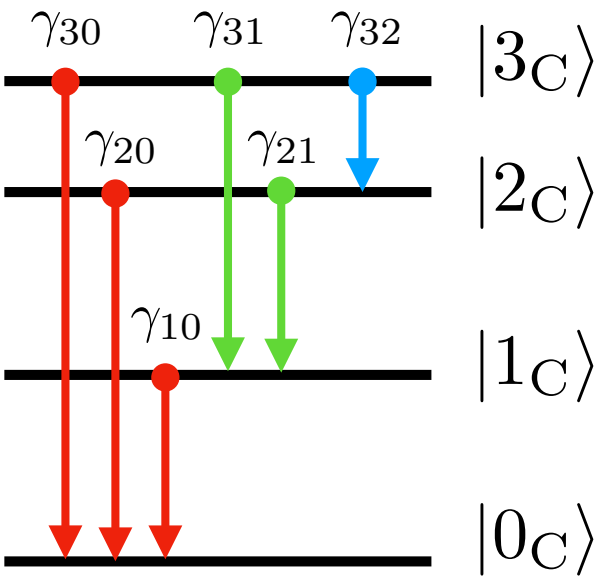

FIGURE 7.2: Schematic representation of a MAD channel acting on a system C of dimension $d_C = 4$: each arrow represents a decaying process where given $j > i$, the upper level $|j_C\rangle$ tends to relax toward the lower level $|i_C\rangle$ at rate γ_{ji}. Notice that by construction the ground state $|0_C\rangle$ is a fixed point of the evolution. An example of a PCDS map can be obtained for instance by imposing $\gamma_{30} = \gamma_{31} = \gamma_{31} = \gamma_{21} = 0$ (in this case A and B are both bi-dimensional subsets spanned by the vectors $|0_C\rangle$, $|1_C\rangle$ and $|2_C\rangle$, $|3_C\rangle$, respectively. The single non-zero decay rate MAD channel $\Omega^{[\gamma]}_{CC}$ is finally obtained by taking $\gamma_{10} = \gamma$ and setting all the other rates equal to zero: notice that in this case restricting the input states to the 3-dimensional subspace spanned by $|0_C\rangle$, $|2_C\rangle$, and $|3_C\rangle$, they will be preserved by the action of the noise.

the set of rates which are explicitly non zero can be split into two distinct groups of γ_{ji} characterized by values of the indexes j, i which span disjoint sets – see caption of Fig. 7.2. For the purpose of the present analysis we shall focus on the special class of these channels characterized by a single non-zero decay rate [CG21b]. Without loss of generality we choose the not null decaying parameter $\gamma \in [0, 1]$ to be the one connecting levels $|0_C\rangle$ and $|1_C\rangle$. We'll indicate then this channel as $\Omega^{[\gamma]}_{CC}$. Under this condition the Kraus set contains only two terms

$$\begin{aligned} \hat{M}^{(01)}_{CC} &\equiv \sqrt{\gamma}\,|0_C\rangle\langle 1_C|\ , \\ \hat{M}^{(0)}_{CC} &\equiv |0_C\rangle\langle 0_C| + \sqrt{1-\gamma}\,|1_C\rangle\langle 1_C| + \sum_{2\leq j\leq d_C-1} |j_C\rangle\langle j_C|\ , \end{aligned} \tag{7.61}$$

which can be easily cast in the PCDS canonical form of Theorem 1. This is done by identifying $\mathcal{H}_{\rm A}$ with the bi-dimensional ($d_{\rm A}=2$) subset spanned by the vectors $|0_{\rm A}\rangle \equiv |0_{\rm C}\rangle$, $|1_{\rm A}\rangle \equiv |1_{\rm C}\rangle$, and $\mathcal{H}_{\rm B}$ with the Hilbert space of dimension $d_{\rm B}=d_{\rm C}-2$ spanned by the vectors $\{|i_{\rm B}\rangle \equiv |(i+2)_{\rm C}\rangle\}_{i=0,\cdots,d_{\rm B}-1}$. Accordingly $\Omega^{[\gamma]}_{\rm CC}$ can be expressed as in Eq. (7.9) with the diagonal terms given respectively by the identity map $\mathrm{Id}_{\rm BB}$ on B, and by the standard qubit Amplitude Damping Channel (ADC) $\Omega^{[\gamma]}_{\rm AA}$, described by the Kraus elements $\hat{M}^{(01)}_{\rm AA} \equiv \sqrt{\gamma}\,|0_{\rm A}\rangle\langle 1_{\rm A}|$ $\hat{M}^{(0)}_{\rm AA} \equiv |0_{\rm A}\rangle\langle 0_{\rm A}| + (1-\gamma)\,|1_{\rm A}\rangle\langle 1_{\rm A}|$. Notice also that any even value of $d_{\rm C}$ can be seen as the dimension of a tensor Hilbert space $\mathcal{H}_{\rm C_1}\otimes\mathcal{H}_{\rm C_2}$ s.t. $d_{\rm C_1}d_{\rm C_2}=d_{\rm C}$. We can then see the MAD channel $\Omega^{[\gamma]}_{\rm CC}$ as a fully correlated ADC on $\mathcal{H}_{\rm C_1}\otimes\mathcal{H}_{\rm C_2}$ analogous to those studied by D'Arrigo et al. in Ref. [DBFM13]. There they studied the case for which $d_{\rm C_1}=d_{\rm C_2}=2$, that damps the 2-qubits state $|11\rangle$ in $|00\rangle$ and leaves the subspace spanned by $|01\rangle$ and $|10\rangle$ untouched.

We now proceed with the explicit evaluation of the quantum capacity of $\Omega^{[\gamma]}_{\rm CC}$. As a preliminary observation we establish two facts that hold true for the entire spectrum of the values of the parameter γ. First of all, as in the case of their qubit counterpart $\Omega_{\rm AA}$, the set of MAD channel $\Omega_{\rm CC}$ is closed under channel composition. In particular given $\gamma_1,\gamma_2\in[0,1]$, we have $\Omega^{[\gamma_1]}_{\rm CC}\circ\Omega^{[\gamma_2]}_{\rm CC}=\Omega^{[\gamma_3]}_{\rm CC}$ with $\gamma_3\equiv\gamma_1+\gamma_2-\gamma_1\gamma_2$. Noticing that γ_3 is larger than γ_1 and γ_2, we can hence invoke the coherent information DPI to establish that $Q(\Omega^{[\gamma]}_{\rm CC})$ must be monotonically decreasing w.r.t. γ, i.e.

$$Q(\Omega^{[\gamma]}_{\rm CC}) \geq Q(\Omega^{[\gamma']}_{\rm CC}) \qquad \forall \gamma\leq\gamma' \,. \tag{7.62}$$

Second we notice that for all γ values we have that the $d_{\rm C}-1$ dimensional subspace $\mathcal{H}'_{\rm C}$, spanned by all the vectors of the basis $\{|i_{\rm C}\rangle\}_{i=0,\cdots,d_{\rm C}-1}$ but $|1_{\rm C}\rangle$, is fully preserved by the action of $\Omega^{[\gamma]}_{\rm CC}$, i.e. $\Omega^{[\gamma]}_{\rm CC}[\hat{\rho}_{\rm CC}]=\hat{\rho}_{\rm CC}\ \forall\ \hat{\rho}_{\rm CC}\in\mathfrak{S}(\mathcal{H}'_{\rm C})$. Accordingly the model allows for the reliable transfer of at least $\log_2(d_{\rm C}-1)$ qubits, leading to the following inequality

$$Q(\Omega^{[\gamma]}_{\rm CC}) \geq \log_2(d_{\rm C}-1) = \log_2(d_{\rm B}+1)\,, \tag{7.63}$$

which subsides the lower bound $Q(\Omega^{[\gamma]}_{\rm CC})\geq\log_2 d_{\rm B}$ that follows from Eq. (7.28).

Let's then proceed with the explicit evaluation of the capacity. To begin with, we remind that the qubit ADC $\Omega^{[\gamma]}_{\rm AA}$ is known to be degradable for $0\leq\gamma\leq 1/2$ and antidegradable for $1/2\leq\gamma\leq 1$ [GF05]. Invoking hence Theorem 2 we can conclude that the MAD channel $\Omega^{[\gamma]}_{\rm CC}$ is degradable if and only if $0\leq\gamma\leq 1/2$. For this values (and only for those values) we can hence compute $Q(\Omega^{[\gamma]}_{\rm CC})$ with the single letter formula in Eq. (7.46). Specifically, remembering that the complementary channel of the qubit ADC $\Omega^{[\gamma]}_{\rm AA}$ for given γ is unitarily equivalent to the qubit ADC $\Omega^{[1-\gamma]}_{\rm AA}$ [GF05], we can write

$$\begin{aligned} Q(\Omega^{[\gamma]}_{\rm CC}) \;=\; & \max_{p\in[0,1]}\Big\{H_2(p)+(1-p)\log_2 d_{\rm B} \\ & + \max_{\hat{\tau}_{\rm AA}\in\mathfrak{S}_{\rm A}}\Big\{pS\left(\Omega^{[\gamma]}_{\rm AA}[\hat{\tau}_{\rm AA}]\right) \\ & - S(p\Omega^{[1-\gamma]}_{\rm AA}[\hat{\tau}_{\rm AA}]+(1-p)|0_{\rm A}\rangle\langle 0_{\rm A}|)\Big\}\Big\}\,, \end{aligned} \tag{7.64}$$

where without loss of generality we identified the vector $|0_{\rm E}\rangle$ of the environment E with the ground state $|0_{\rm A}\rangle$ of A. A numerical evaluation of this function is reported in Fig. 7.3 a) for different choices of $d_{\rm B}$. Notice in particular that for $\gamma = 1/2$ we get

$$Q(\Omega_{\rm CC}^{[1/2]}) = \log_2(d_{\rm B}+1), \tag{7.65}$$

something that can be analytically proven as a direct consequence of Lemma 3. This is due to the fact that in this case $Q(\Omega_{\rm AA}^{[\gamma=1/2]}) = 0$ (the channel $\Omega_{\rm AA}^{[\gamma=1/2]}$ being both degradable and antidegradable), and $\Omega_{\rm AA}^{[\gamma=1/2]}$ admits the pure state $|0_{\rm A}\rangle$ as fixed point [GF05], i.e. $\Omega_{\rm AA}^{[\gamma=1/2]}[|0_{\rm A}\rangle\langle 0_{\rm A}|] = |0_{\rm A}\rangle\langle 0_{\rm A}|$.

What about the capacity of $\Omega_{\rm CC}^{[\gamma]}$ for $\gamma > 1/2$? In this case Eq. (7.64) does not necessarily apply due to the fact that $\Omega_{\rm CC}^{[\gamma]}$ is provably not degradable. Observe that in this regime, at variance with its qubit counterpart $\Omega_{\rm AA}^{[\gamma]}$, $\Omega_{\rm CC}^{[\gamma]}$ is also certainly non antidegradable as a trivial consequence of the bound in Eq. (7.63) which prevents the quantum capacity from being zero. Accordingly the explicit evaluation of $Q(\Omega_{\rm CC}^{[\gamma]})$ for $\gamma > 1/2$ would require in principle to pass through the cumbersome regularization of Eq. (7.26). It turns out however that in this case we can explicitly compute $Q(\Omega_{\rm CC}^{[\gamma]})$ showing that it must keep the constant value it achieved for $\gamma = 1/2$, i.e.

$$Q(\Omega_{\rm CC}^{[\gamma]}) = \log_2(d_{\rm B}+1), \qquad \forall \gamma \in [1/2, 1]\ . \tag{7.66}$$

This indeed follows from Eq. (7.65), the monotonicity condition in Eq. (7.62), and the lower bound in Eq. (7.63) which together imply

$$Q(\Omega_{\rm CC}^{[1/2]}) \geq Q(\Omega_{\rm CC}^{[\gamma]}) \geq \log_2(d_{\rm B}+1)\ . \tag{7.67}$$

It follows then, even if the channel is not degradable for $1/2 < \gamma \leq 1$, that $Q(\Omega_{\rm CC}^{[\gamma]}) = Q^{(1)}(\Omega_{\rm CC}^{[\gamma]})\ \forall \gamma$.

All these results have been summarized in Fig. 7.3 a). In Fig. 7.3 b) instead we report the value of $Q_{\rm ea}(\Omega_{\rm CC}^{[\gamma]})$ as a function of γ which can be easily computed as in Eq. (7.47) that, following the same reasoning that led us to Eq. (7.64), rewrites now as

$$\begin{aligned} Q_{\rm ea}(\Omega_{\rm CC}^{[\gamma]}) \;=\; & \max_{p\in[0,1]} \Big\{ H_2(p) + (1-p)\log_2 d_{\rm B} \\ & + \frac{1}{2} \max_{\hat{\tau}_{\rm AA}\in\mathfrak{S}_{\rm A}} \Big\{ pS\left(\hat{\tau}_{\rm AA}\right) + pS\left(\Omega_{\rm AA}^{[\gamma]}[\hat{\tau}_{\rm AA}]\right) \\ & - S(p\Omega_{\rm AA}^{[1-\gamma]}[\hat{\tau}_{\rm AA}] + (1-p)|0_{\rm A}\rangle\langle 0_{\rm A}|) \Big\} \Big\}\ . \end{aligned} \tag{7.68}$$

Again, it is worth mentioning that in the region $1/2 \leq \gamma \leq 1$, for $d > 2$, the channels are not degradable nor antidegradable but still we are able to compute exactly Q by exploitation of coinciding upper and lower bounds.

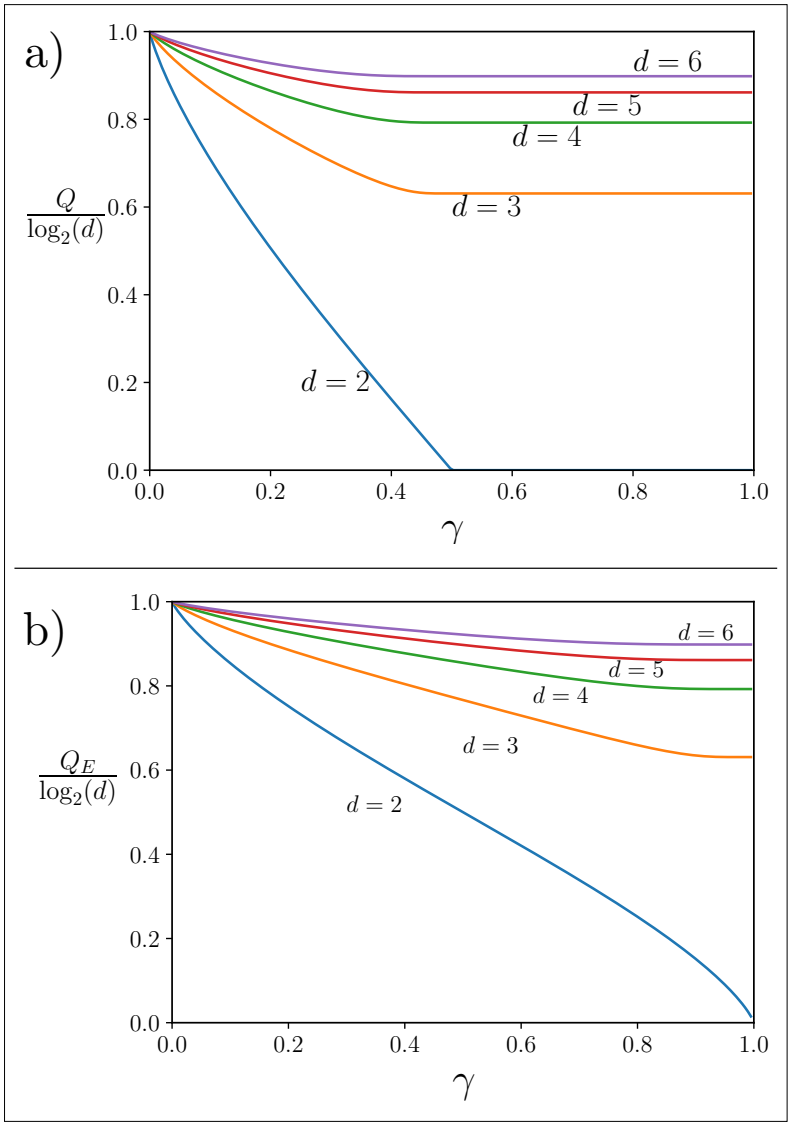

Figure 7.3: Normalized quantum capacities **a)** and entanglement assisted quantum capacities **b)** of single decay MAD channel $\Omega_{\mathrm{CC}}^{[\gamma]}$ for various dimensions d_{C}. Notice that the $d_{\mathrm{C}} = 2$ case corresponds to the qubit ADC [GF05] and the $d_{\mathrm{C}} = 4$ case to the fully correlated ADC of [DBFM13]. The channel is degradable only for $\gamma \leq 1/2$; for higher values of the rate the quantum capacity is constant and equal to $\log_2(d_{\mathrm{B}} + 1)$, see Eq. (7.67). The non increasing functional dependence of $Q(\Omega_{\mathrm{CC}}^{[\gamma]})$ and $Q_{\mathrm{ea}}(\Omega_{\mathrm{CC}}^{[\gamma]})$ upon γ is a consequence of the composition rule of the MAP channels and by the channel DPI.

7.5.3 MAD channel plus block dephasing

As a final example we now consider the capacity of channels obtained by composing the MAD transformations introduced in the previous section with the dephasing channels

$\Delta_{\rm CC}^{(\kappa)}$ that acts over the non diagonal blocks, as shown in Eq. (7.14), i.e. the maps

$$\Omega_{\rm CC}^{[\gamma](\kappa)} \equiv \Delta_{\rm CC}^{(\kappa)} \circ \Omega_{\rm CC}^{[\gamma]} = \Omega_{\rm CC}^{[\gamma]} \circ \Delta_{\rm CC}^{(\kappa)} \, . \tag{7.69}$$

As usual let us start with some preliminary observations. We can invoke the DPI for the quantum capacity and the internal composition rules of the sets $\Omega_{\rm CC}^{[\gamma]}$ and $\Delta_{\rm CC}^{(\kappa)}$. With those we can establish the quantum capacities of $\Omega_{\rm CC}^{[\gamma](\kappa)}$ to be monotonically decreasing in γ and monotonically increasing in $|\kappa|$, i.e.

$$Q(\Omega_{\rm CC}^{[\gamma](\kappa)}) \geq \max\{Q(\Omega_{\rm CC}^{[\gamma'](\kappa)}), Q(\Omega_{\rm CC}^{[\gamma](\kappa')})\} \, , \tag{7.70}$$

for all $\gamma \leq \gamma'$ and for all $|\kappa| \geq |\kappa'|$. Furthermore, again from DPI, it follows that the quantum capacity of $\Omega_{\rm CC}^{[\gamma](\kappa)}$ is always smaller than or equal to the corresponding value associated with the MAD channel $\Omega_{\rm CC}^{[\gamma]}$, as well as the quantum capacity of $\Delta_{\rm CC}^{(\kappa)}$ we computed in Sec. 7.5.1, i.e.

$$Q(\Omega_{\rm CC}^{[\gamma](\kappa)}) \leq \min\{Q(\Omega_{\rm CC}^{[\gamma]}), Q(\Delta_{\rm CC}^{(\kappa)})\} \, . \tag{7.71}$$

In particular for $\kappa = 0$ (full dephasing), from Eq. (7.28) we get

$$Q(\Omega_{\rm CC}^{[\gamma](0)}) = \max\{Q(\Omega_{\rm AA}^{[\gamma]}), \log_2 d_{\rm B}\} \, , \tag{7.72}$$

which, considering that the capacity $Q(\Omega_{\rm AA}^{[\gamma]})$ of the qubit ADC channel $\Omega_{\rm AA}^{[\gamma]}$ is always upper bounded by 1. It is clearly also always smaller than or equal to the lower bound in Eq. (7.63) of $Q(\Omega_{\rm CC}^{[\gamma]})$ as well as smaller than or equal to the value of $Q(\Delta_{\rm CC}^{(0)})$ given in Eq. (7.31).

To compute the exact value of $Q(\Omega_{\rm CC}^{[\gamma](\kappa)})$ for $\kappa \neq 0$, observe that as $\Omega_{\rm CC}^{[\gamma](\kappa)}$ shares the same diagonal block terms of $\Omega_{\rm CC}^{[\gamma]}$. It will enjoy the same degradability properties of the latter – see Theorem 2. In particular this implies that, irrespectively of the value of κ, $\Omega_{\rm CC}^{[\gamma](\kappa)}$ is again degradable if and only if $\gamma \leq 1/2$. Accordingly we can express $Q(\Omega_{\rm CC}^{[\gamma](\kappa)})$ using the single letter formula in Eq. (7.46). In Fig. 7.4 a) we report the solution for the case $d_{\rm C} = 3$ obtained by solving numerically the optimization over the input state $\hat{\tau}_{\rm AA}$ – see Appendix D.4 for details.

To obtain the value of $Q(\Omega_{\rm CC}^{[\gamma](\kappa)})$ also for $1/2 \leq \gamma \leq 1$, where the channel is explicitly not degradable, we resort to produce coinciding upper and lower bounds for such a quantity. Specifically we notice that, irrespectively of the value of γ, if we restrict the possible input states to the subspace spanned by $|0\rangle_{\rm C}$, $|2\rangle_{\rm C}$ we see that $\Omega_{\rm CC}^{[\gamma](\kappa)}$ acts just like the qubit dephasing channel. Its quantum capacity corresponds to the value given in Eq. (7.56) computed at $d_{\rm A} = 1$ [DS05] and which gives our lower bound, i.e.

$$Q(\Omega_{\rm CC}^{[\gamma](\kappa)}) \geq 1 - H_2((1 - |\kappa|)/2) \, . \tag{7.73}$$

An upper bound for $Q(\Omega_{\rm CC}^{[\gamma](\kappa)})$ for $\gamma > 1/2$ instead directly follows from Eq. (7.70) in the form

$$Q(\Omega_{\rm CC}^{[\gamma](\kappa)}) \leq Q(\Omega_{\rm CC}^{[1/2](\kappa)}) \, . \tag{7.74}$$

Now we compute $Q(\Omega_{\rm CC}^{[\gamma](\kappa)})\ \forall\,\kappa$ at $\gamma = 1/2$ and numerically we verify that it coincides with Eq. (7.73). Accordingly we can conclude that

$$Q(\Omega_{\rm CC}^{[\gamma](\kappa)}) = 1 - \frac{H_2(1-|\kappa|)}{2}\ , \qquad \forall \gamma \geq 1/2\ , \tag{7.75}$$

as reported in Fig. 7.4 a). As before, it is worth mentioning that in the region $1/2 \leq \gamma \leq 1$ the channels are not degradable nor antidegradable but still we are able to compute exactly Q by exploitation of coinciding upper and lower bounds.

Finally we perform the maximization in Eq. (7.47), which gives us $Q_{\rm ea}(\Omega_{\rm CC}^{[\gamma](\kappa)})$, reported in Fig. 7.4 b).

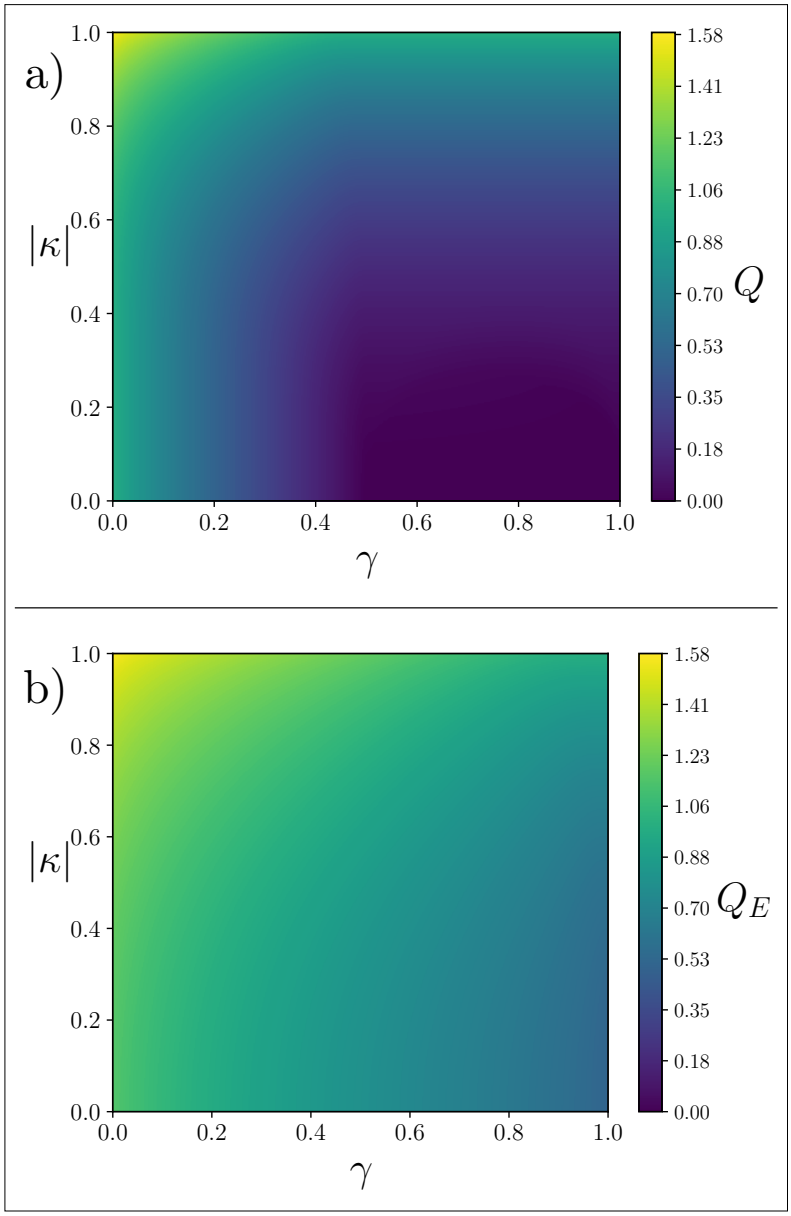

FIGURE 7.4: **a)** Quantum capacity of the channel $\Omega_{\mathrm{CC}}^{[\gamma](\kappa)}$ w.r.t. the damping parameter γ and the dephasing parameter $|\kappa|$. Notice that the map is degradable if and only if $\gamma \leq 1/2$. For $\gamma \geq 1/2$ the capacity no longer depends upon γ and it is given by Eq. (7.75). **b)** Entanglement assisted quantum capacity of the channel $\Omega_{\mathrm{CC}}^{[\gamma](\kappa)}$ w.r.t. the damping parameter γ and the dephasing parameter $|\kappa|$.

7.6 Conclusions

We firstly introduced the new class of *Partially Coherent Direct Sum* channels. We showed that an explicit and compact formula for the quantum capacity and entanglement

assisted quantum capacity is attainable, given suitable degradability conditions of the sub-blocks channels. Since for degradable channels quantum capacity Q and private classical capacity C_{p} are equivalent [Smi08], the degradability provides us also the latter. Since the expression of Q_{ea} differs from the entanglement assisted classical capacity C_{ea} just by a factor $1/2$ [BSST02, BSST02], given the former we have immediately the latter. We are also able to exhibit upper and lower bounds which, in some occasions, also allow us to state exactly the quantum capacity of non degradable channels. We applied the results to instances of the purely dephasing channels, qubit ADC and combinations of the two. The choice of a qubit ADC made here though was just adopted for the sake of simplicity. The same approach can be straightforwardly applied to higher dimensions ADC when known to be degradable [CG21b] or in general to "extend" any other finite dimensional degradable channel. The new approach is immediately generalizable to PCDS composed by $n > 2$ block channels. Moreover, since the maximization is reduced to sub-blocks, the overall problem complexity is considerably lower, making a large class of higher dimensional noisy channels capacities accessible.

8 Conclusions

This thesis goal was to summarize, for how little it could be, our contribution to the literature pertaining Quantum Communication, particularly Quantum Shannon Theory. Our a special interest was primarily devoted towards bounds over some of the known capacities in Chapter 4 and towards quantum capacity and private classical capacity of quantum channels in Chapters 5, 6, 7.

We approached this problem with a perspective over the possible physical realizations of quantum communication schemes. We described the 'flying qubit' model, in which carriers move between communicating parties, and the static model, in which quantum states are transferred through a fixed infrastructure between communicating parties. Our work dealt with both of these two models. We studied information transfer through quantum networks in Chapter 4, where information and states are supposed to travel over a fixed network exploiting local interactions among sites: this is a immediate application of the static model. We then studied in Chapters 5, 6 instances of amplitude damping channels in higher dimensional systems: those kind of noise models can describe discrete encodings in bosonic systems such as photons, that are the paradigmatic example of flying qubit.

As a final synthetic wrap of this thesis we'll recap the main points of each chapter presented and we'll discuss some of the work that can still be done on each subject:

- **Chapter 4**

  Bounding capacities in quantum networks

  We discussed a very generic communication protocol in which communicating parties operate on localized regions of a quantum network equipped with an interaction among sites. By means of the Lieb-Robinson bound we showed that the classical capacity C, entanglement assisted capacity C_{ea}, the quantum capacity Q and the private classical capacity C_{p} of these networks can be bounded from above. This

bounds, with suitable assumptions over the nature of the network interaction, goes to 0 for propagation times that go to 0, recovering the locality of information transmission.

Prospects:

- The number of protocols, and consequently capacities, that are studied in the literature is wider than those approached by our work. A natural follow up would be to extend the analysis, in particular two-way protocols.
- We did not approach the issue of the optimality of our bounds: can we make them tighter?

- **Chapter 5**

  Multi-level amplitude damping channels, a capacity analysis

  We introduced the new class of quantum channels: Multi-level amplitude damping (MAD) channels. These channels emerge as generalization of the qubit amplitude damping channel by mimicking the Kraus operators set structure. We proceeded then at the analysis of quantum capacity, private classical capacity with a study of degradability and antidegradability conditions, and of entanglement assisted quantum and classical capacities.

  Prospects:

  - The analysis of the capacities was only provided for $d = 3$. We think it's implausible to give a dimension-independent solution, but we don't have a proof for that. Further study is needed to understand whether such general analysis can be done or not.
  - If the general analysis can't be done, studying more fixed dimensional cases may help in understanding how the behaviour of such channels scales with the input dimension.
  - Exploring similar channels with different Kraus structure.

- **Chapter 6**

  Resonant multi-level amplitude damping channels channels, a quantum capacity analysis

  We introduced the new class of quantum channels: Resonant multi-level amplitude damping (ReMAD) channels. Different from MAD channels, we constructed them by engineering their Stinespring representation , specifying the transitions between system and environment. We showed that they resemble MAD channels but express a different underlying physics. We studied then degradability and antidegradability in order to approach their quantum capacity and private classical capacity, we computed entanglement assisted quantum and classical capacities.

  Prospects:

  - As for MAD channels, the analysis of the capacities was only provided for $d = 3$. Also in this case we think it's implausible to give a dimension-independent

solution, but again we don't have a proof for that. Therefore similarly as the MAD case, further study is needed to understand whether such general analysis can be done or not.

- As for MAD channels, if the general analysis can't be done, studying more fixed dimensional cases may help in understanding how the behaviour of ReMAD channels scales with the input dimension.
- Exploring similar channels with different Stinespring structure.

- **Chapter 7**

  Partially Coherent Direct Sum channels

  We introduced the class of Partially Coherent Direct Sum channels, generalizing a construction from Fukuda and Wolf. We characterized their structure and show necessary an sufficient conditions for degradability. We exhibited some applications by computing the quantum capacity of composition of physical low dimensional channels shaping higher dimensional channels.

  Prospects:

  - We only approached the issue of quantum and private classical capacities by looking at degradability conditions. The behaviour of other capacities for PCDS channels is still unexplored.
  - We provided some physical examples as applications. A deeper quest over possible emergence of PCDS channels in realistic noise processes is missing.

A

Time-Polynomial Lieb-Robinson bounds for finite-range spin-network models

Preface

What follows is based on the published paper [CG19]:

- S. Chessa, and V. Giovannetti, Time-polynomial Lieb-Robinson bounds for finite-range spin-network models, *Phys. Rev. A* **100**, 052309 (2019).

The Lieb-Robinson bound sets a theoretical upper limit on the speed at which information can propagate in non-relativistic quantum spin networks. In its original version, it results in an exponentially exploding function of the evolution time, which is partially mitigated by an exponentially decreasing term that instead depends upon the distance covered by the signal (the ratio between the two exponents effectively defining an upper bound on the propagation speed). In the present Appendix, by properly accounting for the free parameters of the model, we show how to turn this construction into a stronger inequality where the upper limit only scales polynomially with respect to the evolution time. Our analysis applies to any chosen topology of the network, as long as the range of the associated interaction is explicitly finite. For the special case of linear spin networks we present also an alternative derivation based on a perturbative expansion approach which improves the previous inequality. In the same context we also establish a lower bound to the speed of the information spread which yields a non trivial result at least in the limit of small propagation times.

A.1 Introduction

When dealing with communication activities, information transfer speed is one of the most relevant parameters in order to characterise the communication line performances. This statement applies both to Quantum Communication, obviously, and Quantum Computation, where the effective ability to carry information, for instance from a gate to another one, can determine the number of calculations executable per unit of time. It appears therefore to be useful being able to estimate such speed or, whenever not possible, bound it with an upper value. In the context of communication via quantum spin networks [Bos07] a result of this kind can be obtained exploiting the so called Lieb-Robinson (L-R) bound [LR72, NSY19]: defining a suitable correlation function involving two local spatially separated operators $\hat{A}$ and $\hat{B}$, a maximum group velocity for correlations and consequently for signals can be extrapolated. In more recent years this bound has been generalised and applied to attain results in a wider set of circumstances. Specifically, among others, stick out proofs for the Lieb-Schultz-Mattis theorem in higher dimensions [Has04b], for the exponential clustering theorem [NS06], to link spectral gap and exponential decay of correlations for short-range interacting systems [HK06], for the existence of the dynamics for interactions with polynomial decay [NOS06], for area law in 1-D systems [Has07], for the stability of topological quantum order [BHM10], for information and entanglement spreading [BHV06, EG09, EvdWMK13, EW17], for black holes physics and information scrambling [LSH+13, RS16]. Bounds on correlation spreading, remaining in the framework set by L-R bounds, have been then generalized to different scenarios such as, for instance, long-range interactions [HT13, EvdWMK13, GFFMG14, FFGCG15, MKN17], disordered systems [BO07, BEO09], finite temperature [Has04a, HSGCA17, HG18]. After the original work by Lieb and Robinson the typical shape found to describe the bound has been the exponentially growing in time t and depressed with the spatial distance between the supports of the two operators $d(A, B)$, namely:

$$\|[\hat{A}(t), \hat{B}]\| \lesssim e^{v|t|}\, f(d(A,B)) \,, \tag{A.1}$$

with v positive constant, and $f(\,\cdot\,)$ being a suitable decreasing function, both depending upon the interaction considered, the size of the supports of $\hat{A}$ and $\hat{B}$ and the dimensions of the system [Has04b, NS06, NOS06, HK06]. More recently instances have been proposed [HG18, The14] in which such behaviour can be improved to a polynomial one

$$\|[\hat{A}(t), \hat{B}]\| \lesssim \left(\frac{t}{d(A,B)}\right)^{d(A,B)} \,, \tag{A.2}$$

at least for Hamiltonian couplings which have an explicitly finite range, and for short enough times. Aim of the present work is to set these results on a firm ground providing an alternative derivation of the polynomial version (A.2) of the L-R inequality which, as long as the range of the interactions involved is finite, holds true for arbitrary topology of the spin network and which does not suffer from the short time limitations that instead affects previous approaches. Our analysis yields a simple way to estimate the maximum speed at which signals can propagate along the network. In the second part of the Appendix we focus instead on the special case of single sites located at the extremal

points of a 1-D linear spin chain model. In this context we give an alternative derivation of the t-polynomial L-R bound and discuss how the same technique can also be used to provide a lower bound on $\|[\hat{A}(t), \hat{B}]\|$, which at least for small t is non trivial.

The Appendix is organized as follows. We start in Sec. A.2 presenting the model and recalling the original version of the L-R bound. The main result of the Appendix is hence presented in Sec. A.3 where by using simple analytical argument we derive our t-polynomial version of the L-R inequality. In Sec. A.4 we present instead the perturbative expansion approach for 1-D linear spin chain models. In Sec. A.5 we test results achieved in previous sections by comparing them to the numerical simulation of a spin chain. Conclusions are presented finally in Sec. A.6.

A.2 The model and some preliminary observations

Adopting the usual framework for the derivation of the L-B bound [NS06] let us consider a network $\mathcal{N}$ of quantum systems (spins) distributed on a graph $\mathbb{G} := (V, E)$ characterized by a set of vertices V and by a set E of edges. The model is equipped with a metric $d(x, y)$ defined as the shortest path (least number of edges) connecting $x, y \in V$ ($d(x, y)$ being set equal to infinity in the absence of a connecting path), which induces a measure for the diameter $D(X)$ of a given subset $X \subset V$, and a distance $d(X, Y)$ among the elements $X, Y \subset V$,

$$\begin{aligned} D(X) &:= \max_{x,y} \min\{d(x, y)|x, y \in X\} , \\ d(X, Y) &:= \min\{d(x, y)|x \in X, y \in Y\} . \end{aligned} \tag{A.3}$$

Indicating with $\mathcal{H}_x$ the Hilbert space associated with spin that occupies the vertex x of the graph, the Hamiltonian of $\mathcal{N}$ can be formally written as

$$\hat{H} := \sum_{X \subset V} \hat{H}_X , \tag{A.4}$$

where the summation runs over the subsets X of V with $\hat{H}_X$ being a self-adjoint operator that is local on the Hilbert space $\mathcal{H}_X := \otimes_{x \in X} \mathcal{H}_x$, i.e. it acts non-trivially on the spins of X while being the identity everywhere else. Consider then two subsets $A, B \subset V$ which are disjoint, $d(A, B) > 0$. Any two operators $\hat{A} := \hat{A}_A$ and $\hat{B} := \hat{B}_B$ that are local on such subsets clearly commute, i.e. $[\hat{A}, \hat{B}] = 0$. Yet as we let the system evolve under the action of the Hamiltonian $\hat{H}$, this condition will not necessarily hold due to the building up of correlations along the graph. More precisely, given $\hat{U}(t) := e^{-i\hat{H}t}$ the unitary evolution induced by (A.4), and indicating with

$$\hat{A}(t) := \hat{U}^\dagger(t)\hat{A}\hat{U}(t) , \tag{A.5}$$

the evolved counterpart of $\hat{A}$ in the Heisenberg representation, we expect the commutator $[\hat{A}(t), \hat{B}]$ to become explicitly non-zero for large enough t, the faster this happens, the strongest being the correlations that are dynamically induced by $\hat{H}$ (hereafter we set $\hbar = 1$ for simplicity). The Lieb-Robinson bound puts a limit on such behaviour that

applies for all $\hat{H}$ which are characterized by couplings that have a finite range character (at least approximately). Specifically, indicating with $|X|$ the total number of sites in the domain $X \subset V$, and with

$$M_X := \max_{x \in X} \dim[\mathcal{H}_x] \,, \tag{A.6}$$

the maximum value of its spins Hilbert space dimension, we say that $\hat{H}$ is well behaved in terms of long range interactions, if there exists a positive constant λ such that the functional

$$\|\hat{H}\|_\lambda := \sup_{x \in V} \sum_{X \ni x} |X| \, M_X^{2|X|} e^{\lambda D(X)} \, \|\hat{H}_X\| \,, \tag{A.7}$$

is finite. In this expression the symbol

$$\|\hat{\Theta}\| := \max_{|\psi\rangle} \|\hat{\Theta}|\psi\rangle\| \,, \tag{A.8}$$

represents the standard operator norm, while the summation runs over all the subset $X \subset V$ that contains x as an element. Variant versions [BR12, NS06, HK06] or generalizations [NSY19, NS09] of Eq. (A.7) can be found in the literature, however as they express the same behaviour and substantially differ only by constants, in the following we shall gloss over these differences. The L-R bound can now be expressed in the form of the following inequality [NS06]

$$\|[\hat{A}(t), \hat{B}]\| \leq 2|A||B|\|\hat{A}\|\|\hat{B}\|(e^{2|t|\|\hat{H}\|_\lambda} - 1)e^{-\lambda \, d(A,B)} \,, \tag{A.9}$$

which holds non trivially for well behaved Hamiltonian $\hat{H}$ admitting finite values of the quantity $\|\hat{H}\|_\lambda$. It is worth stressing that Eq. (A.9) is valid irrespectively from the initial state of the network and that, due to the dependence upon $|t|$ on the r.h.s. term, exactly the same bound can be derived for $\|[\hat{A}, \hat{B}(t)]\|$, obtained by exchanging the roles of $\hat{A}$ and $\hat{B}$. Finally we also point out that in many cases of physical interest the pre-factor $|A||B|$ on the r.h.s. can be simplified: for instance it can be omitted for one-dimensional models, while for nearest neighbor interactions one can replace this by the smaller of the boundary sizes of $\hat{A}$ and $\hat{B}$ supports [NS09].

For models characterized by interactions which are explicitly not finite, refinements of Eq. (A.9) have been obtained under special constraints on the decaying of the long-range Hamiltonian coupling contributions [HK06, NS06]. For instance assuming that there exist (finite) positive quantities s_1 and μ_1 (s_1 being independent from total number of sites of the graph $\mathbb{G}$), such that

$$\sup_{x \in V} \sum_{X \ni x} |X| \, \|\hat{H}_X\|[1 + D(X)]^{\mu_1} \leq s_1 \,, \tag{A.10}$$

one gets

$$\|[\hat{A}(t), \hat{B}]\| \leq C_1|A||B|\|\hat{A}\|\|\hat{B}\| \frac{e^{v_1|t|} - 1}{(1 + d(A,B))^{\mu_1}} \,, \tag{A.11}$$

with C_1 and v_1 positive quantities that only depend upon the metric of the network and on the Hamiltonian. On the contrary if there exist (finite) positive quantities μ_2 and s_2 (the latter being again independent from total number of sites of $\mathbb{G}$), such that

$$\sup_{x \in V} \sum_{X \ni x} |X| \, \|\hat{H}_X\| e^{\mu_2 D(X)} \leq s_2 \,, \tag{A.12}$$

we get instead

$$\|[\hat{A}(t),\hat{B}]\| \leq C_2|A||B|\|\hat{A}\|\|\hat{B}\|(e^{v_2|t|}-1)e^{-\mu_2 d(A,B)}\,, \tag{A.13}$$

where once more C_2 and v_2 are positive quantities that only depend upon the metric of the network and on the Hamiltonian. The common trait of these results is the fact that their associated upper bounds maintain the exponential dependence with respect to the transferring t enlightened in Eq. (A.1).

A.3 Casting the Lieb-Robinson bound into a t-polynomial form for finite range couplings

The inequality (A.9) is the starting point of our analysis: it is indicative of the fact that the model admits a finite speed $v \simeq 2\|\hat{H}\|_\lambda/\lambda$ at which correlations can spread out in the spin network. As $|t|$ increases, however, the bound becomes less and less informative due to the exponential dependence of the r.h.s.: in particular it becomes irrelevant as soon as the multiplicative factor of $\|\hat{A}\|\|\hat{B}\|$ gets larger than 2. In this limit in fact Eq. (A.9) is trivially subsided by the inequality

$$\|[\hat{A}(t),\hat{B}]\| \leq 2\|\hat{A}(t)\|\|\hat{B}\| = 2\|\hat{A}\|\|\hat{B}\|\,, \tag{A.14}$$

that follows by simple algebraic considerations. One way to strengthen the conclusions one can draw from (A.9) is to consider λ as a free parameter and to optimize with respect to all the values it can assume. As the functional dependence of $\|\hat{H}\|_\lambda$ upon λ is strongly influenced by the specific properties of the spin model, we restrict the analysis to the special (yet realistic and interesting) scenario of Hamiltonians $\hat{H}$ (A.4) which are strictly short-ranged. Accordingly we now impose $\hat{H}_X = 0$ to all the subsets $X \subset V$ which have a diameter $D(X)$ that is larger than a fixed finite value $\bar{D}$, i.e.

$$D(X) > \bar{D} \qquad \Longrightarrow \qquad \hat{H}_X = 0\,, \tag{A.15}$$

which is clearly more stringent than both those presented in Eqs. (A.10) and (A.12). Under this condition $\hat{H}$ is well behaved for all $\lambda \geq 0$ and one can write

$$\|\hat{H}\|_\lambda \leq \zeta\, e^{\lambda \bar{D}}, \qquad \forall \lambda \geq 0\,, \tag{A.16}$$

with ζ being a finite positive constant that for sufficiently regular graphs does not scale with the total number of spins of the system. For instance for regular arrays of first-neighbours-coupled spins we get $\zeta = 2CM^4\|\hat{h}\|$, where C is the maximum coordination number of the graph (i.e. the number of edges associated with a given site),

$$\|\hat{h}\| := \sup_{X \subset V} \|\hat{H}_X\|\,, \tag{A.17}$$

is the maximum strength of the interactions, and where $M := \max_{x\in V} \dim[\mathcal{H}_x]$ is the maximum dimension of the local spins Hilbert space of the model. More generally for graphs $\mathbb{G}$ characterized by finite values of C it is easy to show that ζ can not be greater than $C^{\bar{D}} M^{C^{\bar{D}}} \|\hat{h}\|$.

Using (A.16) we can now turn (A.9) into a more treatable expression

$$\|[\hat{A}(t),\hat{B}]\| \leq 2|A||B|\|\hat{A}\|\|\hat{B}\|(e^{2|t|\zeta e^{\lambda\bar{D}}}-1)e^{-\lambda\, d(A,B)}\,, \tag{A.18}$$

whose r.h.s. can now be explicitly minimized in terms of λ for any fixed t and $d(A,B)$. As shown in Sec. A.3.1 the final result is given by

$$\begin{aligned}\|[\hat{A}(t),\hat{B}]\| &\leq 2|A||B|\|\hat{A}\|\|\hat{B}\|\left(\frac{2\,e\,\zeta\,\bar{D}\,|t|}{d(A,B)}\right)^{\frac{d(A,B)}{\bar{D}}\mathcal{F}(\frac{d(A,B)}{\bar{D}})} \\ &\leq 2|A||B|\|\hat{A}\|\|\hat{B}\|\left(\frac{2\,e\,\zeta\,\bar{D}\,|t|}{d(A,B)}\right)^{\frac{d(A,B)}{\bar{D}}}\,,\end{aligned} \tag{A.19}$$

where in the second inequality we used the fact that the function $\mathcal{F}(x)$ defined in the Eq. (A.31) below and plotted in Fig. A.1 is monotonically increasing and bounded from above by its asymptotic value 1. At variance with Eq. (A.9), the inequality (A.19) con-

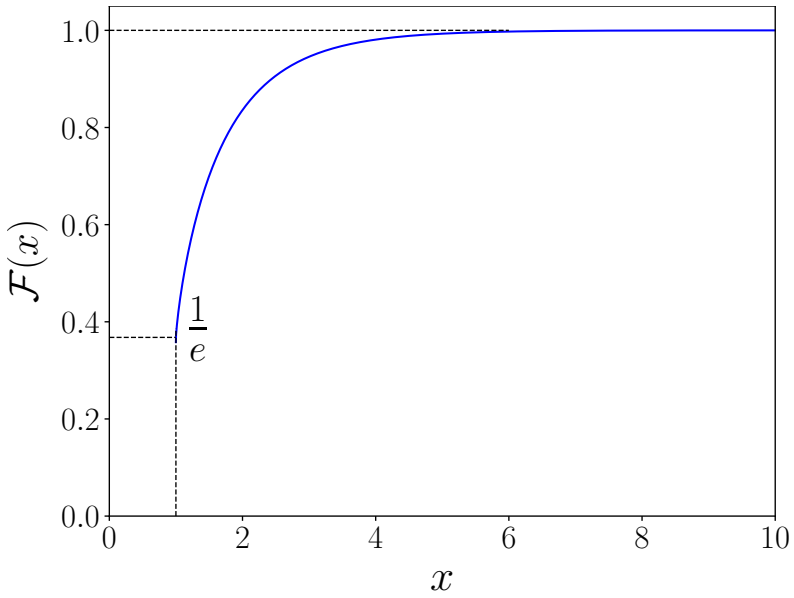

FIGURE A.1: Plot of the function $\mathcal{F}(x)$ entering into the derivation of Eq. (A.19): for $x = \frac{d(A,B)}{\bar{D}} \geq 1$ it is monotonically increasing reaching the value $1/e \simeq 0.37$ for $x = 1$ and quickly approaching the asymptotic value 1 for large enough x.

tains only terms which are explicit functions of the spin network parameters. Furthermore the new bound is polynomial in t with a scaling that is definitely better than the linear behaviour one could infer from the Taylor expansion of the r.h.s. of Eq. (A.9). Looking at the spatial component of (A.19) we notice that correlations still decrease with distance as well as in bounds (A.9), (A.11) and (A.13) but with a scaling $(1/x)^x = e^{-x\log x}$ that is more than exponentially depressed. Also, fixing a (positive) target threshold value $R_* < 1$ for the ratio

$$R(t) := \|[\hat{A}(t),\hat{B}]\|/(2|A||B|\|\hat{A}\|\|\hat{B}\|)\,, \tag{A.20}$$

equation (A.19) predicts that it will be reached not before a time interval

$$t_* = \frac{d(A,B) R_*^{\bar{D}/d(A,B)}}{2e\zeta\bar{D}} \,, \tag{A.21}$$

has elapsed from the beginning of the dynamical evolution. Exploiting the fact that $\lim_{z\to\infty} R_*^{1/z} = 1$, in the asymptotic limit of very distant sites (i.e. $d(A,B) \gg \bar{D}$), this can be simplified to

$$t_* \simeq \frac{d(A,B)}{2e\zeta\bar{D}} \,, \tag{A.22}$$

that is independent from the actual value of the target $R_* \neq 0$, leading us to identify the quantity

$$v_{\max} := 2e\zeta\bar{D} \,, \tag{A.23}$$

as an upper bound for the maximum speed allowed for the propagation of signals in the system.

A.3.1 Explicit derivation of Eq. (A.19)

We start by noticing that by neglecting the negative contribution $-e^{-\lambda\, d(A,B)}$, we can bound the r.h.s. Eq. (A.18) by a form which is much easier to handle, i.e.

$$\|[\hat{A}(t),\hat{B}]\| \leq 2|A||B|\|\hat{A}\|\|\hat{B}\| e^{2|t|\zeta e^{\lambda\bar{D}} - \lambda\, d(A,B)}. \tag{A.24}$$

One can observe that for $t > d(A,B)/(2\zeta\bar{D})$ the approach yields an inequality that is always less stringent than (A.14). On the contrary for $|t| \leq d(A,B)/(2\zeta\bar{D})$, imposing the stationary condition on the exponent term, i.e. $\partial_\lambda(e^{2\,\zeta\, e^{\lambda\overline{D}(X)}|t| - \lambda\, d(A,B)}) = 0$, we found that for the optimal value for λ is provided by

$$\lambda_{\text{opt}} := \frac{1}{\bar{D}} \ln\left(\frac{d(A,B)}{2\,|t|\,\zeta\,\bar{D}}\right), \tag{A.25}$$

which replaced in Eq. (A.24) yields directly (A.19). More generally, we can avoid to pass through Eq. (A.24) by looking for minima of the r.h.s. of Eq. (A.9) obtaining the first inequality given in Eq. (A.19), i.e.

$$\|[\hat{A}(t),\hat{B}]\| \leq 2|A||B|\|\hat{A}\|\|\hat{B}\| \left(\tfrac{2\,e\,\zeta\,\bar{D}\,|t|}{d(A,B)}\right)^{\frac{d(A,B)}{\bar{D}}} \mathcal{F}(\tfrac{d(A,B)}{\bar{D}}) \,. \tag{A.26}$$

For this purpose we consider a parametrization of the coefficient λ in terms of the positive variable z as indicated here

$$\lambda := \frac{1}{\bar{D}} \ln\left(\frac{z d(A,B)}{2\,|t|\,\zeta\,\bar{D}}\right). \tag{A.27}$$

With this choice the quantity we are interested in becomes

$$2|A||B|\|\hat{A}\|\|\hat{B}\|(e^{2|t|\zeta e^{\lambda\bar{D}}}-1)e^{-\lambda\, d(A,B)} = 2|A||B|\|\hat{A}\|\|\hat{B}\|\left(\tfrac{2et\zeta}{x}\right)^{x} f_x(z)\,, \tag{A.28}$$

where in the r.h.s. term for easy of notation we introduced $x = d(A,B)/\bar{D}$ and the function

$$f_x(z) := \frac{e^{xz}-1}{z^x e^x}\,. \tag{A.29}$$

For fixed value of $x \geq 1$ the minimum of the Eq. (A.29) is attained for $z = z_{\rm opt}$ fulfilling the constraint

$$x = -\frac{\ln(1-z_{\rm opt})}{z_{\rm opt}}\,. \tag{A.30}$$

By formally inverting this expression and by inserting it into Eq. (A.28) we hence get (A.26) with

$$\mathcal{F}(x) := \frac{z_{\rm opt}(x)}{1-z_{\rm opt}(x)}\left(\frac{1}{e z_{\rm opt}(x)}\right)^{x}\,, \tag{A.31}$$

being the monotonically increasing function reported in Fig. A.1.

A.4 Perturbative expansion approach

An alternative derivation of a t-polynomial bound similar to the one reported in Eq. (A.19) can be obtained by adopting a perturbative expansion of the unitary evolution of the operator $\hat{A}(t)$ that allows one to express the commutator $[\hat{A}(t),\hat{B}]$ as a sum over a collections of "paths" connecting the locations A and B, see e.g. Eq. (A.41) below. This derivation is somehow analogous to the one used in Refs. [HG18, The14]. Yet in these papers the number of relevant terms entering in the calculation of the norm of $[\hat{A}(t),\hat{B}]$ could be underestimated by just considering those paths which are obtained by concatenating adjacent contributions and resulting in corrections that are negligible only for small times t. In what follows we shall overcome these limitations by focusing on the special case of linear spin chains which allows for a proper account of the relevant paths. Finally we shall see how it is possible to exploit the perturbative expansion approach to also derive a lower bound for $\|[\hat{A}(t),\hat{B}]\|$.

While in principle the perturbative expansion approach can be adopted to discuss arbitrary topologies of the network, in order to get a closed formula for the final expression we shall restrict the analysis to the case of two single sites (i.e. $|A| = |B| = 1$) located at the end of a N-long, 1-D spin chain with next-neighbour interactions (i.e. $d = N-1$). Accordingly we shall write the Hamiltonian (A.4) as

$$\hat{H} := \sum_{i=1}^{N-1}\hat{h}_i\,, \tag{A.32}$$

with $\hat{h}_i$ operators acting non trivially only on the i-th and $(i+1)$-th spins, hence fulfilling the condition

$$[\hat{h}_i, \hat{h}_j] = 0 \,, \qquad \forall |i-j| > 1 \,. \tag{A.33}$$

A.4.1 Upper bound

Adopting the Baker-Campbell-Hausdorff formula we write

$$[\hat{A}(t), \hat{B}] = [\hat{A}, \hat{B}] + \sum_{k=1}^{\infty} \frac{(it)^k}{k!} \left[[\hat{H}, \hat{A}]_k, \hat{B} \right] \,, \tag{A.34}$$

where for $k \geq 1$,

$$[\hat{H}, \hat{A}]_k := \overbrace{[\hat{H}, [\hat{H}, [\cdots, [\hat{H}, [\hat{H}, \hat{A}]] \cdots]]}^{k \text{ times}} \,, \tag{A.35}$$

indicates the k-th order, nested commutator between $\hat{H}$ and $\hat{A}$. Exploiting the structural properties of Eqs. (A.32) and (A.33) it is easy to check that the only terms which may give us a non-zero contribution to the r.h.s. of Eq. (A.34) are those with $k \geq d$. Accordingly we get

$$[\hat{A}(t), \hat{B}] = \sum_{k=d}^{\infty} \frac{(it)^k}{k!} \left[[\hat{H}, \hat{A}]_k, \hat{B} \right] \,, \tag{A.36}$$

which leads to

$$\| [\hat{A}(t), \hat{B}] \| \leq \sum_{k=d}^{\infty} \frac{|t|^k}{k!} \| [[\hat{H}, \hat{A}]_k, \hat{B}] \| \,, \tag{A.37}$$

via sub-additivity of the norm. To proceed further we observe that

$$\| [[\hat{H}, \hat{A}]_k, \hat{B}] \| \leq 2 \|\hat{A}\| \|\hat{B}\| \|2\hat{H}\|^k \,, \tag{A.38}$$

which for sufficiently small times t yields

$$\begin{aligned} \| [\hat{A}(t), \hat{B}] \| &\simeq \frac{|t|^d}{d!} \| [[\hat{H}, \hat{A}]_d, \hat{B}] \| \\ &\leq 2 \|\hat{A}\| \|\hat{B}\| \frac{\left(2 \|\hat{H}\| |t| \right)^d}{d!} \\ &\leq \frac{2 \|\hat{A}\| \|\hat{B}\|}{\sqrt{2\pi d}} \left(\frac{2\, e \|\hat{H}\|\, |t|}{d} \right)^d \,, \end{aligned} \tag{A.39}$$

where in the last passage we adopted the lower bound on $d!$ that follows from the Stirling's inequalities

$$(d/e)^d \sqrt{e^2 d} \geq d! \geq (d/e)^d \sqrt{2\pi d} \,, \tag{A.40}$$

Equation (A.39) exhibits a polynomial behaviour similar to the one observed in Eq. (A.19) (notice that if instead of next-neighbour we had next-$\bar{D}$-neighbours interaction the first

not null order will be the $\lceil \frac{d}{\bar{D}} \rceil$-th one and accordingly, assuming $d/\bar{D}$ to be integer, the above derivation will still hold with d replaced by $d/\bar{D}$). Yet the derivation reported above suffers from two main limitations: first of all it only holds for sufficiently small t due to the fact that we have neglected all the terms of (A.37) but the first one; second the r.h.s of Eq. (A.39) has a direct dependence on the total size N of the system carried by $\|\hat{H}\|$, i.e. on the distance d connecting the two sites. Both these problems can be avoided by carefully considering each "nested" commutator $[[\hat{H}, \hat{A}]_k, \hat{B}]$ entering (A.37). Indeed given the structure of the Hamiltonian and the linearity of commutators, it follows that we can write

$$[[\hat{H}, \hat{A}]_k, \hat{B}] = \sum_{i_1, i_2, \cdots, i_k = 1}^{N-1} [\hat{C}^{(k)}_{i_1, i_2, \cdots, i_k}(\hat{A}), \hat{B}] \,, \tag{A.41}$$

where for $i_1, i_2, \cdots, i_k \in \{1, 2, \cdots, N-1\}$ we have

$$\hat{C}^{(k)}_{i_1, i_2, \cdots, i_k}(\hat{A}) := [\hat{h}_{i_k}, [\hat{h}_{i_{k-1}}, \cdots, [\hat{h}_{i_2}, [\hat{h}_{i_1}, \hat{A}]] \cdots]] \,. \tag{A.42}$$

Now taking into account the commutation rule (A.33) and of the fact that $\hat{A}$ and $\hat{B}$ are located at the two opposite ends of the chain, it turns out that only a limited number

$$n_k \leq \binom{k}{d} d^{k-d} = \frac{k!\, d^{k-d}}{d!(k-d)!} \,, \tag{A.43}$$

of the N^k terms entering (A.41) will have a chance of being non zero. For the sake of readability we postpose the explicit derivation of this inequality (as well as the comment on alternative approaches presented in Refs. [HG18, The14]) in Sec. A.4.3: here instead we observe that using

$$\|[\hat{C}^{(k)}_{i_1, i_2, \cdots, i_k}(\hat{A}), \hat{B}]\| \leq 2\|\hat{A}\|\|\hat{B}\|(2\|\hat{h}\|)^k \,, \tag{A.44}$$

where now $\|\hat{h}\| := \max_i \|\hat{h}_i\|$, it allows us to transform Eq. (A.37) into

$$\begin{aligned} \|[\hat{A}(t), \hat{B}]\| &\leq 2\|\hat{A}\|\|\hat{B}\| \sum_{k=d}^{\infty} n_k \frac{(2|t|\|\hat{h}\|)^k}{k!} \\ &\leq 2\|\hat{A}\|\|\hat{B}\| \frac{\left(2|t|\|\hat{h}\|\right)^d}{d!} \sum_{k=0}^{\infty} \frac{\left(2|t|\|\hat{h}\|d\right)^k}{k!} \\ &= 2\|\hat{A}\|\|\hat{B}\| \frac{\left(2|t|\|\hat{h}\|\right)^d}{d!} e^{2|t|\|\hat{h}\|d} \,, \end{aligned}$$

which presents a scaling that closely resemble to one obtained in Ref. [CSE08] for finite-range quadratic Hamiltonians for harmonic systems on a lattice. Invoking hence the lower bound for $d!$ that follows from (A.40) we finally get

$$\|[\hat{A}(t), \hat{B}]\| \leq \frac{2\|\hat{A}\|\|\hat{B}\|}{\sqrt{2\pi d}} \left(\frac{2\, e \|\hat{h}\|\, |t|}{d} \right)^d e^{2|t|\|\hat{h}\|d} \,, \tag{A.45}$$

which explicitly shows that the dependence from the system size present in (A.39) is lost in favour of a dependence on the interaction strength $\|\hat{h}\|$ similar to what we observed in Sec. A.3. In particular for small times the new inequality mimics the polynomial behaviour of (A.19): as a matter of fact, in this regime, due to the presence of the multiplicative term $1/\sqrt{d}$, Eq. (A.45) tends to be more strict than our previous bound (a result which is not surprising as the derivation of the present section takes full advantage of the linear topology of the network, while the analysis of Sec. A.3 holds true for a larger, less regular, class of possible scenarios). At large times on the contrary the new inequality is dominated by the exponential trend $e^{2|t|\|\hat{h}\|d}$ which however tends to be overruled by the trivial bound (A.14).

A.4.2 A lower bound

By properly handling the identity (A.36) it is also possible to derive a lower bound for $\|[\hat{A}(t), \hat{B}]\|$. Indeed using the inequality $\|\hat{O}_1 + \hat{O}_2\| \geq \|\hat{O}_1\| - \|\hat{O}_2\|$ we can write

$$\begin{aligned} \|[\hat{A}(t), \hat{B}]\| &= \Big\| \sum_{k=d}^{\infty} \frac{(it)^k}{k!} [[\hat{H}, \hat{A}]_k, \hat{B}] \Big\| \\ &\geq \frac{|t|^d}{d!} \|[[\hat{H}, \hat{A}]_d, \hat{B}]\| - \Big\| \sum_{k=d+1}^{\infty} \frac{(it)^k}{k!} [[\hat{H}, \hat{A}]_k, \hat{B}] \Big\| , \end{aligned} \tag{A.46}$$

(notice that the above bound is clearly trivial if $[[\hat{H}, \hat{A}]_d, \hat{B}]$ is the null operator: when this happens however we can replace it by substituting d on it with the smallest $k > d$ for which $[[\hat{H}, \hat{A}]_k, \hat{B}] \neq 0$). Now we observe that the last term appearing on the r.h.s. of the above expression can be bounded by following the same derivation of the previous paragraphs, i.e.

$$\begin{aligned} &\Big\| \sum_{k=d+1}^{\infty} \frac{(it)^k}{k!} [[\hat{H}, \hat{A}]_k, \hat{B}] \Big\| \\ &\qquad \leq 2\|\hat{A}\|\|\hat{B}\| \sum_{k=d+1}^{\infty} n_k \frac{(2|t|\|\hat{h}\|)^k}{k!} \\ &\qquad \leq 2\|\hat{A}\|\|\hat{B}\| \frac{\big(2|t|\|\hat{h}\|\big)^d}{d!} \sum_{k=1}^{\infty} \frac{\big(2|t|\|\hat{h}\|d\big)^k}{k!} \\ &\qquad = 2\|\hat{A}\|\|\hat{B}\| \frac{\big(2|t|\|\hat{h}\|\big)^d}{d!} (e^{2|t|\|\hat{h}\|d} - 1) \\ &\qquad \leq 2\|\hat{A}\|\|\hat{B}\| \left(\frac{2e|t|\|\hat{h}\|}{d} \right)^d \frac{e^{2|t|\|\hat{h}\|d} - 1}{\sqrt{2\pi d}} . \end{aligned}$$

Hence by replacing this into Eq. (A.46) we obtain

$$\begin{aligned}\|[\hat{A}(t),\hat{B}]\| &\geq \frac{|t|^d}{d!}\|[[\hat{H},\hat{A}]_d,\hat{B}]\| \\ &-2\|\hat{A}\|\|\hat{B}\|\left(\frac{2e|t|\|\hat{h}\|}{d}\right)^d \frac{e^{2|t|\|\hat{h}\|d}-1}{\sqrt{2\pi d}} \\ &\geq \frac{2\|\hat{A}\|\|\hat{B}\|}{\sqrt{2\pi d}}\left(\frac{2e|t|\|\hat{h}\|}{d}\right)^d \left(\Gamma_d - (e^{2|t|\|\hat{h}\|d}-1)\right) ,\end{aligned} \tag{A.47}$$

where in the last passage we used the upper bound for $d!$ that comes from Eq. (A.40) and introduced the dimensionless quantity

$$\Gamma_d := \sqrt{\frac{\pi}{2e^2}}\,\frac{\|[[\hat{H},\hat{A}]_d,\hat{B}]\|}{\|\hat{A}\|\|\hat{B}\|(2\|\hat{h}\|)^d} , \tag{A.48}$$

which can be shown to be strictly smaller than 1 (see Sec. A.4.3).

It's easy to verify that as long as Γ_d is non-zero (i.e. as long as $[[\hat{H},\hat{A}]_d,\hat{B}] \neq 0$), there exists always a sufficiently small time $\bar{t}$ such that $\forall\, 0 < t < \bar{t}$ the r.h.s. of Eq. (A.47) is explicitly positive, implying that we could have a finite amount of correlation at a time shorter than that required to light pulse to travel from A to B at speed c. This apparent violation of causality is clearly a consequence of the approximations that lead to the effective spin Hamiltonian we are working on (the predictive power of the model being always restricted to time scales t which are larger than $\frac{d(A,B)}{c}$). More precisely, for sufficiently small value of t (i.e. for $2|t|\|\hat{h}\|d \ll 1$) the negative contribution on the r.h.s. of Eq. (A.47) can be neglected and the bound predicts the norm of $[\hat{A}(t),\hat{B}]$ to grow polynomially as t^d, i.e.

$$\|[\hat{A}(t),\hat{B}]\| \gtrsim \frac{2\|\hat{A}\|\|\hat{B}\|}{\sqrt{2\pi d}}\left(\frac{2e|t|\|\hat{h}\|}{d}\right)^d \Gamma_d , \tag{A.49}$$

which should be compared with

$$\|[\hat{A}(t),\hat{B}]\| \lesssim \frac{2\|\hat{A}\|\|\hat{B}\|}{\sqrt{2\pi d}}\left(\frac{2e|t|\|\hat{h}\|}{d}\right)^d , \tag{A.50}$$

that, for the same temporal regimes is instead predicted from the upper bound (A.45).

A.4.3 Counting commutators

Here we report the explicit derivation of the inequality (A.43). The starting point of the analysis is the recursive identity

$$\hat{C}^{(k)}_{i_1,i_2,\cdots,i_k}(\hat{A}) = [\hat{h}_{i_k},\hat{C}^{(k-1)}_{i_1,i_2,\cdots,i_{k-1}}(\hat{A})] , \tag{A.51}$$

which links the expression for nested commutators (A.42) of order k to those of order $k-1$. Remember now that the operator $\hat{A}$ is located on the first site of the chain. Accordingly, from Eq. (A.33) it follows that

$$\hat{C}_i^{(1)}(\hat{A}) = [\hat{h}_i, \hat{A}] = 0 \,, \qquad \forall i \geq 2 \,, \tag{A.52}$$

i.e. the only possibly non-zero nested commutator of order 1 will be the operator $\hat{C}_1^{(1)}(\hat{A}) = [\hat{h}_1, \hat{A}]$ which acts non trivially on the first and second spin. From this and the recursive identity (A.51) we can then derive the following identity for the nested commutator of order $k = 2$, i.e.

$$\hat{C}^{(2)}_{1,i_2}(\hat{A}) = 0 \,, \qquad \forall i_2 \geq 3 \,, \tag{A.53}$$

$$\hat{C}^{(2)}_{i_1,i_2}(\hat{A}) = 0 \,, \qquad \forall i_1 \geq 2 \text{ and } \forall i_2 \geq 1 \,, \tag{A.54}$$

the only terms which can be possibly non-zero being now $\hat{C}^{(2)}_{1,1}(\hat{A})$ and $\hat{C}^{(2)}_{1,2}(\hat{A}) = [\hat{h}_2, [\hat{h}_1, \hat{A}]]$, the first having support on the first and second spin of the chain, the second instead being supported on the first, second, and third spin. Iterating the procedure it turns out that for generic value of k, the operators $\hat{C}^{(k)}_{i_1,i_2,\cdots,i_k}(\hat{A})$ which may be explicitly not null are those for which we have

$$\begin{cases} i_1 = 1 \,, \\ i_j \leq \max\{i_1, i_2, \cdots, i_{j-1}\} + 1 \,, \qquad \forall j \in \{2, \cdots, k\} \,, \end{cases} \tag{A.55}$$

the rule being that passing from $\hat{C}^{(k-1)}_{i_1,i_2,\cdots,i_{k-1}}(\hat{A})$ to $\hat{C}^{(k)}_{i_1,i_2,\cdots,i_k}(\hat{A})$, the new Hamiltonian element $\hat{h}_{i_k}$ entering (A.51) has to be one of those already touched (except the first one $[\hat{h}_1, A]$) or one at distance at most 1 to the maximum position reached until there. We also observe that among the element $\hat{C}^{(k)}_{i_1,i_2,\cdots,i_k}(\hat{A})$ which are not null, the one which have the largest support are those that have the largest value of the indexes: indeed from (A.51) it follows that the extra commutator with $\hat{h}_{i_k}$ will create an operator whose support either coincides with the one of $\hat{C}^{(k-1)}_{i_1,i_2,\cdots,i_{k-1}}(\hat{A})$ (this happens whenever i_k belongs to $\{i_1, i_2, \cdots, i_{k-1}\}$), or it is larger than the latter by one (this happens instead for $i_k = \max\{i_1, i_2, \cdots, i_{k-1}\} + 1$). Accordingly among the nested commutators of order k the one with the largest support is

$$\hat{C}^{(k)}_{1,2,\cdots,k}(\hat{A}) = [\hat{h}_k, [\hat{h}_{k-1}, \cdots, [\hat{h}_2, [\hat{h}_1, \hat{A}]] \cdots]] \,, \tag{A.56}$$

that in principle operates non trivially on all the first $k+1$ elements of the chain. Observe then that in order to get a non-zero contribution in (A.41) we also need the succession $\hat{h}_i$ entering $\hat{C}^{(k)}_{i_1,i_2,\cdots,i_k}(\hat{A})$ to touch at least once the support of $\hat{B}$. This, together with the prescription just discussed, implies that at least once every element $\hat{h}_i$ between A and B has to appear, and the first appearance of each $\hat{h}_i$ has to happen after the first appearance of $\hat{h}_{i-1}$. In summary we can think each nested commutator of order k as a numbered set of k boxes fillable with elements $\hat{h}_i$ (see Fig. A.2 (a)) and, keeping in mind the rules just discussed, we want to count how many fillings give us non zero commutators. Starting

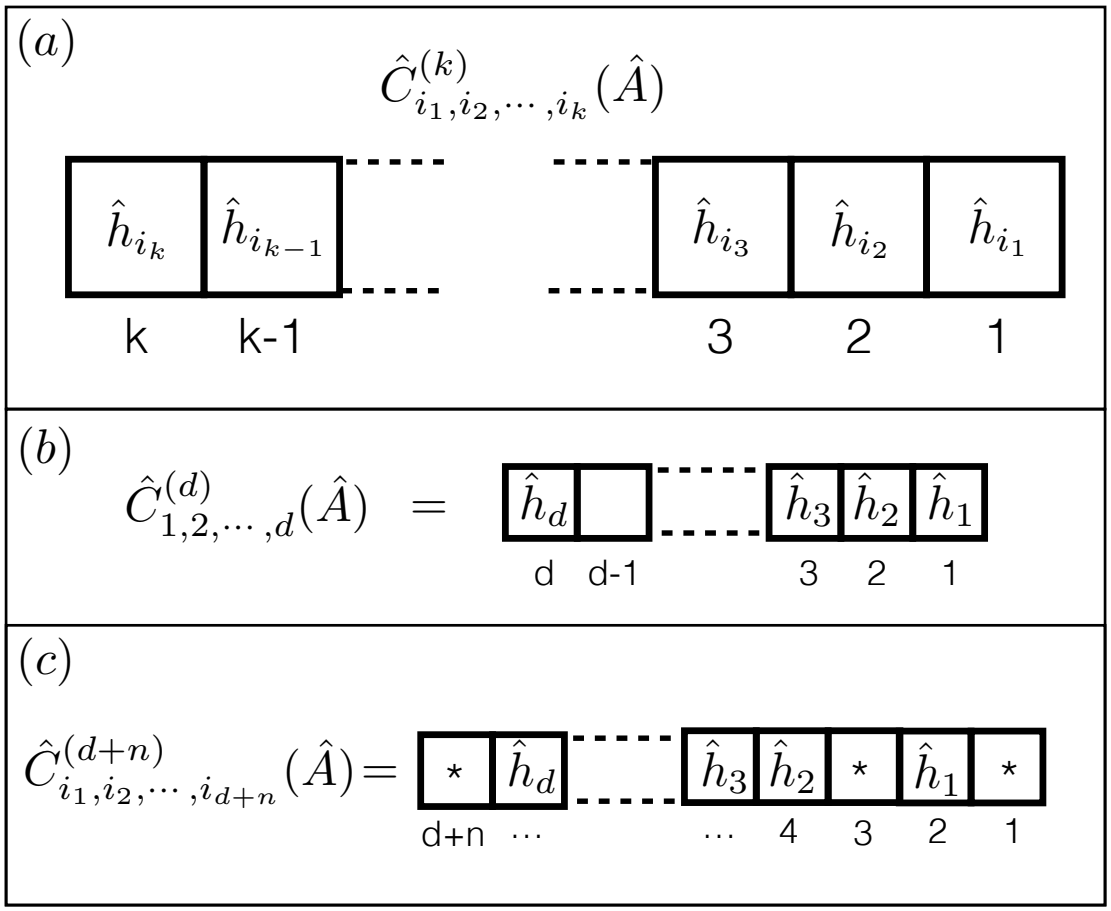

FIGURE A.2: Panel (a): Pictorial representation of the nested commutator $\hat{C}^{(k)}_{1,2,\cdots,k}(\hat{A})$ as a set of boxes, each one fillable with a $\hat{h}_i$; Panel (b): representation of the only nested commutator which for the case $k = d$ admits a non-zero value for the commutation with $\hat{B}$; Panel (c): case $k = d + n$ with $n \geq 1$. Here the boxes indicated with the asterisk can be filled depending on their position, for instance here the box before $\hat{h}_1$ could contain only $\hat{h}_1$ while the one after $\hat{h}_d$ could contain any.

from $k = d$, we have only one possibility, i.e. the element $\hat{C}^{(d)}_{1,2,\cdots,d}(\hat{A})$, see Fig. A.2 (b). This implies

$$\begin{aligned} [[\hat{H},\hat{A}]_d,\hat{B}] &= [\hat{C}^{(d)}_{1,2,\cdots,d}(\hat{A}),\hat{B}] \\ &= [[\hat{h}_d,[\hat{h}_{d-1},\cdots,[\hat{h}_2,[\hat{h}_1,\hat{A}]]\cdots]],\hat{B}]\,, \end{aligned} \tag{A.57}$$

and hence by sub-additivity of the norm, to

$$\|[[\hat{H},\hat{A}]_d,\hat{B}]\| \leq 2\|\hat{A}\|\|\hat{B}\|(2\|\hat{h}\|)^d\,, \tag{A.58}$$

which leads to $\Gamma_d \leq \sqrt{2\pi/e^2} \simeq 0.923$ as anticipated in the paragraph below Eq. (A.48). Consider next the case $k = d+n$ with $n \geq 1$. In this event we must have at least d boxes

filled with each $\hat{h}_i$ between $\hat{A}$ and $\hat{B}$. Once we fix them, the content of the remaining $k = n - d$ boxes (indicated by an asterisk in panel (c) of Fig. A.2) depends on their position in the sequence: if one of those is before the first $\hat{h}_1$ it will be forced to be $\hat{h}_1$, if it's before the first $\hat{h}_2$ it will be $\hat{h}_1$ or $\hat{h}_2$ and so on until the one before the first $\hat{h}_d$, which will be anyone among the $\hat{h}_i$. So in order to compute the number n_k of non-zero terms entering (A.41) we need to know in how many ways we can dispose the empty boxes in the sequence: since empty boxes (as well as the ones necessarily filled) are indistinguishable there are $\binom{k}{n} = \binom{k}{d}$ ways. For each way we'd have to count possible fillings, but there's not a straightforward method to do it so we settle for an upper bound. The worst case is the one in which all empty boxes come after the first $\hat{h}_d$, so that we have d^n fillings, accordingly we can bound n_k with $\binom{k}{n}d^n = \binom{k}{d}d^{k-d}$ leading to Eq. (A.43).

As mentioned at the beginning of the section a technique similar to the one reported here has been presented in the recent literature expressed in [HG18, The14]. These works also results in a polynomial upper bound for the commutator, yet it appears that the number of contributions entering in the parameter n_k could be underestimated, and this underestimation is negligible only at orders $k \simeq d$ or, equivalently, at small times. Specifically in [The14], which exploits intermediate results from [NRSS09, NOS06], the bound is obtained from the iteration of the inequality:

$$C_B(t, X) \leq C_B(0, X) + 2 \sum_{Z \in \partial X} \int_0^{|t|} \mathrm{d}s \; C_B(s, Z) \|\hat{H}_Z\|, \tag{A.59}$$

where $C_B(t, X) = \|[A(t), \hat{B}]\|$, X is the support of A and ∂X is the surface of the set X. The iteration adopted in [The14] produces an object that involve a summation of the form $\sum_{Z \in \partial X} \sum_{Z_1 \in \partial Z} \sum_{Z_2 \in \partial Z_1} \cdots$. This selection however underestimates the actual number of contributing terms. Indeed in the first order of iteration $Z \in \partial X$ takes account of all Hamiltonian elements non commutating with $\hat{A}$, but the next iteration needs to count all non commuting elements, given by $Z_1 \in \partial Z$ *and* $Z \in \partial X$. So the generally correct statement, as in Ref. [NOS06], would be $\sum_{Z \cap X \neq \emptyset} \sum_{Z_1 \cap Z \neq \emptyset} \sum_{Z_2 \cap Z_1 \neq \emptyset} \cdots$. The above discrepancy is particularly evident when focusing on the linear spin chain case we consider here. Taking account only of surface terms in the nested commutators in Eq. (A.37), among all the contributions which can be non-zero according to Eq. (A.55), we would have included only those with $i_{j+1} = i_j + 1$. This corrections are irrelevant at the first order in time in Eq. (A.37) but lead to underestimations in successive orders. In [The14] the discrepancy is mitigated at first orders by the fact that the number of paths of length L considered is upper bounded by $N_1(L) := (2(2\delta - 1))^L$ with δ dimensions of the graph. But again at higher orders this quantity is overcome by the actual numbers of potentially not null commutators (interestingly in the case of 2-D square lattice $N_1(L)$ could be found exactly, shrinking at the minimum the bound, see [GKS92]). Similarly is done in [HG18], where, in the specific case of a 2-D square lattice, to estimate the number of paths of length L a coordination number C is used, which gives an upper bound $N_2(L) := (2C - 1)^L$ that for higher orders is again an underestimation. To better visualize why this is the case, let's consider once more the chain configuration. Following rules of Eq. (A.55) we understood that nested commutators $\hat{C}^{(k)}_{i_1, i_2, \cdots, i_k}(\hat{A})$ with repetitions of indexes. So with growing k the number of possibilities for successive terms in the

commutator grows itself: this is equivalent to a growing dimension $\delta^{(k)}$ or coordination number $C^{(k)}$. For instance we can study the multiplicity of the extensions of the first not null order $\hat{C}^{(d)}_{1,2,\cdots,d}(\hat{A})$. Since the support of this commutator has covered all links between A and B we can choose among d possibilities (not taking into account possible sites beyond B and before A, depending on the geometry of the chain we choose), we'll have then d^{L-d} possibilities at the L-th order: for suitable d and n we shall have $d^{L-d} > N_1(L), N_2(L)$. This multiplicity is relative to a single initial path, so we do not even need to count also the different possible initial paths one can construct with $d+l$ steps s.t. $d+l < L$.

In summary, the polynomial behaviour found previously in the literature is solid at the first order but could not be at higher orders.

A.5 Simulation for a Heisenberg XY chain

Here we test the validity of our results presented in the previous section for a reasonably simple system such as a uniformly coupled, next-neighbour Heisenberg XY chain composed by L spin-1/2, described by the following Hamiltonian:

$$\hat{H} = J \sum_{i=0}^{L-1} \hat{\sigma}_i^x \hat{\sigma}_{i+1}^x + \hat{\sigma}_i^y \hat{\sigma}_{i+1}^y \,. \tag{A.60}$$

As local operators $\hat{A}$ and $\hat{B}$ we adopt two $\hat{\sigma}^z$ operators, acting respectively on the first and last spin of the chain, so that $\|\hat{A}\| = \|\hat{B}\| = 1$. Employing QuTiP [JNN12, JNN13] we perform the numerical evaluation for $\|[\hat{A}(t), \hat{B}]\|$ varying the length of the chain L. (Fig. A.3).

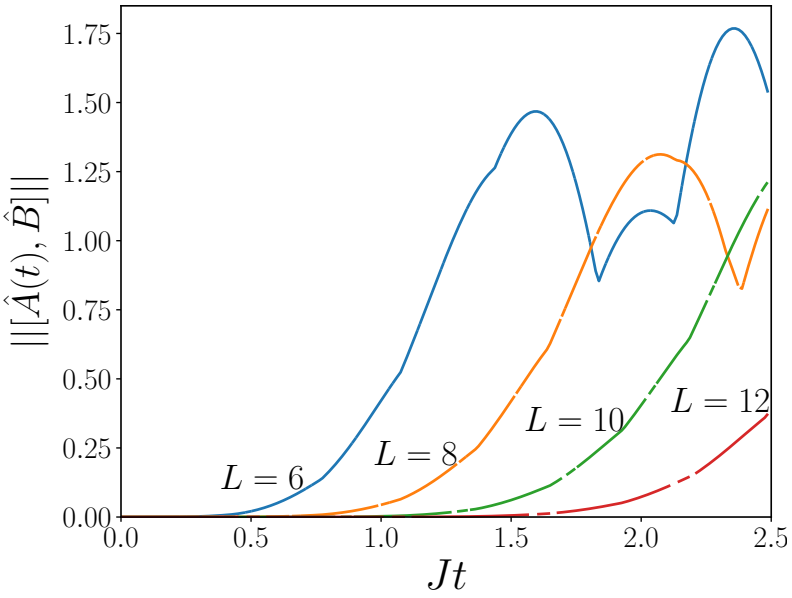

FIGURE A.3: (Color online): Simulation of $\|[\hat{A}(t), \hat{B}]\|$ for different chain lengths L for the Heisenberg XY linear spin-chain.

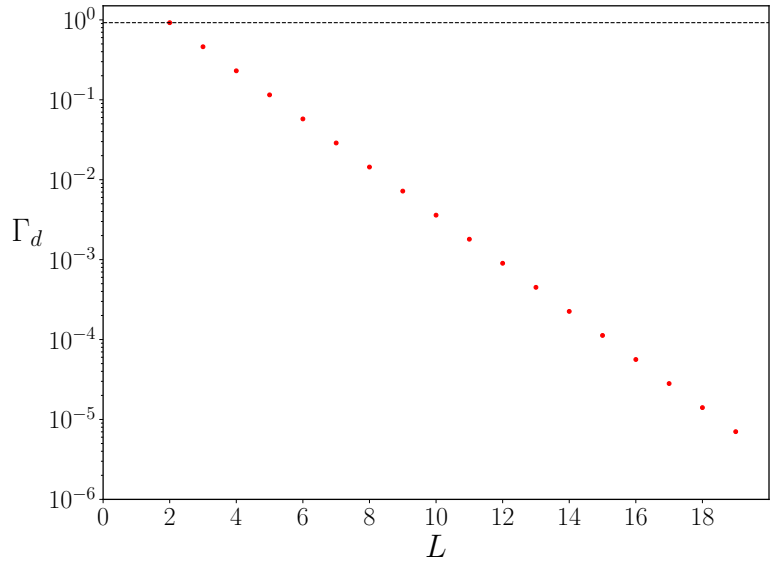

Figure A.4: (Color online): Plot of the value of Γ_d defined in Eq. (A.48) for different values of the chain length L, d being fixed equal to $L-1$. Notice that all values are below $\sqrt{2\pi/e^2}$ (dashed line) which is provably the largest value this parameter can achieve.

We are interested in the comparison between these results with the expressions obtained for the upper bound (A.45), the lower bound (A.47), and the simplified lower bound at short times (A.49). The time domain in which the simplified lower bound stands depends also on the value of the parameter Γ_d specified in Eq. (A.48), which we understood to be $\leq \sqrt{2\pi/e^2}$ but which we need reasonably large in order to produce a detectable bound in the numerical evaluation. In Fig. A.4 values of Γ_d for different chain lengths L (s.t. $d = L - 1$) are reported. The magnitude of Γ_d exhibits an exponential decrease with the size of the chain L. The results of our simulations are presented in Fig. A.5 for the cases $L = 4$ and $L = 10$. The upper bound (A.45), as well as the lower bound (A.47) should result to be universal, i.e. to hold for every t, although being the latter trivial at large times. This condition is satisfied for every L at every t analysed (we performed the simulation for $2 \leq L \leq 12$). For what concerns the simplified lower bound (A.49), we would expect its validity to be guaranteed only for sufficiently small t and as a matter of fact we find the time domain of validity to be limited at relatively small times (see e.g. the histograms in Fig. A.5).

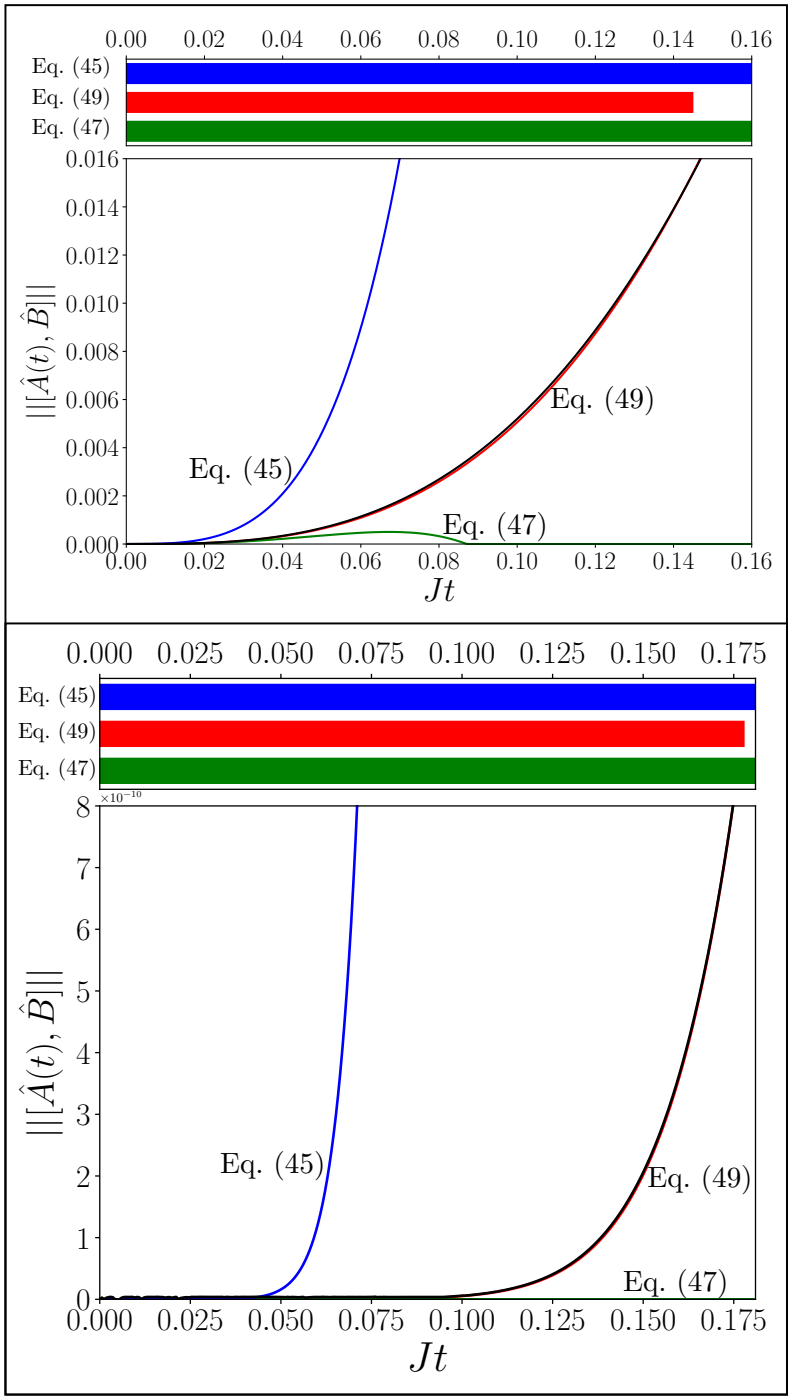

FIGURE A.5: (Color online): Simulation and bounds of the function $\|[\hat{A}(t), \hat{B}]\|$ for a $L = 4$ spin-chain (upper panel) and for a $L = 10$ spin-chain (lower panel). The plot shows upper bound (A.45) (blue curve) lower bound (A.47) (green curve), simplified lower bound (A.49) (red) and numerical simulation (black). The coloured bars above the plots outline the time domain in which the each bound (identified by the same colors) results to be valid. As expected the simplified bound stands only for sufficiently small times. In all cases the simulation and the simplified lower bound are comparable in magnitude so that their curves are hardly distinguishable. In the case of $L = 10$ the complete lower bound (A.47) (green) is considerably small, hence not visible.

A.6 Conclusions

The study of the L-R inequality we have presented here shows that for a large class of spin-network models characterized by couplings that are of finite range, the correlation function $\|[\hat{A}(t), \hat{B}]\|$ can be more tightly bounded by a new constraining function that exhibits a polynomial dependence with respect to time, and which, for sufficiently large distances, allows for a precise definition of a maximum speed of the signal propagation, see Eq. (A.23). Our approach does not rely on often complicated graph-counting arguments, instead is based on an analytical optimization of the original inequality [LR72] with respect to all free parameters of the model (specifically the λ parameter defining via Eq. (A.7) the convergence of the Hamiltonian couplings at large distances). Yet, in the special case of linear spin-chain, we do adopt a graph-counting argument to present an alternative derivation of our result and to show that a similar reasoning can be used to also construct non-trivial lower bounds for $\|[\hat{A}(t), \hat{B}]\|$ when the two sites are located at the opposite ends of the chain. Possible generalizations of the present approach can be foreseen by including a refined evaluation of the dependence upon λ of Eq. (A.7), that goes beyond the one we adopted in Eq. (A.16).

We point out that during the preparation of the manuscript on which this Chapter is based a similar result as the one presented in Eq. (A.50) for a chain appeared in Ref. [CL21].

B

Appendices to *Multi-level amplitude damping channels, a capacity analysis*

B.1 MAD channels: Mathematical prerequisites

Here we review some basic notions on quantum channels and quantum capacities that are extensively used in the main text.

B.1.1 Complementary channels and degradability

A CPTP map $\Phi : \mathcal{L}(\mathcal{H}_\mathrm{A}) \to \mathcal{L}(\mathcal{H}_\mathrm{B})$ can be seen as the evolution induced by an isometry $\hat{V} : \mathcal{H}_\mathrm{A} \to \mathcal{H}_\mathrm{B} \otimes \mathcal{H}_\mathrm{E}$ involving an environment E, called Stinespring dilation [Cho75, Sti55]. Specifically for all input states $\rho_\mathrm{A} \in \mathfrak{S}_\mathrm{A}$ we can write

$$\Phi(\hat{\rho}_\mathrm{A}) = \mathrm{Tr}_\mathrm{E}[\hat{V}\hat{\rho}_A\hat{V}^\dagger]. \tag{B.1}$$

If instead we trace out the degrees of freedom in B we obtain the complementary (or conjugate) channel $\tilde{\Phi} : \mathcal{L}(\mathcal{H}_\mathrm{A}) \to \mathcal{L}(\mathcal{H}_\mathrm{E})$, i.e.

$$\tilde{\Phi}(\hat{\rho}_\mathrm{A}) = \mathrm{Tr}_\mathrm{B}[\hat{V}\hat{\rho}_\mathrm{A}\hat{V}^\dagger]\,. \tag{B.2}$$

Being $\hat{M}_k$ the Kraus operators generating Φ and $|k\rangle_\mathrm{E}$ a basis for the environment, the operator $\hat{V}$ can be written as:

$$\hat{V} = \sum_k \hat{M}_k \otimes |k\rangle_E\,, \tag{B.3}$$

and being

$$\hat{V}\hat{\rho}_\mathrm{A}\hat{V}^\dagger = \sum_{i,j} \hat{M}_i\hat{\rho}_\mathrm{A}\hat{M}_j{}^\dagger \otimes |i\rangle_\mathrm{E}\langle j|\,, \tag{B.4}$$

it's straightforward to verify that Eq. (B.2) can be equivalently expressed as

$$\tilde{\Phi}(\hat{\rho}_{\mathrm{A}}) = \sum_{i,j} \mathrm{Tr}_{\mathrm{B}}[\hat{M}_i \hat{\rho}_{\mathrm{A}} \hat{M}_j{}^{\dagger}] \, |i\rangle_{\mathrm{E}}\langle j| \, . \tag{B.5}$$

A fact that it is worth mentioning, as it will play a fundamental role in our analysis, is that [Hol07] for a channel Φ that is covariant under a unitary representation of some group G, i.e.

$$\Phi(\hat{U}_g^{\mathrm{A}} \hat{\rho} \hat{U}_g^{\mathrm{A}\dagger}) = \hat{U}_g^{\mathrm{B}} \Phi(\hat{\rho}) \hat{U}_g^{\mathrm{B}\dagger} \, , \qquad \forall \hat{\rho} \in \mathfrak{S}(\mathcal{H}), \forall g \in G \, , \tag{B.6}$$

then also the complementary channel $\tilde{\Phi}$ is covariant under the same transformations, i.e.

$$\tilde{\Phi}(\hat{U}_g^{\mathrm{A}} \hat{\rho} \hat{U}_g^{\mathrm{A}\dagger}) = \hat{U}_g^{\mathrm{E}} \tilde{\Phi}(\hat{\rho}) \hat{U}_g^{\mathrm{E}\dagger} \, , \qquad \forall \hat{\rho} \in \mathfrak{S}(\mathcal{H}), \forall g \in G \, , \tag{B.7}$$

where for X=A,B,E, $\hat{U}_g^{\mathrm{X}}$ is the unitary operator that represents the element g of the group G in the output space X.

We finally recall the definition of degradable and anti-degradable channels [DS05]. A quantum channel Φ is said degradable if a CPTP map $\mathcal{N} : \mathcal{L}(\mathcal{H}_{\mathrm{B}}) \to \mathcal{L}(\mathcal{H}_{\mathrm{E}})$ exists s.t.

$$\tilde{\Phi} = \mathcal{N} \circ \Phi, \tag{B.8}$$

while it's said antidegradable if it exists a CPTP map $\mathcal{M} : \mathcal{L}(\mathcal{H}_{\mathrm{E}}) \to \mathcal{L}(\mathcal{H}_{\mathrm{B}})$ s.t.

$$\Phi = \mathcal{M} \circ \tilde{\Phi}, \tag{B.9}$$

(the symbol "$\circ$" representing channel concatenation). Notice that in case Φ is mathematically invertible, a simple direct way to determine whether it is degradable or not is to formally invert (B.8) constructing the super-operator $\tilde{\Phi} \circ \Phi^{-1}$ and check whether such object is CPTP (e.g. by studying the positivity of its Choi matrix) [WPG07, SS07], i.e. explicitly

$$\Phi \text{ invertible} \Longrightarrow \Phi \text{ degradable iff } \tilde{\Phi} \circ \Phi^{-1} \text{ is CPTP} \, . \tag{B.10}$$

Concretely this can be done by using the fact that since quantum channels are linear maps connecting vector spaces of linear operators, they can in turn being represented as matrices acting on vector spaces. This through the following vectorization isomorphism:

$$\begin{gathered} \hat{\rho}_{\mathrm{A}} = \sum_{ij} \rho_{ij} \, |i\rangle_{\mathrm{A}}\langle j| \quad \longrightarrow \quad |\rho\rangle\rangle = \sum_{ij} \rho_{ij} \, |i\rangle_{\mathrm{A}} \otimes |j\rangle_{\mathrm{A}} \in \mathcal{H}_{\mathrm{A}}^{\otimes 2} \\ \Phi(\hat{\rho}_{\mathrm{A}}) \quad \longrightarrow \quad \hat{M}_{\Phi} \, |\rho\rangle\rangle \, , \end{gathered} \tag{B.11}$$

where now $\hat{M}_{\Phi}$ is a $d_{\mathrm{B}}^2 \times d_{\mathrm{A}}^2$ matrix connecting $\mathcal{H}_{\mathrm{A}}^{\otimes 2}$ and $\mathcal{H}_{\mathrm{B}}^{\otimes 2}$ (d_{A} and d_{B} being respectively the dimensions of $\mathcal{H}_{\mathrm{A}}$ and $\mathcal{H}_{\mathrm{B}}$), which given a Kraus set $\{\hat{M}_k\}_k$ for Φ it can be explicitly expressed as

$$\hat{M}_{\Phi} = \sum_k \hat{M}_k \otimes \hat{M}_k{}^{*} . \tag{B.12}$$

Following Eq. (B.8) we have hence that for a degradable channel the following identity must apply

$$\hat{M}_{\tilde{\Phi}} = \hat{M}_{\mathcal{N}} \hat{M}_{\Phi}, \tag{B.13}$$

with $\hat{M}_{\mathcal{N}}$ the matrix representation of the CPTP connecting channel $\mathcal{N}$, implying that the super-operator $\tilde{\Phi} \circ \Phi^{-1}$ is now represented by matrix $\hat{M}_{\tilde{\Phi}} \hat{M}_{\Phi}^{-1}$.

B.1.2 The quantum capacity of a quantum channel

The quantum capacity $Q(\Phi)$ is a measure of how faithfully quantum states can transit from the input to the output of the quantum channel Φ by exploiting proper encoding and decoding procedures that act on multiple transmission stages [Hol19, Wil17, Wat18, HG12], see Sec. 3.3.3 in Chapter 3. A close, yet cumbersome, expression for $Q(\Phi)$ can be obtained in the form [Llo97, Sho02b, Dev05]

$$Q(\Phi) = \lim_{n\to\infty} \max_{\hat{\rho}^{(n)}\in\mathfrak{S}(\mathcal{H}^{\otimes n})} \frac{1}{n} I_{\rm coh}(\Phi^{\otimes n}, \hat{\rho}^{(n)}), \tag{B.14}$$

where $\hat{\rho}^{(n)}$ is a generic joint density matrix belonging to the input Hilbert space $\mathcal{H}^{\otimes n}$ on which the tensor extension $\Phi^{\otimes n}$ of Φ acts. The quantity appearing in the right-hand-side of Eq. (B.14) is the coherent information functional

$$I_{\rm coh}(\Phi^{\otimes n}, \hat{\rho}^{(n)}) \equiv S(\Phi^{\otimes n}(\hat{\rho}^{(n)})) - S(\tilde{\Phi}^{\otimes n}(\hat{\rho}^{(n)})), \tag{B.15}$$

with $S(\cdots) \equiv -{\rm Tr}[\cdots \log_2 \cdots]$ the von Neumann entropy [Hol19] and with $\tilde{\Phi}$ the complementary channel of Φ introduced in the previous section.

The expression in Eq. (B.14) isn't in general easily computable due to the fact that the coherent information functional is typically non sub-additive, making hard to take care of the regularization limit on n: removing it will in general produce just a lower bound to $Q(\Phi)$, i.e.

$$Q(\Phi) \geq Q^{(1)}(\Phi) \equiv \max_{\hat{\rho}\in\mathfrak{S}(\mathcal{H})} I_{\rm coh}(\Phi, \hat{\rho}) \,, \tag{B.16}$$

where now the maximization is performed on all possible input states $\hat{\rho}$ of a single application of Φ. Things however simplify a lot if Φ is antidegradable [CG06] or degradable [DS05]. Indeed in the first case one can invoke a no cloning argument to directly conclude that $Q(\Phi) = 0$. In the second case instead, the gap in Eq. (B.16) closes allowing us to compute $Q(\Phi)$ as

$$Q(\Phi) = Q^{(1)}(\Phi) \equiv \max_{\hat{\rho}\in\mathfrak{S}(\mathcal{H})} I_{\rm coh}(\Phi, \hat{\rho}). \tag{B.17}$$

Besides allowing for the single-letter simplification (B.17), another important consequence of the degradability property (B.8) is the fact that, for channels fulfilling such condition, the coherent information (B.15) is known to be concave [YHD08, WPG07] with respect to the input state $\hat{\rho}$, i.e.

$$I_{\rm coh}(\Phi, \sum_k p_k \hat{\rho}_k) \geq \sum_k p_k I_{\rm coh}(\Phi, \hat{\rho}_k) \,, \tag{B.18}$$

for all statistical ensemble of input states $\{p_k; \hat{\rho}_k\}$. This last inequality allows for some further drastic simplification in particular when the channel Φ is covariant under a group of unitary transformations as in Eq. (B.6). Indeed thanks to results in Ref. [Hol07] and the invariance of the von Neumann entropy under unitary operations we can now observe that

$$\begin{aligned} I_{\rm coh}(\Phi, \hat{U}_g^{\rm A} \hat{\rho} \hat{U}_g^{\rm A\dagger}) &= S(\Phi(\hat{U}_g^{\rm A} \hat{\rho} \hat{U}_g^{\rm A\dagger}) - S(\tilde{\Phi}(\hat{U}_g^{\rm A} \hat{\rho} \hat{U}_g^{\rm A\dagger})) \\ &= S(\hat{U}_g^{\rm B} \Phi(\hat{\rho}) \hat{U}_g^{\rm B\dagger}) - S(\hat{U}_g^{\rm E} \tilde{\Phi}(\hat{\rho}) \hat{U}_g^{\rm E\dagger}) \\ &= I_{\rm coh}(\Phi, \hat{\rho}) \,, \end{aligned} \tag{B.19}$$

for all input states and for all elements g of the group. Given then a generic input state $\hat{\rho}$ of the system, construct the following ensemble of density matrices $\{d\mu(g); \hat{\rho}_g\}$ with $d\mu(g)$ some properly defined probability distribution on G and with $\hat{\rho}_g \equiv \hat{U}_g^{\mathrm{A}} \hat{\rho} \hat{U}_g^{\mathrm{A}\dagger}$. Defining then

$$\Lambda_G[\hat{\rho}] \equiv \int d\mu_g \hat{\rho}_g = \int d\mu_g \hat{U}_g^{\mathrm{A}} \hat{\rho} \hat{U}_g^{\mathrm{A}\dagger} \,, \tag{B.20}$$

the average state of $\{d\mu(g); \hat{\rho}_g\}$ we notice that if Φ is degradable the following inequality holds true:

$$I_{\mathrm{coh}}(\Phi, \Lambda_G[\hat{\rho}]) \geq \int d\mu_g I_{\mathrm{coh}}(\Phi, \hat{U}_g^{\mathrm{A}} \hat{\rho} \hat{U}_g^{\mathrm{A}\dagger}) = I_{\mathrm{coh}}(\Phi, \hat{\rho}) \,, \tag{B.21}$$

where in the last passage we used the invariance (B.19). Accordingly we can now restrict the maximization in Eq. (B.17) to only those input states $\hat{\rho}_G$ which result from the averaging operation (B.20), i.e.

$$Q(\Phi) = Q^{(1)}(\Phi) = \max_{\hat{\rho}_G} I_{\mathrm{coh}}(\Phi, \hat{\rho}_G). \tag{B.22}$$

For the special case of the MAD channels $\mathcal{D}$ introduced in Sec. 5.2, thanks to Eq. (5.4) we can identify the group G with the set of unitary operations which are diagonal in the computational basis $\{|i\rangle\}_{i=0,\cdots,d-1}$. Taking $d\mu_g$ a flat measure, Eq. (B.20) allows us to identify $\Lambda_G[\hat{\rho}]$ with the density matrices of A which are diagonal as well, i.e.

$$\Lambda_G[\hat{\rho}] = \mathrm{diag}[\hat{\rho}] \,, \tag{B.23}$$

and therefore to derive from (B.22) the following compact expression:

$$Q(\mathcal{D}) = Q^{(1)}(\mathcal{D}) = \max_{\hat{\rho}_{\mathrm{diag}}} I_{\mathrm{coh}}(\mathcal{D}, \hat{\rho}_{\mathrm{diag}}), \tag{B.24}$$

which for $d_C = 3$ reduces to Eq. (5.28) of the main text. For completeness we report also an alternative, possibly more explicit way to derive (B.24). This is obtained by observing that a special instance of the unitaries which are diagonal in the computational basis of a MAD channel and hence fulfill the identity (5.4), is provided by the subgroup $\mathcal{O}_D(d)$ formed by the operators represented by the diagonal $d \times d$ matrices for which all the non-zero (and diagonal) elements are ± 1. Clearly the identity operator $\hat{\mathbb{1}}$ is an element of $\mathcal{O}_D(d)$ and the group is finite with 2^d elements. Given then an arbitrary input state $\hat{\rho}$ of A, construct then the ensemble $\{p_k; \hat{\rho}_k\}$ formed by the density matrices $\hat{\rho}_k \equiv \hat{O}_k \hat{\rho} \hat{O}_k^\dagger$, with $\hat{O}_k$ being the k-th element of $\mathcal{O}_D(d)$, and by a flat probability set $p_k = 1/2^d$. It can be shown [STA18] that the average state of $\{p_k; \hat{\rho}_k\}$ is diagonal in the computational basis, i.e.

$$\frac{1}{2^d} \sum_{k=0}^{2^d-1} \hat{O}_k \hat{\rho} \hat{O}_k^\dagger = \mathrm{diag}(\hat{\rho}) \,, \tag{B.25}$$

from which (B.24) can once more be derived as a consequence of (B.22) for all degradable $\mathcal{D}$.

B.1.3 Private Classical Capacity

The private classical capacity $C_{\rm p}(\Phi)$ of a quantum channel Φ quantifies the amount of information that the sender and the receiver of the messages can exchange privately, i.e. without a third party able to extract information from the communication line. This quantity provides a natural upper bound for $Q(\Phi)$, i.e.

$$Q(\Phi) \leq C_{\rm p}(\Phi) \ , \tag{B.26}$$

and a closed formula for it is given in [Dev05, CWY04]:

$$C_{\rm p}(\Phi) = \lim_{n\to\infty} \frac{1}{n} C_{\rm p}^{(1)}(\Phi^{\otimes n}). \tag{B.27}$$

where now, given a generic quantum ensemble $\mathcal{E} := \{p_i, \hat{\rho}_i\}$ at the input of the channel Φ, the one-shot expression $C_{\rm p}^{(1)}(\Phi)$ is computed as

$$C_{\rm p}^{(1)}(\Phi) = \max_{\mathcal{E}} \Big(\chi(\Phi, \mathcal{E}) - \chi(\tilde{\Phi}, \mathcal{E}) \Big) \ , \tag{B.28}$$

with

$$\chi(\Phi, \mathcal{E}) \equiv S(\Phi(\sum_i p_i \hat{\rho}_i)) - \sum_i p_i S(\Phi(\hat{\rho}_i) \ , \tag{B.29}$$

the Holevo information [Hol19, Wil17, Wat18] of the ensemble $\mathcal{E}$ computed at the output of the channel Φ. Since $\chi(\Phi, \mathcal{E})$ is not additive [LWZG09], the relation between the one-shot formula and the asymptotic formula is not trivial, making the computation of the latter difficult in general. Nonetheless if the channel considered is degradable or antidegradable the task of finding the regularized private classical capacity simplifies [Smi08]: indeed for degradable maps Φ we have

$$C_{\rm p}(\Phi) = Q(\Phi) = Q^{(1)}(\Phi). \tag{B.30}$$

while for anti-degradable maps one has $C_{\rm p}(\Phi) = Q(\Phi) = Q^{(1)}(\Phi) = 0$.

B.1.4 Entanglement assisted quantum capacity

The entanglement assisted quantum capacity $Q_{\rm ea}(\Phi)$ of the quantum channel Φ quantifies the amount of quantum information transmittable per channel use assuming the communicating parties to share an arbitrary amount of entanglement. A closed expression for it has been provided in Ref. [BSST99, BSST02] and results in an expression which, in contrast to the quantum capacity formula, doesn't need a regularization w.r.t. to the number of channel uses, i.e.

$$Q_E(\Phi) = \frac{1}{2} \max_{\hat{\rho}\in\mathfrak{S}(\mathcal{H})} I(\Phi, \hat{\rho}), \tag{B.31}$$

where now

$$\begin{aligned} I(\Phi, \hat{\rho}) &\equiv S(\hat{\rho}) + I_{\rm coh}(\Phi, \hat{\rho}) \\ &= S(\hat{\rho}) + S(\Phi(\hat{\rho})) - S(\tilde{\Phi}(\hat{\rho})) \ , \end{aligned} \tag{B.32}$$

is the quantum mutual information functional. As in the case of $C_{\mathrm{p}}(\Phi)$, $Q_E(\Phi)$ provides a natural upper bound for $Q(\Phi)$.

We remind that $I(\Phi, \hat{\rho})$ is concave in the input state [Wil17], i.e.

$$I(\Phi, \sum_k p_k \hat{\rho}_k) \quad \geq \quad \sum_k p_k I(\Phi, \hat{\rho}_k) \; , \tag{B.33}$$

for all ensembles $\{p_k, \hat{\rho}_k\}$. Exploiting this fact, in case the channel Φ is covariant under the action of some group of unitary transformations as in Eq. (B.6), we can hence follow the same derivation detailed at the end of the previous section to claim that

$$Q_{\mathrm{ea}}(\Phi) = \frac{1}{2} \max_{\hat{\rho}_G} I(\Phi, \hat{\rho}_G), \tag{B.34}$$

where now we can restrict the maximization in Eq. (B.31) to only those input states $\hat{\rho}_G$ which result from the averaging operation (B.20). Applying this to the covariance (5.4) of MAD channels with respect to the unitary transformations which are diagonal in the computational basis finally yields to Eq. (5.76) of the main text.

C

Appendices to *Resonant multi-level amplitude damping channels: a quantum capacity analysis*

C.1 Stinespring representation, Kraus operators and complementary channels

A completely positive and trace preserving (CPTP) [Cho75] map $\Phi : \mathcal{L}(\mathcal{H}_{\mathrm{S}}) \to \mathcal{L}(\mathcal{H}_{\mathrm{S}'})$ can be thought as the evolution induced by an isometry $\hat{V} : \mathcal{H}_{\mathrm{S}} \to \mathcal{H}_{\mathrm{S}'} \otimes \mathcal{H}_{\mathrm{E}}$ from the input system S to the output system S' and the environment E. This isometry is called Stinespring dilation [Sti55]. Specifically for all input states $\rho_{\mathrm{S}} \in \mathfrak{S}_{\mathrm{S}}$ we can write the action of Φ as

$$\Phi(\hat{\rho}_{\mathrm{S}}) = \mathrm{Tr}_{\mathrm{E}}[\hat{V}\hat{\rho}_{\mathrm{S}}\hat{V}^{\dagger}]. \tag{C.1}$$

Tracing out the degrees of freedom in S' we obtain instead the complementary (or conjugate) channel $\tilde{\Phi} : \mathcal{L}(\mathcal{H}_{\mathrm{S}}) \to \mathcal{L}(\mathcal{H}_{\mathrm{E}})$, i.e.

$$\tilde{\Phi}(\hat{\rho}_{\mathrm{S}}) = \mathrm{Tr}_{\mathrm{S}'}[\hat{V}\hat{\rho}_{\mathrm{S}}\hat{V}^{\dagger}] \, . \tag{C.2}$$

In general the isometry V can be extended to a unitary matrix $\hat{U} : \mathcal{H}_{\mathrm{S}} \otimes \mathcal{H}_{\mathrm{E}} \to \mathcal{H}_{\mathrm{S}'} \otimes \mathcal{H}_{\mathrm{E}'}$ s.t. Eqs (C.1) and (C.2) become

$$\Phi(\hat{\rho}_{\mathrm{S}}) = \mathrm{Tr}_{\mathrm{E}}[\hat{U}\hat{\rho}_{\mathrm{S}}\hat{U}^{\dagger}] \, , \quad \tilde{\Phi}(\hat{\rho}_{\mathrm{S}}) = \mathrm{Tr}_{\mathrm{S}'}[\hat{U}\hat{\rho}_{\mathrm{S}}\hat{U}^{\dagger}] \, . \tag{C.3}$$

Now, assuming the set of Kraus operators $\hat{M}_k$ generating Φ to be known, and being $|k\rangle_{\mathrm{E}}$ a basis for the environment, the operator $\hat{V}$ can be written as:

$$\hat{V} = \sum_k \hat{M}_k \otimes |k\rangle_{\mathrm{E}} \ , \tag{C.4}$$

and being

$$\hat{V}\hat{\rho}_{\mathrm{S}}\hat{V}^{\dagger} = \sum_{i,j} \hat{M}_i \hat{\rho}_{\mathrm{S}} \hat{M}_j{}^{\dagger} \otimes |i\rangle\langle j|_{\mathrm{E}} \, , \tag{C.5}$$

it's straightforward to verify that Eq. (C.2) can be equivalently expressed as

$$\tilde{\Phi}(\hat{\rho}_{\mathrm{S}}) = \sum_{i,j} \mathrm{Tr}_{\mathrm{S}'}[\hat{M}_i \hat{\rho}_{\mathrm{S}} \hat{M}_j^{\dagger}] \, |i\rangle\langle j|_{\mathrm{E}} \, . \tag{C.6}$$

If instead, as in our case, we want do characterize our channel starting from its action on the levels of S and the environment E like we do in Eq. (6.1) (that is equivalent to specifying $\hat{V}$) we can retrieve Kraus operators. This is done by noticing that

$$\begin{aligned} \hat{V} &= \sum_{s,s',e} V_{s,s'e} \, |s'\rangle_{\mathrm{S}'} |e\rangle_{\mathrm{E}} \langle s|_{\mathrm{S}} \ , \\ \hat{M}_k &= \sum_{s,s'} M_{k\ s,s'} \, |s'\rangle_{\mathrm{S}'} \langle s|_{\mathrm{S}} \ , \end{aligned} \tag{C.7}$$

then by Eq. (C.4) follows

$$M_{k\ s,s'} = V_{s,s'e} \, . \tag{C.8}$$

The isometry $\hat{V}$ for our class of channels is specified by Eqs. (6.1) that give

$$\hat{V} = |0\rangle_{\mathrm{S}'} |0\rangle_{\mathrm{E}} \langle 0|_{\mathrm{S}} + \sum_{j=1}^{d-1} \sqrt{1 - \sum_{l<j} \gamma_{jl}} \, |j\rangle_{\mathrm{S}'} |0\rangle_{\mathrm{E}} \langle j|_{\mathrm{S}} + \sum_{j=1}^{d-1} \sum_{k=1}^{j} \sqrt{\gamma_{j,j-k}} \, |j-k\rangle_{\mathrm{S}'} |k\rangle_{\mathrm{E}} \langle j|_{\mathrm{S}} \, . \tag{C.9}$$

From Eq. (C.8) wee have that if the dimension of S is d

$$\begin{aligned} \hat{K}_0 &= \sum_{l=0}^{d-1} \sqrt{1 - \sum_{l<j} \gamma_{jl}} \, |j\rangle\langle j| \ , \\ \hat{K}_k &= \sum_{l=0}^{d-k-1} \sqrt{\gamma_{k+l,l}} \, |l\rangle\langle k+l| \ . \end{aligned} \tag{C.10}$$

C.2 Degradability and antidegradability

We recall here the definitions of degradable and anti-degradable channels [DS05, CG06]. A quantum channel $\Phi : \mathcal{L}(\mathcal{H}_{\mathrm{S}}) \to \mathcal{L}(\mathcal{H}'_{\mathrm{S}})$ is said degradable if a CPTP map $\mathcal{D} : \mathcal{L}(\mathcal{H}_{\mathrm{S}'}) \to \mathcal{L}(\mathcal{H}_{\mathrm{E}})$ exists s.t.

$$\tilde{\Phi} = \mathcal{D} \circ \Phi \ , \tag{C.11}$$

while it's said antidegradable if it exists a CPTP map $\mathcal{A} : \mathcal{L}(\mathcal{H}_{\mathrm{E}}) \to \mathcal{L}(\mathcal{H}_{\mathrm{S}'})$ s.t.

$$\Phi = \mathcal{A} \circ \tilde{\Phi} \ , \tag{C.12}$$

(the symbol "$\circ$" representing channel concatenation). In case Φ is mathematically invertible, a simple direct way to determine whether it is degradable or not is to formally invert the composition in Eq. (C.11) constructing the super-operator $\mathcal{D} = \tilde{\Phi} \circ \Phi^{-1}$ and check whether such object is CPTP [WPG07, SS07]. This check can be performed by studying the positivity of the Choi matrix $\mathrm{C}_{\mathcal{D}}$ of $\mathcal{D}$, that is

$$\mathrm{C}_{\mathcal{D}} = (I_{\mathrm{R}} \otimes \mathcal{D}_{\mathrm{S}}) \, |\Gamma\rangle\langle\Gamma|_{\mathrm{RS}} \ , \quad \text{with} \quad |\Gamma\rangle_{\mathrm{RS}} = \sum_{i=0}^{d-1} |i\rangle_{\mathrm{R}} \, |i\rangle_{\mathrm{S}} \ . \tag{C.13}$$

Summarizing we have

$$\Phi \text{ invertible} \Longrightarrow \Phi \text{ degradable iff } \mathcal{D} = \tilde{\Phi} \circ \Phi^{-1} \text{ is CPTP} . \tag{C.14}$$

Concretely this inversion can be done by exploiting the fact that quantum channels are linear maps connecting vector spaces of linear operators. They can in turn be represented as matrices acting on vector spaces. This through the following "vectorization" isomorphism:

$$\begin{aligned} \hat{\rho}_{\mathrm{S}} = \sum_{ij} \rho_{ij} |i\rangle\langle j|_{\mathrm{S}} \quad &\longrightarrow \quad |\rho\rangle\rangle = \sum_{ij} \rho_{ij} |i\rangle_{\mathrm{S}} \otimes |j\rangle_{\mathrm{S}} \in \mathcal{H}_{\mathrm{S}}^{\otimes 2} , \\ \Phi(\hat{\rho}_{\mathrm{S}}) \quad &\longrightarrow \quad \hat{\mathrm{M}}_{\Phi} |\rho\rangle\rangle , \end{aligned} \tag{C.15}$$

where now $\hat{\mathrm{M}}_{\Phi}$ is a $d_{\mathrm{S}'}^2 \times d_{\mathrm{S}}^2$ matrix connecting $\mathcal{H}_{\mathrm{S}}^{\otimes 2}$ and $\mathcal{H}_{\mathrm{S}'}^{\otimes 2}$ (d_{S} and $d_{\mathrm{S}'}$ being respectively the dimensions of $\mathcal{H}_{\mathrm{S}}$ and $\mathcal{H}_{\mathrm{S}'}$), which given a Kraus set $\{\hat{K}_i\}_i$ for Φ it can be explicitly expressed as

$$\hat{\mathrm{M}}_{\Phi} = \sum_i \hat{K}_i \otimes \hat{K}_i^* . \tag{C.16}$$

Following Eq. (C.11) we have hence that for a degradable channel the following identity must apply

$$\hat{\mathrm{M}}_{\tilde{\Phi}} = \hat{\mathrm{M}}_{\mathcal{D}} \hat{\mathrm{M}}_{\Phi} , \tag{C.17}$$

with $\hat{\mathrm{M}}_{\mathcal{D}}$ the matrix representation of the CPTP connecting channel $\mathcal{D}$, implying that the super-operator $\tilde{\Phi} \circ \Phi^{-1}$ is now represented by matrix $\hat{\mathrm{M}}_{\tilde{\Phi}} \hat{\mathrm{M}}_{\Phi}^{-1}$.

A completely similar argument can be made for the antidegrading channel $\mathcal{A}$.

C.3 Covariance and coherent information

A feature that's typical of amplitude damping channels is covariance. In brief, we have that [Hol07] for a channel Φ that is covariant under a unitary representation of some group G, i.e.

$$\Phi(\hat{U}_g^{\mathrm{S}} \hat{\rho} \hat{U}_g^{\mathrm{S}\dagger}) = \hat{U}_g^{\mathrm{S}'} \Phi(\hat{\rho}) \hat{U}_g^{\mathrm{S}'\dagger} , \qquad \forall \hat{\rho} \in \mathfrak{S}(\mathcal{H}), \forall g \in G , \tag{C.18}$$

then also the complementary channel $\tilde{\Phi}$ is covariant under the same transformations, i.e.

$$\tilde{\Phi}(\hat{U}_g^{\mathrm{S}} \hat{\rho} \hat{U}_g^{\mathrm{S}\dagger}) = \hat{U}_g^{\mathrm{E}} \tilde{\Phi}(\hat{\rho}) \hat{U}_g^{\mathrm{E}\dagger} , \qquad \forall \hat{\rho} \in \mathfrak{S}(\mathcal{H}), \forall g \in G , \tag{C.19}$$

where for X=S,S',E, $\hat{U}_g^{\mathrm{X}}$ is the unitary operator that represents the element g of the group G in the output space X.

ReMAD channels exhibit a covariance property under the unitary group composed by the following transformations:

$$\hat{U}_S(\theta) = \sum_{j=0}^{d-1} e^{-ij\theta} |j\rangle\langle j|_{\mathrm{S}} , \tag{C.20}$$

$$\hat{U}_E(\theta) = \sum_{j=0}^{d-1} e^{-ij\theta} |j\rangle\langle j|_{\mathrm{E}} , \tag{C.21}$$

with θ real. Specifically:

$$\Phi_{\vec{\gamma}}(\hat{U}_{\mathrm{S}}(\theta)\hat{\rho}\hat{U}_{\mathrm{S}}^{\dagger}(\theta)) = \sum_{k=0}^{d-1}\sum_{j,j'=k}^{d-1} \rho_{j,j'}\, e^{-i(j-j')\theta}\sqrt{\gamma_{j,k}\gamma_{j',k}}\ |j-k\rangle\langle j'-k|_{\mathrm{S}} = \hat{U}_{\mathrm{S}}(\theta)\Phi_{\vec{\gamma}}(\hat{\rho})\hat{U}_{\mathrm{S}}^{\dagger}(\theta)\ , \tag{C.22}$$

and similarly for the complementary channel $\tilde{\Phi}_{\vec{\gamma}}$ we get

$$\tilde{\Phi}_{\vec{\gamma}}(\hat{U}_{\mathrm{S}}(\theta)\hat{\rho}\hat{U}_{\mathrm{S}}^{\dagger}(\theta)) = \sum_{k=0}^{d-1}\sum_{j,j'=k}^{d-1} \rho_{j,j'}\, e^{-i(j-j')\theta}\sqrt{\tilde{\gamma}_{j,k}\tilde{\gamma}_{j',k}}\ |j-k\rangle\langle j'-k|_{\mathrm{E}} = \hat{U}_{\mathrm{E}}(\theta)\tilde{\Phi}_{\vec{\gamma}}(\hat{\rho})\hat{U}_{\mathrm{E}}^{\dagger}(\theta)\ . \tag{C.23}$$

C.3.1 Application to the maximization of coherent information and mutual information

Covariance proves very useful in the computation of the quantum capacity.
As a matter of fact, since for degradable channels the coherent information is concave w.r.t. the input state [YHD08], the covariance of $\Phi_{\vec{\gamma}}$ and $\tilde{\Phi}_{\vec{\gamma}}$ implies that

$$\begin{aligned} I_{\mathrm{coh}}\left(\Phi_{\vec{\gamma}}, \int \frac{d\theta}{2\pi}\hat{U}_S(\theta)\hat{\rho}\hat{U}_S^{\dagger}(\theta)\right) &\geq \int \frac{d\theta}{2\pi} I_{\mathrm{coh}}\left(\Phi_{\vec{\gamma}}, \hat{U}_S(\theta)\hat{\rho}\hat{U}_S^{\dagger}(\theta)\right) \\ &= \int \frac{d\theta}{2\pi} S(\Phi_{\vec{\gamma}}(\hat{U}_S(\theta)\hat{\rho}\hat{U}_S^{\dagger}(\theta)) - S(\tilde{\Phi}_{\vec{\gamma}}(\hat{U}_S(\theta)\hat{\rho}\hat{U}_S^{\dagger}(\theta)) \\ &= I_{\mathrm{coh}}\left(\Phi_{\vec{\gamma}}, \hat{\rho}\right)\ , \end{aligned} \tag{C.24}$$

where in the last equality we made use of the invariance of von Neumann entropy under unitary transformations. Observing then that

$$\int \frac{d\theta}{2\pi}\hat{U}_S(\theta)\hat{\rho}\hat{U}_S^{\dagger}(\theta) = \hat{\rho}^{(\mathrm{diag})} := \sum_{j=0}^{d-1}\rho_{j,j}\ |j\rangle_{\mathrm{S}}\langle j|\ , \tag{C.25}$$

we can conclude that for degradable ReMAD channels the maximization over of (6.23) can be restricted on the set of states $\hat{\rho}^{(\mathrm{diag})}$ which are diagonal in the canonical basis, i.e.

$$C_{\mathrm{p}}(\Phi_{\vec{\gamma}}) = Q(\Phi_{\vec{\gamma}}) = Q^{(1)}(\Phi_{\vec{\gamma}}) = \max_{\hat{\rho}^{(\mathrm{diag})}\in\mathfrak{S}(\mathcal{H}_{\mathrm{S}})} I_{\mathrm{coh}}\left(\Phi_{\vec{\gamma}}, \hat{\rho}^{(\mathrm{diag})}\right)\ . \tag{C.26}$$

Something similar can be applied to the quantum mutual information $I(\Phi,\hat{\rho})$, that can be defined as

$$I(\Phi,\hat{\rho}) = S(\hat{\rho}) + I_{\mathrm{coh}}(\Phi,\hat{\rho})\ . \tag{C.27}$$

Now, the Shannon entropy is always concave w.r.t. the input state but, as we saw before, the coherent information can proved concave only when the channel is degradable. Nevertheless the quantum mutual information is always concave in the input state [Wil17, chapter 13.4.2] and therefore also $I(\Phi)$ can be maximized just over diagonal states if Φ is a ReMAD channel.

C.4 Entanglement assisted quantum and classical capacities

The discovery of protocols such as quantum teleportation [BBC+93] and superdense coding [BW92] showed how entanglement could be leveraged as an additional resource in order to boost the communication performance between two communicating parties. The formalization of these entanglement-assisted protocols in Shannon-theoretic terms was given in [BSST99, BSST02], where the entanglement-assisted classical capacity C_{ea} and entanglement-assisted quantum capacity Q_{ea} were introduced. The peculiarity and the advantage with the definition of these capacities is that they are additive quantities and don't need a regularization. Specifically, recalling the definition of the quantum mutual information $I(\Phi, \hat{\rho})$ in Eq. (C.27), we have:

$$C_{\text{ea}}(\Phi) = \max_{\hat{\rho} \in \mathfrak{S}(\mathcal{H}_{\text{S}})} I(\Phi, \hat{\rho}) \, , \qquad Q_{\text{ea}}(\Phi) = \frac{1}{2} C_{\text{ea}}(\Phi) \, , \tag{C.28}$$

where the definition of $Q_{\text{ea}}(\Phi)$ is justified by the fact that in presence of entanglement a qudit quantum state can be teleported 'spending' two classical $d$its (quantum teleportation) and viceversa two classical $d$its can be communicated by sending a single qudit (superdense coding).

As discussed in App. C.3.1, the quantum mutual information for ReMAD channels can be computed by maximizing just over diagonal states. We report then in Fig. C.1 the evaluation of $C_{\text{ea}}(\Phi_{\vec{\gamma}})$ for a qutrit ReMAD channel at varying γ_{20} and γ_{21} for some instances of γ_{10} values.

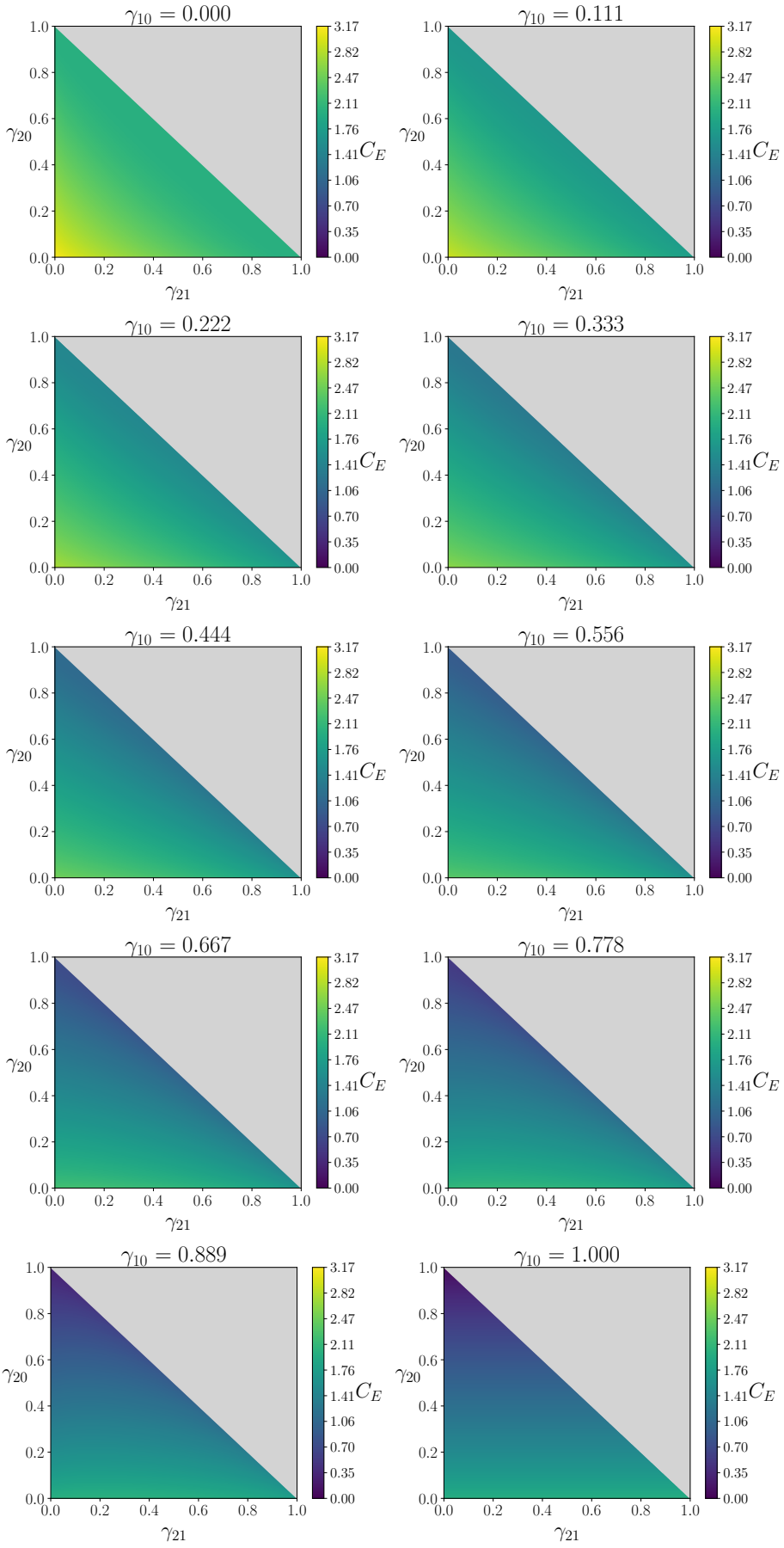

FIGURE C.1: Entanglement assisted classical capacity $C_{\text{ea}}(\Phi_{\vec{\gamma}})$ for different γ_{10}, γ_{21} and γ_{20}. The grey area represents values of γ_{20} and γ_{21} s.t. $\gamma_{20} + \gamma_{21} > 0$ for which the channel is not defined.

D

Appendices to *Partially Coherent Direct Sum channels*

D.1 Necessary and sufficient conditions for PCDS quantum channels

Here we discuss necessary and sufficient conditions for a quantum channel $\Phi_{\rm CC} \in \mathcal{M}^{(\rm cpt)}_{\rm C\to C}$ to admit the PCDS block-structure defined in Eq. (7.8). We start by observing that when introducing this special decomposition we did not explicitly require the diagonal blocks $\Phi_{\rm AA}$ and $\Phi_{\rm BB}$ to be CPT (indeed we merely asked them to be elements of the super-operators sets $\mathcal{M}_{\rm A\to A}$ and $\mathcal{M}_{\rm B\to B}$). This property however is automatically imposed by the CPT constraint on $\Phi_{\rm CC}$ – see the derivation that follows.

We now give an explicit proof of Theorem 1. First of all, assume that the element $\hat{M}^{(j)}_{\rm CC}$ of the Kraus set $\{\hat{M}^{(j)}_{\rm CC}\}_j$ of $\Phi_{\rm CC}$ fulfills the identity in Eq. (7.10). Accordingly for all $\hat{\Theta}_{\rm CC} \in \mathcal{L}_{\rm C\to C}$ we can write

$$\begin{aligned}\Phi_{\rm CC}[\hat{\Theta}_{\rm CC}] &= \sum_j \hat{M}^{(j)}_{\rm CC}\hat{\Theta}_{\rm CC}\hat{M}^{(j)\dagger}_{\rm CC} \\ &= \sum_j \left(\sum_{\rm Y=A,B} \hat{M}^{(j)}_{\rm YY}\right)\hat{\Theta}_{\rm CC}\left(\sum_{\rm X=A,B} \hat{M}^{(j)\dagger}_{\rm XX}\right) \\ &= \sum_j \sum_{\rm X,Y=A,B} \hat{M}^{(j)}_{\rm YY}\hat{\Theta}_{\rm YX}\hat{M}^{(j)\dagger}_{\rm XX}\,, \end{aligned} \tag{D.1}$$

which can be cast into the form of Eq. (7.9) with the super-operators $\Phi_{\rm AA}$, $\Phi_{\rm AA}$, $\Phi^{(\rm off)}_{\rm AB}$, $\Phi^{(\rm off)}_{\rm BA}$ defined as in Eqs. (7.11) and (7.12). Notice in particular that with this choice, for X = A,B the diagonal component writes

$$\Phi_{\rm XX}[\cdots] = \sum_j \hat{M}^{(j)}_{\rm XX}\cdots\hat{M}^{(j)\dagger}_{\rm XX}\,, \tag{D.2}$$

with the operators $\hat{M}^{(j)}_{\mathrm{XX}}$ fulfilling the constraints

$$\begin{aligned}\sum_j \hat{M}^{(j)\dagger}_{\mathrm{XX}}\hat{M}^{(j)}_{\mathrm{XX}} &= \hat{P}_{\mathrm{XX}}\sum_j \hat{M}^{(j)\dagger}_{\mathrm{CC}}\hat{M}^{(j)}_{\mathrm{CC}}\hat{P}_{\mathrm{XX}} \\ &= \hat{P}_{\mathrm{XX}}\hat{I}_{\mathrm{CC}}\hat{P}_{\mathrm{XX}} = \hat{P}_{\mathrm{XX}}\ . \end{aligned} \tag{D.3}$$

This implies that $\{\hat{M}^{(j)}_{\mathrm{XX}}\}_j$ is a proper Kraus set for a map action on X, i.e. that Φ_{XX} is indeed a CPT element of $\mathcal{M}_{\mathrm{X}\to\mathrm{X}}$, as anticipated in the introduction of the present section.

Consider now the reverse property, i.e. assume that exist $\Phi_{\mathrm{AA}} \in \mathcal{M}_{\mathrm{A}\to\mathrm{A}}$, $\Phi_{\mathrm{BB}} \in \mathcal{M}_{\mathrm{B}\to\mathrm{B}}$, $\Phi^{(\mathrm{off})}_{\mathrm{AB}} \in \mathcal{M}^{(\mathrm{off})}_{\mathrm{B}\to\mathrm{A}}$, and $\Phi^{(\mathrm{off})}_{\mathrm{BA}} \in \mathcal{M}^{(\mathrm{off})}_{\mathrm{A}\to\mathrm{B}}$ such that Eq. (7.8) holds true for all possible choices of $\hat{\Theta}_{\mathrm{CC}} \in \mathcal{L}_{\mathrm{C}\to\mathrm{C}}$. Observe then that this in particular implies

$$\begin{aligned} 0 &= \hat{P}_{\mathrm{BB}}\Phi_{\mathrm{CC}}[\hat{P}_{\mathrm{AA}}]\hat{P}_{\mathrm{BB}} = \sum_j \hat{P}_{\mathrm{BB}}M^{(j)}_{\mathrm{CC}}\hat{P}_{\mathrm{AA}}M^{(j)\dagger}_{\mathrm{CC}}\hat{P}_{\mathrm{BB}} \\ &= \sum_j \left(\hat{P}_{\mathrm{BB}}M^{(j)}_{\mathrm{CC}}\hat{P}_{\mathrm{AA}}\right)\left(\hat{P}_{\mathrm{BB}}M^{(j)}_{\mathrm{CC}}\hat{P}_{\mathrm{AA}}\right)^\dagger = \sum_j |M^{(j)}_{BA}|^2\ . \end{aligned}$$

Which is verified if and only if

$$\hat{M}^{(j)}_{\mathrm{BA}} = \hat{M}^{(j)}_{\mathrm{AB}} = 0 \qquad \forall j\ , \tag{D.4}$$

or equivalently if and only if Eq. (7.10) holds true. □

D.2 Complementary maps via Stinespring dilation

Given $\Phi_{\mathrm{XX}} \in \mathcal{M}^{(\mathrm{cpt})}_{\mathrm{X}\to\mathrm{X}}$ a generic CPT transformation acting on an arbitrary system X, we can always express it as

$$\Phi_{\mathrm{XX}}[\cdots] = \mathrm{Tr}_{\mathrm{E}}[\hat{U}_{\mathrm{XEXE}}(\cdots\otimes|0_{\mathrm{E}}\rangle\langle 0_{\mathrm{E}}|)\hat{U}^\dagger_{\mathrm{XEXE}}]\ , \tag{D.5}$$

where E is an auxiliary (environmental) quantum system, $\mathrm{Tr}_{\mathrm{E}}[\cdots]$ is the partial trace over E, $|0_{\mathrm{E}}\rangle$ a pure state vector of the Hilbert space $\mathcal{H}_{\mathrm{E}}$ of E, and finally $\hat{U}_{\mathrm{XEXE}}$ is a unitary transformation on $\mathcal{H}_X \otimes \mathcal{H}_{\mathrm{E}}$. For future purposes it is worth stressing that, by taking the dimensionality of $\mathcal{H}_{\mathrm{E}}$ to be sufficiently large, we can make sure that the dependence of the representation in Eq. (D.5) upon the specific choice of Φ_{XX} is completely carried on by just $\hat{U}_{\mathrm{XEXE}}$. We have then the freedom of fixing $|0_{\mathrm{E}}\rangle$ irrespectively of the map we want to represent. In the above setting a Kraus set for Φ_{XX} is e.g. obtained in terms of the operators

$$\hat{M}^{(j)}_{\mathrm{XX}} = \langle j_{\mathrm{E}}|\hat{U}_{\mathrm{XEXE}}|0_{\mathrm{E}}\rangle\ , \tag{D.6}$$

with $\{|j_{\mathrm{E}}\rangle\}_j$ an orthonormal basis of $\mathcal{H}_{\mathrm{E}}$. The complementary channel of Φ_{XX} instead can be defined as the CPT transformation $\tilde{\Phi}_{\mathrm{EX}} \in \mathcal{M}^{(\mathrm{cpt})}_{\mathrm{X}\to\mathrm{E}}$ that transforms input from X into output of E via the mapping

$$\tilde{\Phi}_{\mathrm{EX}}[\cdots] = \hat{V}_{\mathrm{EE}}\mathrm{Tr}_{\mathrm{X}}[\hat{U}_{\mathrm{XEXE}}(\cdots\otimes|0_{\mathrm{E}}\rangle\langle 0_{\mathrm{E}}|)\hat{U}^\dagger_{\mathrm{XEXE}}]\hat{V}^\dagger_{\mathrm{EE}}\ , \tag{D.7}$$

where now the partial trace is performed over X. In the above expression $\hat{V}_{\rm EE}$ is a unitary operator on E that can be chosen freely. We inserted it to explicitly stress that, as already mentioned in the main text, the complementary channel of a CPT map is defined up to a unitary rotation on the environmental system of the model. Anyway, unless explicitly stated, hereafter we shall assume $\hat{V}_{\rm EE}$ to be the identity operator – notice that under this assumption, thanks to Eq. (D.6), Eq. (D.7) reduces exactly to Eq. (7.17) reported in the main text.

An alternative way to derive Eq. (7.20) can now be obtained by first introducing the unitary operators $\hat{U}_{\rm AEAE} \in \mathcal{L}_{\rm AE\to AE}$ and $\hat{U}_{\rm BEBE} \in \mathcal{L}_{\rm BE\to BE}$ which provide, respectively, the Stinespring representations of Eq. (D.5) of the diagonal components $\Phi_{\rm AA}$ and $\Phi_{\rm BB}$ of the PCDS channel $\Phi_{\rm CC}$. Observe now that while the unitary operator $\hat{U}_{\rm AEAE}$ ($\hat{U}_{\rm BEBE}$) is formally defined on $\mathcal{H}_{\rm A}\otimes\mathcal{H}_{\rm E}$ ($\mathcal{H}_{\rm B}\otimes\mathcal{H}_{\rm E}$) only, we are allowed to extend it to the full space $\mathcal{H}_{\rm C}\otimes\mathcal{H}_{\rm E}$ by imposing the condition $\hat{P}_{\rm B}\hat{U}_{\rm AEAE}=\hat{U}_{\rm AEAE}\hat{P}_{\rm B}=0$ (resp. $\hat{P}_{\rm A}\hat{U}_{\rm BEBE}=\hat{U}_{\rm BEBE}\hat{P}_{\rm A}=0$). With this choice hence we can write the normalization condition for $\hat{U}_{\rm AEAE}$ and $\hat{U}_{\rm BEBE}$ as

$$\begin{aligned}\hat{U}^{\dagger}_{\rm AEAE}\hat{U}_{\rm AEAE} &= \hat{P}_{\rm AA}\otimes\hat{I}_{\rm EE}\,,\\ \hat{U}^{\dagger}_{\rm BEBE}\hat{U}_{\rm BEBE} &= \hat{P}_{\rm BB}\otimes\hat{I}_{\rm EE}\,,\end{aligned} \tag{D.8}$$

with the projectors $\hat{P}_{\rm AA}$ and $\hat{P}_{\rm AA}$ playing the role of the identity transformations on $\mathcal{H}_{\rm A}$ and $\mathcal{H}_{\rm B}$ respectively. In view of these observations a Stinespring representation as in Eq. (D.5) for the PCDS channel $\Phi_{\rm CC}$ can now be assigned by adopting the following coupling

$$\hat{U}_{\rm CECE}=\hat{U}_{\rm AEAE}+\hat{U}_{\rm BEBE}\,, \tag{D.9}$$

which is a unitary transformation on $\mathcal{H}_{\rm C}\otimes\mathcal{H}_{\rm E}$ thanks to Eq. (D.8) and Eq. (7.5). Furthermore, thanks to Eq. (D.6) automatically fulfills the necessary and sufficient PCDS condition in Eq. (7.10). To verify Eq. (7.20) now observe that for an arbitrary vector $|\Psi_{\rm C}\rangle\in\mathcal{H}_{\rm C}$ we can write

$$\begin{aligned}\hat{U}_{\rm CECE}(|\Psi_{\rm C}\rangle\otimes|0_{\rm E}\rangle) &= \hat{U}_{\rm AEAE}(|\Psi_{\rm A}\rangle\otimes|0_{\rm E}\rangle)\\ &\quad+\hat{U}_{\rm BEBE}(|\Psi_{\rm B}\rangle\otimes|0_{\rm E}\rangle)\,,\end{aligned} \tag{D.10}$$

where for X = A,B, $|\Psi_{\rm X}\rangle\equiv\hat{P}_{\rm XX}|\Psi_{\rm C}\rangle$. Tracing over C from the above expression we get that the action of $\tilde{\Phi}_{\rm EC}$ on $|\Psi_{\rm C}\rangle$ can be expressed as

$$\tilde{\Phi}_{\rm EC}[|\Psi_{\rm C}\rangle\langle\Psi_{\rm C}|]=\tilde{\Phi}_{\rm EA}[|\Psi_{\rm A}\rangle\langle\Psi_{\rm A}|]+\tilde{\Phi}_{\rm EB}[|\Psi_{\rm B}\rangle\langle\Psi_{\rm B}|]\,, \tag{D.11}$$

where for X = A,B, $\tilde{\Phi}_{\rm EX}$ is the complementary map of $\Phi_{\rm XX}$, and where we used the fact that $\hat{U}_{\rm AEAE}(|\Psi_{\rm A}\rangle\otimes|0_{\rm E}\rangle)$ lives on $\mathcal{H}_{\rm A}\otimes\mathcal{H}_{\rm E}$ and therefore has zero overlap with the C components of $\hat{U}_{\rm BEBE}(|\Psi_{\rm B}\rangle\otimes|0_{\rm E}\rangle)$, which instead is on $\mathcal{H}_{\rm B}\otimes\mathcal{H}_{\rm E}$.

D.2.1 Structure of the connecting channels

Here we show that if $\Lambda_{\rm EA}$ and $\Lambda_{\rm EB}$ entering in Eq. (7.22) are both CPT then also $\Lambda_{\rm EC}$ is CPT. To see this remember that given $\Phi_{\rm YX}\in\mathcal{M}_{\rm X\to Y}$ a super-operator mapping the

system X into Y, it is CPT if and only if it admits a Kraus set formed by operators $\hat{M}^{(j)}_{\mathrm{YX}}$ that fulfill the normalization condition

$$\sum_j \hat{M}^{(j)\dagger}_{\mathrm{YX}} \hat{M}^{(j)}_{\mathrm{YX}} = \hat{I}_{\mathrm{XX}} \,, \tag{D.12}$$

with $\hat{I}_{\mathrm{XX}}$ the identity on $\mathcal{H}_{\mathrm{X}}$, or alternatively the associated projector in case $\mathcal{H}_{\mathrm{X}}$ is a sub-space on a larger space. Consequently, since we assumed by hypothesis that this is the case for Λ_{EA} and Λ_{EB} appearing in Eq. (7.22), it follows that a Kraus set for Λ_{EC} is given by the set $\{\hat{M}^{(j_1)}_{\mathrm{EA}}, \hat{M}^{(j_1)}_{\mathrm{EB}}\}_{j_1,j_2}$. As indeed we have

$$\begin{aligned} \sum_{j_1} \hat{M}^{(j_1)\dagger}_{\mathrm{EA}} \hat{M}^{(j_1)}_{\mathrm{EA}} + \sum_{j_2} \hat{M}^{(j_2)\dagger}_{\mathrm{EB}} \hat{M}^{(j_2)}_{\mathrm{EB}} &= \hat{P}_{\mathrm{AA}} + \hat{P}_{\mathrm{BB}} \\ &= \hat{I}_{\mathrm{CC}} \,. \end{aligned} \tag{D.13}$$

D.2.2 Pure fixed point channels

Here we show that if the quantum channel $\Phi_{\mathrm{AA}} \in \mathcal{M}^{(\mathrm{cpt})}_{\mathrm{A}\to\mathrm{A}}$ admits as fixed point a pure state $|\Psi^*_{\mathrm{A}}\rangle \in \mathcal{H}_{\mathrm{A}}$, then condition in Eq. (7.48) can be fulfilled by setting $\hat{\rho}^*_{\mathrm{AA}} = |\Psi^*_{\mathrm{A}}\rangle\langle\Psi^*_{\mathrm{A}}|$. To show this, let us consider the unitary operator $\hat{U}_{\mathrm{AEAE}}$ that allows us to express Φ_{AA} and its associated complementary channel Φ_{EA} in the Stinespring representation given by Eqs. (D.5) and (D.7). The fixed point condition of $|\Psi^*_{\mathrm{A}}\rangle$ imposes us to have

$$\Phi_{\mathrm{AA}}[|\Psi^*_{\mathrm{A}}\rangle\langle\Psi^*_{\mathrm{A}}|] = |\Psi^*_{\mathrm{A}}\rangle\langle\Psi^*_{\mathrm{A}}| \,, \tag{D.14}$$

which can be satisfied if and only if the following identity holds true:

$$\hat{U}_{\mathrm{AEAE}}|\Psi^*_{\mathrm{A}}\rangle \otimes |0_{\mathrm{E}}\rangle = |\Psi^*_{\mathrm{A}}\rangle \otimes |0'_{\mathrm{E}}\rangle \,, \tag{D.15}$$

with $|0'_E\rangle$ being some pure state of E. Accordingly from Eq. (D.7) it follows that

$$\tilde{\Phi}_{\mathrm{EA}}[|\Psi^*_A\rangle\langle\Psi^*_A|] = \hat{V}_{\mathrm{EE}}|0'_{\mathrm{E}}\rangle\langle 0'_{\mathrm{E}}|\hat{V}^\dagger_{\mathrm{EE}} \,, \tag{D.16}$$

where now we make explicit use of the freedom of redefining $\tilde{\Phi}_{\mathrm{EA}}$ up to an arbitrary unitary transformation $\hat{V}_{\mathrm{EE}}$. The condition in Eq. (7.48) can finally be enforced by simply selecting $\hat{V}_{\mathrm{EE}}$ so that

$$\hat{V}_{\mathrm{EE}}|0'_{\mathrm{E}}\rangle = |0_{\mathrm{E}}\rangle \,. \tag{D.17}$$

D.3 Generalization to the multi-block decomposition

Consider the case in which the Hilbert space of C decomposes in a direct sum of n different subspaces

$$\mathcal{H}_{\mathrm{C}} = \mathcal{H}_{\mathrm{A}_1} \oplus \mathcal{H}_{\mathrm{A}_2} \oplus \cdots \oplus \mathcal{H}_{\mathrm{A}_n} \,, \tag{D.18}$$

where for $\ell = 1, \cdots, n$, $\mathcal{H}_{\mathrm{A}_\ell}$ represents a Hilbert space of dimension d_{A_ℓ}, with

$$d_{\mathrm{C}} = \sum_{\ell=1}^{n} d_{\mathrm{A}_\ell} \,. \tag{D.19}$$

A PCDS CPT channel $\Phi_{\mathrm{CC}} \in \mathcal{M}^{(\mathrm{cpt})}_{\mathrm{C}\to\mathrm{C}}$ is now defined by the following structural constraint which generalizes the one we presented in Eq. (7.9):

$$\Phi_{\mathrm{CC}} = \sum_{\ell=1}^{n} \Phi_{\mathrm{A}_\ell\mathrm{A}_\ell} + \sum_{\ell\neq\ell'=1}^{n} \Phi^{(\mathrm{off})}_{\mathrm{A}_\ell\mathrm{A}_{\ell'}} \ , \tag{D.20}$$

with $\Phi_{\mathrm{A}_\ell\mathrm{A}_\ell} \in \mathcal{M}_{\mathrm{A}_\ell\to\mathrm{A}_\ell}$ and $\Phi^{(\mathrm{off})}_{\mathrm{A}_\ell\mathrm{A}_{\ell'}} \in \mathcal{M}^{(\mathrm{off})}_{\mathrm{A}_\ell\to\mathrm{A}_\ell}$. Following the same derivation we presented for the $n = 2$ one can verify that the CPT constraint on Φ_{CC} imposes all the diagonal terms $\Phi_{\mathrm{A}_\ell\mathrm{A}_\ell}$ to be CPT as well. Furthermore Theorem 1 still holds true in the following form

Theorem 4. *A quantum channel Φ_{CC} described by a Kraus set $\{\hat{M}^{(j)}_{CC}\}_j$ admits the PCDS structure as in Eq. (7.9) if and only if*

$$\hat{M}^{(j)}_{CC} = \bigoplus_{\ell=1}^{n} \hat{M}^{(j)}_{A_\ell A_\ell} \ , \tag{D.21}$$

or equivalently that $\hat{M}^{(j)}_{A_\ell A_{\ell'}} = 0$, for all j and for all $\ell \neq \ell'$.

In the above expression for all $\hat{\Theta}_{\mathrm{CC}} \in \mathcal{L}_{\mathrm{C}\to\mathrm{C}}$ we defined

$$\hat{\Theta}_{\mathrm{A}_\ell\mathrm{A}_{\ell'}} \equiv \hat{P}_{\mathrm{A}_\ell\mathrm{A}_\ell}\hat{\Theta}_{\mathrm{CC}}\hat{P}_{\mathrm{A}_{\ell'}\mathrm{A}_{\ell'}} \ , \tag{D.22}$$

with $\hat{P}_{\mathrm{A}_\ell\mathrm{A}_\ell}$ being the orthogonal projector on $\mathcal{H}_{\mathrm{A}_\ell}$. Accordingly Eqs. (7.11) and (7.12) get replaced by

$$\begin{aligned} \Phi_{\mathrm{A}_\ell\mathrm{A}_\ell}[\cdots] &= \sum_j \hat{M}^{(j)}_{\mathrm{A}_\ell\mathrm{A}_\ell} \cdots \hat{M}^{(j)\dagger}_{\mathrm{A}_\ell\mathrm{A}_\ell} \ , \\ \Phi^{(\mathrm{off})}_{\mathrm{A}_\ell\mathrm{A}_{\ell'}}[\cdots] &= \sum_j \hat{M}^{(j)}_{\mathrm{A}_\ell\mathrm{A}_\ell} \cdots \hat{M}^{(j)\dagger}_{\mathrm{A}_{\ell'}\mathrm{A}_{\ell'}} \ . \end{aligned} \tag{D.23}$$

Similarly Eq. (7.20) becomes now

$$\tilde{\Phi}_{\mathrm{EC}} = \sum_{\ell=1}^{n} \tilde{\Phi}_{\mathrm{EA}_\ell} \ , \tag{D.24}$$

with $\tilde{\Phi}_{\mathrm{EA}_\ell}$ being the complementary channel of $\Phi_{\mathrm{A}_\ell,\mathrm{A}_\ell}$. Theorem 2 instead is replaced by the more general statement

Theorem 5. *A PCDS quantum channel Φ_{CC} as in Eq. (D.20) is degradable if and only if all its diagonal block terms $\Phi_{A_\ell A_\ell}$ are degradable too.*

It then follows that for Φ_{CC} degradable we can express the quantum capacity as

$$\begin{aligned} Q(\Phi_{\mathrm{CC}}) = \max_{P} \max_{\hat{\tau}_{\mathrm{A}_\ell\mathrm{A}_\ell}} \Big\{ & H(P) + \sum_{\ell=1}^{n} p_\ell S\left(\Phi_{\mathrm{A}_\ell\mathrm{A}_\ell}[\hat{\tau}_{\mathrm{A}_\ell\mathrm{A}_\ell}]\right) \\ & - S\left(\sum_{\ell=1}^{n} p_\ell \tilde{\Phi}_{\mathrm{EA}_\ell}[\hat{\tau}_{\mathrm{A}_\ell\mathrm{A}_\ell}]\right) \Big\} \ , \end{aligned} \tag{D.25}$$

with P a generic probability set $\{p\}_\ell$, $H(P) = -\sum_\ell p_\ell \log p_\ell$ its Shannon entropy, and $\hat{\tau}_{\mathrm{A}_\ell\mathrm{A}_\ell}$ density matrices of $\mathcal{H}_{\mathrm{A}_\ell}$.

D.4 The channel $\Omega_{\mathbf{CC}}^{[\gamma](\kappa)}$ for $d_{\mathbf{C}} = 3$

When $d_{\mathrm{C}} = 3$ a Kraus set of $\Omega_{\mathrm{CC}}^{[\gamma](\kappa)}$ expressed w.r.t. the canonical base elements $\{|0_{\mathrm{C}}\rangle, |1_{\mathrm{C}}\rangle, |2_{\mathrm{C}}\rangle\}$, can be written as

$$\hat{M}_{\mathrm{CC}}^{(0)} = \begin{pmatrix} 1 & 0 & 0 \\ 0 & \sqrt{1-\gamma} & 0 \\ 0 & 0 & \kappa^* \end{pmatrix}, \quad \hat{M}_{\mathrm{CC}}^{(1)} = \begin{pmatrix} 0 & \sqrt{\gamma} & 0 \\ 0 & 0 & 0 \\ 0 & 0 & 0 \end{pmatrix}, \quad \hat{M}_{\mathrm{CC}}^{(2)} = \begin{pmatrix} 0 & 0 & 0 \\ 0 & 0 & 0 \\ 0 & 0 & \sqrt{1-|\kappa|^2} \end{pmatrix}. \tag{D.26}$$

This leads to

$$\Omega_{\mathrm{CC}}^{[\gamma](\kappa)}[\hat{\rho}_{\mathrm{CC}}] = \begin{pmatrix} \rho_{00} + \gamma\rho_{11} & \sqrt{1-\gamma}\rho_{01} & \kappa\rho_{02} \\ \sqrt{1-\gamma}\rho_{01}^* & (1-\gamma)\rho_{11} & \kappa\sqrt{1-\gamma}\rho_{12} \\ \kappa^*\rho_{02}^* & \kappa^*\sqrt{1-\gamma}\rho_{12}^* & \rho_{22} \end{pmatrix}, \tag{D.27}$$

where for $i, j = 0, 1, 2$ we set $\rho_{ij} = \langle i_{\mathrm{C}}|\hat{\rho}_{\mathrm{CC}}|j_{\mathrm{C}}\rangle$, and

$$\tilde{\Omega}_{\mathrm{EC}}^{[\gamma](\kappa)}[\hat{\rho}_{\mathrm{CC}}] = \begin{pmatrix} 1 - \gamma\rho_{11} + |\kappa|^2\rho_{22} & \sqrt{\gamma}\rho_{01} & \kappa^*\sqrt{(1-|\kappa|^2)}\rho_{22} \\ \sqrt{\gamma}\rho_{01}^* & \gamma\rho_{11} & 0 \\ \kappa\sqrt{(1-|\kappa|^2)}\rho_{22}^* & 0 & (1-|\kappa|^2)\rho_{22} \end{pmatrix}, \tag{D.28}$$

for the complementary map defined on a Hilbert space spanned by the vectors $\{|0_{\mathrm{E}}\rangle, |1_{\mathrm{E}}\rangle, |2_{\mathrm{E}}\rangle\}$.

Notice that we can express the input states $\hat{\rho}_{\mathrm{CC}}$ in terms of the $\hat{\tau}_{\mathrm{AA}}$ and $\hat{\tau}_{\mathrm{BB}}$ density matrices as in Eq. (7.33). Eq. (D.28) then can be equivalently written as

$$\tilde{\Omega}_{\mathrm{EC}}^{[\gamma](\kappa)}[\hat{\rho}_{\mathrm{CC}}] = p\tilde{\Omega}_{\mathrm{EA}}^{[\gamma]}[\hat{\tau}_{\mathrm{AA}}] + (1-p)|v_{\mathrm{E}}^{(\kappa)}\rangle\langle v_{\mathrm{E}}^{(\kappa)}|, \tag{D.29}$$

with $\tilde{\Omega}_{\mathrm{EA}}^{[\gamma]}$, the complementary channel of the MAD channel $\Omega_{\mathrm{AA}}^{[\gamma]}$. $\tilde{\Omega}_{\mathrm{EA}}^{[\gamma]}$ is defined by the 2×2 matrix

$$\tilde{\Omega}_{\mathrm{EA}}^{[\gamma]}[\hat{\tau}_{\mathrm{AA}}] = \begin{pmatrix} 1 - \gamma_1\tau_{11} & \sqrt{\gamma_1}\tau_{01} \\ \sqrt{\gamma_1}\tau_{01}^* & \gamma_1\tau_{11} \end{pmatrix}, \tag{D.30}$$

on the Hilbert space spanned by the vectors $|0_{\mathrm{E}}\rangle$ and $|1_{\mathrm{E}}\rangle$. $|v_{\mathrm{E}}^{(\kappa)}\rangle$ in Eq. D.29 is defined as

$$|v_{\mathrm{E}}^{(\kappa)}\rangle \equiv \kappa|0_{\mathrm{E}}\rangle + \sqrt{1-|\kappa|^2}|2_{\mathrm{E}}\rangle, \tag{D.31}$$

which has the same structure of the state in Eq. (7.54) but involves different basis vectors in order to account for the presence of the MAD contribution to $\Omega_{\mathrm{CC}}^{[\gamma](\kappa)}$.

Now, considering the fact that both ADC and dephasing are covariant w.r.t. the action of the group of diagonal orthogonal matrices [CG21b, DBF07], the maximization of the coherent information is attained by exploring only diagonal states. Consequently, from Eq. (7.46) and Eq. (D.29) the quantum capacity is obtained by:

$$\begin{aligned} Q(\Omega_{\mathrm{CC}}^{[\gamma](\kappa)}) = \max_{p\in[0,1]} \{H_2(p) + \max_{\tau_{11}\in[0,1]} \{pH_2(\gamma\tau_{11}) \\ + l_0 \log_2 l_0 + l_+ \log_2 l_+ + l_- \log_2 l_-\}\} \end{aligned} \tag{D.32}$$

where

$$\begin{cases} l_0 = p\tau_{11}\gamma \\ l_+ = \frac{1}{2}(1 - p\gamma\tau_{11} + \\ \qquad \sqrt{4(1-p)p(|\kappa|^2-1)(1-\gamma\tau_{11}) + (1-p\gamma\tau_{11})^2}) \\ l_- = \frac{1}{2}(1 - p\gamma\tau_{11} - \\ \qquad \sqrt{4(1-p)p(|\kappa|^2-1)(1-\gamma\tau_{11}) + (1-p\gamma\tau_{11})^2}). \end{cases} \tag{D.33}$$

Notice how this method allows us to reduce to just 2 the number of parameters involved in the maximization, compared to the at least 8 needed for a generic qutrit state.

References

[AC97] C. Adami and N. J. Cerf. *von Neumann capacity of noisy quantum channels*. Phys. Rev. A, **56** 3470–3483, Nov 1997.

[Ans17] A. Anshu. An upper bound on quantum capacity of unital quantum channels. In *2017 IEEE Information Theory Workshop (ITW)*, pages 214–218, (2017).

[BB14] C. H. Bennett and G. Brassard. *Quantum cryptography: Public key distribution and coin tossing*. Theoretical Computer Science, **560** 7–11, (2014). Theoretical Aspects of Quantum Cryptography – celebrating 30 years of BB84.

[BBC+93] C. H. Bennett, G. Brassard, C. Crépeau, R. Jozsa, A. Peres, and W. K. Wootters. *Teleporting an unknown quantum state via dual classical and Einstein-Podolsky-Rosen channels*. Phys. Rev. Lett., **70** 1895–1899, Mar 1993.

[BČF+06] L. Bartůšková, A. Černoch, R. Filip, J. Fiurášek, J. Soubusta, and M. Dušek. *Optical implementation of the encoding of two qubits to a single qutrit*. Physical Review A, **74**(2) 022325, (2006).

[BdGS02] S. D. Bartlett, H. de Guise, and B. C. Sanders. *Quantum encodings in spin systems and harmonic oscillators*. Phys. Rev. A, **65** 052316, May 2002.

[BDHM10] K. Brádler, N. Dutil, P. Hayden, and A. Muhammad. *Conjugate degradability and the quantum capacity of cloning channels*. Journal of Mathematical Physics, **51**(7) 072201, (2010).

[BDS97] C. H. Bennett, D. P. DiVincenzo, and J. A. Smolin. *Capacities of quantum erasure channels*. Phys. Rev. Lett., **78** 3217–3220, Apr 1997.

[BDSS06] C. H. Bennett, I. Devetak, P. W. Shor, and J. A. Smolin. *Inequalities and separations among assisted capacities of quantum channels*. Phys. Rev. Lett., **96** 150502, Apr 2006.

[BEO09] C. K. Burrell, J. Eisert, and T. J. Osborne. *Information propagation through quantum chains with fluctuating disorder*. Phys. Rev. A, **80** 052319, Nov 2009.

[BEW+17] A. Babazadeh, M. Erhard, F. Wang, M. Malik, R. Nouroozi, M. Krenn, and A. Zeilinger. *High-dimensional single-photon quantum gates: Concepts and experiments.* Phys. Rev. Lett., **119** 180510, Nov 2017.

[BGB07] D. Burgarth, V. Giovannetti, and S. Bose. *Optimal quantum-chain communication by end gates.* Phys. Rev. A, **75** 062327, Jun 2007.

[BHM10] S. Bravyi, M. B. Hastings, and S. Michalakis. *Topological quantum order: Stability under local perturbations.* Journal of Mathematical Physics, **51**(9) 093512, (2010).

[BHP09] K. Brádler, P. Hayden, and P. Panangaden. *Private information via the unruh effect.* Journal of High Energy Physics, **2009**(08) 074–074, aug 2009.

[BHTW10] K. Brádler, P. Hayden, D. Touchette, and M. M. Wilde. *Trade-off capacities of the quantum hadamard channels.* Phys. Rev. A, **81** 062312, Jun 2010.

[BHV06] S. Bravyi, M. B. Hastings, and F. Verstraete. *Lieb-Robinson bounds and the generation of correlations and topological quantum order.* Phys. Rev. Lett., **97** 050401, Jul 2006.

[BJOJ11] K. Brádler, T. Jochym-O'Connor, and R. Jáuregui. *Capacities of grassmann channels.* Journal of Mathematical Physics, **52**(6) 062202, (2011).

[BKL+19] T. Bækkegaard, L. B. Kristensen, N. J. S. Loft, C. K. Andersen, D. Petrosyan, and N. T. Zinner. *Realization of efficient quantum gates with a superconducting qubit-qutrit circuit.* Scientific Reports, **9**(1) 13389, Sep 2019.

[BKN00] H. Barnum, E. Knill, and M. Nielsen. *On quantum fidelities and channel capacities.* IEEE Transactions on Information Theory, **46**(4) 1317–1329, (2000).

[BL21] J. Bausch and F. Leditzky. *Error thresholds for arbitrary Pauli noise.* SIAM Journal on Computing, **50**(4) 1410–1460, (2021).

[BM02] D. Bruss and C. Macchiavello. *Optimal eavesdropping in cryptography with three-dimensional quantum states.* Physical review letters, **88**(12) 127901, (2002).

[BNS98] H. Barnum, M. A. Nielsen, and B. Schumacher. *Information transmission through a noisy quantum channel.* Phys. Rev. A, **57** 4153–4175, Jun 1998.

[BO07] C. K. Burrell and T. J. Osborne. *Bounds on the speed of information propagation in disordered quantum spin chains.* Phys. Rev. Lett., **99** 167201, Oct 2007.

[Bos03] S. Bose. *Quantum communication through an unmodulated spin chain.* Phys. Rev. Lett., **91** 207901, Nov 2003.

[Bos07] S. Bose. *Quantum communication through spin chain dynamics: an introductory overview*. Contemporary Physics, **48**(1) 13–30, (2007).

[BR12] O. Bratteli and D. W. Robinson. *Operator algebras and quantum statistical mechanics*. Springer Berlin, Heidelberg, 2 edition, (2012).

[Brá11] K. Brádler. *An infinite sequence of additive channels: The classical capacity of cloning channels*. IEEE Transactions on Information Theory, **57**(8) 5497–5503, (2011).

[BRS17] A. Bocharov, M. Roetteler, and K. M. Svore. *Factoring with qutrits: Shor's algorithm on ternary and metaplectic quantum architectures*. Phys. Rev. A, **96** 012306, Jul 2017.

[BSST99] C. H. Bennett, P. W. Shor, J. A. Smolin, and A. V. Thapliyal. *Entanglement-assisted classical capacity of noisy quantum channels*. Phys. Rev. Lett., **83** 3081–3084, Oct 1999.

[BSST02] C. Bennett, P. Shor, J. Smolin, and A. Thapliyal. *Entanglement-assisted capacity of a quantum channel and the reverse Shannon theorem*. IEEE Transactions on Information Theory, **48**(10) 2637–2655, (2002).

[BV97] E. Bernstein and U. Vazirani. *Quantum complexity theory*. SIAM Journal on Computing, **26**(5) 1411–1473, (1997).

[BW92] C. H. Bennett and S. J. Wiesner. *Communication via one- and two-particle operators on Einstein-Podolsky-Rosen states*. Phys. Rev. Lett., **69** 2881–2884, Nov 1992.

[BŻ17] I. Bengtsson and K. Życzkowski. *Geometry of Quantum States: An Introduction to Quantum Entanglement*. Cambridge University Press, 2 edition, (2017).

[CDEL04] M. Christandl, N. Datta, A. Ekert, and A. J. Landahl. *Perfect state transfer in quantum spin networks*. Phys. Rev. Lett., **92** 187902, May 2004.

[CDLBO19] D. Cozzolino, B. Da Lio, D. Bacco, and L. K. Oxenløwe. *High-dimensional quantum communication: Benefits, progress, and future challenges*. Advanced Quantum Technologies, **2**(12) 1900038, (2019).

[CEM+15] T. Cubitt, D. Elkouss, W. Matthews, M. Ozols, D. Pérez-García, and S. Strelchuk. *Unbounded number of channel uses may be required to detect quantum capacity*. Nature Communications, **6**(1) 6739, Mar 2015.

[CFG19] S. Chessa, M. Fanizza, and V. Giovannetti. *Quantum-capacity bounds in spin-network communication channels*. Phys. Rev. A, **100** 032311, Sep 2019.

[CG06] F. Caruso and V. Giovannetti. *Degradability of bosonic gaussian channels*. Phys. Rev. A, **74** 062307, Dec 2006.

[CG19] S. Chessa and V. Giovannetti. *Time-polynomial lieb-robinson bounds for finite-range spin-network models*. Phys. Rev. A, **100** 052309, Nov 2019.

[CG21a] S. Chessa and V. Giovannetti. *Partially Coherent Direct Sum Channels*. Quantum, **5** 504, July 2021.

[CG21b] S. Chessa and V. Giovannetti. *Quantum capacity analysis of multi-level amplitude damping channels*. Communications Physics, **4**(1) 22, Feb 2021.

[CGLM14] F. Caruso, V. Giovannetti, C. Lupo, and S. Mancini. *Quantum channels and memory effects*. Rev. Mod. Phys., **86** 1203–1259, Dec 2014.

[Cho75] M.-D. Choi. *Completely positive linear maps on complex matrices*. Linear Algebra and its Applications, **10**(3) 285–290, (1975).

[CL21] C.-F. Chen and A. Lucas. *Operator growth bounds from graph theory*. Communications in Mathematical Physics, **385**(3) 1273–1323, Aug 2021.

[CMH17] M. Christandl and A. Müller-Hermes. *Relative entropy bounds on quantum, private and repeater capacities*. Communications in Mathematical Physics, **353**(2) 821–852, Jul 2017.

[CMW+21] W. Cai, Y. Ma, W. Wang, C.-L. Zou, and L. Sun. *Bosonic quantum error correction codes in superconducting quantum circuits*. Fundamental Research, **1**(1) 50–67, (2021).

[CRS08] T. S. Cubitt, M. B. Ruskai, and G. Smith. *The structure of degradable quantum channels*. Journal of Mathematical Physics, **49**(10) 102104, (2008).

[CSE08] M. Cramer, A. Serafini, and J. Eisert. Locality of dynamics in general harmonic systems. In M. Ericsson and S. Montangero, editors, *Quantum Information and Many Body Quantum Systems*, pages 51–72, Pisa, (2008). Edizioni della Normale Pisa.

[CT05] T. M. Cover and J. A. Thomas. *Elements of Information Theory*. Wiley, 2 edition, (2005).

[CVDC03] T. S. Cubitt, F. Verstraete, W. Dür, and J. I. Cirac. *Separable states can be used to distribute entanglement*. Phys. Rev. Lett., **91** 037902, Jul 2003.

[CWY04] N. Cai, A. Winter, and R. W. Yeung. *Quantum privacy and quantum wiretap channels*. Problems of Information Transmission, **40**(4) 318–336, (2004).

[Dam05] J. N. Damask. *Polarization optics in telecommunications*. Springer Series in Optical Sciences, 1 edition, (2005).

[DBF07] A. D'Arrigo, G. Benenti, and G. Falci. *Quantum capacity of dephasing channels with memory*. New Journal of Physics, **9**(9) 310–310, sep 2007.

[DBFM13] A. D'Arrigo, G. Benenti, G. Falci, and C. Macchiavello. *Classical and quantum capacities of a fully correlated amplitude damping channel*. Phys. Rev. A, **88** 042337, Oct 2013.

[DBFM15] A. D'Arrigo, G. Benenti, G. Falci, and C. Macchiavello. *Information transmission over an amplitude damping channel with an arbitrary degree of memory*. Phys. Rev. A, **92** 062342, Dec 2015.

[Deu85] D. Deutsch. *Quantum theory, the Church-Turing principle and the universal quantum computer*. Proceedings of the Royal Society of London. A. Mathematical and Physical Sciences, **400**(1818) 97–117, (1985).

[Dev05] I. Devetak. *The private classical capacity and quantum capacity of a quantum channel*. IEEE Transactions on Information Theory, **51**(1) 44–55, (2005).

[DiV00] D. P. DiVincenzo. *The physical implementation of quantum computation*. Fortschritte der Physik, **48**(9-11) 771–783, (2000).

[DJ92] D. Deutsch and R. Jozsa. *Rapid solution of problems by quantum computation*. Proceedings of the Royal Society of London. Series A: Mathematical and Physical Sciences, **439**(1907) 553–558, (1992), https://royalsocietypublishing.org/doi/pdf/10.1098/rspa.1992.0167.

[DJP+21] É. Dumur, S. K. J., G. A. Peairs, M.-H. Chou, A. Bienfait, H.-S. Chang, C. R. Conner, J. Grebel, R. G. Povey, Y. P. Zhong, and A. N. Cleland. *Quantum communication with itinerant surface acoustic wave phonons*. npj Quantum Information, **7**(1) 173, Dec 2021.

[Doo49] J. Doob. *Review of "A mathematical theory of communication" by C. E. Shannon*. Mathematical Reviews, **10** 133, (1949).

[DS05] I. Devetak and P. W. Shor. *The capacity of a quantum channel for simultaneous transmission of classical and quantum information*. Communications in Mathematical Physics, **256**(2) 287–303, (2005).

[DSS98] D. P. DiVincenzo, P. W. Shor, and J. A. Smolin. *Quantum-channel capacity of very noisy channels*. Phys. Rev. A, **57** 830–839, Feb 1998.

[EG09] J. Eisert and D. Gross. *Supersonic quantum communication*. Phys. Rev. Lett., **102** 240501, Jun 2009.

[Eke91] A. K. Ekert. *Quantum cryptography based on Bell's theorem*. Phys. Rev. Lett., **67** 661–663, Aug 1991.

[EO06] J. Eisert and T. J. Osborne. *General entanglement scaling laws from time evolution*. Phys. Rev. Lett., **97** 150404, Oct 2006.

[EPBH04] J. Eisert, M. B. Plenio, S. Bose, and J. Hartley. *Towards quantum entanglement in nanoelectromechanical devices*. Phys. Rev. Lett., **93** 190402, Nov 2004.

[ES15] D. Elkouss and S. Strelchuk. *Superadditivity of private information for any number of uses of the channel.* Phys. Rev. Lett., **115** 040501, Jul 2015.

[EvdWMK13] J. Eisert, M. van den Worm, S. R. Manmana, and M. Kastner. *Breakdown of quasilocality in long-range quantum lattice models.* Phys. Rev. Lett., **111** 260401, Dec 2013.

[EW17] J. M. Epstein and K. B. Whaley. *Quantum speed limits for quantum-information-processing tasks.* Phys. Rev. A, **95** 042314, Apr 2017.

[Fan73] M. Fannes. *A continuity property of the entropy density for spin lattice systems.* Communications in Mathematical Physics, **31**(4) 291–294, Dec 1973.

[Fey82] R. P. Feynman. *Simulating physics with computers.* International Journal of Theoretical Physics, **21**(6) 467–488, Jun 1982.

[FF21] K. Fang and H. Fawzi. *Geometric Rényi divergence and its applications in quantum channel capacities.* Communications in Mathematical Physics, **384**(3) 1615–1677, Jun 2021.

[FFGCG15] M. Foss-Feig, Z.-X. Gong, C. W. Clark, and A. V. Gorshkov. *Nearly linear light cones in long-range interacting quantum systems.* Phys. Rev. Lett., **114** 157201, Apr 2015.

[FKG20] M. Fanizza, F. Kianvash, and V. Giovannetti. *Quantum flags and new bounds on the quantum capacity of the depolarizing channel.* Phys. Rev. Lett., **125** 020503, Jul 2020.

[FMHS22] O. Fawzi, A. Müller-Hermes, and A. Shayeghi. A Lower Bound on the Space Overhead of Fault-Tolerant Quantum Computation. In M. Braverman, editor, *13th Innovations in Theoretical Computer Science Conference (ITCS 2022)*, volume 215 of *Leibniz International Proceedings in Informatics (LIPIcs)*, pages 68:1–68:20, Dagstuhl, Germany, (2022). Schloss Dagstuhl – Leibniz-Zentrum für Informatik.

[FST22] O. Fawzi, A. Shayeghi, and H. Ta. *A hierarchy of efficient bounds on quantum capacities exploiting symmetry*, (2022), arXiv:2203.02127.

[FW07] M. Fukuda and M. M. Wolf. *Simplifying additivity problems using direct sum constructions.* Journal of Mathematical Physics, **48**(7) 072101, (2007).

[FW08] J. Fern and K. B. Whaley. *Lower bounds on the nonzero capacity of Pauli channels.* Phys. Rev. A, **78** 062335, Dec 2008.

[FXBJ07] J. Fitzsimons, L. Xiao, S. C. Benjamin, and J. A. Jones. *Quantum information processing with delocalized qubits under global control.* Phys. Rev. Lett., **99** 030501, Jul 2007.

[GB06] V. Giovannetti and D. Burgarth. *Improved transfer of quantum information using a local memory.* Phys. Rev. Lett., **96** 030501, Jan 2006.

[GBDG+14] S. K. Goyal, P. E. Boukama-Dzoussi, S. Ghosh, F. S. Roux, and T. Konrad. *Qudit-teleportation for photons with linear optics.* Scientific Reports, **4**(1) 4543, Apr 2014.

[GF05] V. Giovannetti and R. Fazio. *Information-capacity description of spin-chain correlations.* Phys. Rev. A, **71** 032314, Mar 2005.

[GFFMG14] Z.-X. Gong, M. Foss-Feig, S. Michalakis, and A. V. Gorshkov. *Persistence of locality in systems with power-law interactions.* Phys. Rev. Lett., **113** 030602, Jul 2014.

[GIN18] L. Gyongyosi, S. Imre, and H. V. Nguyen. *A survey on quantum channel capacities.* IEEE Communications Surveys Tutorials, **20**(2) 1149–1205, (2018).

[GJL18a] L. Gao, M. Junge, and N. LaRacuente. *Capacity bounds via operator space methods.* Journal of Mathematical Physics, **59**(12) 122202, (2018).

[GJL18b] L. Gao, M. Junge, and N. LaRacuente. *Capacity estimates via comparison with tro channels.* Communications in Mathematical Physics, **364**(1) 83–121, Nov 2018.

[GKP01] D. Gottesman, A. Kitaev, and J. Preskill. *Encoding a qubit in an oscillator.* Phys. Rev. A, **64** 012310, Jun 2001.

[GKS92] R. K. Guy, C. Krattenthaler, and B. E. Sagan. *Lattice paths, reflections, & dimension-changing bijections.* Ars Combinatorica, **34** 15, (1992).

[GPE+19] T. Giordani, E. Polino, S. Emiliani, A. Suprano, L. Innocenti, H. Majury, L. Marrucci, M. Paternostro, A. Ferraro, N. Spagnolo, and F. Sciarrino. *Experimental engineering of arbitrary qudit states with discrete-time quantum walks.* Phys. Rev. Lett., **122** 020503, Jan 2019.

[Gro96] L. K. Grover. A fast quantum mechanical algorithm for database search. In *Proceedings of the Twenty-Eighth Annual ACM Symposium on Theory of Computing*, STOC '96, page 212–219, New York, NY, USA, (1996). Association for Computing Machinery.

[GSÇ+15] Z. Gedik, I. A. Silva, B. Çakmak, G. Karpat, E. L. G. Vidoto, D. O. Soares-Pinto, E. R. deAzevedo, and F. F. Fanchini. *Computational speed-up with a single qudit.* Scientific Reports, **5**(1) 14671, Oct 2015.

[Gur03] L. Gurvits. Classical deterministic complexity of edmonds' problem and quantum entanglement. In *Proceedings of the Thirty-Fifth Annual ACM Symposium on Theory of Computing*, STOC '03, page 10–19, New York, NY, USA, (2003). Association for Computing Machinery.

[Gur04] L. Gurvits. *Classical complexity and quantum entanglement.* Journal of Computer and System Sciences, **69**(3) 448–484, (2004). Special Issue on STOC 2003.

[Gyo14] L. Gyongyosi. *The structure and quantum capacity of a partially degradable quantum channel.* IEEE Access, **2** 333–355, (2014).

[Has04a] M. B. Hastings. *Decay of correlations in fermi systems at nonzero temperature.* Phys. Rev. Lett., **93** 126402, Sep 2004.

[Has04b] M. B. Hastings. *Lieb-schultz-mattis in higher dimensions.* Phys. Rev. B, **69** 104431, Mar 2004.

[Has07] M. B. Hastings. *An area law for one-dimensional quantum systems.* Journal of Statistical Mechanics: Theory and Experiment, **2007**(08) P08024–P08024, aug 2007.

[Has09] M. B. Hastings. *Superadditivity of communication capacity using entangled inputs.* Nature Physics, **5**(4) 255–257, Apr 2009.

[Hay17] M. Hayashi. *Quantum information theory.* Springer, 2 edition, (2017).

[HG12] A. S. Holevo and V. Giovannetti. *Quantum channels and their entropic characteristics.* Reports on Progress in Physics, **75**(4) 046001, mar 2012.

[HG18] Z. Huang and X.-K. Guo. *Lieb-robinson bound at finite temperatures.* Phys. Rev. E, **97** 062131, Jun 2018.

[Hil21] A. Hill. *Beyond qubits: Unlocking the third state in quantum processors*, Dec 2021.

[HK06] M. B. Hastings and T. Koma. *Spectral gap and exponential decay of correlations.* Communications in Mathematical Physics, **265**(3) 781–804, Aug 2006.

[HL22] C. Hirche and F. Leditzky. *Bounding quantum capacities via partial orders and complementarity*, (2022), arXiv:2202.11688.

[Hol73] A. S. Holevo. *Bounds for the quantity of information transmitted by a quantum communication channel.* Problemy Peredachi Informatsii, **9**(3) 3–11, (1973).

[Hol79] A. S. Holevo. *On capacity of a quantum communications channel.* Problemy Peredachi Informatsii, **15**(4) 3–11, (1979).

[Hol98] A. Holevo. *The capacity of the quantum channel with general signal states.* IEEE Transactions on Information Theory, **44**(1) 269–273, (1998).

[Hol07] A. S. Holevo. *Complementary channels and the additivity problem.* Theory of Probability & Its Applications, **51**(1) 92–100, (2007).

[Hol19] A. S. Holevo. *Quantum Systems, Channels, Information.* De Gruyter, (2019).

[HPK+14] B. Heim, C. Peuntinger, N. Killoran, I. Khan, C. Wittmann, C. Marquardt, and G. Leuchs. *Atmospheric continuous-variable quantum communication.* New Journal of Physics, **16**(11) 113018, nov 2014.

[HRF20] C. Hirche, C. Rouzé, and D. S. França. *On contraction coefficients, partial orders and approximation of capacities for quantum channels*, (2020), arXiv:2011.05949.

[HRP06] M. J. Hartmann, M. E. Reuter, and M. B. Plenio. *Excitation and entanglement transfer versus spectral gap.* New Journal of Physics, **8**(6) 94–94, jun 2006.

[HSGCA17] S. Hernández-Santana, C. Gogolin, J. I. Cirac, and A. Acín. *Correlation decay in fermionic lattice systems with power-law interactions at nonzero temperature.* Phys. Rev. Lett., **119** 110601, Sep 2017.

[HSP10] K. Hammerer, A. S. Sørensen, and E. S. Polzik. *Quantum interface between light and atomic ensembles.* Rev. Mod. Phys., **82** 1041–1093, Apr 2010.

[HT13] P. Hauke and L. Tagliacozzo. *Spread of correlations in long-range interacting quantum systems.* Phys. Rev. Lett., **111** 207202, Nov 2013.

[HTY+11] S. Hermelin, S. Takada, M. Yamamoto, S. Tarucha, A. D. Wieck, L. Saminadayar, C. Bäuerle, and T. Meunier. *Electrons surfing on a sound wave as a platform for quantum optics with flying electrons.* Nature, **477**(7365) 435–438, Sep 2011.

[HW08] P. Hayden and A. Winter. *Counterexamples to the maximal p-norm multiplicativity conjecture for all $p > 1$.* Communications in Mathematical Physics, **284**(1) 263–280, Nov 2008.

[IG12] S. Imre and L. Gyongyosi. *Advanced Quantum Communications: An Engineering Approach.* Wiley-IEEE Press, 1st edition, (2012).

[ITV12] S. S. Ivanov, H. S. Tonchev, and N. V. Vitanov. *Time-efficient implementation of quantum search with qudits.* Phys. Rev. A, **85** 062321, Jun 2012.

[JAT15] R. Jahangir, N. Arshed, and A. H. Toor. *Quantum capacity of an amplitude-damping channel with memory.* Quantum Information Processing, **14**(2) 765–782, Feb 2015.

[JGY+17] L. Ji, J. Gao, A.-L. Yang, Z. Feng, X.-F. Lin, Z.-G. Li, and X.-M. Jin. *Towards quantum communications in free-space seawater.* Opt. Express, **25**(17) 19795–19806, Aug 2017.

[JNN12] J. Johansson, P. Nation, and F. Nori. *Qutip: An open-source python framework for the dynamics of open quantum systems.* Computer Physics Communications, **183**(8) 1760–1772, (2012).

[JNN13] J. Johansson, P. Nation, and F. Nori. *Qutip 2: A python framework for the dynamics of open quantum systems.* Computer Physics Communications, **184**(4) 1234–1240, (2013).

[Key02] M. Keyl. *Fundamentals of quantum information theory.* Physics Reports, **369**(5) 431–548, (2002).

[KFG22] F. Kianvash, M. Fanizza, and V. Giovannetti. *Bounding the quantum capacity with flagged extensions.* Quantum, **6** 647, Feb. 2022.

[KGRS03] A. B. Klimov, R. Guzmán, J. C. Retamal, and C. Saavedra. *Qutrit quantum computer with trapped ions.* Phys. Rev. A, **67** 062313, Jun 2003.

[Kin] C. King. *An application of the Lieb-Thirring inequality in quantum information theory*, pages 486–490. .

[Kin02] C. King. *Additivity for unital qubit channels.* Journal of Mathematical Physics, **43**(10) 4641–4653, (2002).

[Kin03] C. King. *The capacity of the quantum depolarizing channel.* IEEE Transactions on Information Theory, **49**(1) 221–229, (2003).

[Kit95] A. Y. Kitaev. *Quantum measurements and the abelian stabilizer problem*, (1995).

[Kit97] A. Y. Kitaev. *Quantum computations: algorithms and error correction.* Russian Mathematical Surveys, **52**(6) 1191–1249, dec 1997.

[KMNR05] C. King, K. Matsumoto, M. Nathanson, and M. B. Ruskai. *Properties of conjugate channels with applications to additivity and multiplicativity.* , , (2005).

[KNX+20] E. O. Kiktenko, A. S. Nikolaeva, P. Xu, G. V. Shlyapnikov, and A. K. Fedorov. *Scalable quantum computing with qudits on a graph.* Phys. Rev. A, **101** 022304, Feb 2020.

[KOC+03] D. Kaszlikowski, D. K. L. Oi, M. Christandl, K. Chang, A. Ekert, L. C. Kwek, and C. H. Oh. *Quantum cryptography based on qutrit Bell inequalities.* Phys. Rev. A, **67** 012310, Jan 2003.

[Kra71] K. Kraus. *General state changes in quantum theory.* Annals of Physics, **64**(2) 311–335, (1971).

[KRR+17] M. Kues, C. Reimer, P. Roztocki, L. R. Cortés, S. Sciara, B. Wetzel, Y. Zhang, A. Cino, S. T. Chu, B. E. Little, D. J. Moss, L. Caspani, J. Azaña, and R. Morandotti. *On-chip generation of high-dimensional entangled quantum states and their coherent control.* Nature, **546**(7660) 622–626, Jun 2017.

[KSVV02] A. Y. Kitaev, A. Shen, M. N. Vyalyi, and M. N. Vyalyi. *Classical and quantum computation*. Number 47. American Mathematical Soc., (2002).

[KSW20] S. Khatri, K. Sharma, and M. M. Wilde. *Information-theoretic aspects of the generalized amplitude-damping channel*. Phys. Rev. A, **102** 012401, Jul 2020.

[KW20] S. Khatri and M. M. Wilde. *Principles of quantum communication theory: A modern approach*. , , (2020).

[LBA+09] B. P. Lanyon, M. Barbieri, M. P. Almeida, T. Jennewein, T. C. Ralph, K. J. Resch, G. J. Pryde, J. L. O'Brien, A. Gilchrist, and A. G. White. *Simplifying quantum logic using higher-dimensional hilbert spaces*. Nature Physics, **5**(2) 134–140, Feb 2009.

[LKDW18] F. Leditzky, E. Kaur, N. Datta, and M. M. Wilde. *Approaches for approximate additivity of the holevo information of quantum channels*. Phys. Rev. A, **97** 012332, Jan 2018.

[Llo97] S. Lloyd. *Capacity of the noisy quantum channel*. Phys. Rev. A, **55** 1613–1622, Mar 1997.

[LLS18a] F. Leditzky, D. Leung, and G. Smith. *Dephrasure channel and superadditivity of coherent information*. Phys. Rev. Lett., **121** 160501, Oct 2018.

[LLS18b] F. Leditzky, D. Leung, and G. Smith. *Quantum and private capacities of low-noise channels*. Phys. Rev. Lett., **120** 160503, Apr 2018.

[LLS+22a] F. Leditzky, D. Leung, V. Siddhu, G. Smith, and J. Smolin. *The platypus of the quantum channel zoo*, (2022), arXiv:2202.08380.

[LLS+22b] F. Leditzky, D. Leung, V. Siddhu, G. Smith, and J. A. Smolin. *Generic nonadditivity of quantum capacity in simple channels*, (2022), arXiv:2202.08377.

[LLS+22c] F. Leditzky, D. Leung, V. Siddhu, G. Smith, and J. A. Smolin. *The platypus of the quantum channel zoo*, (2022), arXiv:2202.08380.

[LNG+11] G. Lima, L. Neves, R. Guzmán, E. S. Gómez, W. A. T. Nogueira, A. Delgado, A. Vargas, and C. Saavedra. *Experimental quantum tomography of photonic qudits via mutually unbiased basis*. Opt. Express, **19**(4) 3542–3552, Feb 2011.

[LR72] E. H. Lieb and D. W. Robinson. *The finite group velocity of quantum spin systems*. Communications in Mathematical Physics, **28**(3) 251–257, Sep 1972.

[LS09] D. Leung and G. Smith. *Continuity of quantum channel capacities*. Communications in Mathematical Physics, **292**(1) 201–215, Nov 2009.

[LSH+13] N. Lashkari, D. Stanford, M. Hastings, T. Osborne, and P. Hayden. *Towards the fast scrambling conjecture.* Journal of High Energy Physics, **2013**(4) 22, Apr 2013.

[LWL+08] B. P. Lanyon, T. J. Weinhold, N. K. Langford, J. L. O'Brien, K. J. Resch, A. Gilchrist, and A. G. White. *Manipulating biphotonic qutrits.* Phys. Rev. Lett., **100** 060504, Feb 2008.

[LWZG09] K. Li, A. Winter, X. Zou, and G. Guo. *Private capacity of quantum channels is not additive.* Phys. Rev. Lett., **103** 120501, Sep 2009.

[LYF13] B. Li, Z.-H. Yu, and S.-M. Fei. *Geometry of quantum computation with qutrits.* Scientific Reports, **3**(1) 2594, Sep 2013.

[LYGG08] S. Y. Looi, L. Yu, V. Gheorghiu, and R. B. Griffiths. *Quantum-error-correcting codes using qudit graph states.* Phys. Rev. A, **78** 042303, Oct 2008.

[LZE+19] Y.-H. Luo, H.-S. Zhong, M. Erhard, X.-L. Wang, L.-C. Peng, M. Krenn, X. Jiang, L. Li, N.-L. Liu, C.-Y. Lu, A. Zeilinger, and J.-W. Pan. *Quantum teleportation in high dimensions.* Phys. Rev. Lett., **123** 070505, Aug 2019.

[MKF+11] R. P. G. McNeil, M. Kataoka, C. J. B. Ford, C. H. W. Barnes, D. Anderson, G. A. C. Jones, I. Farrer, and D. A. Ritchie. *On-demand single-electron transfer between distant quantum dots.* Nature, **477**(7365) 439–442, Sep 2011.

[MKN17] T. Matsuta, T. Koma, and S. Nakamura. *Improving the lieb–robinson bound for long-range interactions.* Annales Henri Poincaré, **18**(2) 519–528, Feb 2017.

[MMP+15] B. Marques, A. A. Matoso, W. M. Pimenta, A. J. Gutiérrez-Esparza, M. F. Santos, and S. Pádua. *Experimental simulation of decoherence in photonics qudits.* Scientific Reports, **5**(1) 16049, Nov 2015.

[MPGB+18] E. Moreno-Pineda, C. Godfrin, F. Balestro, W. Wernsdorfer, and M. Ruben. *Molecular spin qudits for quantum algorithms.* Chem. Soc. Rev., **47** 501–513, (2018).

[MS00] A. Muthukrishnan and C. R. Stroud. *Multivalued logic gates for quantum computation.* Phys. Rev. A, **62** 052309, Oct 2000.

[MS19] C. Macchiavello and M. F. Sacchi. *Efficient accessible bounds to the classical capacity of quantum channels.* Phys. Rev. Lett., **123** 090503, Aug 2019.

[MVV+16] O. V. Marchukov, A. G. Volosniev, M. Valiente, D. Petrosyan, and N. T. Zinner. *Quantum spin transistor with a heisenberg spin chain.* Nature Communications, **7**(1) 13070, Oct 2016.

[MZL+17] S. Muralidharan, C.-L. Zou, L. Li, J. Wen, and L. Jiang. *Overcoming erasure errors with multilevel systems.* New Journal of Physics, **19**(1) 013026, jan 2017.

[NC10] M. A. Nielsen and I. L. Chuang. *Quantum Computation and Quantum Information: 10th Anniversary Edition.* Cambridge University Press, Cambridge, (2010).

[NJDH+13] P. B. R. Nisbet-Jones, J. Dilley, A. Holleczek, O. Barter, and A. Kuhn. *Photonic qubits, qutrits and ququads accurately prepared and delivered on demand.* New Journal of Physics, **15**(5) 053007, may 2013.

[NOS06] B. Nachtergaele, Y. Ogata, and R. Sims. *Propagation of correlations in quantum lattice systems.* Journal of Statistical Physics, **124**(1) 1–13, Jul 2006.

[NRSS09] B. Nachtergaele, H. Raz, B. Schlein, and R. Sims. *Lieb-robinson bounds for harmonic and anharmonic lattice systems.* Communications in Mathematical Physics, **286**(3) 1073–1098, Mar 2009.

[NS06] B. Nachtergaele and R. Sims. *Lieb-robinson bounds and the exponential clustering theorem.* Communications in Mathematical Physics, **265**(1) 119–130, Jul 2006.

[NS09] B. Nachtergaele and R. Sims. Locality estimates for quantum spin systems. In V. Sidoravičius, editor, *New Trends in Mathematical Physics*, pages 591–614, Dordrecht, (2009). Springer Netherlands.

[NSY19] B. Nachtergaele, R. Sims, and A. Young. *Quasi-locality bounds for quantum lattice systems. i. lieb-robinson bounds, quasi-local maps, and spectral flow automorphisms.* Journal of Mathematical Physics, **60**(6) 061101, (2019).

[Osb06] T. J. Osborne. *Efficient approximation of the dynamics of one-dimensional quantum spin systems.* Phys. Rev. Lett., **97** 157202, Oct 2006.

[Ouy14] Y. Ouyang. *Channel covariance, twirling, contraction and some upper bounds on the quantum capacity.* Quantum Information and Computation, **14** 917–936, Sep 2014.

[PDF+21] J. M. Pino, J. M. Dreiling, C. Figgatt, J. P. Gaebler, S. A. Moses, M. S. Allman, C. H. Baldwin, M. Foss-Feig, D. Hayes, K. Mayer, C. Ryan-Anderson, and B. Neyenhuis. *Demonstration of the trapped-ion quantum ccd computer architecture.* Nature, **592**(7853) 209–213, Apr 2021.

[PHE04] M. B. Plenio, J. Hartley, and J. Eisert. *Dynamics and manipulation of entanglement in coupled harmonic systems with many degrees of freedom.* New Journal of Physics, **6** 36–36, mar 2004.

[Pie73] J. Pierce. *The early days of information theory.* IEEE Transactions on Information Theory, **19**(1) 3–8, (1973).

[Pir21] S. Pirandola. *Satellite quantum communications: Fundamental bounds and practical security.* Phys. Rev. Research, **3** 023130, May 2021.

[PLBG13] Y. Ping, B. W. Lovett, S. C. Benjamin, and E. M. Gauger. *Practicality of spin chain wiring in diamond quantum technologies.* Phys. Rev. Lett., **110** 100503, Mar 2013.

[PLOB17] S. Pirandola, R. Laurenza, C. Ottaviani, and L. Banchi. *Fundamental limits of repeaterless quantum communications.* Nature Communications, **8**(1) 15043, Apr 2017.

[PML+21] M. Pittaluga, M. Minder, M. Lucamarini, M. Sanzaro, R. I. Woodward, M.-J. Li, Z. Yuan, and A. J. Shields. *600-km repeater-like quantum communications with dual-band stabilization.* Nature Photonics, **15**(7) 530–535, Jul 2021.

[RFB05] A. Romito, R. Fazio, and C. Bruder. *Solid-state quantum communication with josephson arrays.* Phys. Rev. B, **71** 100501, Mar 2005.

[RR15] A. Reiserer and G. Rempe. *Cavity-based quantum networks with single atoms and optical photons.* Rev. Mod. Phys., **87** 1379–1418, Dec 2015.

[RRG07] T. C. Ralph, K. J. Resch, and A. Gilchrist. *Efficient toffoli gates using qudits.* Phys. Rev. A, **75** 022313, Feb 2007.

[RS16] D. A. Roberts and B. Swingle. *Lieb-robinson bound and the butterfly effect in quantum field theories.* Phys. Rev. Lett., **117** 091602, Aug 2016.

[SBG+20] R. Sawant, J. A. Blackmore, P. D. Gregory, J. Mur-Petit, D. Jaksch, J. Aldegunde, J. M. Hutson, M. R. Tarbutt, and S. L. Cornish. *Ultracold polar molecules as qudits.* New Journal of Physics, **22**(1) 013027, jan 2020.

[Sch96] B. Schumacher. *Sending entanglement through noisy quantum channels.* Phys. Rev. A, **54** 2614–2628, Oct 1996.

[SD22] S. Singh and N. Datta. *Detecting positive quantum capacities of quantum channels.* npj Quantum Information, **8**(1) 50, May 2022.

[SG21a] V. Siddhu and R. B. Griffiths. *Positivity and nonadditivity of quantum capacities using generalized erasure channels.* IEEE Transactions on Information Theory, **67**(7) 4533–4545, (2021).

[SG21b] V. Siddhu and R. B. Griffiths. *Positivity and nonadditivity of quantum capacities using generalized erasure channels.* IEEE Transactions on Information Theory, **67**(7) 4533–4545, (2021).

[Sha48] C. E. Shannon. *A mathematical theory of communication.* Bell System Technical Journal, **27**(3) 379–423, (1948).

[Shi17] M. E. Shirokov. *Tight uniform continuity bounds for the quantum conditional mutual information, for the holevo quantity, and for capacities of quantum channels*. Journal of Mathematical Physics, **58**(10) 102202, (2017).

[Sho94] P. Shor. Algorithms for quantum computation: discrete logarithms and factoring. In *Proceedings 35th Annual Symposium on Foundations of Computer Science*, pages 124–134, (1994).

[Sho02a] P. W. Shor. *Additivity of the classical capacity of entanglement-breaking quantum channels*. Journal of Mathematical Physics, **43**(9) 4334–4340, (2002).

[Sho02b] P. W. Shor. The quantum channel capacity and coherent information. In *Lecture notes, MSRI Workshop on Quantum Computation (Quantum Information and Cryptography)*, Nov 2002.

[Sid21] V. Siddhu. *Entropic singularities give rise to quantum transmission*. Nature Communications, **12**(1) 5750, Oct 2021.

[Sim97] D. R. Simon. *On the power of quantum computation*. SIAM Journal on Computing, **26**(5) 1474–1483, (1997).

[SJG+] J. S. Sidhu, S. K. Joshi, M. Gündoğan, T. Brougham, D. Lowndes, L. Mazzarella, M. Krutzik, S. Mohapatra, D. Dequal, G. Vallone, P. Villoresi, A. Ling, T. Jennewein, M. Mohageg, J. G. Rarity, I. Fuentes, S. Pirandola, and D. K. L. Oi. *Advances in space quantum communications*. IET Quantum Communication, **2**(4) 182–217, .

[Smi08] G. Smith. *Private classical capacity with a symmetric side channel and its application to quantum cryptography*. Physical Review A, **78**(2) 022306, (2008).

[SN96] B. Schumacher and M. A. Nielsen. *Quantum data processing and error correction*. Phys. Rev. A, **54** 2629–2635, Oct 1996.

[SRS08] G. Smith, J. M. Renes, and J. A. Smolin. *Structured codes improve the bennett-brassard-84 quantum key rate*. Phys. Rev. Lett., **100** 170502, Apr 2008.

[SS96] P. W. Shor and J. A. Smolin. *Quantum error-correcting codes need not completely reveal the error syndrome*, (1996), arXiv:quant-ph/9604006.

[SS07] G. Smith and J. A. Smolin. *Degenerate quantum codes for Pauli channels*. Physical review letters, **98**(3) 030501, (2007).

[SS08] G. Smith and J. A. Smolin. Additive extensions of a quantum channel. In *2008 IEEE Information Theory Workshop*, pages 368–372, (2008).

[SSdRG11] N. Sangouard, C. Simon, H. de Riedmatten, and N. Gisin. *Quantum repeaters based on atomic ensembles and linear optics.* Rev. Mod. Phys., **83** 33–80, Mar 2011.

[SSW93] C. E. Shannon, N. J. A. Sloane, and A. D. Wyner. *Claude Elwood Shannon: Collected Papers.* IEEE Press, (1993).

[SSWR17] D. Sutter, V. B. Scholz, A. Winter, and R. Renner. *Approximate degradable quantum channels.* IEEE Transactions on Information Theory, **63**(12) 7832–7844, (2017).

[STA18] *Effect of diagonal orthogonal matrices.* Mathematics Stack Exchange, (2018).

[Sti55] W. F. Stinespring. *Positive functions on C*-algebras.* Proceedings of the American Mathematical Society, **6**(2) 211–216, (1955).

[SW97] B. Schumacher and M. D. Westmoreland. *Sending classical information via noisy quantum channels.* Phys. Rev. A, **56** 131–138, Jul 1997.

[SY08] G. Smith and J. Yard. *Quantum communication with zero-capacity channels.* Science, **321**(5897) 1812–1815, (2008).

[SZS+18] A. R. Shlyakhov, V. V. Zemlyanov, M. V. Suslov, A. V. Lebedev, G. S. Paraoanu, G. B. Lesovik, and G. Blatter. *Quantum metrology with a transmon qutrit.* Phys. Rev. A, **97** 022115, Feb 2018.

[TCV20] B. M. Terhal, J. Conrad, and C. Vuillot. *Towards scalable bosonic quantum error correction.* Quantum Science and Technology, **5**(4) 043001, jul 2020.

[The14] K. Them. *Towards experimental tests and applications of lieb-robinson bounds.* Phys. Rev. A, **89** 022126, Feb 2014.

[TWW17] M. Tomamichel, M. M. Wilde, and A. Winter. *Strong converse rates for quantum communication.* IEEE Transactions on Information Theory, **63**(1) 715–727, (2017).

[VBD+15] G. Vallone, D. Bacco, D. Dequal, S. Gaiarin, V. Luceri, G. Bianco, and P. Villoresi. *Experimental satellite quantum communications.* Phys. Rev. Lett., **115** 040502, Jul 2015.

[vN27] J. von Neumann. *Thermodynamik quantenmechanischer gesamtheiten.* Nachrichten von der Gesellschaft der Wissenschaften zu Göttingen, Mathematisch-Physikalische Klasse, **1927** 273–291, (1927).

[vN18] J. von Neumann. *Mathematical Foundations of Quantum Mechanics: New Edition.* Princeton University Press, (2018).

[Wat12] S. Watanabe. *Private and quantum capacities of more capable and less noisy quantum channels.* Phys. Rev. A, **85** 012326, Jan 2012.

[Wat18] J. Watrous. *The Theory of Quantum Information*. Cambridge University Press, Cambridge, (2018).

[WFD19] X. Wang, K. Fang, and R. Duan. *Semidefinite programming converse bounds for quantum communication*. IEEE Transactions on Information Theory, **65**(4) 2583–2592, (2019).

[WHSK20] Y. Wang, Z. Hu, B. C. Sanders, and S. Kais. *Qudits and high-dimensional quantum computing*. Frontiers in Physics, **8** 479, (2020).

[Wie83] S. Wiesner. *Conjugate coding*. SIGACT News, **15**(1) 78–88, jan 1983.

[Wil17] M. M. Wilde. *Quantum Information Theory*. Cambridge University Press, Cambridge, 2 edition, (2017).

[WPG07] M. M. Wolf and D. Perez-Garcia. *Quantum capacities of channels with small environment*. Physical Review A, **75**(1) 012303, (2007).

[WPGP+12] C. Weedbrook, S. Pirandola, R. García-Patrón, N. J. Cerf, T. C. Ralph, J. H. Shapiro, and S. Lloyd. *Gaussian quantum information*. Rev. Mod. Phys., **84** 621–669, May 2012.

[WTB17] M. M. Wilde, M. Tomamichel, and M. Berta. *Converse bounds for private communication over quantum channels*. IEEE Transactions on Information Theory, **63**(3) 1792–1817, (2017).

[YHD08] J. Yard, P. Hayden, and I. Devetak. *Capacity theorems for quantum multiple-access channels: classical-quantum and quantum-quantum capacity regions*. IEEE Transactions on Information Theory, **54**(7) 3091–3113, (2008).

[YMP+20] S. Yu, Y. Meng, R. B. Patel, Y.-T. Wang, Z.-J. Ke, W. Liu, Z.-P. Li, Y.-Z. Yang, W.-H. Zhang, J.-S. Tang, C.-F. Li, and G.-C. Guo. *Experimental observation of coherent-information superadditivity in a dephrasure channel*. Phys. Rev. Lett., **125** 060502, Aug 2020.